Role of microRNAs in podocyte structure and function

DISSERTATION ZUR ERLANGUNG DES DOKTORGRADES DER NATURWISSENSCHAFTEN (DR. RER. NAT.) DER FAKULTÄT FÜR BIOLOGIE UND VORKLINISCHE MEDIZIN DER UNIVERSITÄT REGENSBURG

vorgelegt von

Sandra Meisinger

aus

Traunstein

im Jahr

2021

Das Promotionsgesuch wurde eingereicht am:

Die Arbeit wurde angeleitet von:
Prof. Dr. Ralph Witzgall

Unterschrift:

Sandra Meisinger

I. Table of content

II. List of figures

III. List of tables

1. Introduction

1.1. Small non-coding RNAs

1.1.1. Types of small non-coding RNAs

Non-coding RNAs (ncRNA) are a large group of endogenous RNAs which have no protein coding capacity. However, they have important functions like regulation of gene transcription and translation or post-transcriptional modifications. Around 80 % of the genome is transcribed for ncRNA as identified by the ENCODE (Encyclopedia of DNA elements) project (The ENCODE Project Consortium, 2004; Pennisi, 2012). ncRNAs are divided into two groups: small non-coding RNAs (<200 nt) and long non-coding RNAs (>200 nt). Small non-coding RNAs (sncRNA) include small- interfering RNAs (siRNAs), piwi-interacting RNAs (piRNAs) and microRNAs (miRNAs).

All sncRNAs are able to interfere or regulate the expression of specific genes. Complementary nucleotide sequences induces mRNA cleavage resulting in no gene translation, e.g. single-stranded piRNAs, which are part of the riboprotein complexes and ensure germ-line stability by transposons silencing (Moyano and Stefani, 2015). miRNAs, which is the best studied group of sncRNAs and main interest of the present work, are short, single stranded non-coding RNAs with an average size of 22 nucleotides (18-25 nt) that regulate many target mRNAs and therefore play important role in many biological processes.

1.1.2. Classification of miRNAs

The first miRNA lin-4 was identified in 1993 by the Ambros and Ruvkun group (Lee et al., 1993; Wightman et al., 1993). Since then, 38.589 hairpin precursor and 48.860 mature miRNAs in 271 organisms have been detected and listed on the online database mirBase (Griffiths-Jones, 2004; Griffiths-Jones et al., 2006; Griffiths-Jones et al., 2008; Kozomara and Griffiths-Jones, 2011, 2014; Kozomara et al., 2019). According to their discovery, miRNAs precursors are numbered chronologically. The miRNA precursor is indicated by a non-capitalized “r“, e.g. mir-30 and the prefix shows the specimen (e.g. hsa for *homo sapiens,* mmu for *mus musculus*). If a precursor is encoded by two different loci in the genome, the precursor is numbered, e.g. hsa-mir-101-1 and hsa-mir-101-2. The two mature miRNAs originating from a common precursor are named after the arm of the precursor they are derived from, e.g. miR-145-5p or miR-145-3p. If two or more miRNAs have an identical so-called “seed region”, i.e. sequence position 2 to 7, they are grouped into one family (e.g. miR-29a-3p

and miR-29b-3p are members of the miR-29 family). Additionally, miRNAs can be localized as clusters, meaning that a group of miRNA hairpin precursors within a distance of 10 kb are processed, e.g. miR-17~92 cluster (Griffiths-Jones et al., 2008). The primary transcript of the cluster is a polycistron that is processed into seven different miRNAs (He et al., 2005).

1.1.3. Canonical pathway of miRNA biogenesis

Biogenesis of miRNAs

MicroRNAs are known to have regulatory functions and are involved in various biological processes like differentiation, apoptosis and proliferation. Genomic organization of primary transcripts as well as the sequence of mature miRNA are highly conserved between different species e.g. human and mouse. Over the past decade, the function and biogenesis of miRNA was elucidated in detail.

miRNAs are either encoded as individual genes (monocistronic), as clusters (polycistronic) or from introns (intronic). The primary miRNA (pri-miRNA) containing hairpins and 5' and 3' flanking sequences are derived from RNA polymerase II or III (Pol II / Pol III) activity (Kim, 2005; Treiber et al., 2019). In the nucleus, the pri-miRNA is further processed by the microprocessor, consisting of the RNase III enzyme Drosha and the DiGeorge critical region 8 (DGCR8) dimer (Fig. 1.1). The resulting preliminary-miRNA (pre-miRNA) consists of a single hairpin with a 5' phosphate, 3' hydroxyl group and a 2-nucleotide overhang. After transportation into the cytoplasm through the export receptor exportin 5 (Exp5), the pre-miRNA is processed by the RNase enzyme III Dicer. Dicer cleaves the pre-miRNA close to the terminal loop to generate a miRNA duplex, consisting of 20-25 nucleotides. Together with the trans-activation-responsive RNA-binding protein (TRBP), Dicer and Argonaute protein (AGO) assemble into the RNA-induced silencing complex (RISC). At this step, one strand of the miRNA is transferred to one member of the Argonaute protein family (Treiber et al., 2019). In mammalian cells, the AGO family consists of four members (AGO 1-4) with only AGO 2 possessing catalytic activity. In humans, the heat shock protein 90 (HSP90) dimer binds to Argonaute proteins, thus keeping it in an open conformation to allow miRNA loading (Meister, 2013). Only one strand is loaded into AGO proteins, while the other strand is discarded (passenger strand). Afterwards, loaded AGO proteins convert into a closed conformation and detach from Dicer to form the functional RISC (Meister, 2013; Treiber et al., 2019).

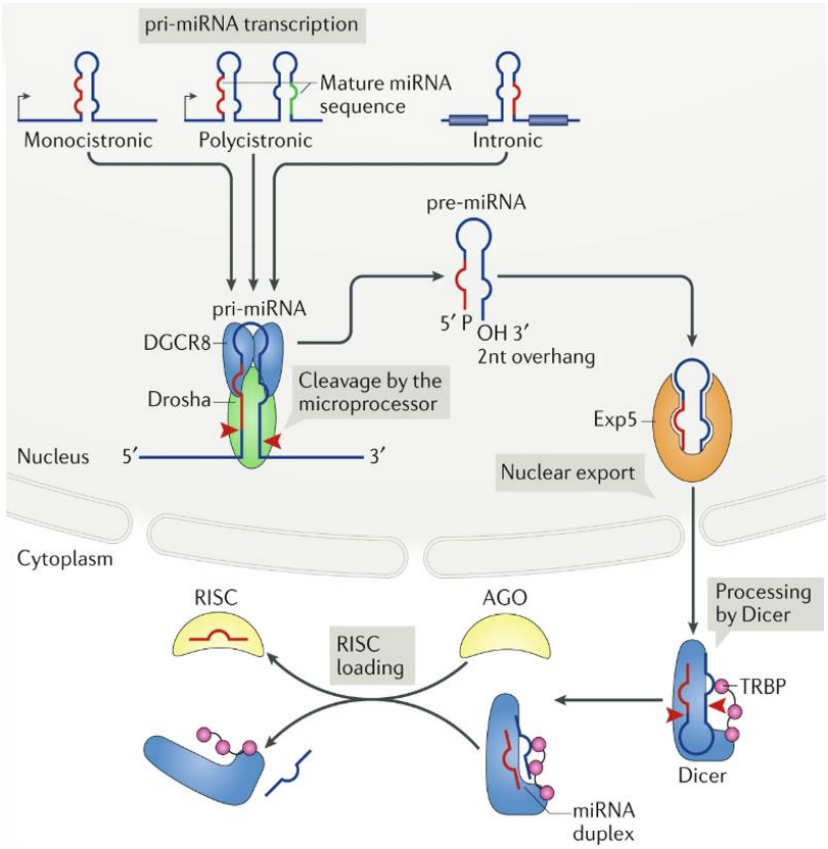

Figure 1.1 ***Canonical pathway of miRNA biogenesis****. Primary transcript is encoded as either monocistronic, polycistronic or intronic. After processing by Drosha, the pre-miRNA is exported from the nucleus into the cytoplasm via Exp5. The RNAse III Dicer further cleaves the miRNA resulting in a mature double-stranded miRNA. One of the strands is loaded into Argonaute proteins forming the functional RISC. Abbreviations: Pri-miRNA: primary microRNA, DGCR8: DiGeorge critical region 8, pre-miRNA: preliminary miRNA, P: Phosphate, OH: hydroxyl group, Exp5: Exportin 5, TRBP: trans-activation-responsive RNA-binding protein, AGO: Argonaute proteins, RISC: RNA-induced silencing complex (Treiber et al., 2019). Permission was kindly granted by Springer Nature.*

Posttranscriptional regulation of target mRNA

After miRNA loading into the AGO proteins, the functional RNA-induced silencing complex (RISC) is formed. The loaded miRNA strand serves as a guide for the RISC to the target mRNA. Thereby, the RISC mainly binds to the complementary sequence within the 3’ untranslated region (UTR). However, it can also bind to the 5’ UTR or the coding sequence (e.g. miR-619-5p (Atambayeva et al., 2017)), which is less frequent. If perfect complementarity between the miRNA and mRNA occurs, target mRNA is cleaved by AGO 2 leading to direct degradation. In most cases, there is a partial complementarity between miRNA and mRNA (Fig. 1.2). The nucleotides 2 to 7/8, known as the “seed region”, is essential for the miRNA-mRNA interaction resulting in translationally silencing and degradation (Meister, 2013). The degradation of mRNA is initiated by deadenylation and decapping. AGO proteins recruit trinucleotide repeat-containing gene 6 (TNRC6), a member of the GW protein family, which interact

with the cytoplasmic deadenylase complexes PAN2–PAN3 and CCR4–NOT. This complex shortens the poly(A)-tail of the mRNA, and indicates mRNA decapping through decapping protein 1-2 complex (DCP1/DCP2) together with additional cofactors at the 5’ end. Finally, the mRNA is degraded from the 5’-to-3’ by the exoribonuclease 1 (XRN1) (Jonas and Izaurralde, 2015; Treiber et al., 2019).

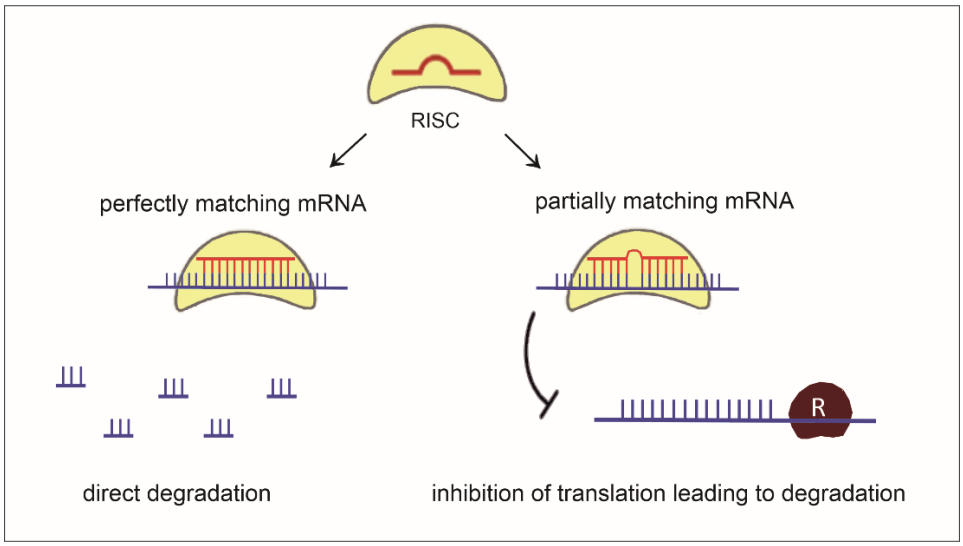

Figure 1.2 ***Posttranscriptional regulation of target mRNA.*** *After RISC forming, mRNA regulation depends on complementary between the miRNA and the target mRNA. Perfectly matching miRNA-mRNA leads to cleavage through AGO2 and direct degradation of the mRNA. Partially matching miRNA-mRNA leads to inhibition of translation followed by degradation. Abbreviations: R: Ribosome, RISC: RNA-induced silencing complex [modified from (Treiber et al., 2019)]. Permission was kindly granted by Springer Nature.*

1.1.4. Non-canonical pathway of miRNA biogenesis

Beside the classical canonical pathway of miRNA biogenesis, also two non-canonical pathways exist: a Drosha-independent or Dicer-independent pathway.

The Drosha-independent pathway is used by mirtrons, which are miRNA originated from introns (Fig. 1.1). After splicing, mirtrons function as pre-miRNA and are therefore are transported into the cytoplasm without Drosha cleavage. The hairpin structure of mirtrons possesses a unique characteristic which allows distinction of the canonical pre-miRNA (Treiber et al., 2019). Another miRNA class originates from 5’ end of Pol-II-transcribed genes, which harbor a 5’ 7-methylguanylate cap. The m^7G-cap eases the export by the cap-binding complex-exportin 1 (Exp1) and dicer cleavage. Due to the 5’ cap, miRNA loading into the RISC is limited to the 3p arm of the miRNA (Treiber et al., 2019).

For the Dicer-independent pathway, one specific miRNA with a unique structure was identified. The mir-451 is encoded with a short 17 nucleotide long stem region (Fig. 1.3 A). This short stem region

leads to a loss of Dicer recognition (Cheloufi et al., 2010). Dicer needs at least a 19 nucleotide long double strand for miRNA processing. For miRNA maturation, the mir-451 is directly loaded into AGO2 and cleaved (Fig. 1.3 B). AGO2 cuts the mir-451 at the opposite of nucleotide 10/11 and produces a 30 nt long fragment. Afterwards, the poly(A)-specific ribonuclease (PARN) trims the miRNA to the typical 22-26 nt mature miR-451 (Herrera-Carrillo and Berkhout, 2017).

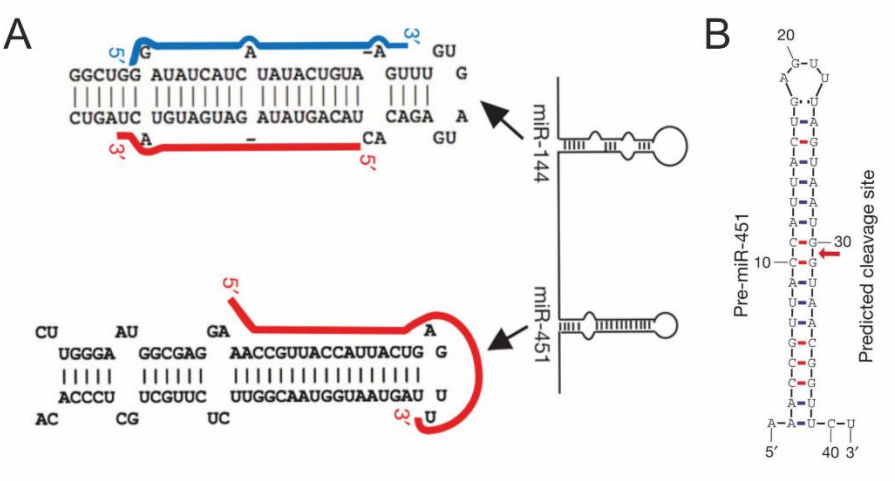

Figure 1.3 ***Dicer-independent miRNA precursor.*** *(A) mir-451 hairpin structure in comparison with the mir-144. mir-451 codes for one mature miRNA (miR-451-5p), while mir-144 codes for two mature miRNAs (blue: miR-144-5p, red= miR-144-3p); (B) cleavage site of AGO2 at the opposite of nucleotide 10/11 in the mir-451 [modified from (Cheloufi et al., 2010)]. Permission was kindly granted by Springer Nature.*

1.1.5. Regulation of miRNA biogenesis

miRNAs are important regulators of gene expression and therefore for various biological processes. However, miRNA expression can also be regulated in different ways. Since miRNAs are generated by RNA polymerase II or III from primary transcripts, their expression can be regulated by transcription factors. The two transcription factors p63 and p73 (tumor protein 63 and 73) directly regulate miR-200 family, which play an important role in epithelial-mesenchymal transition (EMT) (Knouf et al., 2012). The transcription factor *Lmx1b* (LIM homeobox transcription factor 1 beta) forms a regulatory circuit with the miR-135a-2 in the midbrain (see 1.2.3). Post-translational modifications like phosphorylation, ubiquitination or DNA methylation are another method to regulate miRNA expression. Phosphorylation of TRBP by MAPK ERK increases the stability of Dicer-TRBP complex and stimulates miRNA production (Paroo et al., 2009; Treiber et al., 2019). Under hypoxic conditions, phosphorylated AGO2 leads to impaired interaction between AGO2 and Dicer, and therefore to reduced miRNAs (Shen et al., 2013; Treiber et al., 2019). mTor activation increases the level of p53 inhibitor E3 ubiquitin-protein ligase MDM2. MDM2 serves as an E3 ubiquitin ligase of Drosha, which leads to proteasome-

mediated degradation and reduced miRNA processing (Ye et al., 2015; Treiber et al., 2019). Changes in methylation are often associated with cancer progression. DNA hypermethylation of the miR-132 promotor reduces its expression and leads to poor prognosis in colorectal cancer (Qin et al., 2015; Gulyaeva and Kushlinskiy, 2016). RNA-binding proteins serve as post-transcriptional modifiers, which can have a positive or negative effect on miRNA expression in all steps of biogenesis, e.g. RSIC loading. TDP43 disrupts the loading of miR-1 and miR-206 (King et al., 2014) while hnRNP D0 (AU-rich element RNA-binding protein 1) supports loading of let-7b into RISC (Yoon et al., 2015; Treiber et al., 2019). Another regulation of miRNAs is based on specific sequences within the miRNA itself, leading to instability and fast decay. In the miR-29b, uracils at the nucleotide position 9-11 lead to fast degradation, showing that U-rich sequences seem to be a trigger for degradation (Zhang et al., 2011). For the miR-382, the seven nucleotides of the 3'terminus are necessary for its instability (Bail et al., 2010).

1.2. The mammalian kidney

1.2.1. Anatomy, function and inner structure

The kidneys are two bean-shaped organs that are located subphrenic on both sides of the body. The main functions of the kidneys are the filtration of the blood, control of electrolyte and fluid level, regulation of blood pressure and secretion of hormones (Moorthy and Blichfeldt, 2009). The functional unit of the kidney is the nephron, which consists of the glomerulus and the tubule system (Fig. 1.4). Per day, 180 L of primary urine is filtered in the glomerulus and concentrated to 1.5 L urine per day in the tubule system (Tryggvason and Wartiovaara, 2005). Reabsorption of water and electrolytes also take place in the tubule system. The kidney can be divided into two major segments: the cortex and the medulla. In the adult kidney, glomeruli are only present in the cortex together with the convoluted proximal and distal tubule segments. In the medulla, the loop of Henle is found consisting of *tubulus proximalis pars recta*, the two *tubulus intermedius* segments and the *tubulus distalis pars recta.* The collecting tube is present in the cortex and the medulla (Fig. 1.4).

In mice, an average of 10.000-14.000 glomeruli with a size of about 80 µm are found (Liu et al., 2013). In humans, each kidney contains 1.2 – 1.4 million glomeruli with a size of about 0.2 mm (Wennemuth, 2017; Lüllmann-Rauch and Asan, 2019).

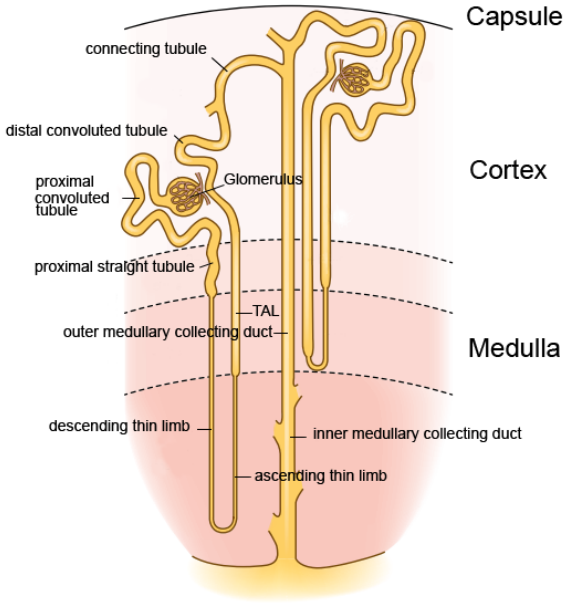

Figure 1.4 ***Schematic overview of the functional unit (nephron) of the mammalian kidney.*** *The nephron consists of the glomerulus and tubule system. Within the glomerulus, blood filtration to primary urine takes place, which is resorbed by the following tubule system. Abbreviations: TAL (thick ascending limb) [modified from (Mount, 2014)]. Permission was kindly granted by The Clinical Journal of the American Society of Nephrology.*

1.2.2. The glomerulus and the filtration barrier

The glomerulus consists of a unique bundle of capillaries, which lie within the Bowman's capsule and is derived from the afferent arteriole. Within the capillary tuft, the blood is filtered to primary urine, which flows into the Bowman's space, followed by the tubule system. The glomerular tuft is stabilized by the so-called mesangium, consisting of the mesangial matrix and cells. The mesangial matrix is produced by the cells and is composed of matrix proteins like collagens, fibronectin or laminin (Maezawa et al., 2013). The inside of Bowman's capsule is lined by the parietal epithelial cells (PECs), which changes at the vascular pole to the inner visceral layer formed by the podocytes (Fig. 1.5A). Together with the glomerular basement membrane and the fenestrated endothelium, the podocytes form the filtration barrier (Fig. 1.5 D) (Pollak et al., 2014). The filtration of the blood to primary urine by the glomerular filtration barrier allows the passage of molecules based on their size and charge. Normally only small and medium sized molecules (i.e. 1.6-1.8 nm) can pass the barrier, however damage to any of the three components leads to dysfunctional filtration and proteinuria, i.e. proteins larger than > 4.2 nm can pass through the barrier (Pollak et al., 2014).

Podocytes

These highly specialized epithelial cells cover the glomerular tuft and typically form different processes (Fig. 1.5 B-C). From the cell body, major processes are floating out, forming smaller foot processes. The major processes are connected by microtubules and intermediate filaments, while the foot processes are stabilized by an actin-based cytoskeleton (Ichimura et al., 2003). Between the interdigitating foot processes of two neighboring podocytes is a delicate protein structure, the slit diaphragm, consisting of various proteins which are important for podocyte signaling and normal glomerular filtration (e.g. nephrin, Neph1, podocin)(Huber and Benzing, 2005). The slit diaphragm is also linked to the actin cytoskeleton by linker proteins such as CD2AP.

The foot processes are attached to the underlying glomerular basement membrane (GBM), an extracellular matrix compartment which is secreted from the podocytes and the glomerular endothelial cells. Integrins are localized to the basal membrane and link to the actin cytoskeleton of the podocytes. Therefore, mutations of the adhesion proteins lead to a disruption of podocyte-GBM adhesion and further to proteinuria, podocyte effacement and glomerular basement membrane defects (Pozzi et al., 2008; Kang et al., 2010).

Due to the fact that podocytes are not able to replicate by mitosis, putative podocyte replacement mechanisms have been discussed in the last years. For example, parietal cells (PECs) are proposed to substitute podocytes by migrating to the glomerular tuft and differentiate into podocytes (Appel et al., 2009). Another possibility is the compensation of podocyte loss by hypertrophy of neighboring podocytes (Wiggins, 2007).

The glomerular basement membrane

The glomerular basement membrane (GBM) is the layer between the endothelium and the podocytes. It represents the extracellular matrix component, which is synthesized by the endothelial cells and the podocytes (Miner, 2012) . The GBM consists of three layers: the *lamina densa,* the *lamina rara interna* and the *lamina rara externa.* The four major macromolecules of the GBM are laminin, type IV collagen, nidogen and heparan sulfate proteoglycan (Miner, 2012). The extracellular matrix glycoprotein laminin is important for the structural assembly of the GBM and for cell-matrix interactions, while type IV collagen is critical for the maintenance of normal integrity and function (Rabelink et al., 2015). Collagen IV builds a cross-linked network to which the other components can bind (Pöschl et al., 2004). Nidogen 1 and 2 are major components of basement membranes, which can bind to laminin and collagen IV to form ternary complexes (Miosge et al., 2002). The major heparan sulfate proteoglycan of the GBM is

agrin, which has a highly negative charge due to sulfated glycosaminoglycan side chains. Therefore, agrin is important for the negative charge of the GBM (Miner, 2012).

The Endothelium

The glomerular endothelium is characterized by numerous fenestrations, allowing the flow of the blood. The fenestrations of the endothelium are observed as transcytoplasmic holes with a size of 60-80 nm. They contain no diaphragm or express plasmalemmal vesicle-associated protein 1 (PV-1), a type II transmembrane glycoprotein which is an integral part of the diaphragm (Satchell and Braet, 2009). Each fenestration is surrounded by a network of actin microfilaments, which might be important for shape determining of the endothelial cells (Vasmant et al., 1984). These cells have a gelatinous surface coating, the glycocalyx, which negatively charged and consists of proteoglycans and glycoproteins (e.g. syndecan, selectins or integrins.). They serve as backbone molecules for the connection to the endothelium. The glycocalyx also covers the fenestrations which prevents not only big molecules, but also negatively charged molecules (albumin, 3.6 nm) from passing. Therefore, it plays an important role for the permeability of the endothelium (Reitsma et al., 2007; Weinbaum et al., 2007; Haraldsson et al., 2008).

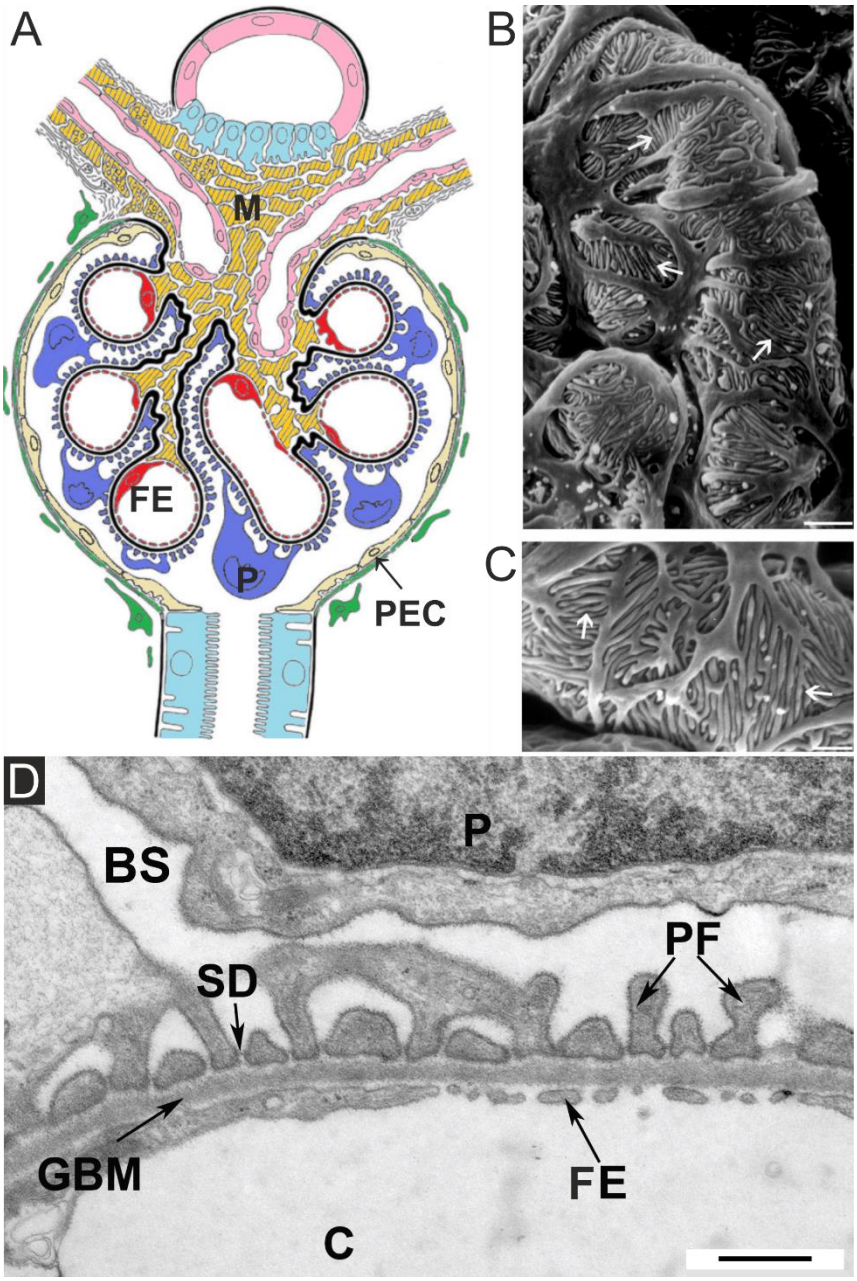

Figure 1.5 ***Structure of the glomerulus and the glomerular filtration barrier (GFB).*** *(A) Schematic figure of the glomerulus. The capillary tuft is stabilized by mesangial cells (M) and lined by the fenestrated endothelium (FE). Blood capillaries are covered by podocytes (P), which build the slit diaphragm in between their interdigitating processes. The primary urine is conducted from the Bowman space, bordered by parietal epithelial cells (PEC), to the tubular system [modified from (Hausmann et al., 2010)]. (B-C) Electron micrographs of interdigitating processes of neighboring podocytes covering the glomerular tuft (scanning EM). White arrows indicate interdigitating foot processes (Kriz and Lemley, 2015). (D) Electron micrograph of the filtration barrier consisting of interdigitating podocyte foot processes with slit diaphragms in between, the glomerular basement membrane and the fenestrated endothelium. Abbreviations: P: podocyte; BS: Bowman's space; PF: foot processes; SD: slit diaphragm; GBM: glomerular basement membrane; FE: fenestrated endothelium; C: capillary; scale bar: 500 nm (micrographs by H. Othmen, Institute for Molecular & Cellular Anatomy, University of Regensburg). Permission for Figure A, B and C was kindly granted by The Journal of the American Society of Nephrology.*

1.2.3. Proteins and their important roles in kidney function

Kidney function strongly depends on the interplay of the proteins expressed in the three components of the filtration barrier, e.g. proteins of the slit diaphragm or GBM. Mutations within the proteins often lead to severe kidney damage, characterized by podocyte foot process effacement, glomerular basement thickening and proteinuria.

CD2AP

CD2-associated protein was first identified 1998 by its role in T cell activation (Dustin et al., 1998). In the kidney, CD2AP is an essential component for the slit diaphragm and many mutations in CD2AP lead to renal diseases, e.g. congenital nephrotic syndrome or FSGS (Takano et al., 2019). CD2AP directly interacts with the actin cytoskeleton by connecting it to plasma membrane proteins (Lehtonen et al., 2002). Moreover, CD2AP interacts with podocin and nephrin, forming a signaling complex and sensor of mechanical stress (Huber et al., 2003). Together with nephrin, CD2AP interacts with PI3K (Phosphoinositide 3-OH kinase) and stimulates AKT (Protein kinase B) signaling, which controls many cellular processes like cell proliferation, survival and metabolism. Induced AKT activation by nephrin, podocin and CD2AP lead to inhibition of detachment-induced apoptosis (anoikis) in podocytes. Podocyte depletion and death is one characterization of glomerulosclerosis and a lack of CD2AP lead to apoptotic cell death of podocytes (Huber et al., 2003). Interestingly, Cd2ap deficient mice suffer from defects in podocyte foot processes and extracellular matrix deposition (Shih et al., 1999).

FYN

FYN is a family member of the Scr (SCR proto-oncogene, non-receptor tyrosine kinase) kinase family and has a size of 59 KDa (Uddin et al., 2020). FYN tyrosine phosphorylates the two slit diaphragm components Neph1 and nephrin. Phosphorylation of both proteins is necessary for the recruitment of specific proteins, e.g. NCK adapter protein or Grb2. Both interactions – nephrin with NCK and Neph1 with Grb2 – induces actin polymerization (Verma et al., 2006; Garg et al., 2007). In *Fyn* $^{-/-}$ mice the majority of foot processes are effaced (Verma et al., 2003), which is defined as the retraction of the foot processes forming a broad, uniform layer leading to loss of slit diaphragm (Verma et al., 2006). Increased nephrin and Neph1 phosphorylation through FYN might result in increased actin polymerization and therefore easing podocyte injury due to stiffer cytoskeleton (Burghardt et al., 2013).

LMX1B

The LIM homeobox transcription factor 1 beta (LMX1B) is associated with the kidney disease Nail-Patella Syndrome. The disease is characterized with abnormalities in nails, knees and open angle glaucoma (10 %). Approximately, 40 % of NPS patients also suffer nephropathy, which leads to end-stage renal failure in 10 % of patients (Witzgall, 2017). More than 180 mutations within LMX1B has been identified until now which comprises missense, nonsense and frameshift mutations (Harita et al., 2017). In NPS patient, the filtration barrier shows podocyte effacement and a thickened GBM with electron lucent zones (Heidet et al., 2003). LMX1B regulates a number of other podocyte proteins, e.g. CD2AP, podocin or ABRA. In *Lmx1b* knock-out mice, reduced levels of Cd2ap and podocin were detected. Binding of LMX1B to the promoter of these two proteins could be demonstrated in NIH 3T3 cells (Miner et al., 2002). Inducible podocyte specific *Lmx1b* knock-out mice showed dysregulation of actin cytoskeleton organization after 1 week of induction. Microarray studies revealed that several actin-associated proteins like Abra (Actin-binding Rho activating protein) or Arl4c (ADP-ribosylation factor-like 4C) were increased. Chromatin immunoprecipitation and gel shift assays showed that LMX1B binds to the FLAT elements (Far linked AT rich elements) in the promoter region of *ABRA* and *ARL4C* (Burghardt et al., 2013).

As a transcription factor, LMX1B regulates the expression of specific genes which can lead to silencing or enhancing. Therefore, miRNAs might also be regulated by LMX1B. In 2013, Anderegg et al. demonstrated a regulatory negative feedback loop between *Lmx1b* and the miR-135a-2 in the midbrain. On one hand, *Lmx1b* drives the expression of miR-135a-2, while on the other hand the miRNA negatively regulates *Lmx1b* levels. Together they modulate the *Wnt1*/Wnt signaling pathway, which determines the size of midbrain and the dopaminergic progenitor pool (Anderegg et al., 2013).

Nephrin and Neph1

One main component of the slit diaphragm is nephrin (NPHS1), a transmembrane protein of the immunoglobulin family (Welsh and Saleem, 2011). Mutations of nephrin lead to congenital nephrotic syndrome in children and reduced levels are often observed in diabetic nephropathy (Li and He, 2015). Nephrin is known to interact with many other slit diaphragm and podocyte proteins. Together with Neph1, it forms a protein complex which seems to function as a transmembrane receptor. Absence of either proteins lead to proteinuria and failed foot process formation (Donoviel et al., 2001; Garg et al., 2007).

Nephronectin

Nephronectin (NPNT) a basal lamina protein, is expressed in podocytes and localized to the GBM, where it interacts with α8β1-integrin. The α8β1-integrin is produced in mesangial cells, and therefore this receptor-ligand interaction connects the GBM to the mesangium through specialized adhesion structures. In *NPHS*2:Cre-*Npnt* knockout mouse model, the GBM-mesangial adhesions are disrupted and α8β1-integrin is mislocalized. Increased mesangial cell number and matrix is observed in affected glomeruli due to *Npnt* loss leading to decreased stability of capillary tufts. Thus, it shows the importance of the GBM-mesangial interaction for the glomerular structure (Zimmerman et al., 2018).

Podocin

Podocin, transcribed from *NPHS2* gene, is localized to the insertion site of the slit diaphragm where it regulates nephrin recruitment and signaling (Huber et al., 2001). Moreover, podocin regulates the ion channel TRPC6 (Transient receptor potential cation channel, subfamily C, member 6), which is a sensor of mechanically and osmotically induced membrane stretch. This allows the podocytes to remodel its cytoskeleton and to react to mechanical stimuli (Huber et al., 2007).

SPARC

Another important extracellular matrix protein is SPARC (Secreted protein acidic and rich in cysteine), which is known to play a role in mediating podocyte detachment. Under normal conditions, SPARC expression level is low in podocytes, however it increases after podocyte injury. In a passive nephrotoxic nephritis model using SPARC $^{+/+}$ and SPARC $^{-/-}$ mice, increased SPARC levels were observed leading to accelerating glomerulosclerosis in the SPARC $^{+/+}$ mice compared to the null-mutant mice. Also, podocyte number was decreased in SPARC $^{+/+}$ mice indicating podocyte detachment (Sussman et al., 2009).

VEGFA

The most important protein for the endothelium is VEGFA (Vascular epithelial growth factor A), which is a major regulator of angiogenesis and vascular permeability (Eremina et al., 2007). It is produced in large amounts by the podocytes during fetal development and also in the mature glomerulus, however in lower doses. One of the main functions of VEGFA is the induction of fenestration in the glomerular endothelium, which is supported by manipulation of VEGFA doses in different studies (Eremina et al., 2007; Satchell and Braet, 2009). Downregulation of VEGFA leads to missing fenestration (Eremina et

al., 2003) as well as to GBM thickening and proliferation of mesangial cells (Zhang et al., 2010). In contrast, overexpression of VEGFA results in collapsing glomerulopathy and reduced number of endothelial cells. Moreover, affected glomeruli displayed lack of well- formed slit diaphragms (Eremina et al., 2003; Satchell and Braet, 2009).

1.3. Role of miRNAs for kidney structure and function

1.3.1. Podocyte specific loss of miRNA

The decisive evidence of the important role of miRNA for kidney function was demonstrated in 2008 by three studies (Harvey et al., 2008; Ho et al., 2008; Shi et al., 2008). Mice harboring *loxP* sites flanking exon 23 of the miRNA processing enzyme Dicer, which contains the second part of RNAse III domain (Harfe et al., 2005), are crossed with mice expressing Cre recombinase under control of the *NPSH2* promoter (Moeller et al., 2003). Cre recombinase recognizes and cleaves at the *loxP* sites leading to a constitutive podocyte-specific deletion of exon 23 and therefore to altered miRNA biogenesis. *Dicer* knockout mice develop proteinuria three to five weeks after birth ending in end-stage renal failure and death. Glomerular injury occurred in affected mice consisting of glomerular tuft collapse, hypertrophy with crescent formation, wrinkling of the GBM and podocyte foot processes effacement. Moreover, expression of some podocyte specific proteins was altered in knockout podocytes. Although, WT1 (Harvey et al., 2008; Ho et al., 2008) and α-actin (Harvey et al., 2008) are normally expressed in knockout mice, whereas synaptopodin (Harvey et al., 2008; Shi et al., 2008), podocin (Ho et al., 2008; Shi et al., 2008), nephrin (Ho et al., 2008) and podocalyxin (Harvey et al., 2008) are reduced. Microarray expression profiling revealed 68 mRNA to be upregulated in knockout podocytes, of which 15 mRNA contain possible binding sites of the miR-30 family (Shi et al., 2008). This finding indicates a role of the miR-30 family in podocytes, which was also suggested by Harvey et al. (2008). *In situ* hybridization against mature miRNAs showed that miR-30a is absent in podocytes of knockout glomeruli due to a podocyte-specific loss of Dicer when compared to wildtype glomeruli, while the epithelial and mesangial expressed miR-126 and miR-145 were expressed normally (Harvey et al., 2008). In addition, other miRNAs were also identified to be expressed in glomeruli like the miR-23b, miR-24 or miR-26a (Ho et al., 2008),which might also be involved in podocyte function.

In 2011, Zhdanova et al. used a constitutive as well as an inducible podocyte-specific *Drosha* knockout mouse line to investigate if described *Dicer* knockout phenotype is due to miRNA loss and not due to an additional alternative function of Dicer. Mice with Cre recombinase under the control of NPHS2 promoter were crossed with mice harboring a *loxP* site flanking exon 9 of Drosha, the first miRNA

processing enzyme (Chong et al., 2008). Two to three weeks after birth, knockout mice develop proteinuria followed by renal failure and death after four to eight weeks. Affected mice suffered first from podocyte effacement and mild wrinkling of GBM. With the progression, glomeruli showed glomerular tuft collapse, pseudo-crescent formation and segmental or global sclerosis. Moreover, the glomerular injury is accompanied with loss of podocyte-specific markers like synaptopodin, podocin, nephrin and WT1. This phenotype resembles the *Dicer* knockout phenotype, except of WT1 expression, which is normal in *Dicer* knockout mice but decreased in *Drosha* knockout mice. To investigate if miRNAs are not only important for development but also for podocyte maintenance, an inducible TetOn (tetracycline-controlled transcriptional activation) *Drosha* knockout was used in the same study. After two weeks of doxycycline administration adult mice showed the first signs of proteinuria. In electron microscopy, the phenotype of the inducible knockout mice resemble the phenotype of the constitutive *Drosha* knockout (Zhdanova et al., 2011). Thus, the study of Zhdanova et al. not only demonstrated that the observed phenotype is due to miRNA loss but also the important role of miRNA for podocyte development and maintenance.

1.3.2. miRNA role in kidney health and disease

miRNAs are involved in the regulation of various biological processes, like cell proliferation, migration and differentiation. Therefore, dysregulation of miRNAs is associated with the development of different diseases. Downregulation of miR-30 family leads to a dysregulation of calcium/calcineurin signaling, which results in podocyte cytoskeleton damage (Wu et al., 2015). Podocyte damage is a key feature, especially in glomerular diseases like FSGS (Trionfini and Benigni, 2017). Gebeshuber et al. (2013) demonstrated that increased miR-193a induces FSGS in mice leading to strong podocyte foot processes effacement. miR-193a inhibits the expression of Wilm's tumor protein 1 (WT1), which is essential for the development and maintenance of podocytes. Diabetic nephropathy (DN) is characterized with podocyte loss, matrix accumulation and basement membrane thickening. miR-29c controls podocyte apoptosis and is increased *db/db* mice. By targeting Sprouty homolog 1, increased miR-29c activates Rho kinase resulting in fibronectin assembly and apoptosis (Long et al., 2011). In patients with lupus nephritis (LN) the downregulation of miR-130b is negatively correlates with abnormal activation of IFN pathway by targeting IFN regulatory factor 1 (IRF-1) (Han et al., 2016).

2. State of the art and aims of the present work

Over the last decades, more than 38.000 miRNAs were identified in several species (Griffiths-Jones, 2004; Griffiths-Jones et al., 2006; Griffiths-Jones et al., 2008; Kozomara and Griffiths-Jones, 2011, 2014; Kozomara et al., 2019) and their role in health and disease has been analyzed in many studies. However, their potential target mRNAs are still not established completely. For a better understanding of the role of miRNAs for kidney structure and filtration function, it is necessary to identify target genes of specific miRNAs.

Therefore, main focus of the present work was the identification of podocyte-specific miRNA- mRNA interactions that play an important role for podocyte structure and function. Therefore, different approaches were used:

1. **Identification of podocyte-specific miRNA-mRNA interactions and effect on podocyte structure and function**

In previous studies potential miRNA regulated target genes were identified (Baumgarten et al., unpublished). In context of this work, nine of those putative interactions between miRNAs and their target mRNAs were analyzed using a luciferase assay: *Arrdc3*-miR-19b-3p; *Fosb*-miR-347b-5p/miR-19b-3p; *Npnt*-miR-101b-3p; *Per1*-miR-29a-3p; *Serinc3*-miR-340-5p; *Sparc*-miR-29a-3p; *Stt3a*-miR-340-5p; *VegfA*-miR-503-5p; *Zfp36*-miR-29a-3p.

In addition, generated mir-30a-5p and mir-146b-5p knockout cell lines (Baumgarten et al., unpublished) were used to analyze the effect of miRNA loss in podocytes for differentiation.

2. **miRNAs as regulators of transcription factor *Lmx1b/LMX1B*?**

Transcription factors like Lmx1b are known to regulate miRNA expression. However, they can also be a potential target of miRNA regulation. Using podocytes from Lmx1b knockout and wildtype mice, *deep sequencing* analysis identified specific miRNA which were subsequently used for *in silico* predictions (miRWalk2) by Baumgarten (2017) and Zaparty (unpublished). To identify the interactions between *Lmx1b/LMX1B* and the predicted miRNAs, luciferase assays were used.

3. Investigation of effect of miRNA loss in murine podocytes for target mRNAs

Using an inducible-podocyte specific *Dicer* knockout mouse line (Baumgarten et al., unpublished), the effect of miRNA loss in the kidney was analyzed. Beside the analysis of the phenotype of knockout mice by different methods like SDS-PAGE, H&E staining and ultrastructural visualization, the effect on identified target mRNA expression was investigated. For this, freshly isolated podocytes from *Dicer* knockout mice were used to analyze the mRNA expression level by qPCR analysis.

3. Materials and methods

3.1. Materials

3.1.1. Equipment and instruments

Equipment	source
Absorbance microplate reader "Sunrise"	TECAN
Agarose gel electrophoresis chamber “Horizon 58”	Gibco
Agarose gel electrophoresis chamber “OwlTM EasyCastTM B2”	Thermo Fisher
Autoclave "2540ML"	Tuttnauer
Autoclave "5050 ELV"	Tuttnauer
Bunsen burner	Usbeck
Cell separation magnet “IMagnetTM”	BD Bioscience
Cell sorter “FACSAria II”	BD Bioscience
Centrifuge " hitachi himac CT15RE"	VWR
Centrifuge "Multifuge 3L-R"	Heraeus
Centrifuge "Multifuge 3SR+"	Heraeus
Centrifuge "Pico"	Heraeus
Centrifuge "Pico 17"	Heraeus
Centrifuge “Sigma-Aldrich 3K20”, rotor 12158	Braun
Centrifuge "Z 300"	Hermle
CO_2 incubator “CB210”	Binder
Cold Light Source "KL-1500-T"	Schott
Compressor	Jun-Air
Cooling plate	Medax
Drying closet "Venti-line"	VWR
Electrophoresis power supply "PS608"	Life technologies
Freezer -20°C	Privileg
Freezer -80°C	VWR
Gel Documentation System “GelDoc XR+”	BioRad
Gel electrophoresis cell “Mini Protean Tetra Cell”	BioRad
Glassware (beakers, bottles, flasks)	Schott, VWR
Heating plate with a magnetic stirrer " MR 3001"	Heidolph
Hybridization oven "HB-1000"	UVP
Hybridization oven "OV3"	Biometra
Ice machine	Ziegra
Incubator "Kelvitron t"	Heraeus
Incubator "Multitron standard"	Infors
Incubator	Memmert
Laboratory pH Meter "CG 842"	Schott
Luminometer "Centro XS^3 LB 960"	Berthold
Luminometer "Mithras LB480"	Berthold
Laminar flow bench “HERA safe"	Heraeus
Laminar flow bench “Lamin Air HA 2448 GS"	Heraeus

Microtom "RM2255"	Leica
Metal Block Thermostats "LS1"	VLM
Microwave “8016 G"	Privileg
Multi-dispenser “HandyStep® electronic”	Brand
Neubauer counting chamber (depth 0.1 mm)	Marienfeld
Paraffin embedding module “EG1150 H”	Leica
Pipettor “IPS Pipetboy acu”	Integra Bioscience
Pipettes	Brand, Gilson
qPCR Cycler "LightCycler 480 II"	Roche
Refrigerators	SEQ/Privileg
Rocking platform shaker "Duomax 1030"	Heidolph
Spectrophotometer "NanoDrop 2000"	Thermo Scientific
Tissue float bath "1052"	GFL
Tissue processor “TP-1020”	Leica
Thermal cycler "MyCyclerTM"	Biorad
Thermal Cycler "T100"	Biorad
Thermo Shaker "TS-100"	Hartenstein
Tweezers	DUMONT
Ultrapure water unit "Seralpur PRO 90 CN"	Seral
UV/VIS spectrophotometer "U-2000"	Hitachi
Vacuum gas pump	VWR
Vortexer "Vortex-Genie 2"	Scientific Ind.
Weighing scale "Kern 770"	KERN & Sohn
Weighing scale "LP-4202"	VWR
Weighing scale "SE 622"	VWR

3.1.2. Microscopes

Microscopes	Source	Camera	Source
Microscope "CME"	Leica		
Microscope "Eclipse TS100"	Nikon		
Microscope "DM750"	Leica	ICC50 HD	Leica
Transmission Electron Microscope EM "902"	Zeiss		
Inverted microscope "Axiovert 200M"	Zeiss	pco.edge	Visitron Systems GmbH
"Axiovert 200"	Zeiss	pco.panda	sCMOS technology
LSM 710_NLO	Zeiss	Axiocam MR R3	Zeiss

3.1.3. Software and tools

Software	Version	Purpose	Company
CorelDraw	2019	Data and image processing	
FileMaker Pro	6	Database	FileMaker, Inc.
ImageLab	6.0.0	Gel documentation	BioRad
ImageJ		Image processing	National Institutes of Health

LightCycler 480	1.5.0	RNA quantification	Roche
Microsoft Excel	Office 2019	Data processing, diagrams	Mircosoft
Microsoft Power Point	Office 2019		Mircosoft
Microsoft Word	Office 2019		Mircosoft
Magellan™	7.2	Photometric measurement	TECAN
NanoDrop 2000/2000c	1.6	Photometric measurement	Thermo Scientific
OriginPro		Data processing, diagrams	OriginLab
SnapGeneViewer	4.2.6	Gene/plasmid handling	GSL Biotech, LL
ZEN 2.3 SP1 (black)	14.0.0.0	Image recording	Zeiss
LAS V4	V4.12	Image recording	Leica
pco.camware 4		Image recording	sCMOS technology
VisiView		Image recording	Visitron Systems GmbH

Internet databases and tools	internet address
BLAST	www.ncbi.nlm.nih.gov/blast
ensembl	www.ensembl.org
mirBase	www.mirbase.org
MirWalk2	http://zmf.umm.uni-heidelberg.de/apps/zmf/mirwalk2/
miR2Disease	http://mir2disease.org/
Primer3	www.primer3.ut.ee/
PubMed NCBI	www.ncbi.nlm.nih.gov/pubmed
UCSC genome browser	https://genome.ucsc.edu/
Mouse podocytes mRNA expression Database	https://hpcwebapps.cit.nih.gov/ESBL/Database/Podocyte_Transcriptome/index.htm

3.1.4. Consumables

Consumables	Source
96-well plate white	Greiner bio-one
96-well light cycler plate	Th. Geyer GmbH
96-well light cycler plate sealing tape	Sarstedt
Autoclave tape	Brand
Bottle top filter for sterile filtration (500 ml,0.2 µM)	Sarstedt
Cell culture dishes (P3, P6, P10)	Sarstedt
Cell culture flasks (25 cm^2, 75 cm^2)	Sarstedt
Cell culture plates (12 well, 24 well)	Sarstedt
Cell scraper 25 cm	Sarstedt
Cell strainer 30 µm	Miltenyi Biotec
Cell Stainer 100 µm	BD Falcon
CycroPure tubes 1.8 mL	Sarstedt
Dispenser tips (1.25, 2.5, 5, 12.5 mL)	VWR
Filters for sterile filtration (20µm, 45 µm)	Sarstedt
Glass pasteur pipettes (150mm)	VWR
Glass pasteur pipettes (250mm)	Kimble

Glass coverslips, 12mm	R. Langenbrinck
GenePulser electroporation cuvettes	BioRad
Gloves, nitirile	Roth
Hypodermic needles	B.Braun
MF-Milipore membrane filter 0.025 µm pore size	Millipore
Micro tubes PCR-PT (2 mL)	Sarstedt
Microscope cover glass (24x60 mm)	Roth
Microscope slides	Roth
Microscope slides, SuperFrost® Plus	Thermo Fisher
Microtome blade	Leica
Parafilm	Pechiney Plastic
PCR tubes 0.2 mL	Sarstedt
Petri dish (92x16 mm)	Sarstedt
Pipette tips	Sarstedt
Pipette tips with filter	Sarstedt
Polystrene cuvettes	Sarstedt
Reaction tubes (1.5 mL, 2 mL)	Sarstedt
Roundbottom tube with cell strainer, 35 µM	BD Falcon
Scalpels	B.Braun
Serological pipettes (1, 2, 5, 10, 25 mL)	Sarstedt
Syringes	Henke Sass Wolf
Task wipes	Kimteck
Tubes (15 mL, 50 mL)	Sarstedt
Weighing paper MN 226, 90x115 mm	Macherey-Nagel

3.1.5. Kits, enzymes, antibodies and markers

Kits for RNA work

Kit name	Cat No. /ID	Source
DNA-free™ Kit DNase Treatment and Removal Reagents	AM1906	life technologie
iScript DNA synthese Kit	1708896	BioRad
miRVana miRNA isolation kit, with/without phenol	AM1560/1561	life technologie
RNase free DNase set	79254	Qiagen
RNeasy Mini Kit	74104	Qiagen
RNeasy Micro Kit	74004	Qiagen
miRNeasy Micro Kit	217084	Qiagen

Kits for DNA work

Kit name	Cat No. /ID	Source
E.Z.N.A. Gel Extraction Kit	D2500-01	VWR
GeneJET Plasmid Miniprep Kit	K0502	Thermo Scientific
Plasmid Plus Midi Kit	12945	Qiagen
QIAquick Gel Extraction Kit	28704	Qiagen
QIAquick Nucleotide Removal Kit	28304	Qiagen

Wizard Plus Midipreps DNA Purification System	A7640	Promega

Enzymes

modifying enzymes	Cat No. /ID	Source
Alkaline phosphatase	M0290 S	NEB
Collagenase Type II	LS004176	Worthington-Biochemical
DNase I	A3778,0050	AppliChem
E.coli poly-A polymerase (EPAP)	M0276S	NEB
Pfu DNA Polymerase	M7741	Promega
Phusion High-Fidelity DNA Polymerase	M0530S	NEB
Pronase E	1.07433.0001	Merck
Proteinase K	7528.4	Roth
Taq DNA Polymerase	M0267 S	NEB
T4 DNA Ligase	M0202 S	NEB
T4 PNK	M0201 S	NEB

restriction enzymes	Cat No. /ID	Source
*Bgl*II	R0144L	NEB
*Hind*III-HF	R3104L	NEB
*Sac*I –HF	R3156L	NEB
*Spe*I-HF	R3133L	NEB

Markers	Cat No. /ID	Source
1 kb Plus DNA Ladder	N3200S	NEB
PageRuler Prestained Protein Ladder	26616	Thermo Scientific
Ultra Low Range DNA Ladder II, peqGOLD	732-3300	VWR
TriDye Ultra Low Range DNA Ladder	N0558S	NEB

Antibodies and staining solutions

Primary antibodies

Name	dilution	Species	Cat No. /ID	source
α-α-actinin 4	1:200	Rabbit	0042-05	Immuno Globe

Secondary antibodies

Name	dilution	Species	Cat No./ID	source
Alexa Fluor ® 568 donkey	1:600	Donkey	Ab175470	Invitrogen polyclonal

Staining solutions

Name	Cat No. /ID	source
HSC CellMask Red Staining	H32712	Thermo Scientific
miRCURY LNA™ microRNA Mimics	479997	Exiqon

3.1.6. Chemicals and reagents

Chemicals	**Source**
ß-mercaptoethanol	Merck
2-dodecenyl succinic anhydride	Sigma
Acetic acid, glacial	Sigma
Agarose (NEEO quality, ultra quality)	Roth
Ampicillin sodium salt	Roth
APS (ammoniumpersulfate)	Fluka
ATP (adenosine triphosphate, 100 mM)	Thermo Scientific
ATP powder for luciferase assay substrate	PJK
Acrylamide 30 %/ Bisacrylamide, 0.8 % solution	Serva
Bromophenol blue	Pharmacia Biotech
BSA (Bovine serum albumin)	Roth
Chloroform	Merck
Coelenterazine, 1000x stock	PJK
Coenzyme A for luciferase assay	PJK
Coomassie Brillant Blue R-250	Serva
Creatinine	Merck
D-Luciferin	PJK
DABCO (1,4-Diazabicyclo[2.2.2]octan)	Roth
DEPC (Diethylpyrocarbonate)	Roth
DePeX	Serva
DMP30	Roth
DMEM (Dulbecco's modified Eagle's medium) high glucose	Sigma
DMSO (Dimethylsulfoxidase)	Sigma
dNTPs (Deoxynucleotide triposphate)	Thermo Scientific
Doxycyline hyclate	AppliChem
DTT (1,4-Dithio-DL-threitol)	Roth
Dynabeads™ M-450, tosylactivated	invitrogen by life technologies
Ethanol	Sigma
Eosin	Agar scientific
Ethidium bromide	Sigma
FCS (fetal calf serum)	PAN Biotech
Ficoll™ 400	Serva
Glucose	Merck
Glutaraldehyde, 25 %	Serva
Glycidyl ethers	Sigma
Gylcerol	Roth
Glycogen	PeqLab

Hematoxylin, Gill No. 3	Sigma
Hemalum solution acc. to Mayer	Roth
HEPES (4-(2-hydroxyethyl)-1-piperazineethanesulfonic acid)	Roth
Horse serum	PAA
Hydrochloric acid 1M	VWR
Hydrochloric acid 37 %	VWR
Isopropanol	Merck
ITS-G (Insulin-Transferrin-Selenium, 100x)	Gibco
Kanamycin sulfate	AppliChem
Lead citrate, 3 % (Ultrostain 2)	Leica
Lipofectamine, 3000	invitrogen by life technologies
Magnesium sulfate	Merck
Magnesium chloride	Merck
Methanol	Roth
Methyl nadic anhydride	Sigma
Narcoren	Merial
P3000 reagent	invitrogen by life technologies
Paraplast Plus ®	Leica
Passive lysis buffer, 5x	Promega
Perodic acid	Merck
PFA (paraformaldehyde)	Merck
Picric acid	Sigma
Potassium acetate	Merck
Potassium chloride	Merck
Potassium dihydrogen phosphate	Merck
Potassium dihydrogen phosphate	Merck
Potassium disulfate	Rieder-deHaen
Propidium iodide	AppliChem
qPCR mastermix: Sensifast Sybr No-Rox	Bioline
qPCR mastermix: Takyon No-Rox Sbyr	Eurogentec
RNase away	Molecular BioProducts
RPMI medium 1640 with L-Glutamine	Sigma
Roti-Quant	Roth
SDS (Sodium dodecylsulfate)	Serva
Sodium acetate	Roth
Sodium azide	Merck
Sodium cacodylate trihydrate	Fluka
Sodium chloride	Roth
Sodium citrate dihydrate	Merck
Sodium EDTA	Roth
Sodium hydroxide solution, 1M	Roth
Sodiumhydroxide pellets	Merck
Sodium phosphate dibasic heptahydrate	Merck
Sucrose	VWR
Schiff's reagent	Roth
TEMED (Tetramethylethylenediamine)	Roth
Tissue-TEK	Sakura Finetek

Tricine	Roth
Tris base	Roth
Triton-X-100	Roth
Trypsin-EDTA-solution	Sigma
Trichloroacetic acid	Riedel-deHaen
Trifast	PeqLab
TurboFECT	Thermo Scientific
Xylene cyanol FF	Serva
Xylol	Merck

3.1.7. Plasmids and cell lines

Plasmid	Resistance	Modification	Source
pMIR-Report-TK (modified)	Ampicillin	CMV promotor changed to TK; Renilla luciferase expressed on same plasmid	Ambion, modified (AG Prof. Meister)
pSuper (modified)	Kanamycin	Ampicillin resistance changed to kanamycin	oligoengine, modified (AG Prof. Meister)
CMV-d2eGFP-empty	Ampicillin		Addgene, Ebert et al. (2007)

Cell lines and bacterial strains		Source
HEK293T	human embryonic kidney cells	ATCC
hPCL	human podocyte cell line, AB 8/13	Saleem et al. (2002)
DH5α	*E.coli* strain	DSMZ
TOP10	*E.coli* strain	life technologies

3.1.8. Media, solutions and buffers

Commercial buffer and solutions

Buffer and solutions	Cat No. /ID	Source
ThermoPol ® reaction Buffer	B9004S	NEB
T4 DNA Ligase Reaction Buffer	B0202S	NEB
CutSmart ® buffer	B7204S	NEB
NEBuffer ™ 3.1	B7203S	NEB
Phusion ® HF buffer	B0518S	NEB
Pfu 10x reaction Buffer	M776A	Promega
HBSS modified, premixed powder	H1387-10L	Sigma

Media and solutions for bacterial work

LB-Medium	
premixed powder	10 g in 500 mL H_2O

LB-Agar plates	
premixed powder	8.75 g in 250 mL H_2O

Ampicillin stock	
Ampicillin	1 g in 10 mL H_2O

Kanamycin stock	
Kanamycin	0.5 g in 10 mL H_2O

Solutions and buffers for mouse work and genotyping

Induction solution	
Doxycycline	20 mg/mL
Sucrose	50 mg/mL
	in H_2O

Tail buffer	
Tris buffer pH 8.0	100 mM
EDTA	5 mM
SDS	0.2 %
NaCl	200 mM
	ad H_2O to 250 mL

50x TAE buffer	
Tris base (M=121.14g)	2 M
EDTA	100 mM
in H_2O, adjusted to pH 8.0 with acetic acid	

5x Loading dye	
Ficoll type 400	1.5 g/L
Na_2EDTA pH 8.0	50 nM
SDS	5 g/L
Bromophenol blue/xylene cyanol FF	1.25 g/L
	ad H_2O

Solutions and buffers for SDS-PAGE

4x Lower Tris buffer	
Tris base pH 8.8	1.5 M
SDS	0.4 %
	in H_2O

4x Upper Tris buffer	
Tris base pH 6.8	0.5 M
SDS	0.4 %
	in H_2O

10 % acrylamide separating gel solution	
30 % Acrylamide/0.8 % Bisacrylamide	6 mL
4x Lower Tris buffer	4.5 mL
H_2O	7.5 mL
10 % APS	50 µL
TEMED	10 µL

Stacking gel solution	
30 % Acrylamide/0.8 % Bisacrylamide	1.3 mL
4x Upper Tris buffer	2.5 mL
H_2O	6.1 mL
10 % APS	50 µL
TEMED	10 µL

1x SDS gel running buffer	
Glycine	0.19 M
Tris-Cl	25 mM
SDS	3.5 mM
	in H_2O

5x Laemmli sample buffer	
Tris-Cl pH 6.8	60 mM
SDS	2 %
Glycerol	10 %
ß-mercaptoethanol	5 %
Bromophenol blue	0.01 %
	in H_2O

Coomassie blue staining solution	
Coomassie Brilliant Blue R-250	3 mM
Methanol	45 %
Acetic acid	10 %
	in H_2O

Coomassie blue destaining solution	
Methanol	45 %
Acetic acid	10 %
	in H_2O

Solutions and buffers for epon embedding

Epon	
Glycidyl ethers	46 g
2-dodecenyl succinic anhydride	28.5 g
Methyl nadic anhydride	25.1 g
DMP30	1.5 g

DMP30 was added to the solution after incubation for 15 min at 50°C and 5 min stirring on a magnetic mixer. Afterwards the solution was stirred for another 5 min.

Solutions and buffers for tissue and cell fixation

4 % Paraformaldehyde	
PFA	20 g
H_2O	400 mL
NaOH 1M	15 drops
10x PBS	50 mL
	ad to 500 mL H_2O
adjusted to pH 7.4 with 1M hydrochloric acid	

2 % Glutaraldehyde	
GA	25 % in 0.1 M Caco buffer

Caco buffer	
Sodium cacodylate trihydrate	0.1 M

Solutions and buffers for tissue and cell staining

Eosin solution	
Eosin	0.1 %
Acetic acid	2-3 drops/100 mL in H_2O

Periodic acid	
Perodic acid	1 % in H_2O
Sulfite water	
Potassium disulfate	10 %
HCL	1M in H_2O

Solutions and buffers for podocyte isolation and FACS

Hank's buffered salt solution (HBSS) was prepared by solving 9.7 g of premixed salt solution powder in 1 L of H_2O followed by the adjustment to pH = 7.4. The buffer was filter-sterilized and stored at 4°C.

HBSS buffer	
$CaCl_2$	1.26 mM
KCl	5.37 mM
KH_2PO_4	0.44 mM
NaCl	0.138 M
Na_2HPO_4	0.33 mM
$MgSO_4$	0.81 mM
D-Glucose	5.55 mM

Beads solution	
Magnetic beads, tosylactivated	50 µL
HBSS buffer, pH 7.4	in 10 mL

Beads with enzyme solution	
Dynabeads™ M-450, tosylactivated	10 µL
Digestion solution	in 2 mL

Beads were washed with HBSS for 1-3 times before adding to working solution (HBSS buffer or digestion solution).

Digestion solution	
Pronase E	1 mg/mL
Collagenase Type II	1 mg/mL
DNase I	50 U/mL
	in HBSS buffer, pH 7.4

FACS buffer	
FCS	0.2 %
	in 1x PBS, pH 7.4

Solutions and buffers for DNA preparation from bacteria

P1-buffer	
Tris-Cl, pH 8.0	20 mM
EDTA, pH 8.0	10 mM
RNase A	100 µg/mL
	in H_2O

P2-buffer	
NaOH	0.2 M
SDS	1 %
	in H_2O

P3-buffer	
Potassium acetate, pH 5.5	3 M
	in H_2O

Solutions and buffers for Luciferase Assay

Renilla luciferase substrate	
Na_2EDTA	2.2 mM
K_xPO_4 pH 5.1	0.22 M
BSA	0.44 mg/mL
NaCl	1.1 M
NaN_3	1.3 mM

The buffer was adjusted to pH 5.0 and filter-sterilized. Aliquots of 10 mL were prepared and stored at -20°C. Prior to luciferase assay, 1 µL /mL of 1000x coelenterazine stock solution was added to the buffer.

1000x Coelenterazine stock solution	
Coelenterazine	1 mg
Methanol	1,653 mL

Firefly luciferase substrate	
D-Luciferin	470 µM
ATP	530 µM
Coenzyme A	270 µM
Tricine	20 mM
$MgSO_4$*7 H_2O	5.34 mM
EDTA	0.1 mM
	in H_2O

D-Luciferin was added after the buffer was adjusted to pH 8.0, followed by sterile filtration, aliquoting (7.5 mL) and storage at -80°C. Prior to luciferase assay, 33.3 µL/mL of 1M DTT was added.

3.2. Mouse Work

3.2.1. Breeding and handling

Mice were kept in the conventional animal laboratory at University of Regensburg in euro standard type cages II or III. Animals had free access to unlimited water and food and a 12h day/night cycle.

Breeding was started with 2-month-old animals and separation of the litter from mother took place after 21 to 28 days. Offspring either were marked with footpad tattoos or ear punches before separation. Tail biopsies or ear punch tissue was used for genotyping.

3.2.2. Used mouse lines

mT/mG x P2.5 Cre mice

For the isolation of podocytes, a mouse strain was generated with sortable green fluorescent podocytes. A mouse containing an Cre recombinase under the regulation of a 2.5 kb fragment of the *NPHS2* promotor (Moeller et al., 2003) was crossed with a double fluorescent Cre reporter mouse containing the *mT/mG* cassette ((Muzumdar et al., 2007) kindly provided by T. Huber). This mouse line expresses membrane-targeted tandem dimer Tomato (mT) in non-recombined cells and membrane-targeted green fluorescent protein EGFP (mG) in recombined cells after Cre excision. This allows for the differentiation and sorting of green fluorescent podocytes and red fluorescent epithelial and mesangial cells by Fluorescent activated cell sorting (FACS).

mT/mG x P 2.5 rtTA x LC1 x Dicer flox mice

To investigate the consequences of miRNA loss in adult mice, an inducible podocyte-specific dicer knockout mouse model was generated (Baumgarten et al., unpublished). In these mice, two *loxP* sites flanking the exon 23 of *Dicer* are inserted, leading to the deletion of most of the second RNaseIII domain (Harfe et al., 2005). The mouse line (kindly provided by Prof. Dr. Schweda) was crossed with a mouse line carrying *mT/mG* cassette (Muzumdar et al., 2007) and an Cre recombinase under the control of a promoter activated by reverse tetracycline transactivator (rtTA; TetOn system). rtTA was placed under the control of the podocyte-specific P2.5 promoter *NPHS2*. Through administration of doxycycline, podocyte-specific expression of Cre recombinase was induced, resulting in the deletion of RNaseIII domain of *Dicer* and the tomato cassette. *Cre* mediated expression of EGFP allows for the FACS analysis of green fluorescent podocytes isolated from murine glomeruli. Animals with wildtype *Dicer* gene not harboring the *loxP* sites for Cre recombinase recognition were used as control animals.

mT/mG x P2.5 rtTA x LC1 x Lmx1b flox mice

Inducible, podocyte-specific *Lmx1b* knockout mice (Burghardt et al., 2013) were crossed with double fluorescent *Cre* reporter mouse containing *mT/mG* cassette (Muzumdar et al., 2007). In these mice, exons 4 and 6 are flanked with *loxP* sites, which after administration of doxycycline, resulted in a *Lmx1b* knockout in podocytes. Moreover, tomato cassette was excised from the genome, resulting in green fluorescent podocytes due to the expression of GFP. This allows for FACS analysis of enriched podocytes from *Lmx1b* knockout mice and control mice, which harbor the wildtype *Lmx1b* genes without Cre recombinase recognition sites.

3.2.3. Genotyping of transgenes

DNA isolation

Genotyping for all transgenes was performed by PCR using isolated DNA from tail biopsies or ear punch tissue.

Tissue samples of animals were digested at 50°C overnight in 400-500 µL tail buffer and 4-5 µL proteinase K solution (20 mg/mL) under rotation. Afterwards, samples were vortexed and centrifuged at 14.000 rpm for 30 min. For DNA precipitation, the supernatant was mixed with 400-500 µL of isopropanol and centrifuged at 14.000 rpm for 30 min. After supernatant removal, the pellet was washed with 70 % ethanol, centrifuged for 15 min at 14.000 rpm and dried for 30 min at 37°C. DNA was dissolved in 50 µL water overnight at 50°C under rotation.

PCR

Isolated DNA was used for determination of genotypes by PCR using different primers (Tab. 1). Additionally, a known sample and water were used as template for the positive and negative control for each PCR.

Table 3.1 ***Oligonucleotides for PCR from genomic DNA for Genotyping.*** *mut: product size of animals harboring the mutation; wt: product size of wildtype animals; pos: product size of animals harboring transgene*

Primer name	**Sequence 5'→ 3'**	**PCR product size**
Cre forward	TGGACATGTTCAGGGATCGC	pos: 613 bp
Cre reverse	TCAGCTACACCAGAGACGGA	
mT/mG forward	CTCTGCTGCCTCCTGGCTTCT	wt: 330 bp mut: 250 bp
mT/mG reverse 1	CGAGGCGGATCACAAGCAATA	
mT/mG reverse 2	TCAATGGGCGGGGGTCGTT	
rtTA forward	GCAAGACTTTCTGCGGAACA	pos: 340 bp
rtTA reverse	GAAAAGGAAGGCAGGTTCGG	
Dicer_flox forward	CCTGACAGTGACGGTCCAAAG	wt: 351 bp mut: 420 bp
Dicer_flox reverse	CATGACTCTTCAACTCAAACT	
Lmx1b_flox forward	AGGCTCCATCCATTCTTCTC	wt: 220 bp
Lmx1b_flox reverse	CCACAATAAGCAAGAGGCAC	mut: 330 bp

The standard 25 µL reaction mix for genotyping consists of the following components:

Thermopol 10x reaction buffer (own lab)	2.5 µL
Primer (10 µM), each	0.5 µL
dNTPs (10 mM)	0.5 µL
H_2O	18.25 µL
Taq Polymerase (own lab)	0.25 µL
DNA solution (100 ng/µL)	2.5 µL

Table 3.2 ***Standard PCR program for genotyping***

Denaturation of DNA	95°C	5 min	
Denaturation of amplicon	95°C	30 sec	35 cycles
Annealing	58°C	30 sec	
Elongation	68°C	1 min	
Final Elongation	68°C	5 min	

Agarose gel electrophoresis

For determination of size, PCR products were analyzed by agarose gel electrophoresis. Therefore, 2 g of agarose was dissolved in 100 mL 1x TAE buffer and heated in a microwave. After the addition of 50 µL ethidium bromide (1 mg/ml), the gel solution was poured into the gel tray containing a comb and set for solidification (30 min). Each sample was mixed with 6.25 µL of 5x loading dye (< 300 bp xylene cyanol FF, > 300 bp bromophenol blue) and 12.5 µL was loaded into the well. As a DNA standard, 7µL of 1kb Plus DNA Ladder (NEB) was used. Gel electrophoresis was performed at 160 V for 35-40 min in 1x TAE buffer. For visualization and documentation of the results, the GelDocXR+ system (BioRad) was used.

3.2.4. Induction of *Dicer* knockout and analysis of urine samples

For induction of the dicer knockout, *mT/mG x P2.5rtTA x LC1 x Dicer-flox* mice received 2 mg/mL doxycycline and 50 mg/mL sucrose in drinking water for 3 to 41 days, depending on the respective trial period (Fig. 3.1). The drinking solution was freshly prepared every two days. Over the induction time, urine samples were collected on several days during the trial period, as well as on perfusion day. Urine samples were used for quantitative and qualitative analysis of urine proteins using SDS-PAGE and creatinine-protein ratio. Parallel body weight was monitored over the trial period.

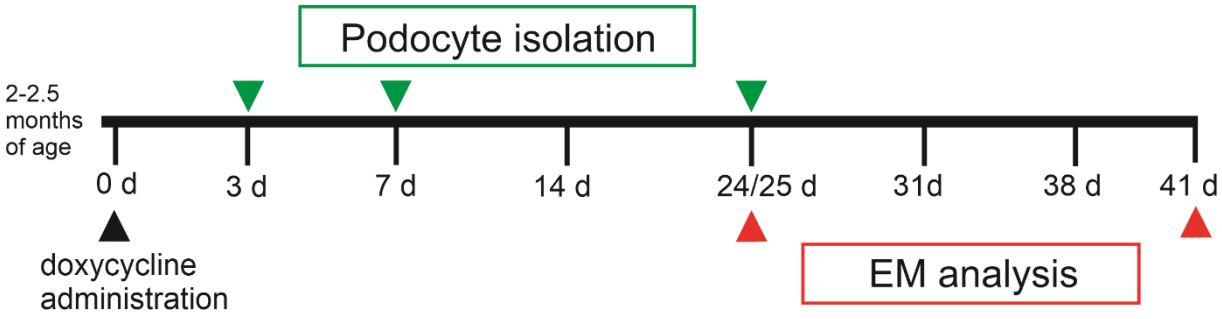

Figure 3.1 ***Monitoring of urine and body weight over the respective trial period.*** *Dicer knockout are induced in 2-2.5 month old mice by administration of doxycycline. Urine samples as well as body weight are measured on induction day and day 3, 7, 14, 24-25, 31, 38 and 41 postinduction. Mice are perfused on day 3, 7 and 24 for podocyte isolation or on day 24 and 41 for EM analysis.*

SDS-PAGE

Protein separation was conducted by SDS-PAGE using the Mini Protean 3 gel system (BioRad). Acrylamide separation gel (10 %) was poured into the apparatus and covered with a thin layer of isopropanol. After 45-60 min, the gel was polymerized and excessive isopropanol could be removed. After that, the stacking gel was cast on top and a comb was inserted.

After polymerization, gels were inserted into a gel chamber with 1x SDS running buffer and pre-run for 20 min at 220 V. The urine sample (1 µL) was mixed with H_2O and 5x Laemmli Loading dye and heated for 5min at 95°C. Additionally as control samples, different BSA (bovine serum albumin) concentrations were used (1, 3 and 10 µg). Together with 3 µL of prestained protein marker (Thermo Scientific) the samples were loaded on the gel and run at 150 V for 5min for sample setting. Afterwards, voltage was increased to 250 V for 30 min.

For staining, part of the stacking gel was removed, and the gel was stained with Coomassie blue solution for 15 min at room temperature. For destaining, gel was washed with water and placed into Coomassie blue destaining solution until BSA control samples were clearly visible.

Urine creatinine and protein measurement

Creatinine is a byproduct of protein metabolism and creatine phosphate. Creatinine can pass unchanged through the kidney filtration barrier and thereby can serve as a control parameter for kidney health. Serum creatinine, as well as urine creatinine can be measured.

Urine creatinine concentration was determined by Jaffe reaction. Creatinine reacts with picric acid in alkaline medium and produces an orange color.

Urine samples were diluted 1:100 (50µL) and pipetted in doubles in a 96 well plate. A blank sample (H_2O) and creatinine standard curve samples (0.03mg/mL, 0.015 mg/mL, 0.0075 mg/mL and 0.00375 mg/mL) were also pipetted in doubles. To each well 150 µL master mix was added using a multi-dispenser and incubated for 30 min at room temperature in the dark.

Master mix for urine creatinine measurement:

Trichloroacetic acid	1.2 M	50 µL/well
Picric acid	8 g/L	50 µL/well
NaOH	1.6 M	50 µL/well

Absorbance of creatinine-picric complex is measured at 540 nm with a photometric plate reader (Tecan Sunrise). Calibration was performed using the creatinine standard curve, of which linear regression yielded the y-intercept and slope. All samples were corrected by blank ratio. Creatinine mass concentration (ß) was calculated by the following equation:

$$ß\left(creatinine\frac{mg}{mL}\right) = \frac{Urine\ sample_{corr.A520nm} * y - intercept}{slope} * dilution\ factor$$

Bradford assay

For whole protein content investigation in urine samples, Bradford assay was used. For this, urine samples were diluted 1:200 and BSA standards were diluted from a 10 g/L stock solution (4 mg/L, 8mg/L, 16 mg/L, 40 mg/L, 80 mg/L and 160 mg/L). Respectively, 50 µL of the urine samples, BSA standard samples and bank (water sample) were pipetted in doublets into a 96-well plate. Additionally, 200 µL Roti-Quant solution (1:4 dilution) was given into each well using a multi-dispenser in fast succession. After 5 min incubation at room temperature, samples absorbance were measured at 450 nm and 595 nm using photometric plate reader (Tecan Sunrise). Samples were corrected with 450/595nm ratio of blank sample and calibrated using the BSA standard curve.

Protein mass concentration (ß) was calculated by the equation:

$$ß\left(protein\ \frac{\mu g}{\mu L}\right) = \frac{Urine\ sample_{corr.\frac{A450}{595nm}} * y - intercept}{slope} * dilution\ factor$$

3.3. Work with kidney samples

3.3.1. Kidney fixation perfusion

Mice were anesthetized by intraperitoneal injection of Narcoren working solution (1:50 dilution; 0.12–0.16 mg/g bodyweight) and tail biopsies were taken for re-genotyping. First, the *peritoneum* was opened and the *arteria* and *vena iliaca communis* were clamped. In addition, the aorta was clamped beneath the renal arteries. After removal of fat tissue, a small cut was made into the abdominal aorta where the tubing was inserted and fixed with a string. The *vena cava inferior* was cut, aorta clamp was removed, and perfusion fixation was performed using fixation solution (4 % PFA in 1x PBS) with a constant pressure of 180-200 mbar for three minutes. Fixated kidneys were extracted, halved vertically to the longitudinal axis and placed into snap cap vials with either 4 % PFA in 1xPBS (paraffin embedding) or 2 % glutaraldehyde in 0.1 M sodium cacodylate buffer (epon embedding).

3.3.2. Preparation for EM analysis

3.3.2.1. Epon embedding

Kidney samples were kept for post-fixation in 2 % glutaraldehyde in 0.1 M sodium cacodylate buffer for at least two days at 4°C under constant shaking. Accordingly, kidneys were cut into 2x2mm thick pieces and washed three times with 0.1 M sodium cacodylate buffer for 20 min. Kidney samples were incubated in 1 % osmium tetroxide for 1-2 hours, followed by another washing step and dehydration with an increased ethanol series (50 %, 70 %, 90 %, 96 %, 100 %) and 100 % acetone for 30 min. Tissue samples were incubated overnight in an epon/acetone mixture (1:1 ratio) and with freshly produced epon for 3h at 37°C. For final polymerization, the samples were incubated for 1-2 days at 60°C.

3.3.2.2. Section preparation for EM analysis

Tissue sections were quartered and cut with an ultramicrotome at a thickness of 50 nm and placed on 1 % pioloform coated copper slot grids. After washing with filtered double distilled H_2O (ddH_2O), the grids were incubated for 30 min with 1 % uranyl acetate and 3 % lead citrate solution in the dark for contrasting. Sections were washed 10 times with ddH_2O. Per mouse, TEM pictures of two glomeruli were taken at different magnifications with the EM 902: 400x, 700x, 3.000x, 7.000x and 20.000x.

3.3.3. Paraffin embedding and slice preparation

Kidney halves for paraffin embedding were fixed in 4 % paraformaldehyde in 1x PBS for 1-2 days at 4°C at constant shaking. Tissue samples were washed two times with 1x PBS and placed in an automated tissue processor. Samples were incubated in an increasing isopropanol series (50 %, 70 %, 80 %, 96 %, 3x 100 %) for 90 min, followed by incubation in 100 % xylol (2x) for 90 min and 60°C melted paraffin (3x) for 240 min. Kidney samples were placed with the cut edge on bottom of the base mold together with an embedding cassette. Heated paraffin was dispensed from a heated Paraffin dispensing module and the base mold was placed on a cooling plate (-20°C). After paraffin hardening, the block was removed from the base mold and stored at room temperature. Paraffin blocks were cooled before tissue sections were cut with a thickness of 5-6 µm using a microtome. Section slices were unfolded in a 40°C water bath and two slices were placed on one microscope slide. Subsequently, slices were dried on a heating plate at 40°C and quality controlled with a light microscope. Finally, tissue slices were dried overnight at 37°C before proceeding to section staining.

3.3.4. Staining of kidney sections

3.3.4.1. Deparaffinization and rehydration

Before staining, paraffin was removed from sections using a descending series of alcohol. For this, slides were placed into a staining tray and moved from the different reservoirs. Sections were incubated for 10 min twice in 100 % xylol and for 1-2 min in 100 % isopropanol. Afterwards, the sections were incubated for 1-2 min in 96 %, 80 %, 70 % and 50 % isopropanol. Sections were shortly placed in distilled H_2O for rehydration.

3.3.4.2. H&E staining

After deparaffinization and rehydration, sections were stained with hematoxylin and eosin. Sections were stained for 3 min at RT with filtered hematoxylin solution (basophilic staining) and washed shortly in tap water. To remove excess staining solution, sections were differentiated two times in 0.1 % HCL in 70 % isopropanol and washed for 10 min under running tap water. Additionally, slices were incubated in freshly prepared 0.1 % eosin solution (acidophilic staining) for 40-45 sec at RT and washed with H_2O.

3.3.4.3. PAS reaction

After deparaffinization and rehydration, sections were first incubated in freshly prepared 1 % periodic acid solution for 10 min at RT and washed 3x shortly in H_2O. Consequently, unsubstituted glycol groups were oxidized into two neighboring aldehyde groups. Slices were stained for 15 min with Schiff's reagent, which binds to the aldehyde groups leading to a color change. Afterwards, sections were differentiated three times in freshly prepared sulfite water for 1 min and washed for 5min with tap water. For cell nucleus staining, slices were placed in a hemalum solution for 3-5 min followed by washing for 5 min and differentiation in 0.1 % HCL in 70 % isopropanol. Finally, sections were washed again for 5 min with tap water.

3.3.4.4. Dehydration and light microscope analysis

After H&E staining or PAS reaction, the sections were dehydrated by an ascending series of alcohol. Therefore, the sections were incubated for a short period (3s-3min) in 70 %, 80 %, 96 % and twice in 100 % isopropanol. Before mounting, the sections were incubated twice for 5-10 min in 100 % xylol. Dehydrated sections were mounted with DePeX embedding medium and digitalized with the Leica DM750 using different magnifications (10x and 40x).

3.3.5. Glomeruli isolation by magnetic beads perfusion

The magnetic bead perfusion protocol was based on the protocol published by Boerries et al. (2013) with slight modifications. Mice were anesthetized by intraperitoneal injection of Narcoren working solution (1:50 dilution; 0.12–0.16 mg/g bodyweight) and tail biopsies were taken for re-genotyping. *Peritoneum* was opened and kidneys were extract with their renal arteries and part of the aorta for *ex vivo* perfusion. Through the *arteria renalis,* each kidney was perfused with 1 mL of HBSS buffer followed by 4 mL of bead solution and 1 mL of beads-digestion solution. After the removal of the capsule, kidneys were chopped into small pieces and digested with 2 mL digestion solution for 10 min on a shaking rotator plate at 37°C. The digested kidneys were filtered through a 100 µm cell strainer twice and centrifuged for 5 min (4°C, 1.500 rpm). The pellet was resuspended with 2 mL HBSS buffer and transferred into a 2 mL tube. For glomeruli collection, the cell solution was placed into a magnetic collector for 7 min on ice. Collected glomeruli were washed only once with HBSS buffer and resuspended with 2 mL digestion solution.

3.3.5.1. Single cell preparation with enzymatic digestion

For detachment of podocytes from glomeruli, the solution was incubated for 45 min at 37°C in a thermomixer at 1.400 rpm. During the incubation time, samples were treated as described as follows:

Table 3.3 ***Digestion steps for podocyte detachment***

Time	Procedure
5 min	pipet up and down with glass pipet
10 min	vortex and pipet up and down with glass pipet
15 min	draw through 27 G needle for 3 times
20 min	Vortex and pipet up and down with glass pipet
25 min	pipet up and down with glass pipet
30 min	vortex and passed through a 200 µl pipet tip put on a 1000 µl pipet tip
35 min	pipet up and down with glass pipet
40 min	vortexed 3 times and passed through a 200 µl pipet tip put on a 1000 µl pipet tip
45 min	draw through 27 G needle for 3 times

After incubation, samples were checked for detached green fluorescent podocytes by fluorescence microscopy (Axiovert 200). If intact glomeruli were still observed, the digestions steps can be extended to detach all podocytes.

The samples were again placed into the magnetic collector to remove beads, and remaining glomeruli and tubular fragments. The supernatant was collected and filtered through a 30 µm cell strainer (MACS Miltenyi Biotec) and washed with HBSS buffer. After centrifugation (5 min, 1.500 rpm, 4°C), the pellet was resuspended with 475 µL FACS buffer (0.2 % FCS in 1x PBS) and 25 µL propidium iodide solution (stock solution 1 mg/mL) for staining of non-viable cells. The cell solution was filtered into a tube with a cell-strainer cap and placed on ice.

3.3.5.2. FACS sample preparation and separation of podocytes and mesangial/epithelial cells

Fluorescent activated cell sorting (FACS) was performed at the Department for Internal Medicine III, University Hospital Regensburg. BD FACSAria IIu sorter (BD Biosciences) separated green fluorescent podocytes and red fluorescent cell fraction containing mesangial cells, epithelium cells and podocytes without Cre expression. Sorted cells were pelleted (10 min, 1.500 rpm, 4°C), supernatant was discarded and dry cell pellets were snap frozen in liquid N_2 and stored at -80°C or directly used for RNA isolation.

3.4. RNA work

3.4.1. Handling of RNA material

Working with RNA requires careful handling because of the chemical instability of RNA and the presence of RNases. Water, solutions, and buffers for RNA preparation were processed with 1mL/L diethylpyrocarbonate (DEPC) overnight followed by autoclaving at 121°C to prevent RNA degradation. Plastic ware, pipettes and lab bench were treated with RNase Away spray before RNA isolation. Gloves were worn at every preparation step and only filtered pipettes tips were used.

3.4.2. RNA isolation and quantification

RNA samples for qPCR analysis were isolated from cultured cells or freshly isolated murine podocytes and stored at -80°C.

3.4.2.1. Isolation of small RNA fraction (< 200 nt)

miRNA was isolated using the miRVana Kit (Ambion) according to manufacturer's protocol. Cell pellet was lysated with 500-600 µL lysis/binding buffer and vortexed. Lysate was incubated for 10 min on ice with 1/10 volume of miRNA homogenate additive followed by RNA extraction using a volume of Phenol:Chloroform-mixture that was equal to the amount of used lysis/binding buffer. After vortexing for 1 min and centrifugation at 10.000 rpm for 5 min, the upper aqueous phase was carefully removed and transferred into a new tube. 1/3 volume of 100 % ethanol was mixed with the aqueous phase and passed through the first filter cartridge at 10.000 rpm for 15 sec, containing the long RNA fraction. Filtrate was mixed with 2/3 of 100 % ethanol and passed through a second filter cartridge, which carries the small RNA fraction. Both filter cartridges were washed with 700 µL miRNA washing buffer 1 and

twice with 500 µL miRNA washing buffer 2/3. After filter cartridges were spin dried for 1 min, the filters were placed into a new tube and eluted with 70-100 µL 95°C preheated DEPC-H_2O. Long RNA fraction was further concentrated and cleaned using RNeasy Micro Kit (Qiagen) (see 3.4.2.2). RNA concentration was measured using a NanoDrop photometer and stored at -80°C.

Additionally, a DNase digestion could be performed by adding 0.1 volume of 10x DNase I Buffer and 1 µL rDNase I to the RNA in a 50 µL reaction volume. The reaction was incubated for 1h at 37°C. Afterwards, 0.1 volume of DNase Inactivation Reagent was added to the reaction mix and incubated for 2 min with occasional mixing. After centrifugation for 1.5 min at 10.000 x g, supernatant was transferred to a new tube.

3.4.2.2. Isolation of total and long RNA fraction (> 200 nt)

Total RNA was isolated using RNeasy Micro Kit (Qiagen). RNA was lysed with 350 µL RLT buffer, mixed with one volume of 70 % ethanol and transferred to the RNeasy MinElute spin column. After centrifugation at 8.000 g for 15 sec, a DNase digestion step (DNase Kit I, Qiagen) was included using a modified protocol. After washing with 350 µL RW1 buffer, the sample was incubated for 1h at 28°C with DNase I in RDD buffer and washed again with 350 µL RW1 buffer. Samples were washed with 500 µL RPE buffer and 80 % ethanol, followed by spin drying for 5 min. Sample was eluted with 14-20 µL RNase-free H_2O and stored at -80°C. For purification of long RNA fraction (see above), protocol starts with second step (mixture with 70 % ethanol). RNA concentration was measured with a NanoDrop photometer.

3.4.2.3. cDNA synthesis

cDNA synthesis of miRNAs/small RNAs

For the generation of miRNA templates long enough for qPCR, a protocol for miRNA elongation from Hurteau et al. (2006) was used. Here a poly-A-tail was added to the miRNA by the *E.coli* poly (A) polymerase (EPAP, NEB). In addition, an adapter primer consisting of a universal sequence and a poly T-sequence was annealed to the poly-A-tail.

miRNA elongation reaction mix:

isolated RNA sample	0.2-0.5 µg
E. coli buffer reaction buffer, 10x	2 µL
ATP, 10 mM	2 µL
EPAP [5.000 units/mL]	1 µL
Nuclease free H_2O/DEPC-H_2O	ad to 20 µL

For poly-A-tail synthesis, the reaction mix was incubated for 30 min at 37°C in a PCR cycler (BioRad). Afterwards, the reaction mix was denatured at 65°C for 15-20 min and cooled to 4°C.

For poly-A-tail annealing, 1 µL of 100 µM Universal PCR primer was added to the miRNA elongation reaction mix and heated at 65°C for 5 min. Accordingly, the reaction mix was slowly cooled down 1°C/min till 25°C, followed by a rapid cool-down to 4°C. Before cDNA synthesis, the reaction mix was split into the sample and non-RT control sample, which only lacks the reverse transcriptase. For the cDNA generation with the iScript Select cDNA synthesis kit (BioRad), the poly-A-poly-T-double strand was used as a starting point.

cDNA synthesis reaction mix:	cDNA sample	non-RT control sample
Poly-A-tail reaction mix	18 µL	3µL
iScript select 5x reaction buffer	5 µL	1.25 µL
iScript reverse transcriptase	1.25 µL	-
nuclease free H_2O/DEPC-H_2O	0.75 µL	0.75 µL

First, the reaction mix was incubated for 5 min at 25°C, followed by the cDNA synthesis at 42°C for 60 min. The reaction mix was then denatured at 85°C for 5min and rapidly cooled down to 4°C.

cDNA preparation for total/long RNA

cDNA synthesis was performed with iScript Select cDNA Synthesis kit (BioRad) in a PCR cycler.
RNA reaction mix was incubated at 25°C for 5 min and incubated for 60 min at 42°C for cDNA synthesis. After denaturation at 85°C for 5min, the reaction mix was rapidly cooled down to 4°C.

cDNA synthesis reaction mix:	cDNA sample	non-RT control sample
RNA sample	< 1 µg	< 1 µg
iScript select 5x reaction buffer	4 µL	4 µL
random primer mix	2 µL	2 µL
iScript reverse transcriptase	1 µL	-
nuclease free H_2O/DEPC-H_2O	ad 20 µL	ad 20 µL

3.4.2.4. Quantitative real-time PCR analysis

Quantitative RT-PCR was used for relative quantification of RNA levels using the LightCycler480II. cDNAs were prediluted 1:2 to 1:10 depending on the amount of used RNA. For each target or reference genes. a dilution standard series (1:2, 1:4, 1:8, 1:16, 1:32) of each cDNA was used to measure primer pair efficiency. The efficiency was measured by the 2nd derivative maximum analysis method (non-linear regression line) by the LightCycler software (version 1.5.0.39) using the formula:

$$E = 10^{\frac{-1}{slope}}$$

Furthermore, a melting curves analysis was performed for each well to monitor and exclude possible synthesis of more products. cDNA samples were diluted 1:8 and pipetted in triplets in a 96-well plate. For each cDNA, a non-RT control was treated like cDNA sample and analyzed for each target/reference genes. Relative advanced quantification of unknown cDNA samples were performed with the efficiencies of each target/reference and the CP-values using the LightCycler software.

As reference gene, snRNA U6 was used for small RNA quantification and Lamin A/C and S9 were used for long RNA quantification.

qPCR reaction mix:

cDNA/nRT	2 µL
Primer forward (10 mM)	1 µL
Primer reverse (10 mM)	1 µL
H_2O	6 µL
qPCR Mastermix	10 µL

Table 3.4 ***Standard program for qPCR analysis***

Pre-incubation	95°C	7 min	
Amplification	95°C	10 sec	55 cycles
	50-62°C	10 sec	
	72°C	10 sec	
Melting curve	95°C	5 min	
	40°C	1 min	
	97°C	2.2°C/min	
Cooling	40°C	30 sec	

For relative quantitation, the annealing temperature depends on target gene. For both small and long RNAs an annealing temperature of 62°C were used.

Table 3.5 ***Primer for qPCR analysis of mRNA targets***

Primer name	**Sequence 5' → 3'**
*Cd2ap*_Forward	AACTCACAACGCTCAGGAGGA
*Cd2ap*_Reverse	TGTGCAAC GATCCGGGA
*Dicer*_Forward	GCAAGGAATGGACTCTGAGC
*Dicer*_Reverse	GGGGACTTCGATATCCTCTTC
*Dusp1*_Forward	GCGCTCCACTCAAGTCT
*Dusp1*_Reverse	TGCACTGTCAGGCACACTA
*Fyn*_Forward	TCTGCGATCAGCAAACATTC
*Fyn*_Reverse	CTTCAATCAACCGAGCCAAT
*Lamin A/C*_Forward	TGACTTGGTGTGGAAGGCG
*Lamin A/C*_Reverse	CAGTGGAGTTGATGAGAGCGG
*Npnt*_Forward	AAAGGCCATCTACCAGACC
*Npnt*_Reverse	GCTGACCCCTCTTTCGATTT
S9_Forward	TGAAGCTGGATTACATCCTG
S9_Reverse	GGGATGTTCACCACCTG
*Sparc*_Forward	CCACACGTTTCTTTGAGACC
*Sparc*_Reverse	GATGTCCTGCTCCTTGATGC
*VegfA*_Forward	CTGTACCTCCACCATGCCAAGT
*VegfA*_Reverse	AGATGTCCACCAGGGTCTCAAT

Table 3.6 ***Primer for qPCR analysis of miRNA targets.***

Primer name	**Sequence 5' → 3'**
U6_Forward	CGCTTCGGCAGCACATATAC
U6_Reverse	TTCACGAATTTGCGTGTCAT
Universal Primer	AACGAGACGACGACAGACTTT
miR-19b-3p	GCAAATCCATGCAAAACTGA
miR-29a-3p	AGCACCATCTGAAATCGGTTA
miR-30a-5p	TGTAAACATCCTCGACTGGAA
hsa-miR-101a-5p	CAGTTATCACAGTGCTGATGC
mmu-miR-101a5p	CAGTTATCACAGTGCTGATGC
miR-135a-5p	TATGGCTTTTTATTCCTATGTG
miR-149-5p	CTGGCTCCGTGTCTTCACTC
miR-210-3p	CTGTGCGTGTGACAGCGG
miR-378a-3p	ACTGGACTTGGAGTCAGAAGG
miR-615-3p	TCCGAGCCTGGGTCTCCCTCT
miR-615-5p	GGGTCCCCGGTGCTCGGAT

3.5. Cell culture work

3.5.1. Handling and culturing

Cells were cultivated in 25 cm^2 or 75 cm^2 cell culture flasks with a filter cap and kept in a 5 % CO_2-incubator at 95 % relative humidity. Culture work was performed in a laminar flow bench, which was cleaned with 70 % ethanol before each use. All used solutions and plasticware were either bought sterile or sterilized through filtration or autoclaving at 121°C.

HEK293T cells

HEK293T cells were cultured in DMEM with 10 % FCS and kept at 37°C. Medium was changed every two to three days and cells were subcultured at an 80 % confluency.

hPCL cells

Originally, the human podocyte cell line „8/13“ was established at lab of P. Mundel (Saleem et al., 2002). Cells were cultivated in RPMI with 10 % FCS and 1 % ITS-G and kept at 33°C for proliferation. Medium was changed every two to three days and subcultured depending on cell density. For differentiation, cells were seeded at a density of 7200/cm^2 and after 24h shifted to 37°C.

3.5.2. Freezing

For freezing, cells were grown to a confluency of 80 % in a 75cm^2 flask and washed once with 1x PBS. Cells were detached with 1ml trypsin and incubated for 5 min at 33°C or 37°C. Afterwards, cells were resuspended in growth medium and centrifuged at 300 xg for 5min at 4°C. The cell pellet was resuspended in 4 mL freezing medium containing FCS and 10 % dimethyl sulfoxide (DMSO) and separated into three cryovials. After slowly freezing the cells down to -80°C, cells were stored at -80°C for short term storage or in liquid nitrogen for long term storage.

3.5.3. Thawing

Frozen cells were rapidly thawed to room temperature and diluted in 10 mL growth medium. After centrifugation at 300 xg for 5 min, diluted freezing medium was removed. The cell pellet was resuspended in growth medium and seeded in cell culture flasks.

3.5.4. Harvesting

After the determination of cell concentration by counting cells in all four quarters of a Neubauer chamber, cells were seeded according to the amount required. Cells were then harvested 24 h after seeding. For this, cells were washed twice with 1x PBS and scraped from the plate with a cell scraper. The cell suspension was centrifuged at 350 xg for 10 min at 4°C. The cell pellet was shock-frozen in liquid nitrogen and stored at -80°C. For hPCL cells, either proliferating or differentiated cells can be used. Differentiated cells were harvested after 14 days after the temperature shift to 37°C.

3.5.5. HSC CellMask Red staining

To investigate if miRNA knockout in hPCL cells lead to problems in differentiation, knockout cells were stained with HSC CellMask Red staining and cell area size was measured. Therefore, hPCL knockout cells (mir-30a-5p and 146b-5p) were seeded at a density of 7.200 cells/cm^2 in a 24 well plate containing a cover slip. After 24h cells were shifted to 37°C for differentiation and incubated for 14 days. Afterwards the cover slips were washed 2-3 times with 1x PBS and incubated for 15 min in 4 % PFA for fixation. After another washing step with 1x PBS, cover slips were incubated for 15 min in 0.1 % Triton-X-100. After permeabilization, cells were washed again with 1x PBS followed by incubation with cell mask staining solution (2 µL 10 mg/mL staining stock solution in 10 ml 1x PBS) for 30 min without light irradiation. Before mounting the cells with DAPCO on a glass slide, the cells were washed again with 1x PBS. For each knockout cell line two clones and one control was analyzed. Cells were analyzed by fluorescence/confocal microscopy at 588/612 (LSM 710_NLO) with a 20x objective.

10 mg/mL staining stock solution:

Component A	250 µg
Component B (DMSO)	25 µL

The evaluation was performed with the ImageJ software. First, the median filter was used to reduce noise followed by the threshold setting. By using the watershed function, attached cells were split into single cells. After using the function “analyzing particles”, the results were transferred in Microsoft Excel and sorted after area size. From all analyzed cells, the mean value was calculated as well as the standard deviation. Cells, which were smaller than 200 μm^2 were excluded. For significance, the unpaired student’s t-test was performed.

3.5.6. Mimic transfection of hPCL cells

hPCL cells were seeded at a density of 7.200 cell/cm^2 in a 12 well plate containing cover slips. After 24h cells in each well were transfected with miRCURY LNA™ microRNA Mimics reaction mixture (control, 30a-5p or 146b-5p) with different end concentrations (10 nM, 50 nM, 100 nM).

Mimic stock solution [66.6 µM]:

miRNA mimic, dried	5nmol
nuclease free H_2O	75 µL

Transfection reaction mixture:

Mimic stock solution, prediluted [0.1, 0.5, 1 pmol/µL]	10 µL
RPMI medium, without FCS	100 µL
P3000 reagent [2µL/µg DNA]	0.2 µL
Lipofectamine 3000	3 µL

The transfection reaction mixture was incubated for 15 min at RT and 100 µL was added to each well. The next day, cells were shifted to 37°C for differentiation and incubated for 14 days. The medium was changed three times per week, and the cells were used for immunostaining after two weeks.

3.5.7. Immunostaining

Mimic treated cells were washed twice with 1x PBS. For fixation, cells were incubated in 4 % PFA for 8 min at room temperature and washed three times with 1x PBS. After incubation in 0.05 % Triton-X-100 for 30 min, cells were blocked with 5 % horse serum in 1x PBS for 30 min. Afterwards, cells were incubated with the primary antibody α-α-actinin 4 (1:200 in 5 % horse serum in 1x PBS) for 2h at RT. After washing the cells three times, the cells were incubated with the second antibody Alexa Fluor 568

donkey α-rabbit (1:600 in 5 % horse serum in 1x PBS) for 30 min at RT. Cells were mounted with DAPCO after washing with 1x PBS and analyzed with a fluorescence microscope (Axiovert 200M). Samples only treated with the secondary antibodies served as controls. The evaluation of sample area size was performed according to the method described in chapter 3.5.5.

3.6. DNA work

3.6.1. Generation of constructs harboring 3'UTR of potential target mRNA

3.6.1.1. Preparation of vector

For constructs harboring the 3'UTR of target mRNAs a modified pMIR-Report vector was used (see 3.1.7). The plasmid coded a targeted firefly luciferase and additionally a renilla luciferase as an untargeted internal standard. Also, the CMV promoter was exchanged for a TK promoter and it harbors the ampicillin resistance gene.

The pMIR-Report plasmid was digested with the restriction enzymes *Spe*I-HF and *Sac*I-HF for 2 h at 37°C. After 1h, 1µL of alkaline phosphatase was added to the digesting mixture.

Vector digestion mixture:

pMIR-Report plasmid	> 1 µg
CutSmart 10x buffer	2 µL
SpeI-HF [20 U/ µL]	0.5 µL
SacI-HF [20 U/µL]	0.5 µL
H_2O	ad 20 µL

After digestion, the vector was cleaned via agarose gel electrophoresis. For this, the vector was loaded into a 1 % agarose gel running with 1x TAE buffer for 0.5-1 h at 160 V. The digested vector band was cut out from the gel using a scalpel and isolated using the QIAquick Gel Extraction Kit (Qiagen) according to the manufacturer's protocol. Three to six volumes (> 2 % agarose gel) of QG buffer was given to 1 volume of gel (100 mg gel ~ 100 ml) and incubated at 50°C for 10 min to allow for the gel to dissolve. After addition of 1 volume 100 % isopropanol, the mixture was passed through a spin column at 13.000 rpm for 1 min at RT. Then the column was treated again with 500 µL QG and washed twice with 750 µL PE buffer (13.000 rpm, 1min, RT). The DNA was eluted in 30-50 µL H_2O after spin drying for 2 min at 13.000 rpm. The concentration was measured using the NanoDrop 2000 photometer.

3.6.1.2. Preparation of Inserts

Amplification of 3'UTR fragments

The 3'UTR inserts of the wildtype target mRNAs was generated by PCR using sequence specific primers harboring the recognition site of used restriction enzymes *Spe*I-HF and *Sac*I-HF. As template, genomic DNA from HEK293T /hPCL cells for human constructs or DNA from *P2.5 Cre x mT/mG* mice for murine constructs was used. Due to the size and the containing of internal *Sac*I restriction site in the 3'UTR of *Lmx1b/LMX1B*, the 3'UTR was divided into four fragments.

Table 3.7 ***Oligonucleotides for PCR amplification of human and murine 3'UTR fragments from genomic DNA.***

Primer name	**Sequence 5' → 3'**
pMIR-Report/TK_*Arrdc3*_front forward	TGAAGCAACACTAGTCTGAGTCAA
pMIR-Report/TK_*Arrdc3*_front reverse	TCAGCAAAACTGAGCTCCAACATAT
pMIR-Report/TK_*ARRDC3*_front forward	TGCCCCACTAGTTGAAGGAAC
pMIR-Report/TK_ *ARRDC3*_front reverse	GATTCAAATAGAGCTCCAAACAATTA
pMIR-Report/TK_*Fosb* forward	ACCTAATCCCAAACCCCACC
pMIR-Report/TK_*Fosb* reverse	GTCCAGGGAAAACAGACACT
pMIR-Report/TK_*FOSB* forward	CTCATGAGGACTAGTTTATG
pMIR-Report/TK_*FOSB* reverse	TCGGAGCTCCATTGAATTG
pMIR-Report/TK_*Npnt*_1 forward	CTGAAGTACTAGTAAAGAGCACC
pMIR-Report/TK_*Npnt*_1 reverse	GGAAGAGCTCGGTGGCAG
pMIR-Report/TK_*NPNT*_1 forward	GGGGGAAAATAAACTAGTAAGCC
pMIR-Report/TK_*NPNT*_1 reverse	CAAAAAAAAACAGAGCTCAAAAAACAA
pMIR-Report/TK_*Npnt*_2 forward	GTGTCTTCACTAGTAAGGCCTT
pMIR-Report/TK_*Npnt*_2 reverse	AAAGATACACGAGCTCCACAAG
pMIR-Report/TK_*NPNT*_2 forward	TAATGTACTAGTGTGGCGGTGG
pMIR-Report/TK_*NPNT*_2 reverse	GAACCTGGGAGAGCTCAATTGA
pMIR-Report/TK_*Per1* forward	AACAGCACTAGTTAGACTCCATTT
pMIR-Report/TK_*Per1* reverse	TTCATTTCACGAGCTCTTGGGTT
pMIR-Report/TK_*Serinc3* forward	AGCTGAGACTAGTGTGTCAAGGA
pMIR-Report/TK_*Serinc*3 reverse	TGTCAGATTGATTTGGAGCTCTCTAAA
pMIR-Report/TK_*SERINC3* forward	GTCGGGACTAGTGCTGAACC
pMIR-Report/TK_S*ERINC3* reverse	GAATAGGAGCTCCCTGACTAGA
pMIR-Report/TK_*Sparc* forward	CAAGGATCTGGTGATACTAGTTC
pMIR-Report/TK_*Sparc* reverse	AGTGCCTAGAGCTCCCGG
pMIR-Report/TK_*SPARC* forward	CTTGTGAACTAGTTCCACTCCTT
pMIR-Report/TK_*SPARC* reverse	GAGGAGGAGCTCTGCAGG
pMIR-Report/TK_*STT3A* forward	ATCGAGGCTTGACTAGTACATAAATGT
pMIR-Report/TK_*STT3A* reverse	CTACAAACAGAGCTCTCAATCAGC
pMIR-Report/TK_*VegfA* forward	ATGTGACTAGTCAAGGCGGTG
pMIR-Report/TK_*VegfA* reverse	TATATGAGCTCATGTGGGTGG

pMIR-Report/TK_*VEGFA* forward	ATGTGACTAGTCGAGGCGGT
pMIR-Report/TK_*VEGFA* reverse	GACACCAATAACATTAGAGCTCTTAA
pMIR-Report/TK_*Zfp36* forward	TGAGTGACTAGTGCCTACCTA
pMIR-Report/TK_*Zfp36* reverse	AAAAAGACAGAGCTCATCTCAGTT
pMIR-Report/TK_*Lmx1b*_1.construct forward	CTACTCCAACTAGTGCTCCTAC
pMIR-Report/TK_*Lmx1b*_1.construct reverse	CTGTCCAAGAGCTCTGGGTC
pMIR-Report/TK_*Lmx1b*_2.construct forward	TGGGGGAAGCTTAAACTAGTTCG
pMIR-Report/TK_*Lmx1b*_2.construct reverse	CCCAGAGACAGGAAATTAACCCA
pMIR-Report/TK_*Lmx1b*_3.construct forward	CCCATCTCTGTCTCACTAGTGCA
pMIR-Report/TK_*Lmx1b*_3.construct reverse	CCAGAGCTCTGAGTCCATCTTCC
pMIR-Report/TK_*Lmx1b*_4.construct forward	TAGGACTAGTGGGACGCTGCA
pMIR-Report/TK_*Lmx1b*_4.construct reverse	GGTGGTGAGCTCGAAACGCTA
pMIR-Report/TK_*LMX1B*_1.construct forward	CCTTAACTAGTCTCAGCGAC
pMIR-Report/TK_*LMX1B*_1.construct reverse	GTCCGAGAGCTCTGGGT
pMIR-Report/TK_*LMX1B*_2.construct forward	ACGGCCACTAGTCTCCCAGC
pMIR-Report/TK_*LMX1B*_2.construct reverse	TCGCTGACCTAGTGAGCTCCTT
pMIR-Report/TK_*LMX1B*_3.construct forward	GGCCAAACTAGTTGCCTGACAT
pMIR-Report/TK_*LMX1B*_3.construct reverse	CCAGAGCTCAAGGATGGAGC
pMIR-Report/TK_*LMX1B*_4.construct forward	GCACCAACTAGTGTGAGGGA
pMIR-Report/TK_*LMX1B*_4.construct reverse	GGTGGTGTGGTGAGCTCTAAT

For most of the inserts, the *Taq* polymerase was used for amplification at a temperature of 50°C. Only for *VegfA*, the *Phusion* polymerase was used. For *Serinc3* an annealing temperature of 54°C and 52°C for mPer1 was used. For the amplification of *Npnt*_2 (50°C) and *NPNT*_2 (52°C) the *Pfu* polymerase was used. For the amplification of the *Lmx1b*/*LMX1B* constructs with the *Taq* polymerase different annealing temperature were used: *Lmx1b*_4.construct and *LMX1B*_1.construct (60°C); *LMX1B*_2.construct and *LMX1B*_4.construct (62°C); *LMX1B*_3.construct (51°C); *Lmx1b*_2.construct (54°C) and *Lmx1b*_3.construct (58°C, Bachelor thesis N. Malagimani 2019).

PCR Mastermix:

Thermopol 10x reaction buffer/ Phusion HF 5x buffer	2.5 µL / 5 µL
Primer Forward (10 µM)	1 µL
Primer Reverse (10 µM)	1 µL
dNTPs (10 µM)	1 µL
genomic DNA (100 ng/µL)	1 µL
Taq Polymerase/ *Phusion* Polymerase	0.25 µL
H_2O	ad 25 µL

In addition, 0.1 µL *Pfu* polymerase was added to each 25 µL PCR master mix with the *Taq* polymerase to enable proof-reading (3'→5' exonuclease activity).

Table 3.8 ***Standard PCR program for 3'UTR insert amplification with Taq Polymerase***

Denaturation of DNA	95°C	5 min	
Denaturation of amplicon	95°C	30 sec	35 cycles
Annealing	50-54°C	1 min	
Elongation	68°C	1 min/kb	
Final Elongation	68°C	5 min	

Table 3.9 ***Standard PCR program for 3'UTR insert amplification with Phusion Polymerase***

Denaturation of DNA	98°C	5 min	
Denaturation of amplicon	98°C	30 sec	35 cycles
Annealing	50-54°C	1 min	
Elongation	72°C	30 sec/kb	
Final Elongation	72°C	5 min	

The PCR products were loaded to 1-2 % agarose gel for purification and isolated using the QIAquick Gel Extraction Kit (Qiagen, see 3.6.1.1.).

Digestion and purification

Isolated 3'UTR inserts were digested with *Spe*I-HF and *Sac*I-HF for 2 h at 37°C. Afterwards, the mixture was purified using the QIAquick Nucleotide Removal Kit (Qiagen). Shortly, five volumes of PNI buffer were added to the mixture and passed through a spin column at 6.000 rpm for 1 min at RT. The column was washed with 750 µL PE buffer (6.000 rpm, 1 min, RT) and spin dried for 1 min at 13.000 rpm. The DNA was eluted with 30-50 µL H_2O and quantified using a NanoDrop 2000 photometer.

3.6.1.3. Ligation of insert and vector

For ligation, pMIR-vector and the 3'UTR insert were mixed in a molar ratio between 1:3 and 1:5. The ligation mixture was mixed and incubated overnight in a water bath, slowly cooling down from 16°C to 4°C. As negative control, a ligase reaction mixture was performed with a linearized vector alone and no insert.

Ligation reaction mix:

pMIR-vector	50-100 ng
3'UTR insert	50-100 ng

T4 DNA Ligase reaction buffer 10x	2 µL
T4 DNA Ligase	1 µL
H_2O	ad 20 µL

3.6.1.4. Electroporation

The day following ligation, the enzymatic reaction was deactivated by heating the mixture at 65°C for 10 min. Before electroporation, the ligation mix was dialyzed on a dialysis filter paper in a petri dish filled with water for 1 h at RT. Then it was mixed in an electroporation cuvette with 40 µL of freshly thawed electrocompetent *E. coli* suspension. After electroporation at 2.500 V, the cells were immediately diluted in 1 mL LB medium and incubated for 1 h at 37°C in a shaking incubator. 100 µL of cell suspension and the resuspended pellet was plated on LB agar plates containing ampicillin (100 µg/mL) for selection and incubated at 37°C overnight.

3.6.1.5. DNA preparation and screening of positive clones

The following day, colonies were picked from the plates and transferred to 4 mL of LB medium containing ampicillin and incubated overnight at 37°C in a shaking incubator. Then plasmids were isolated from the bacterial cells. Each 4 mL cell suspension was collected by centrifugation at 13.000 rpm for 2 min at RT and pellet was resuspended with 250 µL of P1 buffer. After adding 250 µL P2 buffer and 350 µL P3 buffer, the mixture was centrifuged for 10 min at 13.000 rpm. Supernatant was removed carefully and transferred into a new tube with 500 µL isopropanol (13.000 rpm, 10 min). The pellet was washed with 500 µL 70 % ethanol (13.000 rpm, 5 min) and dried for 1 min at 13.000 rpm. The DNA was eluted with 50 µL H_2O and concentration was measured with a NanoDrop 2000 photometer. For screening of positive clones, isolated plasmids were digested with *Spe*I-HF and *Sac*I-HF for 1h at 37°C and analysis using agarose gel electrophoresis. Clones showing a digested insert of the right size were sequenced to exclude point mutations.

3.6.1.6. Plasmid isolation for cell transfection

After exclusion of any point mutations, the plasmids were incubated in a 50-100 mL culture overnight and isolated using the Wizard Plus Midipreps DNA Purification System (Promega). The bacterial cells were pelleted at 4000 xg for 15 min at 4°C and resuspended with 3 mL of Cell Resuspension solution. After adding 3 mL of Lysis buffer and 3 mL of Neutralization buffer, the lysate was transferred to a centrifuge tube and centrifuged at 14.000 g for 15 min at 4°C. The supernatant was passed through a filter and mixed with 10 mL of Resin. The mixture was then passed through a column using vacuum. After washing the column twice with 15 mL washing buffer, the column was spin dried at 13.000 rpm

for 2 min. The DNA was eluted with 250 µL H_2O (preheated to 70°C) and quantified using a NanoDrop 2000 photometer. The isolated plasmid was used for cell transfection. As alternative to the Promega Kit also the Plasmid Plus Midi Kit (Qiagen) can be used. Shortly, the bacterial cells were pelleted at 4.000 xg for 15 min at 4°C and resuspended in 2 mL P1 buffer. After the addition of 2 mL P2 buffer and incubation for 3 min at RT, 2 mL of P3 buffer was added to the lysate. The lysate was transferred to the QIAfilter Cartridge, incubated for 10 min and filtered into a tube. BB buffer (2 mL) was added to the cleared lysate before transferring it to QIAGEN Plus spin column and passing it through the column by vacuum. Afterwards, the DNA was washed twice with 700 µL ETR buffer (10.000 xg, 1 min, RT) and spin dried. The DNA was eluted using 250 µL H_2O. The isolated plasmid was used for cell transfection.

3.6.2. Generation of constructs harboring point mutation in 3'UTR of target mRNA

3.6.2.1. Preparation of point-mutated 3'UTR insert

3'UTR constructs containing destroyed putative miRNA binding sites were generated by inserting point mutations at the position 2, 4 and 6 of the miRNA seed region. For the PCR amplification of 3'UTR harboring the mutated binding site, a forward and reverse primer containing the mutations were generated (Tab. 3.10). Two PCRs were performed with one of the flanking primers and the primer harboring the mutated binding site.

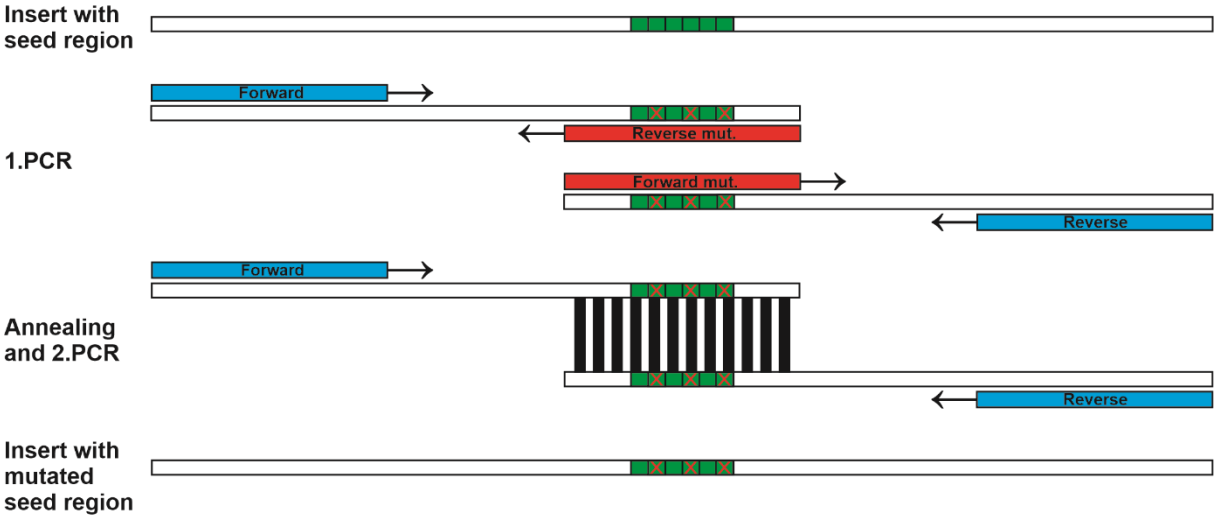

Figure 3.2 ***Generation of point-mutated 3'UTR insert.*** *Flanking primers of the 3'UTR (blue) and primers containing the mutations (red) were used to generate two fragments. After annealing and amplification of the two fragments, the 3'UTR insert containing the mutated seed region was generated.*

The PCR program was performed as shown above for the amplification of the wildtype 3'UTR. The PCR products were cleaned by agarose gel electrophoresis and isolated using the QIAquick Gel Extraction Kit (Qiagen). After gel extraction, the two PCR fragments were annealed in a molar ratio of 1:1. After heating to 98°C for 10 min, the mixture was then slowly cooled down to 28°C (-1°C/min) and rapidly cooled down 4°C. Afterwards, the following reagents were added to the annealing mix:

Reaction mix:

Annealing mix	20.5 µL / 17.5 µL
Thermopol 10x reaction buffer /Phusion HF 5x buffer	2.5 µL / 5 µL
dNTPs (10 µM)	1 µL
Taq / Phusion Polymerase	0.25 µL / 0.3 µL
H_2O	ad 25 µL

The reaction mix was incubated for 15 min at 68°C or 72°C. Afterwards, the inserts were amplified with the flanking primer in a second PCR. The PCR was performed with an annealing temperature of 50°C.

Full-length amplification mix of mutated 3'UTR:

Reaction mix	25 µL
Flanking forward primer (10 µM)	1 µL
Flanking reverse primer (10 µM)	1 µL
Thermopol 10x reaction buffer/ Phusion HF 5x buffer	0.5 µL/ 1 µL
H_2O	2.5 µL/ 2 µL

The full-length PCR product were loaded into an agarose gel and isolated by the QIAquick Gel Extraction kit (Qiagen). To ensure the right insertion of mutations, the PCR product was sequenced.

Table 3.10 ***Primer for mutated 3'UTR amplification***

Primer name	**Sequence 5' → 3'**
pMIR-Report/TK_*NPNT*_101-3p forward	GGAAGAAGTTATCCAAAGTAGTATGTAA
pMIR-Report/TK_*NPNT*_101-3p reverse	TAATAAACAAGATGTTACATACTACTTTGG
pMIR-Report/TK_*Sparc*_29a-3p first forward	CCTGGGGATAAGATCCGAACATA
pMIR-Report/TK_*Sparc*_29a-3p first reverse	ATTCAGTTAAATCTATGTTCGGATCTTAT
pMIR-Report/TK_*Sparc*_29a-3p second forward	TAACTGAATACATTAACGATCCGAAA
pMIR-Report/TK_*Sparc*_29a-3p second reverse	CTTTGTTTTTTTTTTTTTTTCGGATCGTTA

pMIR-Report/TK_*SPARC*_29a-3p first forward	GCCTGGAGACAAGATCCGAACA
pMIR-Report/TK_*SPARC*_29a-3p first reverse	TTCACTTAAATCTATGTTCGGATCTTGT
pMIR-Report/TK_*SPARC*_29a-3p second forward	ATTAACGATCCGAAAAATGAAAATTCTAAC
pMIR-Report/TK_*SPARC*_29a-3p second reverse	GTTAGAATTTTCATTTTTCGGATCGTT
pMIR-Report/TK_*VegfA*_503-5p forward	GATTCGCCATTTTCTTATATCTGATCCAA
pMIR-Report/TK_*VegfA*_503-5p reverse	GGGCTTGGCGATTTTGGATCAGAT
pMIR-Report/TK_*VEGFA*_503-5p forward	CTTGATCCAAAATCACCGAGCC
pMIR-Report/TK_*VEGFA*_503-5p reverse	GGGCTCGGTGATTTTGGATCAAGAA

After digestion with the used restriction enzymes, the insert was ligated into the pMIR-vector. Ligation of mutated 3'UTR insert and the pMIR-vector was performed according to the same protocol of the wildtype 3'UTR. Electroporation, plasmid isolation and screening for positive clones were also performed according to the described protocol in chapters 3.6.1.4-6.

3.6.3. Generation of plasmid construct harboring overexpressed miRNA

3.6.3.1. Preparation of vector

As a vector for constructs harboring overexpressed miRNA, a modified pSuper plasmid was used (see 3.1.7). In the plasmid the puromycin resistance was replaced by a kanamycin resistance.

The plasmid was digested by *Hind*III-HF and *Bgl*II in two separate steps.

First digestion of pSuper plasmid:

pSuper plasmid	5 µg
CutSmart 10x buffer	5 µL
*Hind*III-HF [20 U/ µL]	2.5 µL
H_2O	ad 50 µL

The first digesting mixture was incubated for 1h at 37°C. Before the second digestion, the mixture was dialyzed in a petri dish filled with water on a dialysis filter paper for 1h at RT.

Second digestion of pSuper plasmid:

pSuper plasmid/*Hind*III-HF	44 µL
10x NEBuffer 3.1	5.5 µL
*Bgl*II [10 U/µL]	5 µL
Alkaline phosphatase	1 µL
H_2O	ad 55 µL

The second digestion was performed for 1h at 37°C. The vector was loaded on a 1 % agarose gel running for 1h at 140 V and subsequently extracted from the gel (see above).

3.6.3.2. Preparation of inserts

The inserts of overexpressed miRNA were designed according to the pSuper manual (Oligoengine). Oligonucleotides containing the hairpin precursor of the mature miRNA sequence are diluted to 3 mg/mL concentration and phosphorylated. The phosphorylated forward and the reverse oligonucleotides were mixed in a molar ratio of 1:1 and annealed. The annealed oligos contain overhangs at both ends corresponding to the restriction sites of the vector backbone.

Oligonucleotide phosphorylation mixture:

Oligonucleotide Forward	1 µL
Oligonucleotide Reverse	1 µL
T4 DNA Ligase 10x buffer	2 µL
T4 PNK	1 µL
H_2O	ad 20 µL

Oligonucleotide phosphorylation mixture was incubated for 45 min at 37°C. For annealing of the oligonucleotides, the mixture was heated to 98°C for 10 min followed by incubation at 70°C for 10 min. Afterwards, the mixture was cooled down to 37°C within 15 min (-2°C/min).

Table 3.11 ***Oligonucleotides for annealing and cloning of pSuper overexpression vector***

Primer name	**Sequence 5' → 3'**
pSuper_135_5p_Forward	GATCCCCTATGGCTTTTTATTCCTATGTGATTCAAGAGATCACATA GGAATAAAAAGCCATATTTTTA
pSuper_135_5p_Reverse	AGCTTAAAAATATGGCTTTTTATTCCTATGTGATCTCTTGAATCAC ATAGGAATAAAAAGCCATAGGG
pSuper_h378a-3p_Forward	GATCCCCACTGGACTTGGAGTCAGAAGGCTTCAAGAGAGCCTTC TGACTCCAAGTCCAGTTTTTTA
pSuper_h378a-3p_Reverse	AGCTTAAAAAACTGGACTTGGAGTCAGAAGGCTCTCTTGAAGCC TTCTGACTCCAAGTCCAGTGGG
pSuper_m378a-3p_Forward	GATCCCCACTGGACTTGGAGTCAGAAGGTTCAAGAGACCTTCTG ACTCCAAGTCCAGTTTTTTA
pSuper_m378a-3p_Reverse	AGCTTAAAAAACTGGACTTGGAGTCAGAAGGTCTCTTGAACCTTC TGACTCCAAGTCCAGTGGG
pSuper_210-3p_Forward	GATCCCCCTGTGCGTGTGACAGCGGCTGATTCAAGAGATCAGCC GCTGTCACACGCACAGTTTTTA
pSuper_210-3p_Reverse	AGCTTAAAAACTGTGCGTGTGACAGCGGCTGATCTCTTGAATCA GCCGCTGTCACACGCACAGGGG

pSuper_615-3p_Forward	GATCCCCTCCGAGCCTGGGTCTCCCTCTTTTCAAGAGAAAGAGGGAGACCCAGGCTCGGATTTTTA
pSuper_615-3p_Reverse	AGCTTAAAAATCCGAGCCTGGGTCTCCCTCTTTCTCTTGAAAAGAGGGAGACCCAGGCTCGGAGGG
pSuper_615-5p_Forward	GATCCCCGGGGGTCCCCGGTGCTCGGATCTTCAAGAGAGATCCGAGCACCGGGGACCCCCTTTTTA
pSuper_615-5p_Reverse	AGCTTAAAAAGGGGGTCCCCGGTGCTCGGATCTCTCTTGAAGATCCGAGCACCGGGGACCCCCGGG
pSuper_h101-5p_Forward	GATCCCCCAGTTATCACAGTGCTGATGCTTTCAAGAGAAGCATCAGCACTGTGATAACTGTTTTTA
pSuper_h101-5p_Reverse	AGCTTAAAAACAGTTATCACAGTGCTGATGCTTCTCTTGAAAGCATCAGCACTGTGATAACTGGGG
pSuper_m101a-5p_Forward	GATCCCCTCAGTTATCACAGTGCTGATGCTTCAAGAGAGCATCAGCACTGTGATAACTGATTTTTA
pSuper_m101a-5p_Reverse	AGCTTAAAAATCAGTTATCACAGTGCTGATGCTCTCTTGAAGCATCAGCACTGTGATAACTGAGGG

3.6.3.3. Ligation of insert and vector

The ligation reaction, which contains 0.2 mg/mL of the pSuper vector, 2 µL of the annealed oligonucleotide-mixture, 1 µL of T4 DNA Ligase 10x buffer and 1 µL T4 DNA ligase, was incubated overnight in a 16°C water bath slowly cooled down to 4°C. As negative control, a ligase reaction mixture was performed with a linearized vector alone and without insert. The next day, the ligation reaction was deactivated by incubation at 65°C for 10 min and dialyzed on a dialysis filter paper. Electroporation was performed with electrocompetent *E. coli* suspension and cell suspension was plated on LB agar plates containing kanamycin as selection.

3.6.3.4. Screening of positive clones using colony-PCR

On the next day, colonies were picked from the plates and used for colony-PCR. Thereby, colonies were lysed in 50 µL H_2O by heating to 95°C for 5 min. After centrifugation, 20 µL of the supernatant was used as DNA template for the PCR reaction with primer against the pSuper vector. As a positive control a pSuper vector with an insert was used, and as negative control an empty vector. The colonies were cultured in 4 mL LB-medium containing kanamycin in parallel.

Colony-PCR mixture:

Plasmid DNA	21 µL
Thermopol 10x reaction buffer	2.5 µL
Primer T7 (10 µM)	0.25 µL
Primer M13 (10 µM)	0.25 µL

dNTPs (10 mM)	0.5 µL
Taq Polymerase	0.5 µL

Table 3.12 ***Amplification program for colony-PCR***

Denaturation of DNA	95°C	30 sec	
Denaturation of amplicon	95°C	30 sec	35 cycles
Annealing	50°C	30 sec	
Elongation	68°C	30 sec	
Final Elongation	68°C	2 min	

3.6.3.5. Overexpression test by qPCR analysis

Successful overexpression was tested by qPCR analysis. For this, HEK293T cells were transfected with the pSuper control or respective miRNA pSuper plasmid and harvest 24 h later. After isolation of small RNA (see 3.4.2.1) and additional cDNA synthesis (see 3.4.2.3), qPCR analysis was performed (see 3.4.2.4). Relative miRNA expression was compared to expression level of cells transfected with control pSuper. snRNA U6 was used as internal standard.

3.7. Luciferase assay

To investigate putative miRNA-mRNA interactions predicted by *in silico* predictions, luciferase assays were performed.

3.7.1. Seeding and transfection of cells

HEK293T cells were seeded with a density of 50.000 cells per well in a 24 well plate. After 24h, for each well a mixture containing 200 ng luciferase plasmid and 300 ng pSuper plasmid in 100 µL DMEM medium was prepared. After adding 2 µL Turbofect transfection reagent, the mixture was incubated for 20 min at RT. Afterwards, the mix was added to the wells and incubated again for 24h. For each condition, six biological replicates were transfected on three different days. Each of these replicates,

was performed in three technical replicates. Additionally, a transfection control using a pVMVd2eGFP-vector was added for each plate, which was used for background correction.

3.7.2. Harvesting of the transfected cells

After 24h, cells were washed with 1x PBS and lysed with 70 µL 1x passive lysis buffer (Promega). After shaking for 15 min at RT, lysates were collected and centrifuged at 14.000 rpm for 10 min at 4°C. Supernatant was transferred in a new tube and stored at -80°C.

3.7.3. Luciferase assay measurement and analysis

To analyze mRNA-miRNA interaction by luciferase assay, 3 µL of cell lysate were mixed with 22 µL H_2O and pipetted onto a 96 well plate. Three technical replicas were measured for each biological replicate. Firefly and renilla luminescence were measured with a luminometer (Berthold). First, 20 µL of firefly luciferase substrate was injected into each well and firefly luminescence was measured after a delay of 3 sec. Afterwards, 20 µL of renilla luciferase substrate was injected and renilla luminescence was measured after a delay of 3 sec.

For analysis, the background of non-transfected cells was subtracted from the measured values of the transfected cells. Then, the ratio of firefly luminescence intensity to renilla luminescence intensity was calculated.

4. Results

4.1. Investigation of miRNA-mRNA interactions

In previous studies potential miRNA regulated target genes were identified by Baumgarten et al. (unpublished). In context of this work, nine putative interactions between miRNAs and their target mRNAs were analyzed:

Arrdc3 – miR-19b-3p

Fosb – miR-374b-5p /miR-19b-3p

Npnt – miR-101b-3p

Serinc3 – miR-340-5p

Sparc – miR-29a-3p

VegfA – miR-503-5p

Per1 – miR-29a-3p

Zfp36 – miR-29a-3p

Stt3a – miR-340-5p

4.1.1. Generation of required constructs for luciferase assay

For investigation of putative miRNA-mRNA interactions using luciferase assays, the required constructs were generated as described in 3.6. After PCR amplification, the respective amplicon was extracted and digested with the two restriction enzymes *Spe*I- HF and *Sac*I-HF. Afterwards, the insert was cloned into the modified pMIR-Report plasmid behind the firefly luciferase (see 3.6). The derived constructs are shown in Tab 4.1.

Table 4.1 ***Generated constructs for investigation of miRNA-mRNA interactions by luciferase reporter assay.*** *[1] Primer position in transcript sequence. Primer sequences and full length 3'UTR are shown in the supplement (see Fig. 9.4-9.18).*

mRNA Target	Transcription-ID	Primer position[1]	Amplicon size [bp]	Insert size [bp]	construct name
Arrdc3	ENSMUST00000099356.9	1.471-1.494/2.704-2.728	1.258	1.238	pMIR_3'UTR_*Arrdc3*
ARRDC3	ENST00000265138.4	1.456-1.476/4.144-4.169	2.714	1.297	pMIR_3'UTR_Arrdc3
Fosb	ENSMUST00000003640	2.978-2.998/3.606-3.627	650	641	pMIR_3'UTR_*Fosb*
FOSB	ENST00000353609.8	2.992-3.011/3.617-3.635	644	631	pMIR_3'UTR_Fosb
Npnt_1	ENSMUST00000042744.15	4.324-4.346/4.614-4.629	308	297	pMIR_3'UTR_*Npnt-1*
NPNT_1	ENST00000379987.6	4.259--4.281/4.575-4.602	344	320	pMIR_3'UTR_Npnt-1
Npnt_2	ENSMUST00000042744.15	2.174-2.205/2.374-2.385	212	194	pMIR_3'UTR_*Npnt-2*
NPNT_2	ENST00000379987.6	3.902-3.923/4.158-4.179	278	262	pMIR_3'UTR_Npnt-2
Serinc3	ENSMUST00000017851.3	1.521-1.543/2.492-2.518	998	976	pMIR_3'UTR_*Serinc3*
SERINC3	ENST00000342374.5	1.525-1.544/2.439-2.460	936	924	pMIR_3'UTR_Serinc3
Sparc	ENSMUST00000018737.12	1.197-1.219/1.947-1.964	758	735	pMIR_3'UTR_*Sparc*
SPARC	ENST00000231061.9	965-987/1.705-1.722	758	745	pMIR_3'UTR_Sparc

VegfA	ENSMUST00000142351.8	1.573-1.593/1.904-1.923	351	339	pMIR_3'UTR_*VegfA*
VEGFA	ENST00000372067.7	1.591-1.611/2.174-2.199	486	465	pMIR_3'UTR_VegfA
Per1	ENSMUST00000021271.13	4.055-4.078/4.670--4.692	637	621	pMIR_3'UTR_*Per1*
Zfp36	ENSMUST00000051241.6	985-1.005/1.761-1.784	800	785	pMIR_3'UTR_*Zfp36*
STT3A	ENST00000392708.9	2.198-2.224/4.520-4.543	2.346	2.326	pMIR_3'UTR_Stt3a

In case of the human sequence of *PER1* and *ZFP36* as well as the murine sequence of *Stt3a* different approaches like modifications of PCR conditions, use of different polymerases and various primer designs were used. However, sequence could not be amplified.

To identify conserved miRNA binding sites between murine and human 3'UTRs, alignment analysis (see below) was performed for each mRNA and its respective miRNA using NCBI Blast software.

4.1.2. Luciferase assay for confirmation of putative miRNA-mRNA pairs

To confirm possible miRNA interaction with the 3'UTR of the target mRNAs, luciferase reporter assays were performed. Therefore, HEK293T cells were co-transfected with the pMIR-Report plasmid and the pSuper plasmid (see 3.1.7). The pMIR-Report plasmid codes for a firefly luciferase containing the 3'UTR of the target mRNA and an untargeted renilla luciferase, which serves as internal control. The pSuper plasmid of respective miRNA is overexpressed as shRNA and tested beforehand using qPCR analysis (see supplement, Fig. 9.1). For control, cells were transfected with a pSuper construct overexpressing an artificial miRNA based on the CXCR4 sequence (Ebert et al., 2007) to provide comparable environments. For each candidate 3'UTR, six biological replicates are repeated three times (see 3.7). Using an unpaired student's t-test, p-values were calculated for possible miRNA-mRNA pair compared to the respective control.

In each experiment, the transfection efficiency was monitored. HEK293T cells were transfected with a plasmid coding for eGFP and efficiency was controlled by fluorescence microscopy (Fig.4.1). Control transfection displayed a high efficiency (~90 %), which was reproducible in each single experiment.

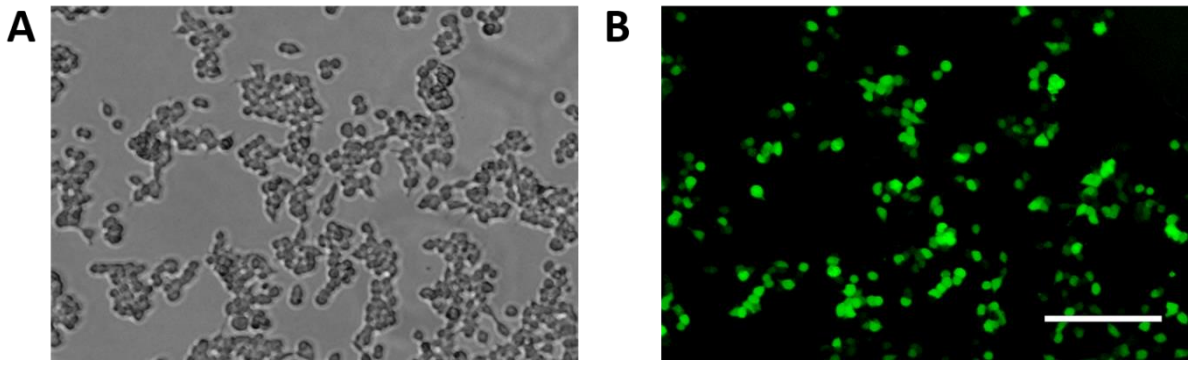

Figure 4.1 ***Transfection efficiency test.*** *HEK293T cells are transfected with plasmid coding for eGFP. (A) transmitted-light picture; (B) fluorescent picture. Scale bar 50 µm*

In the case of significant reproducible miRNA-induced reduction of firefly/renilla ratio for both murine and human constructs, the seed region of the predicted miRNA was mutated at positions 2, 4 and 6. Destruction of the miRNA binding site lead to a derepression of firefly intensity of construct harboring the mutated seed region when compared to the construct with wildtype 3'UTR.

Arrestin domain containing 3 (*Arrdc3*/*ARRDC3*)

The 3'UTR of transcripts *Arrdc3/ARRDC3* consists of 2.616 bp and 2.769 bp, respectively. The front part of the murine transcript was cloned by S. Baumgarten (Tab 4.1) into the pMIR-Report plasmid (see 3.6.1). The human 3'UTR was amplified completely (2.714 bp), but due to internal *Sac*I-restriction site the cloned construct consists only of 1297 bp (front part of the 3'UTR, cloned by S. Baumgarten).

Within the 3'UTR of *Arrdc3/ARRDC3*, two binding sites of the predicted miR-19b-3p exists, which are conserved between the murine and human constructs (Fig. 4.2).

A
```
murine 358   TTCCT---ATTTGAAAATTTGCACATGCTCAATGCTTACATTGTGCAGTTCAGTGTCACT  414
             |||  |   |||||||||||||||||||||||||||||||||||| ||||   ||||||
human  360   TTCTTTTGATTTGAAAATTTGCACATGCTCAATGCTTACATTGTGCGGTTCGACGTCACT  419
```

B
```
murine 926   AGGTGAATGCATCACTTGCCAAACTGTTGGAATGCCGTCTAtgttt-gttgcactgttat  984
             |||||||  ||||||||||||||||||||||||||||  | | |||||  |||||||||||  |
human  894   AGGTGAACGCATCACTTGCCAAACTGTTGGAATGCTATTTGTGTTTTGTTGCACTGTTTT  953
```

Figure 4.2 ***Alignment of 3'UTR of Arrdc3/ARRDC3 containing the binding sites of miR-19b-3p (bold green) at (A) position 373-378/378-383 and (B) 973-978/942-947.***

After co-transfection of HEK293T cells using the murine and human 3'UTR constructs with the respective pSuper overexpressing miR-19b-3p, the ratio of firefly to renilla luciferase luminescence (FLuc/RLuc) was analyzed.

Overexpression of miR-19b-3p lead to a significant reduction of 24 % of firefly luciferase activity of pMIR_3'UTR-*Arrdc3* compared to the control condition, showing an effect of the miRNA on *Arrdc3* expression (Fig. 4.3 A). Coexpression of pSuper_miR-19b-3p had no significant effect (reduction of 8 %) (Fig. 4.3 B) on luciferase intensity of pMIR_3'UTR-*ARRDC3*.

miR-19b-3p seems to regulate the murine *Arrdc3* and within the 3'UTR two binding sites exists. Functionality of both binding sites was not further examined, because repression of luciferase activity was not conserved for murine and human constructs.

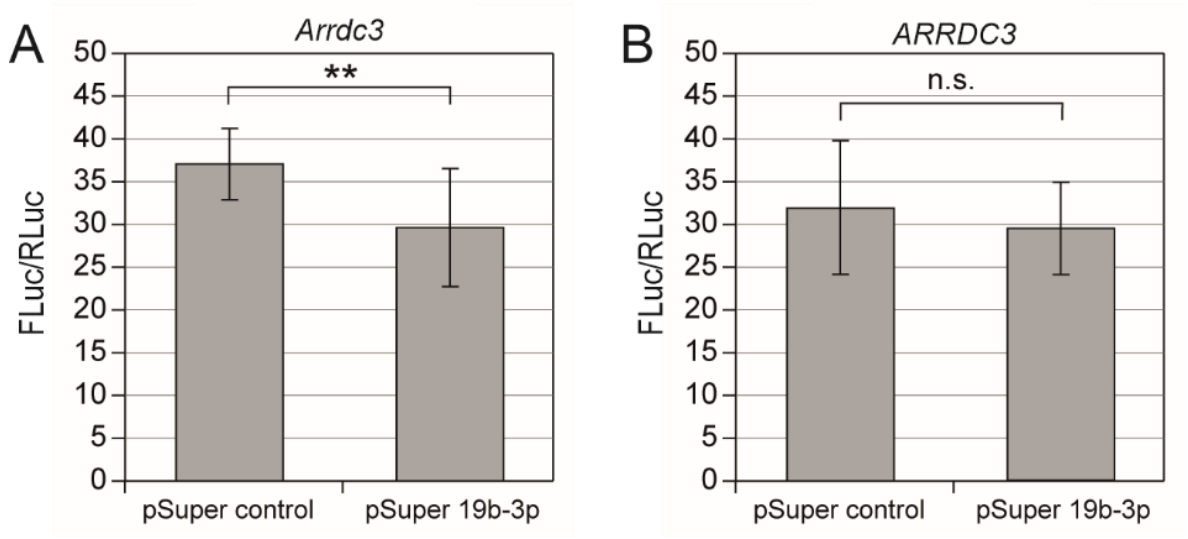

Figure 4.3 ***Luciferase assay of Arrdc3 and ARRDC3 3'UTR****. Cells were transfected with respective pMIR plasmid and either with control or miRNA pSuper construct. (A) pMIR_3'UTR-Arrdc3 and (B) pMIR_3'UTR-ARRDC3 were used for co-transfection of HEK293T cells together with control or overexpressed miR-19b-3p pSuper construct. Data are shown as mean value ± SEM of all samples per condition (n=18), P-value: ** p<0.01; n.s. not significant.*

FBJ osteosarcoma oncogene B (*Fosb*/*FOSB*)

Both 3'UTR of *Fosb* and *FOSB* consists of length of 2.145 bp and 2.167 bp, respectively. Over almost the complete 3'UTR length, high homology was observed between murine and human sequence. The 5'end of 3'UTR was cloned into the pMIR-Report plasmid, which contain the binding site for the predicted miRNAs (Tab 4.1). pMIR_3'UTR-*Fosb* contains one miR-374b-5p binding site and one miR-19b-3p binding site, while pMIR_3'UTR-*FOSB* contains binding sites for the miR-374b-5p (Fig. 4.4)

```
A murine 1493  CCAGCTATTTATCCCTTTCCTGGTTCCCAAAAAGCACTtatatctattatgtataaataa  1552
               ||||||||||||||||||||||| || ||| ||| ||||||||||||||||||| |||
  human  1525  TTAGCTATTTATCCCTTTCCTGGTTTCCGAAAGGCAATTATATCTATTATGTATAAGTAA  1584

  murine 1553  atatattatatGAgtgtgcgtgtgtgtgcgtgtgcgtgcgtgcgtgcgtgcgtgcg-A  1611
               |||||||||||||  ||||  |||||||||||| ||||| ||| ||| | || |  | |
  human  1585  ATATATTATATGGATGTG--TGTGTGTGCGTGCGCGTGAGTGTGTGAGCGCTTCTGCA  1642

B murine 2005  CTGTATTTGTGAttttttttcattttgtttttttgtatttttGCACCTGACCCCGGGGGTGC  2064
               |||||  |||||            || | ||||||||||||||| ||||||||||||  ||
  human  2043  CTGTACTTGTG-----------GTTCTCTTTTTGTATTTTGCATCTGACCCCGGGGG-GC  2090
```

Figure 4.4 ***Alignment of the 3'UTR of Fosb and FOSB containing (A) the binding sites of the miR-374b-5p (bold dark green) and (B) the binding site of miR-19b-3p (bold green)****. Positions of miR-374b-5p binding sites in 3'UTR sequence: 1557-1562 (murine), 1561-1566 and 1589-1594(human); position of miR-19b-3p binding site in 3'UTR sequence: 2043-2048(murine).*

Co-transfection of HEK293T cells with pMIR_3'UTR-*Fosb* and overexpressed miRNA-pSuper plasmid lead to no significant reduction of firefly activity compared to co-transfected cell with control-miRNA plasmid (Fig. 4.5 A). Presence of miR-19b-3p lead to a small reduction of luminescence ratio (4 %) whereas miR-374b-5p lead to no decreased luminescence intensity in both constructs (Fig. 4.5 A, B).

Taken together, both predicted miRNAs seem to have no effect on the luciferase activity indicating no functional binding sites.

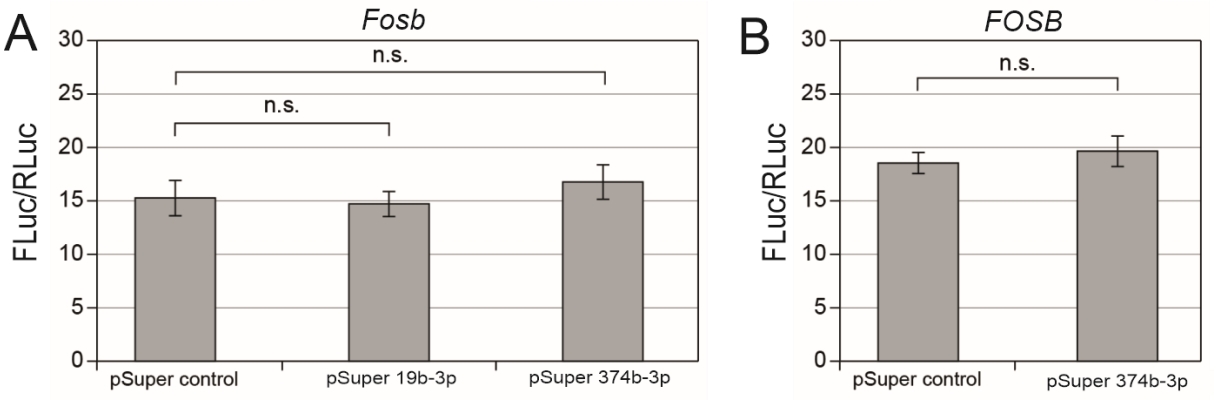

Figure 4.5 ***Luciferase reporter assay of 3'UTR of Fosb/FOSB with respective miRNA or control pSuper****. (A) pMIR_3'UTR-Fosb and (B) pMIR_3'UTR-FOSB were used for co-transfection of HEK293T cells with either control or respective miRNA pSuper plasmid. Data are shown as mean value ± SEM of all samples per condition (n=18), P-value: n.s not significant*

Nephronectin (*Npnt/NPNT*)

The 3'UTR of *Npnt* and *NPNT* both consist of about 2.680 bp and show high sequence similarity. For investigation of the predicted miR-101-3p –*Npnt/NPNT* interaction, the 5'end of both 3'UTRs were cloned into the pMIR-Report plasmid (Tab 4.1, Fig. 4.6).

```
murine 2555  GAAGTTATCCAAAGTACTGTATAACATCTTGTTTATTATTTAATGTTCTCTCAAGTGAGA  2614
             |||||||||||||||||||||||||||||||||||||||||||||||||| ||| || | | |
human  2554  GAAGTTATCCAAAGTACTGTATAACATCTTGTTTATTATTTAATGTTTTCTAAAATAAAA  2613
```

Figure 4.6 ***Alignment of the 3'UTR of Npnt and NPNT containing the binding sites of the miR-101-3p (bold orange) at position 2570-2575/2569-2574 in 3'UTR sequence****.*

The murine construct (297 bp) was cloned and analyzed previously (Baumgarten et al., unpublished), showing a significant reduction of firefly luminescence through the mmu-miR-101b-3p. For the human construct, consisting of 320 bp, a significant reduction of luciferase activity about 16 % compared to the control was measured (Fig. 4.7 A).

To verify the interaction, miR-101-3p binding site in the 3'UTR of *NPNT* was destroyed (see 3.6.2). Luciferase reporter assay showed in presence of miR-101-3p a significant and reproducible derepression of 17 % of luciferase activity for the constructs harboring the destroyed miRNA seed region compared to wildtype construct (Fig. 4.7 B).

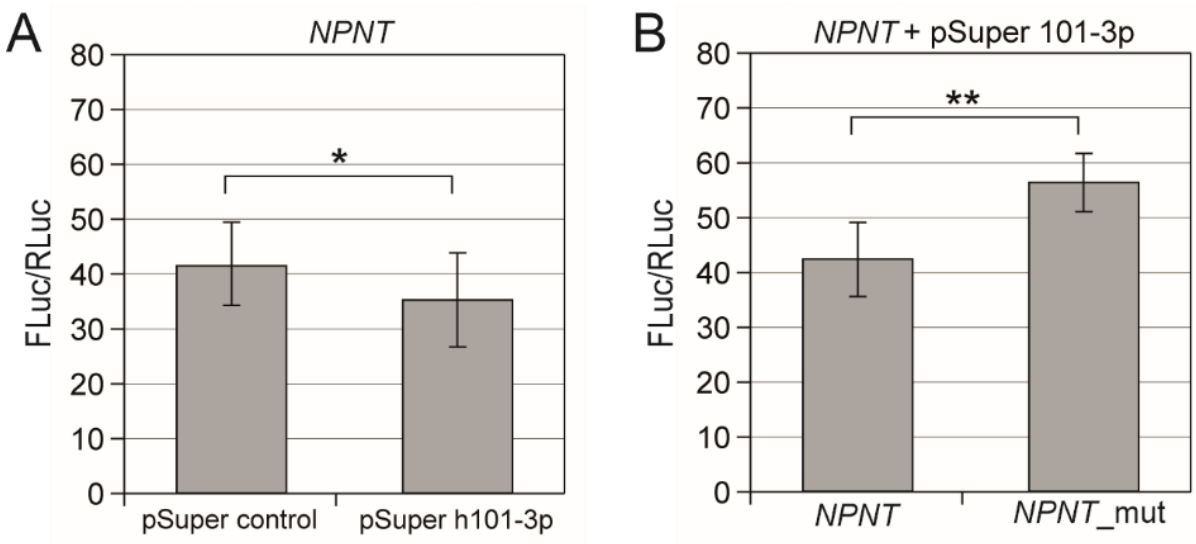

Figure 4.7 ***Luciferase assay of wildtype and mutated NPNT 3'UTR.*** *(A) pMIR_3'UTR-NPNT-1 was used for co-transfection of HEK293T cells with control or miR-101-3p pSuper construct. (B) Binding site of miR-101-3p was destroyed by insertion of mutation in 3'UTR of NPNT; luminescence intensity of construct harboring mutated seed region was compared to pMIR_3'UTR-NPNT. Data are shown as mean value ± SEM of all samples per condition (n=18), P-value: n.s not significant, ** p<0.01*

In 2017, Müller-Deile demonstrated a specific downregulation of *NPNT* by the miR-378a-3p, which was observed by luciferase reporter assay in HEK293 cells (Müller-Deile et al., 2017). The previous cloned pMIR_3'UTR-*Npnt-1* contained the predicted binding site by Müller-Deile and was used to analyze the binding site of miR-378a-3p at position 2480-2485 (Fig. 4.8 A). For the binding site at position 365-370, a construct of 194 bp containing the 5'end of murine 3'UTR was cloned (pMIR_3'UTR-*Npnt-2*, Tab 4.1). For the interaction between the human *NPNT* 3'UTR and pSuper_miR-378a-3p, a 262 bp long construct was cloned into the pMIR-Report plasmid containing the predicted binding site by Müller-Deile (Fig. 4.8 B).

A murine 2435 tttttAATGATTCATTTCCTTCTTGGTCATGTAACTGCACAGCTG**A**T**T**CAGAAGAAAGGG 2494

murine 336 CAT------TCTGTGCAAATGG-TATTCTGTGATCT**GTCCAG**TGTTGTACCATGAGTAGT 388

B human 2101 TTTCAGAttttttttttttttAAGAGATCCTTCAAGGAACACA**GT**T**CAG**AGAGATTTTCAT 2160

Figure 4.8 ***3'UTR of Npnt/NPNT containing the binding sites of the miR-378a-3p (bold black).*** *(A) Binding site in pMIR_3'UTR-Npnt-1 at position 2480-2485 was predicted by Müller-Deile et al. (2017), while binding site at position 365-370 in pMIR_3'UTR-Npnt-2 was found by own scanning. (B) Binding site of miR-378a-3p in pMIR_3'UTR-NPNT-2 at position 2143-2148. Red indicating mismatch letter.*

For both murine and human constructs, no reduction of luminescence intensity was measured compared to the control (Fig. 4.9).

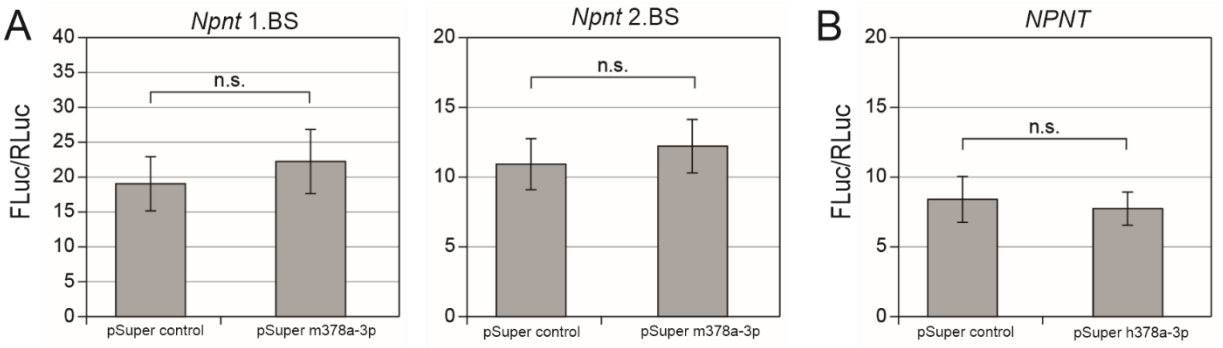

Figure 4.9 ***Luciferase reporter assay of 3'UTR of Npnt/NPNT with pSuper_miR-378a-3p or control****. (A) Constructs containing either the binding site at position 2481-2486 or 365-370 of miR-378a-3p were used for co-transfected of HEK293T cells with the respective miRNA construct. (B) pMIR_3'UTR-Npnt-2 was used for co-transfection of HEK293T cells with miR-378a-3p or control pSuper construct. Data are shown as mean value ± SEM of all samples per condition (n=18), P-value: n.s not significant*

Taken together, a regulatory interaction between the miR-101-3p and the human transcript was demonstrated as shown previously for the murine transcript. By destroying the seed region of the miRNA, no more binding was observed showed by derepression of luminescence compared to the

construct harboring the wildtype 3'UTR. The reported interaction between the human *NPNT* and the miR-378a-3p by Müller-Deile et al. (2017) could not be confirmed, at least under the chosen conditions.

Serine incorporator 3 (*Serinc3*/*SERINC3*)

To investigate the putative interaction between *Serinc3*/*SERINC3* and the miR-340-5p, the first part of the 3'UTR was cloned into the pMIR-Report plasmid. The 3'UTR of *Serinc3* has a total length of 2.168 bp and the *SERINC3* a length of 2.855 bp. Within the 3'UTR of *Serinc3* three binding sites of miR-340-5p exists, with the first two being conserved at the same position with the human 3'UTR. The pMIR_3'UTR-*SERINC3* contains a total of four miR-340-5p binding sites (Fig. 4.10).

```
murine 121  CAGGTTTATATCAAAAGGCAAGATTGAGTAATGCTTGATGCAGAATCTGAGCTT-TCata  179
            ||||||||||||| ||||  ||||||| ||||||||||||||||||  | ||| ||||
human  123  CAGGTTTATATCAGAAGGTGAGATTGAATAATGCTTGATGCAGAATCGAAACTTCTCATT  182

murine 300  AAGAGAATTCTTTATAAAGACCTGTAGATTCCTACAACTTTGGTTTAAGTTTTAAGTTAG  359
            |||||| ||||||||||||| ||||||| ||| |  |||||||||||||  | |||| |||
human  264  AAGAGAGTTCTTTATAAAG-CCTGTAGGTTCTTTTAACTTTGGTTTAAAATGTAAGATAG  322

murine 360  AAGATTGTTGGATATTTAAGGCTATTTTTA----ATTTCTATTACAGTCTCCTTAAAAAC  415
             | | ||||||||||||| |||| ||  |||    |||| |||| |||| ||||| ||||
human  323  GAAAATGTTGGATATTTGAGGCCATGCTTAATATATTTTATATTGCAGTATCCTTTAAAAG  382

murine 545  TTGAGTTCCTTTACTTACTTTTTATAC----TA-CACTGATGCTGCTTGATAGAAGTCTG  599
            |||||||  || | ||||||||| |||    || || |||  |||||||||  |||||||
human  569  TTGAGTTTTTTAATTTACTTTTTTTACACTGTAGCATTGAGACTGCTTGATTCAAGTCTG  628

human  841  AGCTTTTATAGTTAGCAGCCATTCTTTATTTTCTGGATAGCCAGGTTTTATCACGCTTCT  900
```

Figure 4.10 ***Alignment of the 3'UTR of Serinc3 and SERINC3 containing the binding sites of the miR-340-5p (bold purple).*** *The first two binding sites are conserved at the same position (125-130/127-132 and 310-315/274-279) between the murine and human construct. Further positions of miR-340-5p: 565-570 (murine), 358-363 and 845-850 (human).*

For luciferase reporter assay, cloned constructs (Tab 4.1) were used for co-transfection of HEK293T cells with either the pSuper control plasmid or the pSuper miR-340-5p plasmid. In the pMIR_3'UTR-*Serinc3* no marked reduction of luciferase activity (4 %) was shown, suggesting no effect of the miR-340-5p. For the human construct a significant reduction of luciferase activity of 10 % was observed compared to the control.

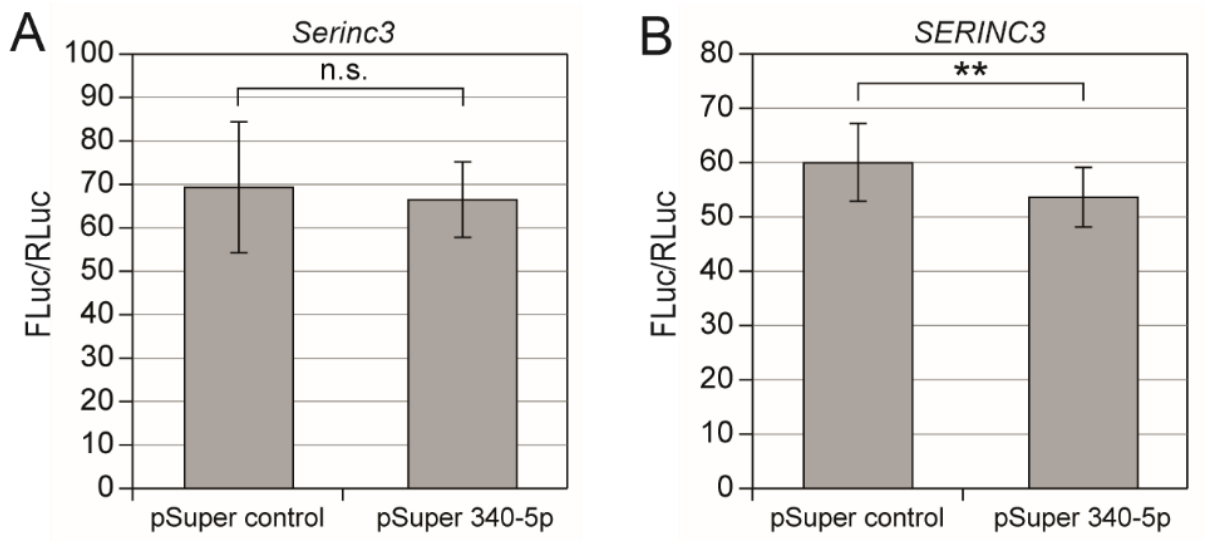

Figure 4.11 ***Luciferase reporter assay of 3'UTR of Serinc3/SERINC3 with respective miRNA or control plasmid****. (A) pMIR_3'UTR-Serinc3 and (B) pMIR_3'UTR-SERINC3 were used for co-transfection of HEK293T cells with either control or miR-340-5p pSuper plasmid. Data are shown as mean value ± SEM of all samples per condition (n=18), P-value: n.s not significant, ** p<0.01*

Within the 3'UTR of *Serinc3*/*SERINC3* more binding sites (3/4) of the predicted miR-340-5p exist. Further experiments to reveal functional binding site were not performed due to the effect of the miR-340-5p only on the human *SERINC3*.

Secreted acidic cysteine rich glycoprotein (*Sparc*/*SPARC*)

The 3'UTR of *Sparc* shows high sequence homology with the human transcript and each contain two binding sites of the miR-29a-3p (Fig. 4.12). Almost the complete length of the murine 3'UTR and the first half of the human 3'UTR was cloned into the pMIR-Report plasmid (Tab 4.1).

```
murine 120  CTGTTCCGCCTGGGGATAAGGTGCTAACATAGATTTAACTGAATACATTAACGGTGCTaa  179
            |||||  ||||||  ||  ||||||||||||||||||||  ||||||||||||||||||||
human  114  TTGTTCTGCCTGGAGACAAGGTGCTAACATAGATTTAAGTGAATACATTAACGGTGCTAA  173
```

Figure 4.12 ***Alignment of the 3'UTR of Sparc/SPARC containing the binding sites of the miR-29a-3p (bold cyan).*** *Position of binding sites in murine and human 3'UTR: 139-144/133-138 (1 binding site) and 172-177/166-171 (2.binding site).*

Overexpression of miR-29a-3p lead to significant reduced luminescence intensity in both murine and human 3'UTR of *Sparc*/*SPARC* (Fig. 4.13). Firefly/renilla intensity was reproducible and significantly reduced about 44 % for the pMIR_3'UTR-*Sparc* compared to the control. For the pMIR_3'UTR-*SPARC*, luciferase activity was decreased about 34 %, showing a strong effect of miR-29a-3p.

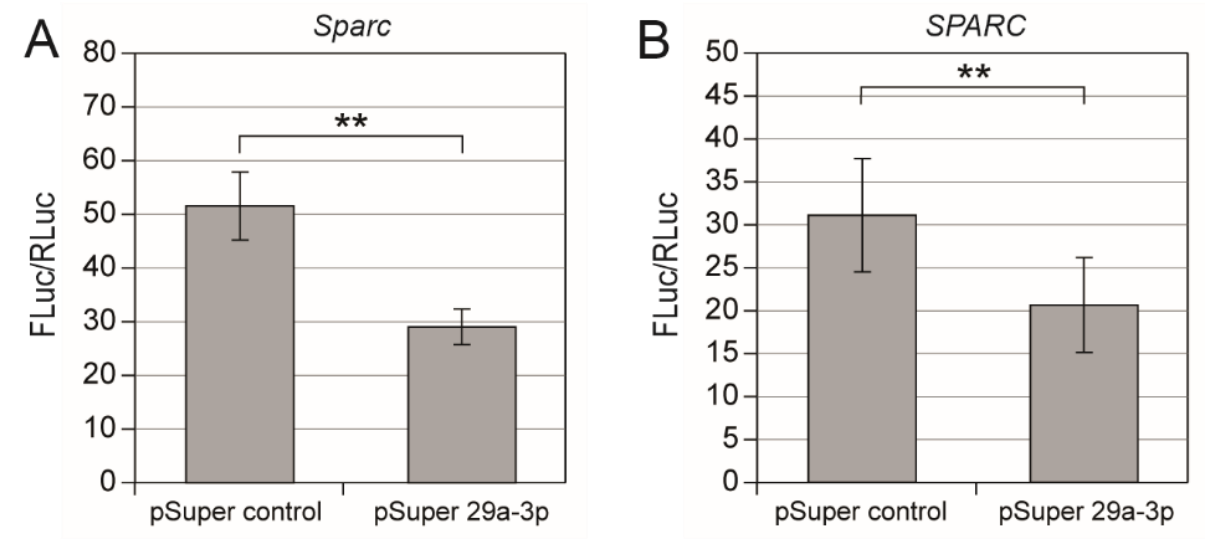

Figure 4.13 ***Luciferase reporter assay of 3'UTR of Sparc/SPARC with respective miRNA or control plasmid****. (A) pMIR_3'UTR-Sparc and (B) pMIR_3'UTR-SPARC were used for co-transfection of HEK293T cells with either control or miR-29a-3p pSuper plasmid. Data are shown as mean value ± SEM of all samples per condition (n=18), P-value: ** p<0.01*

To confirm the predicted seed region of miR-29a-3p, positions 2, 4 and 6 were mutated separately for each binding site. Destroying the first binding site (position 139-144/133-138) lead to a significant increase of luciferase activity by about 28 % for the construct harboring murine mutated 3'UTR and about 41 % for the construct harboring human mutated 3'UTR. About 29 % and 48 % derepression of luciferase activity was measured for constructs containing the mutated second binding site (positon: 172-177/166-171). Deletion of both binding sites had an accumulative effect, leading to a stronger derepression of firefly/renilla intensity about 79 % for murine and 73 % for human construct (Fig. 4.14).

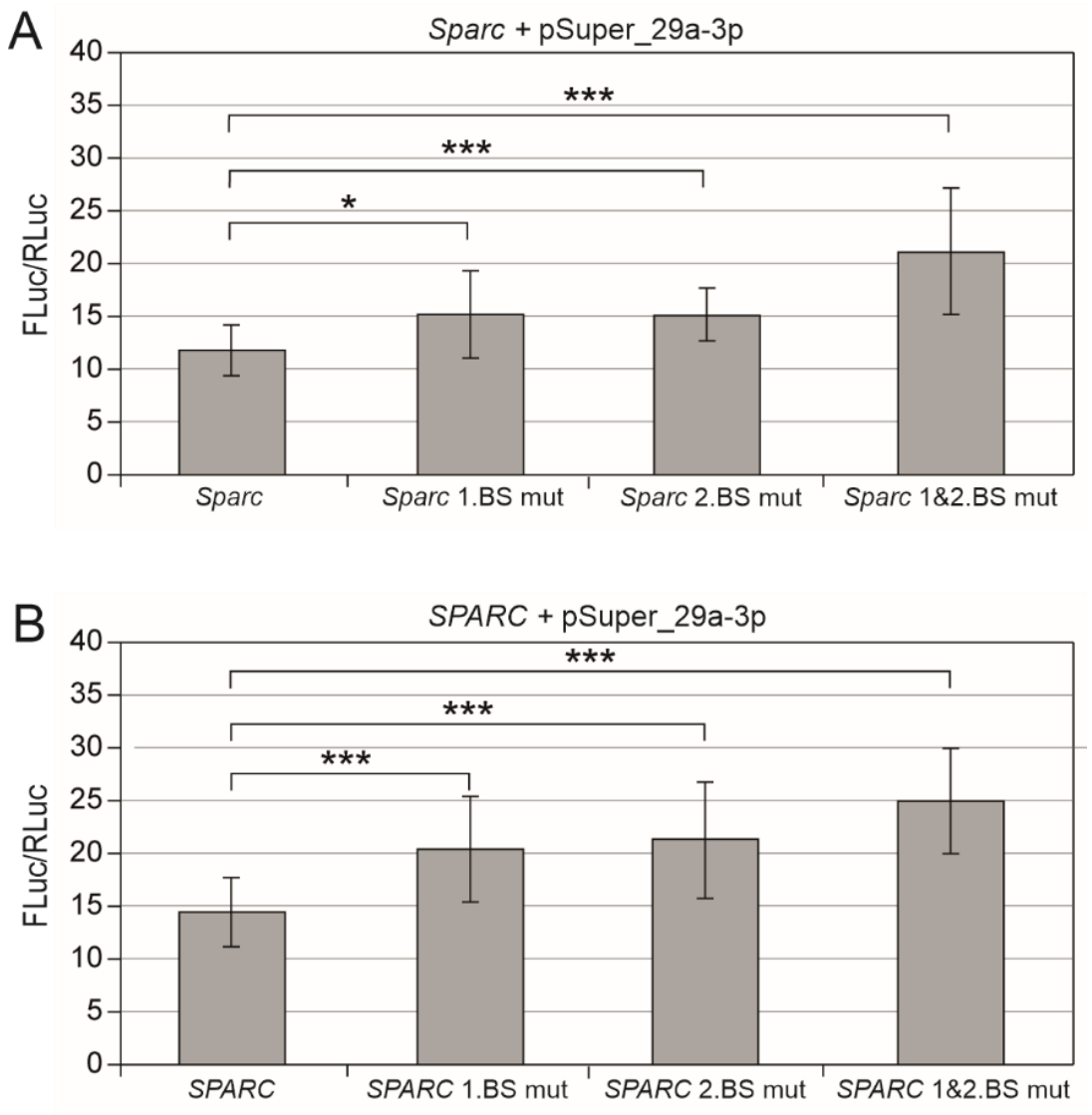

Figure 4.14 ***Luciferase reporter assay of mutated murine and human 3'UTR of Sparc/SPARC****. (A)First binding site, second binding site and both binding sites were destroyed separately in murine construct, (B) first binding site, second binding site and both binding sites were destroyed separately in the human construct. Data are shown as mean value ± SEM of all samples per condition (n=18), P-value: * p<0.05, *** p<0.001, Bonferroni corrected*

Vascular endothelial growth factor A (*VegfA*/*VEGFA*)

The 3'UTR of *VegfA*/*VEGFA* comprises of 315 and 1.947 nucleotides, respectively. Homologue sequence of murine and human 3'UTR (Tab 4.1) containing miR-503-5p seed region were cloned into the pMIR-Report plasmid (Fig.4.15).

```
murine 225  TCCCTCGTGGGACTGGATTCGCCATTTTCTTATATCTGCTGCTAAATCGCCAAGCCCGGA  284
            |||||| ||| | ||||||||||||||| || |   |||||||||||| || ||||||||
human  262  TCCCTCTTGGAATTGGATTCGCCATTTTATTTTTCTTGCTGCTAAATCACCGAGCCCGGA  321
```

Figure 4.15 ***Alignment of the 3'UTR of VegfA/VEGFA containing the binding site of the miR-503-5p (bold blue) at position 272-277/309-314****.*

Luciferase reporter assays performed in presence of miR-503-5p demonstrated a regulatory effect on the murine and human constructs. A significant repression of luciferase intensity of 15 % and 19 % was observed compared to the control (Fig. 4.16), indicating a specific interaction.

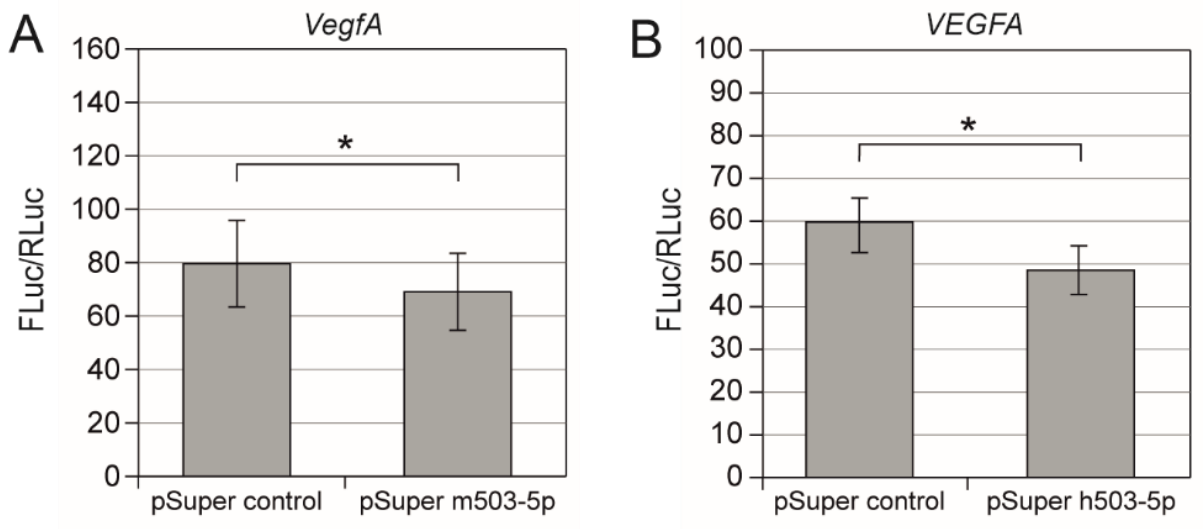

Figure 4.16 ***Luciferase reporter assay of 3'UTR of VegfA/VEGFA with respective miRNA or control****. (A) pMIR_3'UTR-VegfA and (B) pMIR_3'UTR-VEGFA were used for co-transfection of HEK293T cells with either control or miR-503-5p pSuper plasmid. Data are shown as mean value ± SEM of all samples per condition (n=18), P-value: ** p<0.01*

For confirmation of the observed regulation, the seed region of miR-503-5p was destroyed in both of the murine and human 3'UTR. Mutation within the binding site lead to a significant derepression of firefly/renilla intensity of about 8 % for the murine construct harboring mutated seed region compared to the construct containing the wildtype 3'UTR. For the mutated human construct, a derepression of luminescence intensity of about 15 % by the miR-503-5p could be shown compared to the wildtype 3'UTR construct (Fig. 4.17). Taken together, a specific interaction between *VegfA*/*VEGFA* and the miR-503-5p could be verified.

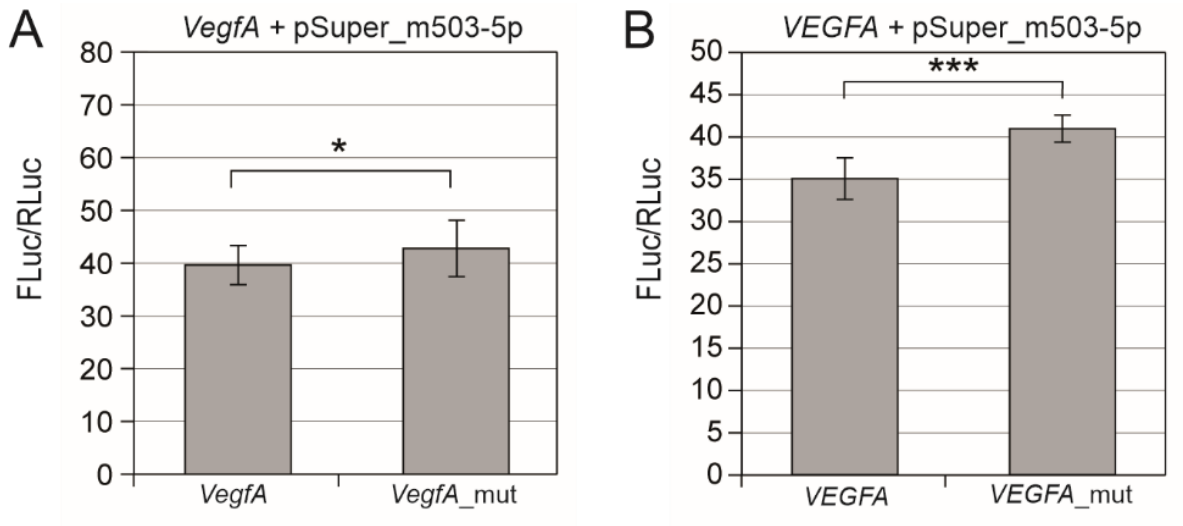

Figure 4.17 ***Luciferase reporter assay of mutated 3'UTR of VegfA/VEGFA****. (A) Seed region of miR-503-5p was destroyed in the murine 3'UTR and (B) in the human 3'UTR. FLuc/RLuc was compared between construct harboring the mutated seed region and the construct with wildtype 3'UTR. Data are shown as mean value ± SEM of all samples per condition (n=18), P-value: * p<0.05, *** p<0.001*

Period circadian protein homolog 1 (*Per1*), Zinc finger protein 36 (*Zfp36*) and subunit of the oligosaccharyl-transferase complex, homolog A (*STT3A*)

The murine transcript of *Per1* contains a 3'UTR with a length of 601 nucleotides, which was cloned completely into the pMIR-Report plasmid (Tab 4.1). For *Zfp36* only the murine 3'UTR was cloned for luciferase assay. For generating the required constructs of human homologue of *PER1* and *ZFP36* different approaches, e.g. modification of PCR condition, different polymerase or primer additions, did not lead to successful cloning.

Both 3'UTR of *Per1*/*PER1* (Fig. 4.18 A) and *Zfp36*/*ZFP36* (Fig. 4.18 B) contain a binding site for the miR-29a-3p, which was predicted by *in silico* predictions.

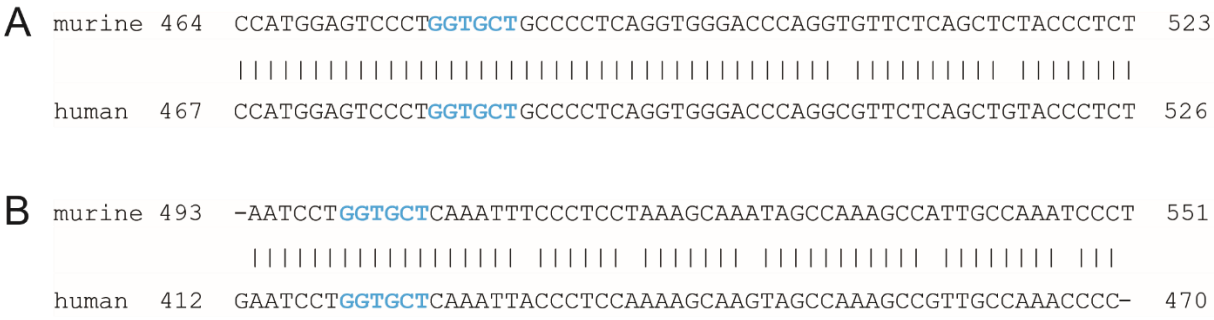

Figure 4.18 ***Alignment of the 3'UTRs of mRNA targets.*** *(A) miR-29a-3p binding site (bold cyan) in Per1/PER1 at position 477-482/480-485. (B) miR-29a-3p binding site (bold cyan) in Zfp36/ZFP36 at position 500-505/419-424.*

In case of the predicted interaction between miR-340-5p and the transcript *Stt3a*/*STT3A*, the human 3'UTR was cloned (Tab 4.1). The complete length of the 3'UTR consists of 2.281 nucleotides, which shows high sequence similarity to the murine 3'UTR. Each species contains four binding sites for the miR-340-5p (Fig. 4.19).

```
murine 73    ---ATATGCAGTTTATAAGAAC--AGCCGGATGGGGTTAGAATTGTCTGCAAGTTTTGCC  127
                |||||||||||  |||||||   | | ||||||   | ||||||||||| ||||||||  |
human  80    TTAATATGCAGTTTGTAAGAACAAAACTGGATGGCATCAGAATTGTCTGGAAGTTTTGTC  139

murine 128   CTGGACAATATGGGCTGGGCCAAGTGAAATGATTTTTATAATTCTGAGCAGGTTACCAAA  187
              |||  ||  ||||||||||||||| |||||||||||||||||||| | ||||||||||||
human  140   TTGGGCAGTATGGGCTGGGCCAAATGAAATGATTTTTATAATTCTAAACAGGTTACCAAA  199

murine 580   T-TCTTTAGAAGCTCTTTGGCTTTATAA  606
             | ||  |||||  ||||||||  ||||||||
human  587   TATCCTTAGACGCTCTTTGACTTTATAA  614

murine 1298   TATGTGCTTAGGTGTACTTGTATACCTAAGG-GCTTTTCCTT-CAAACCGGTGTATGTAC  1355
              ||  ||||   || || ||||||| | | ||  |||  |||| ||||||  | ||| |||
human  1418   TA--TGCTGTTGTATATTTGTATAGCCAGGGCACTTAGCCTTCCAAACCAATTTATATAC  1475

murine 1416   AAATACATTATTTGATTTATATACAGAACTACTGCCTAGTGGGAAAGGTTAACCTGA--G  1473
              || ||||||| ||||||| |||| ||||    |   |||||| | ||||||  ||||
human  1530   AAGTACATTACTTGATTTCTATAAAGAA----TCTTTAGTGGAAGAGGTTATTCTGAATT  1585

murine 1474   ACTTATCAATATGATTAACA----TTACAGGTTATTAGTAAGCTTTCTCTATAGTATAAA  1529
              | ||||||||||||||| |    ||| |  |||||| | | ||| || |||| |||| |
human  1586   ATTTATCAATATGATTAATACCAGTTAGAAATTATTAATGATCTTCCTTTATACTATACA  1645
```

Figure 4.19 ***Alignment of the 3'UTR of Stt3a/STT3A containing the binding sites of the miR-340-5p (bold purple).*** *Position of binding sites in 3'UTR: murine: 84-89, 162-167, 600-605, 1431-1436; human: 174-179, 608-613, 1467-1472, 1633-1638.*

No repression of luminescence intensity was observed for the proteins compared to the control, suggesting no effect of the predicted miRNAs under the chosen conditions (Fig. 4.20).

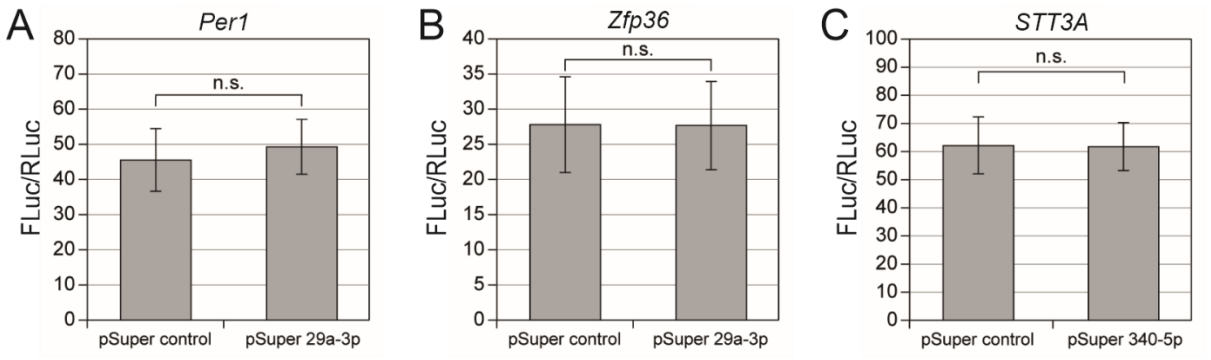

Figure 4.20 ***Luciferase reporter assay of 3'UTR of mRNA targets with respective miRNA or control****. (A) pMIR_3'UTR-Per1 and (B) pMIR_3'UTR-Zfp36 were used for co-transfection of HEK293T cells with control or miR-29a-3p plasmid. (C) pMIR_3'UTR-STT3A was used for co-transfection of HEK293T cells with control or miR-340-5p plasmid. Data are shown as mean value ± SEM of all samples per condition (n=18), P-value: n.s not significant*

In summation, from the nine investigated predictions, three could be demonstrated to be specific and conserved in murine and human: *Npnt/NPNT*, *Sparc/SPARC* and *VegfA/VEGFA* (Tab. 4.2). For two targets only in one species a significant repression of luciferase activity was observed (*Arrdc3*, *SERINC3*). For four targets no regulation could be shown (*Fosb/FOSB*, *Per1*, *Zfp36*, *STT3A*).

Table 4.2 ***Analyzed miRNA-mRNA interactions in podocytes****. ✓: interactions shown, ✓✓: interaction verified by mutation of seed region, x: interactions negatively tested, n.det: interaction not analyzed yet.*

Target 3'UTR	predicted miRNA	conserved binding site	interaction confirmation for transcripts	
			murine	human
Arrdc3/ARRDC3	miR-19b-3p	yes	✓	x
Fosb/FOSB	miR-374b-5p	yes	x	x
	miR-19b-3p	no	x	
Npnt/NPNT	mmu-miR-101b-3p/hsa-miR-101-3p	yes	✓✓	✓✓
	miR-378a-3p	yes	x	x
Serinc3/SERINC3	miR-340-5p	yes	x	✓
Sparc/SPARC	miR-29a-3p	yes	✓✓	✓✓
VegfA/VEGFA	miR-503-5p	yes	✓✓	✓✓
Per1	miR-29a-3p	yes	x	n.det
Zfp36	miR-29a-3p	yes	x	n.det
STT3A	miR-340-5p	yes	n.det	x

4.2. Role of miRNAs for podocyte function and structural maintenance

To further investigate the role of two specific miRNAs for podocyte function and maintenance, mir-30a-5p and mir-146b-5p knockout in hPCLs (human Podocyte cell line) were generated using TALEN genome editing method (Baumgarten, 2017). The immortalized podocyte cell line, derived from isolated human podocytes transfected with retroviral construct coding for the SV40 large T antigen (Saleem et al., 2002), proliferates at 33°C and differentiates for two weeks when cultured at 37°C. TALE (Transcription activator-like effector) nucleases are used for directed genomic knockout of protein coding genes as well as for miRNA knockout. They comprise a non-specific DNA cleaving nuclease fused to a sequence specific DNA binding domain (Joung and Sander, 2013). TALEN pairs, each composed of a sequence specific TALE array (against human genomic locus of either mir-30a-5p or mir-146b-5p) and a part of an unspecific nuclease, binds to the DNA and generates double-strand breaks in the genome.

Knockout cell lines showed abnormalities in podocyte structure compared to control cells, such as missing distinct patterns of specific proteins, size differences and missing arborization (Baumgarten et al., unpublished). To confirm the fact that knockout cells seem to have problems with differentiation, the cell area of the control and knockout cells was determined.

4.2.1. Measurement of cell area using Cell Mask Staining Red HSC

After two weeks of differentiation, hPCL-control and knockout cells were stained with Cell Mask RED HSC and analyzed by fluorescence/confocal microscopy (see 3.5.5). Due to clonal variation, two clones were used for each condition (mir-30a-5p knockout, mir-146b-5p knockout or control).

As already shown by Baumgarten et al. (unpublished) mir-30a-5p and mir-146b-5p knockout cells stayed smaller in size compared to control cells. Both control cells displayed properly differentiated and bigger cells in comparison to both knockout cell lines (Fig. 4.21 A). To verify the difference in size between control and knockout cells, cell area was measured using ImageJ software (see 3.5.5). Unpaired student's t-test revealed significantly smaller knockout cells compared to control cells, indicating that they do not differentiate properly (Fig. 4.21 B).

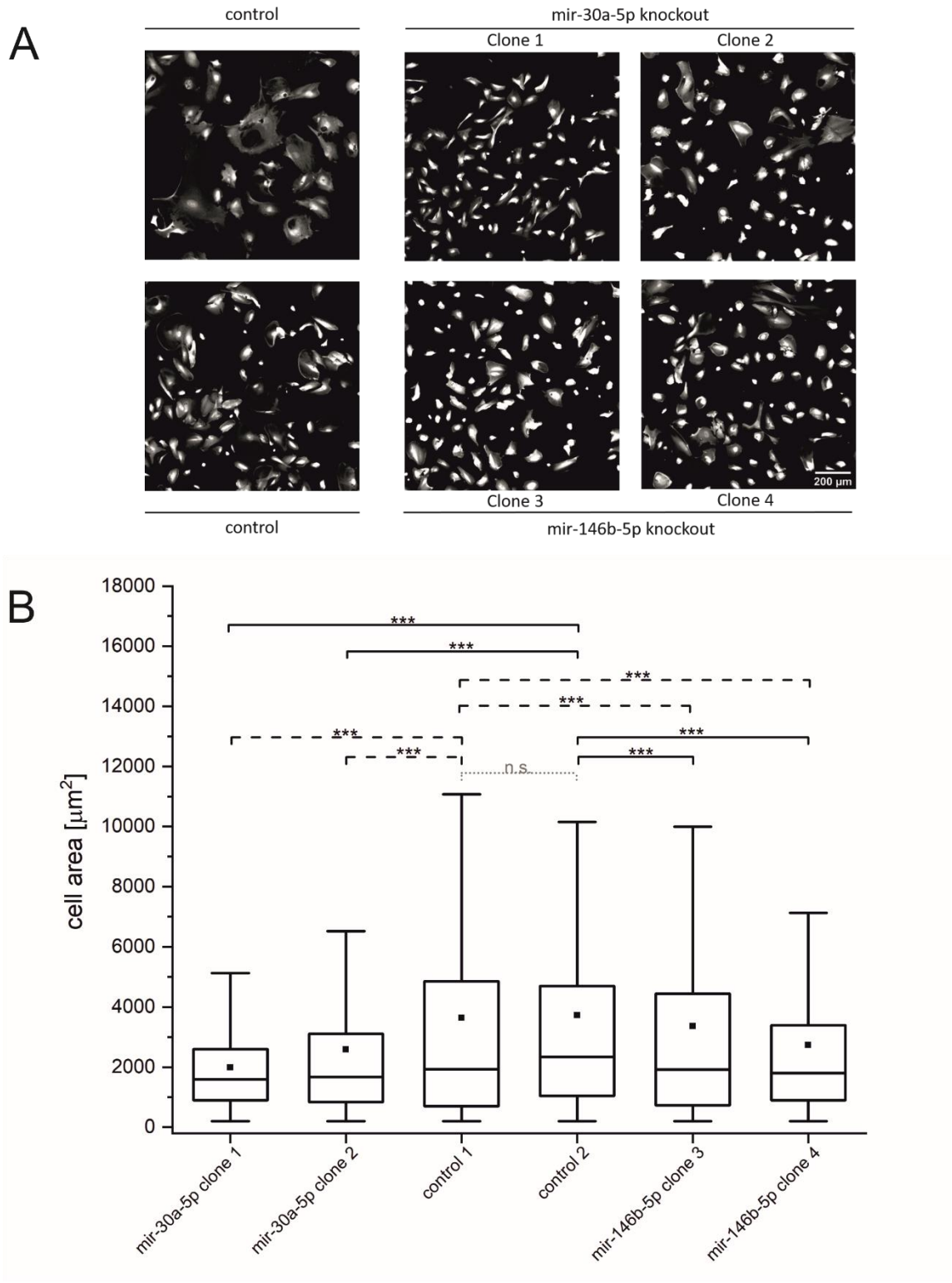

Figure 4.21 ***Cell Mask staining of differentiated hPCL-control and knockout cell lines (A) and cell area measurement (B).*** *Control cell lines were transfected with only on TALEN plasmid. Analysis of three cover slips per cell line. Abbreviations: n.s. not significant, *** p>0.001, Bonferroni corrected*

4.2.2. Rescue experiment using miRNA-mimics

Due to the observed phenotype of hPCL-knockout cells, a rescue experiment was performed. Here, knockout and control cells were transfected with either a control- mimic or a miRNA-mimic. miRNA-mimics are designed to simulate naturally occurring, mature miRNAs and can be used for miRNA-gain-of-function studies (Wang, 2011). They consist of three RNA strands: a guide RNA strand consisting of the sequence of the miRNA and a passenger strand, which is divided into two LNA-enhanced RNA strands (Exiqon). Once introduced into cells, it mimics an endogenous miRNA that can bind to its target genes and perform posttranscriptional regulation.

After two weeks of differentiation, cells were immuno-stained with α-actinin-4 antibody. miRNA-mimic is paired with a GFP-tag allowing the visualization of positive transfection (see 3.5.6 and 3.5.7). To investigate if mimic-transfection allows knockout cells to differentiate properly again, cell area is measured. In a pretrial experiment, different concentrations of miRNA-mimic were tested with one control cell line and the mir-146b-knockout cell line. Mimic-concentration of 10 nM showed no green fluorescent signal, neither in the control nor the knockout cell lines, indicating that the used concentration was too low (data not shown). In cells transfected with 50 nM mimic concentration (Fig. 4.22), α-actinin-4 staining was demonstrated as distinct pattern and a weak GFP signal was observed in some cells (similar in control and knockout cells). However, background noise prevents cell area measurement because a clear separation of cell body and background noise through threshold setting (ImageJ, Analyzing particles) could not be obtained. Using a higher concentration of 100 nM, almost no cells were left on the cover slips indicating that mimic transfection lead to cell death. Remaining cells were not transfected and thus survived (data not shown).

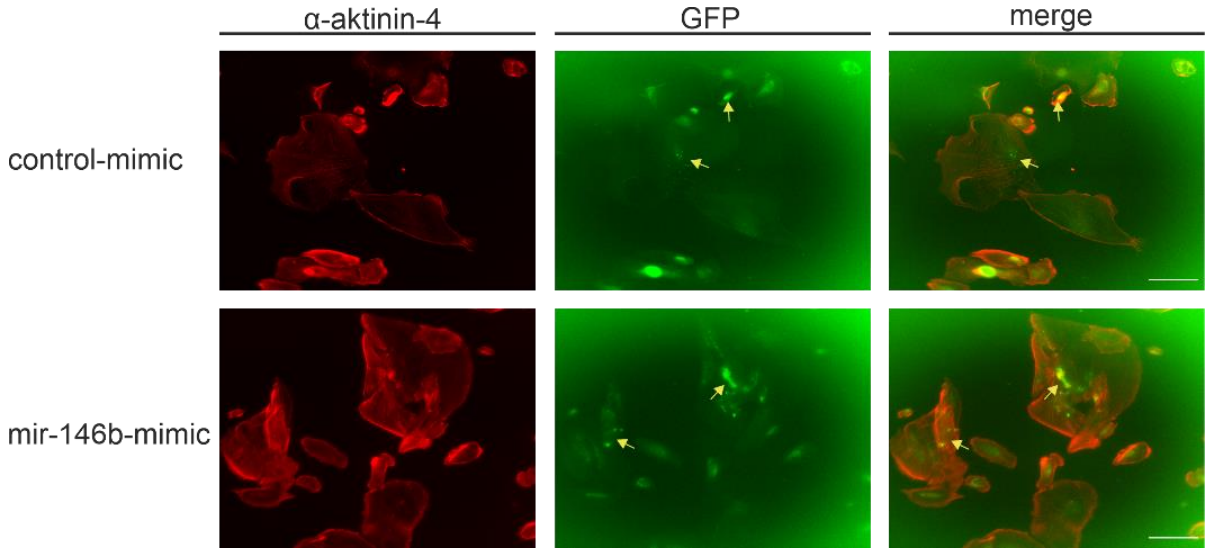

Figure 4.22 ***Immunostaining of mir-146b-5p knockout cell line with control or mir-146b-mimic (50 nM).*** *Representative staining of α-aktinin-4 (red channel) and GFP-tagged mimic (green channel). Yellow arrow indicates positive GFP signal.*

Taken together, knockout cells were not able to differentiate properly and stayed smaller than control cells. Knockout cells showed almost no formation of processes, neither short and rounded nor long, spindle-like projections as described by Saleem et al. (2002).

Pretrial experiments to rescue knockout cells demonstrated that mimic-concentration of 50 nM showed positive GFP signals however, it was very low. Strong background makes it difficult to measure cell area. Higher concentration (100 nM) was toxic for cells leading to massive cell death.

4.3. miRNA-mediated regulation of transcription factor *Lmx1b/LMX1B*

In 2013, it was demonstrated that *Lmx1b* is not only a regulator of miRNAs, but is also regulated by miRNAs itself (Anderegg et al., 2013). In the midbrain, a regulatory negative feedback loop between *Lmx1b* and the miR-135a-2 was shown. To investigate if *Lmx1b* in podocytes is also regulated by miRNAs, *in silico* predictions (miRWalk2) were used to identify putative miRNA binding sites (Zaparty, unpublished).To verify the interactions between *Lmx1b*/*LMX1B* and the predicted miRNAs, luciferase assays were used.

4.3.1. Putative miRNA-mRNA interaction in *Lmx1b*/Lmx1b

In silico analysis predicted five miRNA binding sites for the 3'UTR of *Lmx1b*/*LMX1B*: miR-149-5p, miR-210-3p, miR-615-3p, miR-615-5p, miR-101a-5p and miR-135a-5p.

The longest transcript of murine *Lmx1b* (ENSMUST00000041730.11) comprises a 3'UTR of 3.671 nucleotides, while the human 3'UTR (ENST00000355497.10) consists of 4.581 nucleotides. The murine and human 3'UTR was cloned separately as four fragments into pMIR-Report plasmid containing the binding sites of predicted miRNAs (Fig. 4.23).

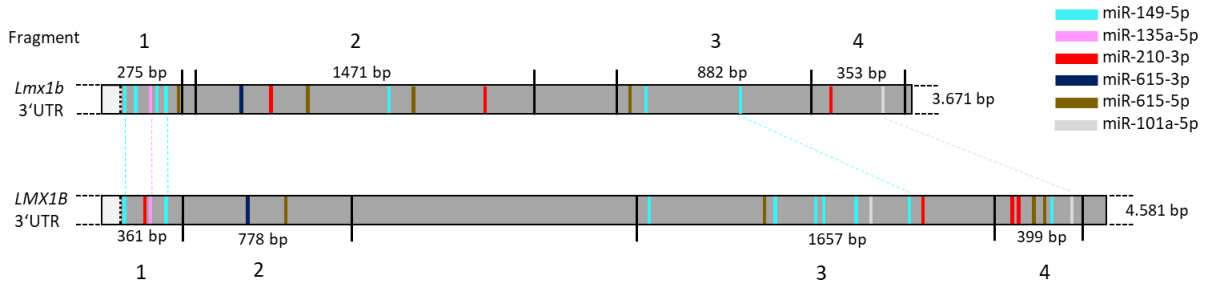

Figure 4.23 ***3'UTR of Lmx1b/LMX1B with cloned fragments****. Inserts containing the predicted binding sites of miR-149-5p (**cyan**), miR-135a-5p (**pink**), miR-210-3p (**red**), miR-615-3p (**blue**), miR-615-5p (**brown**) and miR-101a-5p (**gray**).*

4.3.2. Luciferase assays for screening of putative miRNA regulation

Fragment 1 of murine and human 3'UTR

Cloned insert of murine and human *Lmx1b*/*LMX1B* covers the 5'end of the 3'UTR (position 1.673-1.964/1.627-1.984 bp). Both 3'UTR fragments show high homology over their complete length, but not all predicted binding sites are conserved between the human and murine transcript (Fig. 4.24).

```
murine 1    GAGCCAGCCGGGCCGCATGGACGCTTGGGCCTGGGCCTAGGGTGGA--GCCACAGGCCTC  58
            ||||||||| ||| ||| ||||||||||||  |||||| ||| |||  ||||   |||||
human  1    GAGCCAGCCAGGC-GCACGGACGCTTGGGCAGGGGCCTGGGGGGGGACTGCCA---GCCTC  56

murine 59   TGCAGCCAGCC-GGCC-CCCCAGCCCACCAC-CCGCTCAGACTCTTCAGACAGCCATACG  115
            ||| ||||||| |||| |||| ||||  | | |||| ||||||   ||||||||||||||
human  57   TGCGGCCAGCCTGGCCACCCCCGCCCTGCTCTCCGCACAGACTA--CAGACAGCCATACG  114

murine 116  GTGCCCTCCCCTCGGCCAGCCAGACCTGGCTCAAGTGCCCACCGGGCACAGCCAGGCAAG  175
            ||||||||||||||||||  | |||| |    ||||||   ||| ||||||||  |  |
human  115  GTGCCCTCCCCTCGGCCAGCTGGGCCTGACCACTGTGCCCGTTGGGTACAGCCAGACC-G  173

murine 176  GCAGATGGGTGCAGCCTGGGCAGGGACTGTGTCCTGCCCACAGAGACCTTGTGACCCCTG  235
            | |||||||  |||||||||||||| |||||||||||||||||||||||| | |||
human  174  GTAGATGGGCACAGCCTGGGCAGGGGCTGTGTCCTGCCCACAGAGACCTTGTCATCCCCA  233
```

Figure 4.24 ***Alignment of the 3'UTR fragment of Lmx1b/LMX1B.*** *Predicted seed binding sites are indicated as follows:* ***cyan****: miR-149-5p,* ***pink****: miR-135a-5p,* ***red****: miR-210-3p,* ***brown****: miR-615-5p.*

The overexpression of miR-149-5p seems to have no effect on the luciferase activity of pMIR_3'UTR-*Lmx1b*-1 and pMIR_3'UTR-*LMX1B*-1. In case of the miR-135a-5p, overexpression lead only for the human construct to show a significant reduction of luciferase activity (8 %). Anderegg et al. (2013) demonstrated a strong regulation (~40 %) through miR-135a-5p in murine *Lmx1b*. However, the interaction could not be confirmed within the present work at least under the chosen conditions. For pMIR_3'UTR-*Lmx1b*-1, a repression of luminescence intensity of 6 % was observed by overexpression of miR-135a-5p, however no significant difference to the control was detected. Coexpression of pSuper_miR-615-5p and pMIR_3'UTR-*Lmx1b*-1 showed no effect, as well as co-transfection of cells with pSuper_miR-210-3p and pMIR_3'UTR-*LMX1B*-1 (Fig. 4.25).

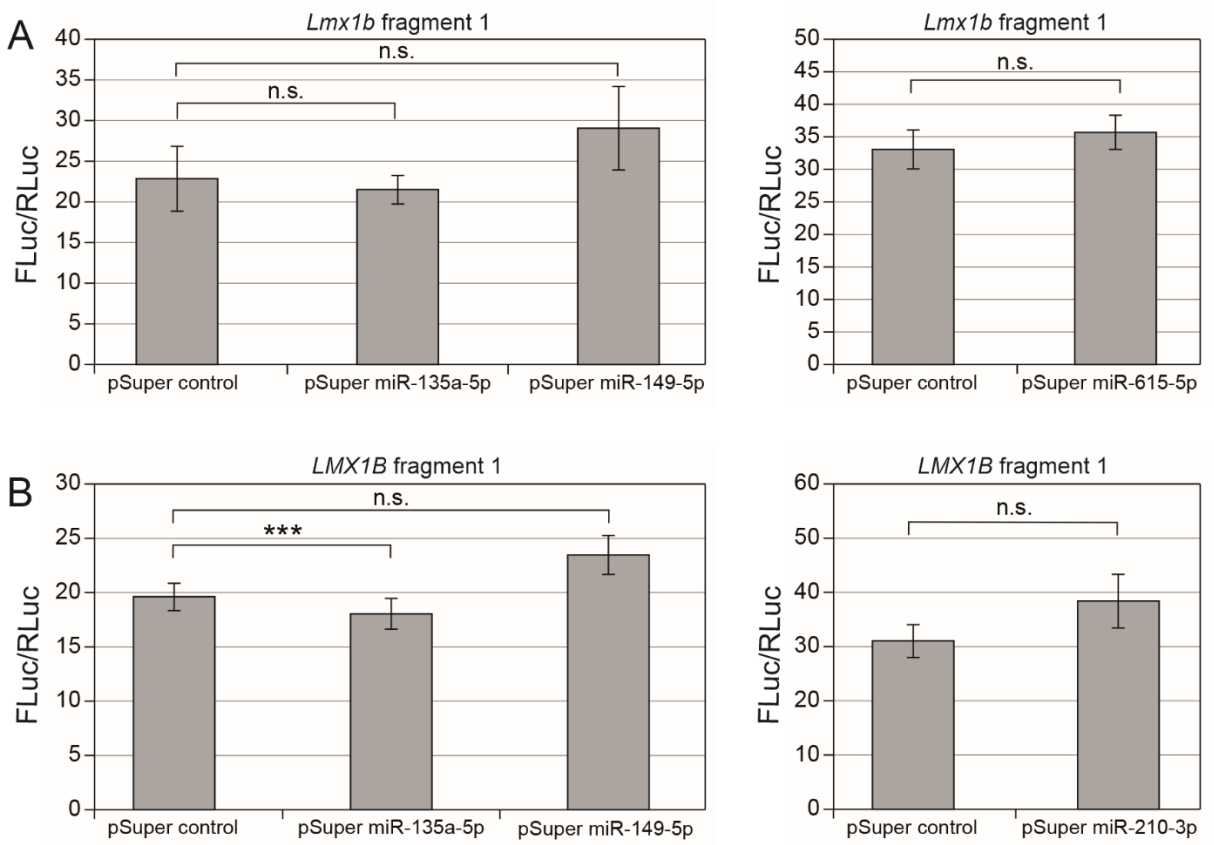

Figure 4.25 ***Luciferase assay of fragment 1 of Lmx1b/LMX1B 3'UTR.*** *(A) pMIR_3'UTR-Lmx1b-1 was used for co-transfection of HEK293T cells with control pSuper or overexpressed miR-135a-3p, miR-149-5p and miR-615-5p pSuper plasmid. (B) pMIR_3'UTR-Lmx1b-1 was used for co-transfection of HEK293T cells with control pSuper or miR-135a-5p, miR-149-5p and miR-210-3p pSuper plasmid. Data are shown as mean value ± SEM of all samples per condition (n=18), P-value: n.s. not significant, *** p<0.001, Bonferroni corrected*

Fragment 2 of murine and human 3'UTR

Fragment 2 of murine and human 3'UTR shows no sequence similarity or conserved miRNA binding sites (position 2.021-3.606/1.983-2.779 bp). pMIR_3'UTR-*Lmx1b*-2 contains binding sites of miR-615-3p, miR-615-5p, miR-149-5p and miR-210-3p (Fig. 4.26 A). The pMIR_3'UTR-*LMX1B*-2 contains binding sites of miR-615-3p and miR-615-5p (Fig. 4.26 B). Despite several tries with different polymerases and genomic DNA samples, the construct contains one point-mutation 198 bp downstream of miR-615-5p (see supplement, Fig 9.2). However, due to the distance to the seed region, a possible effect of the point-mutation on miRNA binding was accepted.

A

```
murine 481    AACAGTTATACGGGTGTCCTGCGCTGGAGACCACTTCCCCTTCTGGTTAGCTCGGGGGAT  540

murine 901    ACAGACCTGGGTGGACCCCAGGCTCTGTACAGGTCATGACTGCCAGGGCAGGAGGGTAGT  960
murine 961    CACAAACCTACAGGTCCCAGGGCAAAGCTGGAGTCCAGAGAACCCAGTATACACAGACCT  1020
murine 1021   CAGCAGACACTCCAGATGGAGAGGACCTCAAGAGTCTGACCCTTGGTACCATCCGATACT  1080
murine 1081   TAACTCCCTCGGTCCTTCTTCTTACCCAGGGCCAGCGATGGCCAGCTGCCCTCCTTGTGG  1140
murine 1141   GCTCCCCTGACCCTCAATCTCCTCTTGCCTGTCAGCTGAGGCTGTCCGCTGGCAGGGCTC  1200
murine 1201   CTGACCTTAGCCAGCTCGCACTCAACAAGGCCAGCACCTTCTCTGCTCTTGGCACCTTAG  1260
murine 1261   CTCTGCTGATGCGGCTTAGGTCTCATGACTTTGGAGCCCCATCCTTGTTCCATAATGACC  1320
murine 1321   CCCCTCCCCGGGGCCTCACACAGGCACAGTGACAAGCTACAAACTCCTTCAATATGTGTG  1380
murine 1381   GATGGGATGTTGATTGCTTAGAGCCCATGGAAGACCACCGCTTGTACCTGGTTGCCTTTC  1440
murine 1441   CTTTTGTTGGCTCAGTCAGCTTGGGGCGTTACTCTGAAGCCACTGTATCTGTTCCCTCTG  1500
murine 1501   TCTCAGCTGCATCAGGTCAGCCCTGTGGGGCGCCCCACAGAATCCTTGCACAGTTATAGG  1560
murine 1561   CCACCAGCATTTCAGCCTCCTGAGTCACCCCCAGCCCCCAGTCTCCTGGACTCTTCCTGC  1620
murine 1621   CTGAAGCTGAAGCAGCCGTGGTTCTTTCCTTGTCAcccccccccCGCACACCACCCCCCA  1680
```

B

```
human  541    AGGAGGCGGGCTCGGAGCCTGAGCCTGGGCAGGCGCAAAGGGACAGAGAGGCACGTGCAG  600
human  601    ACACATGCACACTTGCAGACAAACCCACGCAAACACACACACAGCTGTATGGGGACACCA  660
human  661    GAAGGGACAGGGATGCTCAGCGGGTCTGTCCTGCCTTGTCAGAAAGAGAAAAGGAGGCCA  720
human  721    GGCAGGGGACCCCCCAGTTCTTAAGAGCGATTGGAAAGGGAGGAAGGGGAGAGGAAGAGG  780
```

Figure 4.26 ***3'UTRs of Lmx1b/LMX1B fragment 2.*** *(A) Binding sites in murine 3'UTR and (B) in human 3'UTR. Seed regions are indicated as followed: miR-615-3p (**blue**), 615-5p (**brown**), miR-149-5p (**cyan**) and miR-210-3p (**red**).*

Luciferase reporter assay of pMIR_3'UTR-*Lmx1b*-2 and pSuper overexpressing miR-149-5p, miR-615-5p and miR-615-3p showed no repression of luminescence intensity. miR-210-3p overexpression lead to a significant reduction of luciferase activity of 6 % for construct with murine 3'UTR compared to the control, indicating a regulatory effect of the miRNA (Fig. 4.27 A).

Overexpression of miR-615-5p show no reduction of firefly luciferase activity for pMIR_3'UTR-*LMX1B*-2, while presence of miR-615-3p has an effect. The repression of luciferase activity compared to co-transfection of cells with pSuper control plasmid amounts to 9 % (Fig. 4.27 B).

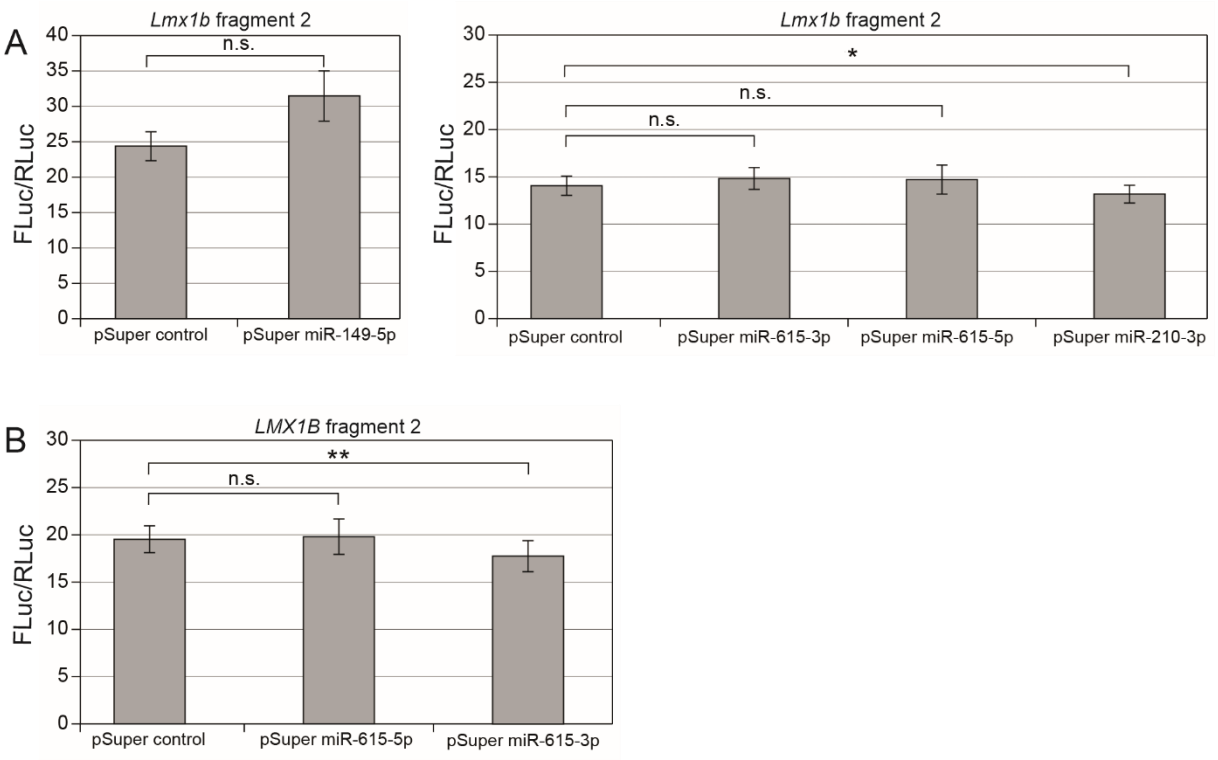

Figure 4.27 ***Luciferase assay of fragment 2 of Lmx1b/LMX1B 3'UTR.*** *(A) pMIR_3'UTR-Lmx1b-2 was used for co-transfection of HEK293T cells with control pSuper or overexpressed miR-149-5p, miR-615-3p, miR-615-5p and miR-210-3p pSuper plasmid. (B) pMIR_3'UTR-LMX1B-2 was used for co-transfection of HEK293T cells with control pSuper or miR-615-3p and miR-615-5pp Super plasmid. Data are shown as mean value ± SEM of all samples per condition (n=18), P-value: n.s. not significant, * p<0.05, ** p<0.01, Bonferroni corrected*

Fragment 3 of murine and human 3'UTR

Fragment 3 of 3' UTR of *Lmx1b*/*LMX1B* (position 4.000-4.898/4.112-5.777 bp) shows only partial high homology at the back part (Fig. 4.28 B). The front part displays no homology between the murine and human fragments (Fig. 4.28 A). While the murine fragment contains binding sites of the miR-615-5p and miR-149-5p, the human fragment also presents also binding sites of miR-101a-5p and miR-210-3p. The pMIR_3'UTR-*LMX1B*-3 construct contains two point-mutations 74 bp upstream and 5 bp downstream of miR-149-5p binding site at position 3652-3657 (see supplement, Fig. 9.3). Different approaches with various polymerases and DNA material were not able to result in mutation-free cloning of the construct. Due to the close vicinity of the mutations, a possible effect on miRNA binding cannot be excluded, but was inevitably accepted.

Figure 4.28 ***3'UTR of Lmx1b/LMX1B fragment 3.*** *(A) 3'UTR with no homology between murine and human construct. (B) Alignment of back part of 3'UTR. Binding site of miRNAs: miR-615-5p (**brown**), miR-149-5p (**cyan**), miR-101a-5p (**black bold**) and miR-210-3p (**red**).*

For both predicted miRNAs miR-149-5p and miR-615-5p no repression of firefly/renilla intensity of pMIR_3'UTR-*Lmx1b*-3 could be measured, suggesting no effect of miRNA on targeted expression

(Fig. 4.29 A). Same result was observed for the pMIR_3'UTR-*LMX1B*-3 as well as for the predicted miR-210-3p. The overexpression of miR-101a-5p showed a significant reduction of luminescence intensity of 17 % for the pMIR_3'UTR-*LMX1B*-3 compared to the control, indicating functional binding site (Fig. 4.29 B).

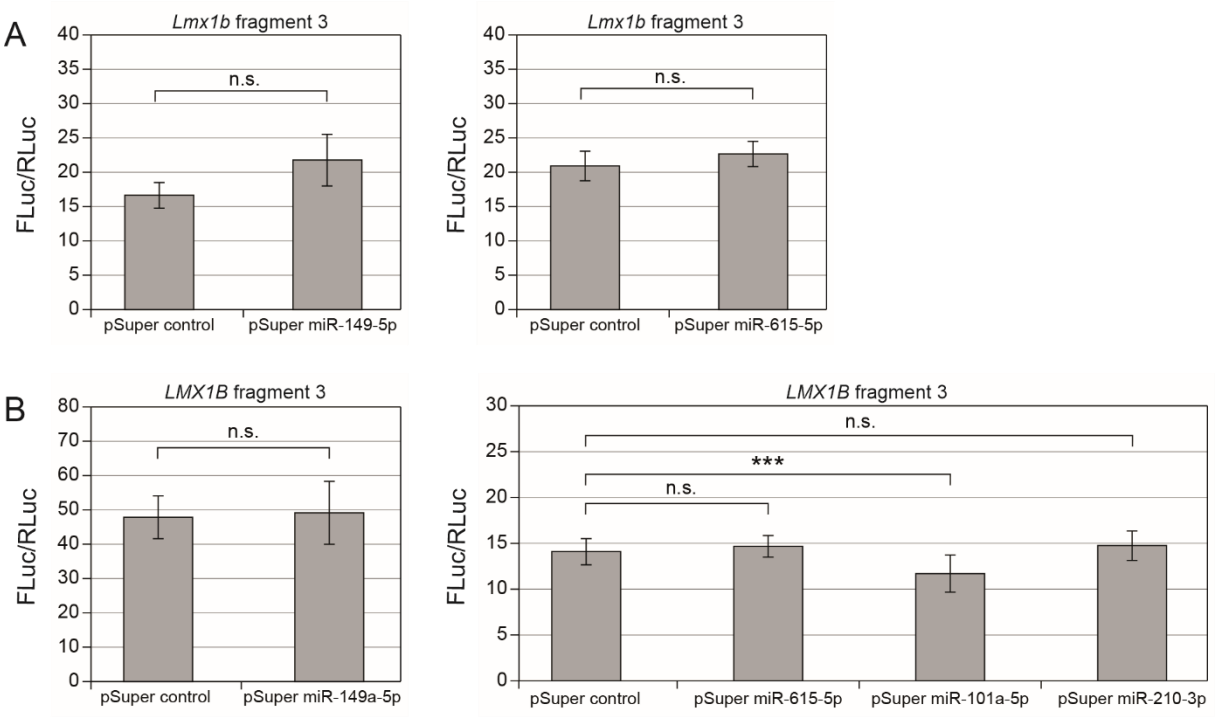

Figure 4.29 ***Luciferase assay of fragment 3 of Lmx1b/LMX1B 3'UTR.*** *(A) pMIR_3'UTR-Lmx1b-3 was used for co-transfection of HEK293T cells with control pSuper or overexpressed miR-149-5p and miR-615-5p pSuper. (B) pMIR_3'UTR-LMX1B-3 was used for co-transfection of HEK293T cells with control pSuper or miR-149-5p, miR-615-5p, miR-101a-5p and miR-210-3p pSuper. Data are shown as mean value ± SEM of all samples per condition (n=18), P-value: n.s. not significant, *** p<0.001, Bonferroni corrected*

Fragment 4 of murine and human 3'UTR

The 3'end of murine and human *Lmx1b*/*LMX1B* 3'UTR display high sequence similarity over the full length (position 4.906-5.268/5.778-6.193 bp). However, not all predicted binding sites are conserved (Fig. 4.30).

There are two binding sites for miR-210-3p located in murine or human 3'UTR, which were not functional as no reduction of luciferase activity could be observed. Only presence of miR-101a-5 lead to a highly significant repression of luciferase activity of about 15 % of the pMIR_3'UTR-*LMX1B*-4 compared to the control. However, no significant effect was detected for the pMIR_3'UTR-*Lmx1b*-4 (5 %) (Fig. 4.31 A). Luciferase reporter assays revealed no significant repression of firefly/renilla intensity for the human construct by the miR-149-5p and miR-615-5p.

```
murine 3236  ATGCGTGGAAGGGGCAGcacactcacacacgtgcgc--------acacactcacacccga  3287
              || | |||| ||||  ||| ||||||| |  ||||        |||||||||||| |
human  4097  -TGGGGGGAAAGGGCTCCACGCTCACACGCACGCGCTCGCACACACACTCACACCTGG  4155

murine 3288  a---acaaggaggct--------------------cacacaTGGCCTGGGAGCAGGGAGA  3324
             |   ||| |||||||                     ||||  |||||||||  | ||| ||
human  4156  ACGCACACGGAGGCTTGCGGACCCATACTCACAGGCACATGTGGCCTGGGGACTGGGGGA  4215

murine 3325  -CAGGAAGGACCCTTC-AACATGTGGCCCTTGACAGGGGCAATTGCCAATG-GTCTCTGG  3381
              |||||| ||||| || ||||| |||||||||  |||  | ||||||||||| | ||||
human  4216  GCAGGAAAGACCCCTCCAACATTTGGCCCTTGGAAGGCACCATTGCCAATGAGCCTCTTT  4275

murine 3382  GCTGCTGCCCTGC------CCTGGGGTCCCGCTTGGAGGGCGTTTGTTGCAGCTGGACTG  3435
             |||| | |||         |||||||  ||  | ||||  |        ||| ||   ||
human  4276  GCTGGTTCCCCCGACCCCACCTGGGGGTCCCATGGGAGCCCAGCCCAGCCAGGTG---TG  4332

murine 3436  GGGCCAGGCCACCCATCGTATTCTTTCCGTTTACCTTGTACAGACTG----------CCC  3485
             |||   |||||||   |  |||| |   |||| ||||||||||| |          |||
human  4333  GGGATGGGCCACCGGCC--ATTCCT---GTTTTCCTTGTACAGACAGATTCTCACTACCC  4387

murine 3486  GCCTGCCATCCCCACACACATTTTATTTAATAACTTGTCATTGTTAAATTATTTATTAGC  3545
              || ||||||||||| ||||||||||||||||||||||||||||||||||||||||||
human  4388  ACCCGCCATCCCCAGACACATTTTATTTAATAACTTGTCATTGTTAAATTATTTATTAGC  4447
```

Figure 4.30 ***Alignment of 3'UTR fragment 4 of Lmx1b/LMX1B****. Predicted miRNA binding site are indicated as followed:* ***red****: miR-210-3p,* ***brown****: miR-615-5p,* ***cyan****: miR-149-5p,* ***bold black****: miR-101a-5p.*

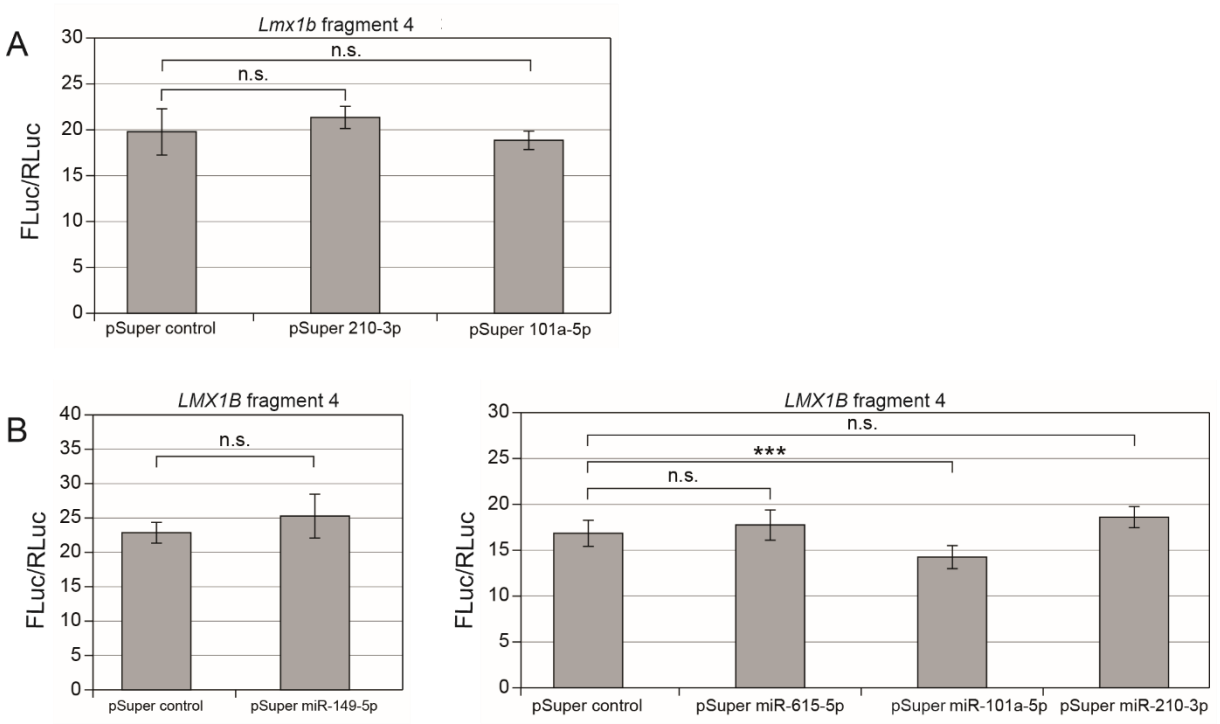

Figure 4.31 ***Luciferase assay of fragment 4 of Lmx1b/LMX1B 3'UTR.*** *(A) pMIR_3'UTR-Lmx1b-4 was used for co-transfection of HEK293T cells with control pSuper or overexpressed miR-210-3p and miR-101a-5p pSuper plasmid. (B) pMIR_3'UTR-LMX1B-4 was used for co-transfection of HEK293T cells with control pSuper or miR-149-5p, miR-615-5p, miR-101a-5p and miR-210-3p pSuper. Data are shown as mean value ± SEM of all samples per condition (n=18), P-value: n.s. not significant, *** p<0.001, Bonferroni corrected*

Taken together, only one miRNA seems to regulate the murine *Lmx1b* transcript. In presence of miR-210-3p, a significant repression of luciferase intensity was measured for the construct harboring the miRNA seed region at position 1665-1670 in 3'UTR sequence compared to the control. The second binding site at position 3269-3274 however, showed no effect, suggesting that the first binding site is the one that is functional. For the human transcript, overexpression of three miRNAs showed significant reduction of luciferase activity. Beside miR-135a-5p and miR-615-3p, which both contain one binding site in fragment 1 and 2, respectively, of human 3'UTR, both binding sites of miR-101a-5p (position 3485-3490, 4417-4422 in 3'UTR sequence) seem to be functional. Overexpression of miRNA in both 3'UTR-constructs (fragment 3 and 4) lead to significant reduction of luciferase activity of 15 to 17 %. Thus, repression of luciferase intensity by predicted miRNAs was only observed in one species.

4.4. Podocyte-specific inducible *Dicer* knockout in mice

As described in previous studies, a constitutive podocyte-specific deletion of *Dicer* and as well as inducible podocyte-specific deletion of *Drosha* in mice lead to glomerular injury and podocyte effacement (Harvey et al., 2008; Ho et al., 2008; Shi et al., 2008; Zhdanova et al., 2011). These results demonstrated the importance of miRNA for development and maintenance of podocyte. However, no inducible podocyte-specific *Dicer* knockout mouse has been described yet. Therefore and to investigate the effect of Dicer loss in adult mice, an inducible podocyte-specific *Dicer* knockout mouse model was generated (S. Baumgarten). Kidneys of knockout, heterozygous and wildtype mice after three weeks and six weeks of doxycycline administration were analyzed with respect to histological and ultrastructural abnormalities.

4.4.1. Genomic organization of *Dicer* knockout mouse

In these mice, exon 23 of *Dicer* and the *mT/mG* cassette is flanked by two *lox p* sites (see 3.2.2). Induction of Dicer knockout and deletion of mTomato was applied after 10-12 weeks after birth by administration of doxycycline for three to six weeks. Knockout mice (*Dicer* $^{lox/lox}$), heterozygous mice (*Dicer* $^{lox/+}$) as well as control mice (*Dicer* $^{+/+}$) were used.

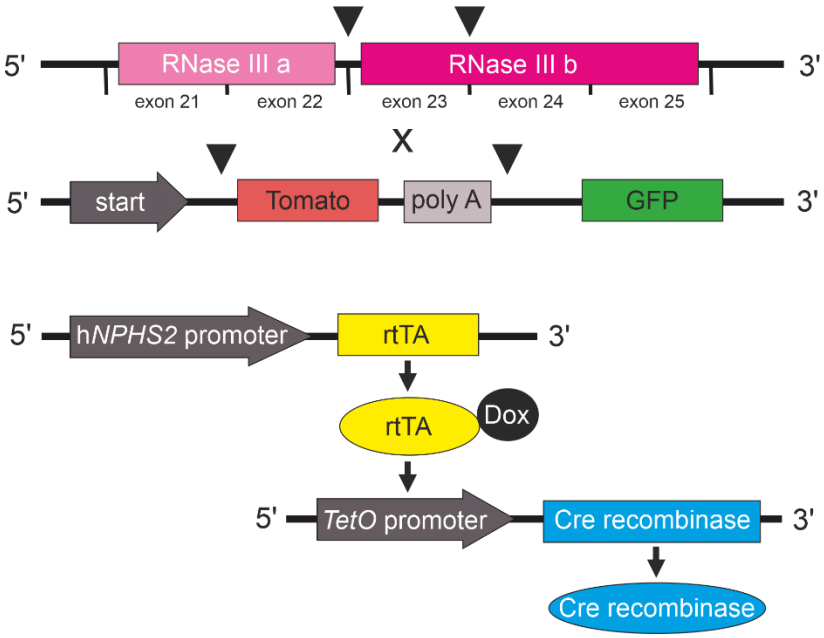

Figure 4.32 ***Scheme of Dicer and mT/mG constructs****. Lox p sites (black arrowheads) are flanking exon 23 of Dicer and mT/mG cassette. rtTA activation, which is under the control of podocyte-specific promoter, leads to expression of Cre recombinase. Abbreviations: RNase IIIa/b: RNAse domains III, GFP: green fluorescent protein, NPHS2: podocin, rtTA: reverse tetracycline transactivator, TetO: Tet-On promoter, Dox: doxycycline [modified from (Baumgarten, 2017)].*

4.4.2. Detection of proteinuria

Urine samples were collected on several days and body weight was monitored over the trial period of 41 days of induction.

SDS-PAGE revealed beginning proteinuria in *Dicer* knockout mice after 24 to 25 days (Fig. 4.33 A). Protein amount in urine varies within each mouse. Three animals developed a stronger proteinuria (10 µg) compared to the other two mice with about 1 µg protein (Fig. 4.33 A, upper right). After 38 days, proteinuria further progressed in all mice. Both wildtype and heterozygous *Dicer* mice showed no proteinuria over the total experimental time.

Protein/creatinine ratio confirmed the results that wildtype and heterozygous mice show no proteinuria. After 24 days all knockout mice developed a distinct proteinuria (SDS-PAGE), however protein-creatinine ratio demonstrated no significant difference compared to the two control mice (Fig. 4.33 B). With further progression, protein-creatinine ratio was significantly increased in knockout mice.

Consistent with those observations, body weight of knockout mice began to decrease after onset of proteinuria. From day 31 onwards, knockout mice lost between 16-34 % of weight until day 41 (see supplement, Tab. 9.1). Weight of heterozygous mice was similar to the wildtype mice (average body weight of ~23 g), which stayed stable over the trial period (Fig. 4.33 C).

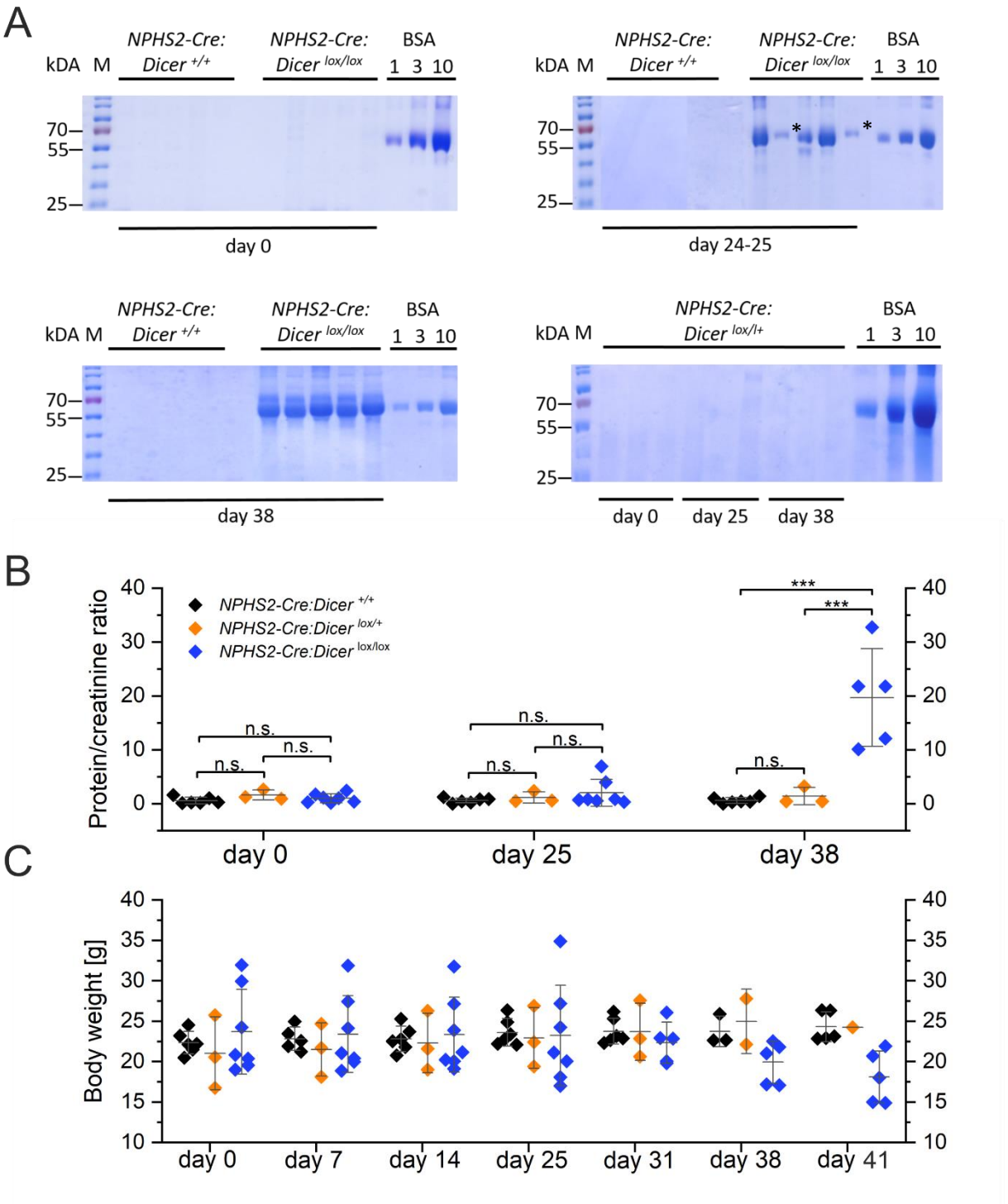

Figure 4.33 ***Coomassie stained urine gels, protein to creatinine ratio and body weight.*** *(A) Urine samples of Dicer $^{+/+}$ and Dicer $^{lox/lox}$ mice from days before induction (upper left), day 24 to 25 (upper right) and day 38 (lower left) as well as urine samples from heterozygous mice (lower right); * indicating lower proteinuria (1µg) compared to other mice. (B) Protein to creatinine ratio of Dicer $^{+/+}$, Dicer $^{lox/+}$ and Dicer $^{lox/lox}$ mice. (C) Body weight monitoring showed beginning weight loss of knockout mice after 31 days, but no significant difference was observed; Abbreviations: n.s. not significant, *** p>0.001 .*

4.4.3. Renal phenotype of *Dicer* knockout mice and control mice

Kidney sections were investigated using hematoxylin/eosin staining and PAS reaction of 6 µm thick paraffin sections (Fig. 4.34).

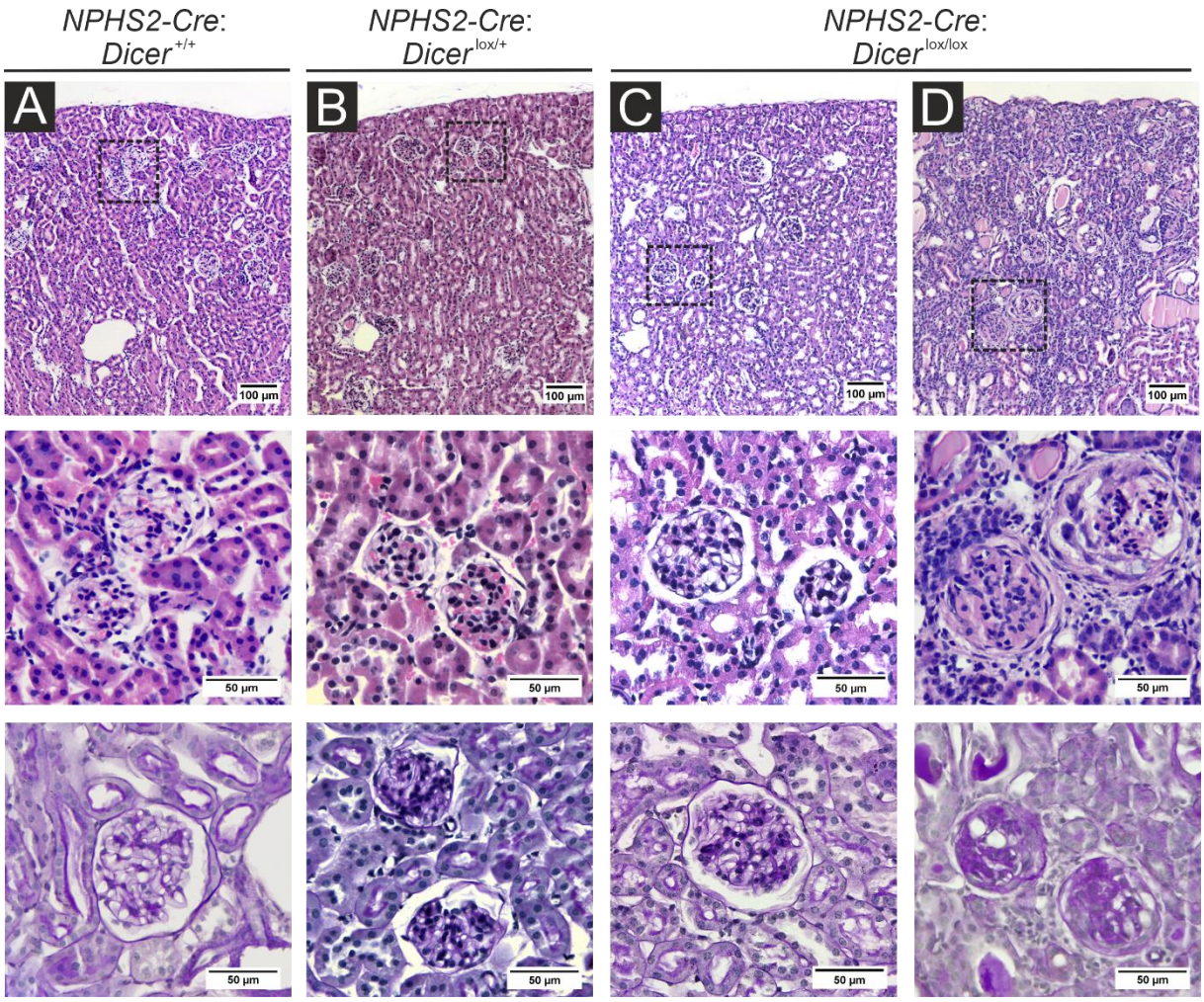

Figure 4.34 ***Histological analysis of kidney sections from Dicer $^{+/+}$, Dicer $^{lox/+}$ and Dicer $^{lox/lox}$ mice after six weeks of induction****. (A) Dicer wildtype mice and (B) heterozygous mice after 41 days postinduction. (C) Dicer knockout mice at day 24 and (D) after 41 days of induction; HE staining (first and second lane, x10 and x40) and PAS reaction (third lane, x40). Boxes mark the magnified glomeruli depicted in the middle panel.*

After 41 days of induction, knockout mice showed strong signs of proteinuria. Renal tubule displayed mild dilation with proteinaceous casts compared to both control (wildtype and heterozygous) mice. Affected glomeruli showed matrix proliferation and glomerular tuft collapse as well as vacuolization of epithelial cells (Fig. 4.34 D). With the onset of proteinuria at day 24 (Fig. 4.34 C), glomeruli appeared histological normal, however in some glomeruli possible start of focal sclerosis was seen. No abnormalities were detected within the glomeruli of wildtype and heterozygous mice (Fig. 4.34 A-B).

Electron micrographs of ultrastructure of wildtype and heterozygous *Dicer* mice showed regular formed podocyte foot processes, glomerular basement membrane and fenestrated endothelium (Fig. 4.35 A, B). After three weeks, filtration barrier of *Dicer* knockout mice displayed slight ultrastructural defects. Most podocytes still form regular foot processes, however few displayed broadening and loss of filtration slit diaphragms (Fig. 4.35 C). With further progression, podocytes were strongly effaced and no normal formed foot processes were observed (Fig. 4.35 D).

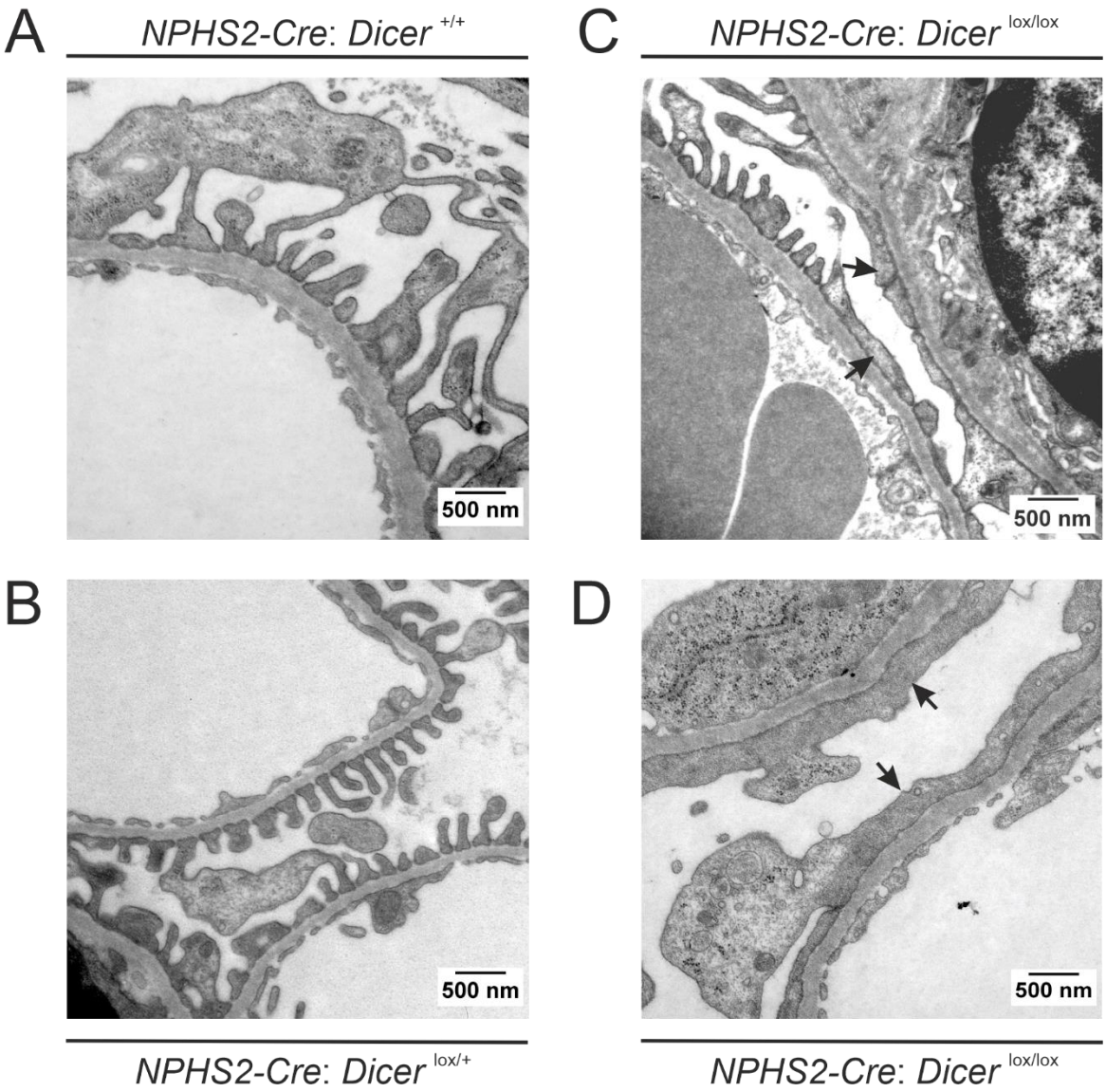

Figure 4.35 ***Electron microscopy of filtration barrier from Dicer $^{+/+}$, Dicer $^{lox/+}$ and Dicer $^{lox/lox}$ mice.*** *Representative micrographs from (A) wildtype after 41 days, (B) heterozygous animals after 41 days, (C) knockout mice after 24 days and 41 days (D). Arrows indicate podocyte foot process effacement, x20.000.*

These structural abnormalities display the dysfunction of the filtration barrier in knockout mice compared to wildtype and heterozygous mice as shown in constitutive *Dicer* knockout mice (Harvey et al., 2008; Ho et al., 2008; Shi et al., 2008). The phenotype of inducible *Dicer* knockout mice corresponds to the described phenotype of constitutive *Dice*r mice, which results from dicer deletion and consequent loss of miRNAs.

4.5. Investigation of target mRNA levels in the *Dicer* knockout mouse

To investigate the effect of miRNA loss in podocytes on mRNA targets, the generated mouse line with inducible podocyte-specific *Dicer* knockout was used. After 24 days of induction, knockout mice showed beginning proteinuria and abnormalities in ultrastructure compared to control mice (see 4.4). To observe mRNA levels at beginning of proteinuria, knockout mice were induced for 24 days based on results from SDS-PAGE (see 4.4.2.). Additional three and seven days of induction were used as early time points.

4.5.1. Analysis of urine and body weight

Dicer knockout in adult (10-12 weeks) mice was induced by administration of doxycycline for the chosen trial period at three, seven and 24 days. Seven control (*NPHS2-Cre*: *Dicer* $^{+/+}$) and five knockout (*NPHS2-Cre: Dicer* $^{lox/lox}$) mice were given doxycycline for three days. For the induction time of seven days, eight animals were used for each group. Six animals per group (control, knockout) were used for 24 days of induction.

Urine samples were collected (see 3.2.4) and checked for proteinuria by SDS-PAGE and protein to creatinine ratio was measured. Knockout mice, induced for three and seven days, showed no proteinuria after respective trial period, which was confirmed by protein to creatinine ratio measurement (Fig. 4.36 A-B; D-E).

After 24 days, only one knockout mouse showed slight proteinuria compared to the control group (Fig. 4.36 C). In former experiments, almost all knockout mice (n=5) displayed clear proteinuria on day 24, although protein quantity varies from individual to individual (see 4.4.2). Nevertheless, mice were killed on day 24 to maintain the same experimental conditions. Proteinuria varies between animals, however based on experience from former experiments (see 4.4.2), proteinuria was detected until day 26. Therefore, it can be assumed that also the used mice would have shown signs of proteinuria on the following day. As expected from SDS-PAGE, protein to creatinine ratio revealed no significant

difference between knockout and control animals (Fig. 4.36 F). In the pilot experiment protein/creatinine ratio also displayed no significant difference between control and knockout mice which suffered from distinctive proteinuria as shown by SDS-PAGE (see 4.4.2). Therefore, it is likely that abnormalities might already have occurred on the molecular level, which did not reflect significantly as proteinuria in SDS-PAGE or protein/creatinine ratio.

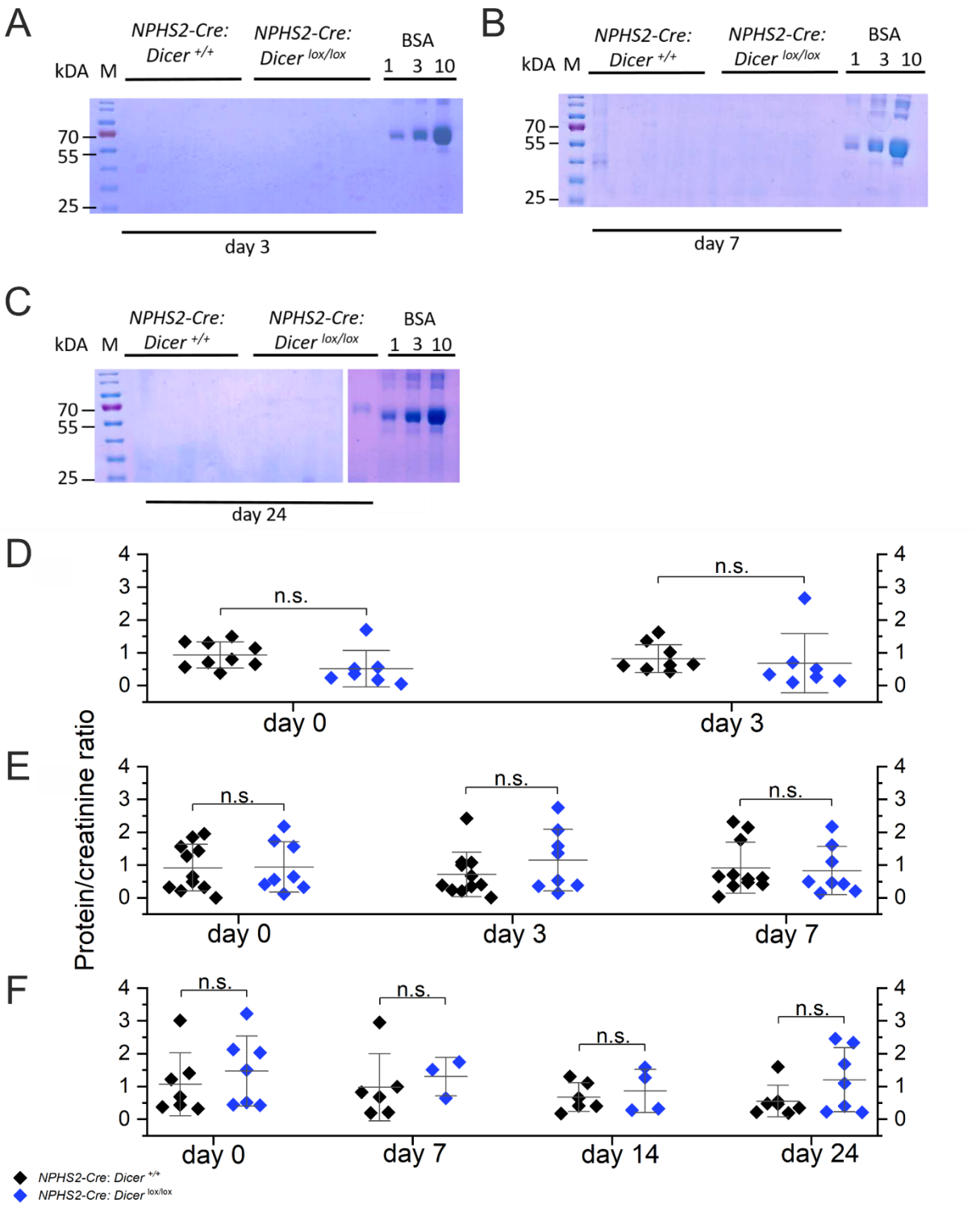

Figure 4.36 ***Urine gel of Dicer knockout and control mice and protein-creatinine ratio.*** *(A-C) representative coomassie stained urine gels of Dicer knockout and control animals after three days, seven days and 24 days of induction; Albumin size: 66 kDA. (D-F) Protein-creatinine ratio demonstrated no significant difference between knockout and control mice; one dot represents one animal; Abbreviations: n.s. not significant.*

Moreover, body weight was controlled periodically. No significant differences were observed in body weight of *Dicer* knockout mice compared to control animals (Fig. 4.37). After three days induction, two mice in each group (control, knockout) lost weight about 1-2 %, which is a normal fluctuation (see supplement, Tab 9.2). This extends also to four control mice with a trial period of seven days (weight loss: 1-3 % respectively). Weight loss of more than 20 % of starting weight would be considered as stress condition.

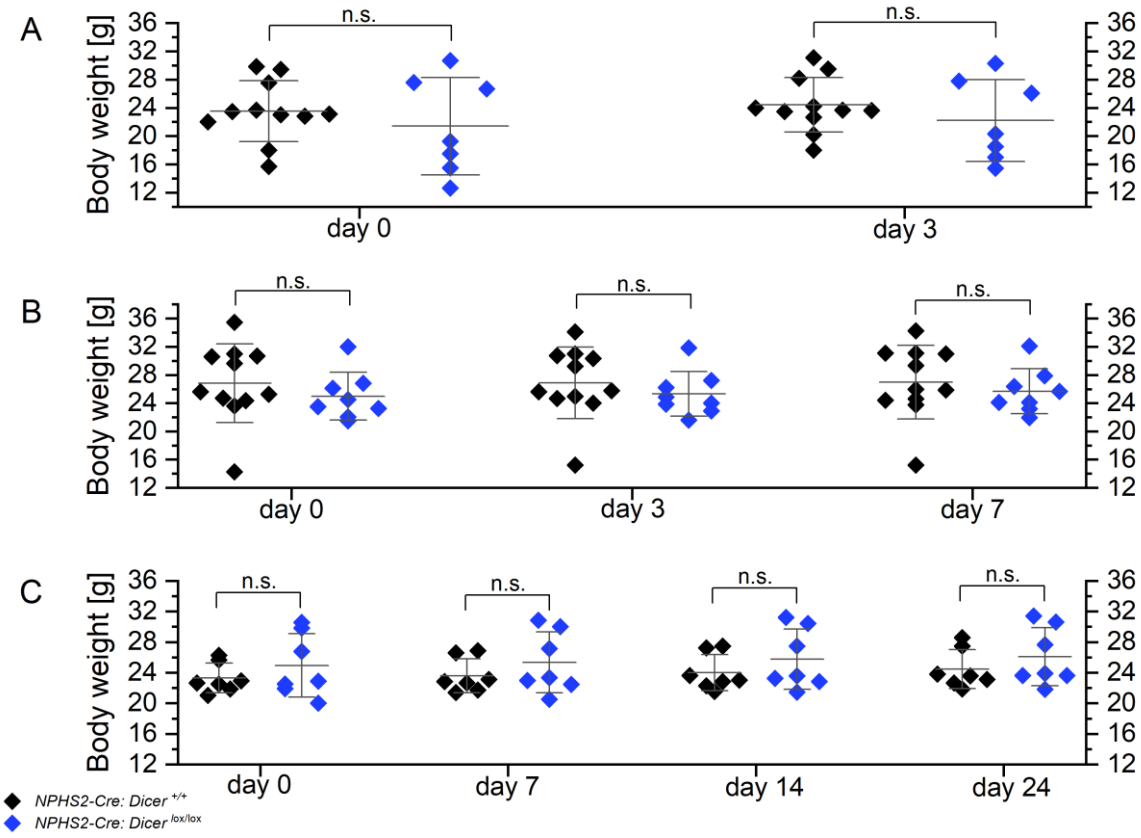

Figure 4.37 ***Body weight of Dicer knockout mice and control mice over respective trial period.*** *Mice were treated with doxycycline for three days (A), seven days (B) and 24 days (C) and body weight was monitored from induction day (day 0) to respective perfusion day; one dot represents one animal; Abbreviations: n.s. not significant.*

4.5.2. Fluorescence activated cell sorting analysis (FACS)

Administration of doxycycline lead to *Dicer* knockout and to the deletion of tomato cassette, allowing for the transcription of the mGFP cassette. Since Cre recombinase is under the control of *NPHS2* promotor, green fluorescence and *Dicer* knockout occurs in podocytes. The other kidney cell types, i.e. mesangial, endothelial and tubuli cells, express tomato (Fig. 4.38 A). After second digestion step (see 3.3.5), podocytes are detached from the glomeruli. Due to the difference in fluorescence, glomeruli cell populations are separated from suspension using FACS analysis (Fig. 4.38 B-D).

Podocytes from *NPHS2-Cre*: *Dicer* $^{+/+}$ and *NPHS2-Cre*: *Dicer* $^{lox/lox}$ mice for each condition (3d, 7d and 24d of induction) were isolated by magnetic bead perfusion and subsequently sorted by FACS.

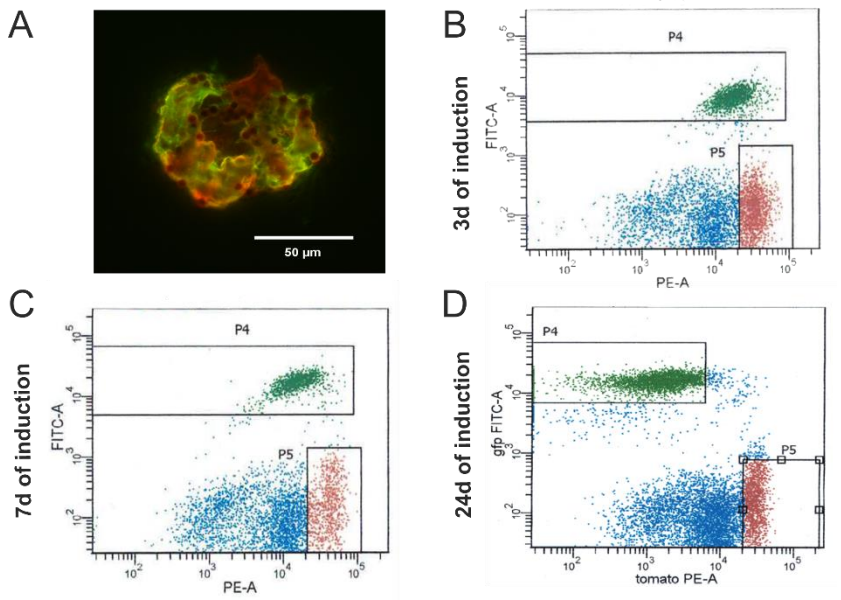

Figure 4.38 ***Green and red fluorescent cell populations of isolated glomeruli (A) and subsequent FACS analysis (B-C)****. After digestion of green fluorescent podocytes from glomerular structure, cells are separated by FACS after three days, seven days and 24 days of induction. Only marked cells (P4 and P5) are sorted.*

In addition to the green podocytes and red fluorescent cells (P4 and P5), other cells are seen by FACS analysis (Fig. 4.38 B-D), which show no significant strong red or green fluorescence and were therefore excluded.

Turnover of mT in the cells varies from tissue to tissue and analysis at an early time point revealed double-labeled cells, which fluorescent yellow (Muzumdar et al., 2007). Samples from three and seven days induced mice also display additional tomato expression in mGFP expressing podocytes (Fig. 4.38 B, C). After 24 days (Fig. 4.38 D), a shift of podocyte population was observed, which is based on complete turnover of mT cells, i.e. only mGFP is expressed in podocytes, which corresponds to the observation of Muzumdar et al. (2007).

For *Dicer* knockout and control mice, in most cases the number of sorted podocyte cell number exceed 100.000 cells, which was set as an approximate value (Tab. 4.3). Podocytes from mice with same genotype were pooled for a better RNA yield if cell number was markedly lower than 100.000 cells.

Table 4.3 ***Sorted cell numbers of green podocytes and red fraction from murine glomeruli.*** *[1]pooled samples for RNA isolation*

		Podocytes	Red fraction		Podocytes	Red fraction
3d of induction	*NPHS2-Cre: Dicer +/+*	43.380	89.000	*NPHS2-Cre:Dicer lox/lox*	95.500	31.800
		60.000	152.600		114.000	60.600
		88.426	72.875		168.000	127.000
		143.197	65.222		366.392	140.273
		98.464	72.875		90.000	206.000
		135.520	95.075		54.500	29.170
		131.856	146.601		175.000	99.800
		92.500	122.500			
		98.500	67.137			
		Podocytes	**Red fraction**		**Podocytes**	**Red fraction**
7d of induction	*NPHS2-Cre: Dicer +/+*	131.800	194.800	*NPHS2-Cre:Dicer lox/lox*	115.000	86.200
		41.500	35.300		40.300	52.330
		103.574	42.400		226.798	139.684
		190.982	43.600		234.790	71.000
		140.400	78.800		150.000	79.000
		100.000	73.000		175.900	170.200
		101.297	75.429		160.643	122.121
		141.710	202.531		202.963	155.142
		60.264	181.974			
		43.346	81.386			
		Podocytes	**Red fraction**		**Podocytes**	**Red fraction**
24d of induction	*NPHS2-Cre: Dicer +/+*	111.763	50.563	*NPHS2-Cre:Dicer lox/lox*	126.000	59.000
		153.399	64.106		100.499	110.362
		100.000	122.000		110.000	120.000
		51.000	34.700		116.000	160.000
		59.000	36.500		44.000	48.000
		90.000	73.000		39.555	168.500
		100.000	40.900		110.000	75.900

4.5.3. Investigation of mRNA target by qPCR analysis

After isolation and subsequent FACS, podocytes were used for RNA isolation. Total RNA from murine podocytes was isolated using the RNeasy Micro Kit. For validation of miRNA deletion, small RNA fraction was isolated separately beside the long RNA fraction using a combination of the miRVana™ miRNA isolation kit and RNeasy Micro Kit (see 3.4.2.1-2) from podocytes of seven day induced mice. After cDNA synthesis (see 3.4.2.3), long RNA fraction was used for investigation of mRNA expression level.

Dicer deletion lead to a dysregulation of miRNA levels and thus to altered regulation of mRNA target expression. miRNA binding to target mRNAs lead to its degradation and additionally to reduced mRNA expression. So it could be presumed that altered miRNA regulation lead to possible increased mRNA expression. To investigate such aberrations in mRNA level, qPCR analysis of identified miRNA-regulated target mRNAs was performed using *Dicer* knockout and control mice.

***Dicer* expression level**

To check if *Dicer* deletion was successful, qPCR was performed in three induced *Dicer* knockout and control animals. After three days, no clear *Dicer* signal was detectable in the knockout mice compared to the control. PCR product of *Dicer* (size: 70 bp) was observed as distinct band in the control animal (*) but not in the knockout animal, indicating no *Dicer* mRNA after three days of induction (Fig. 4.39). PCR of *Dicer* in knockout mice displayed a pattern of unspecific products with either smaller (~50 bp, arrow) or much bigger size (~700 bp, arrowhead) in sample and standard curve concentrations. Negative controls showed a similar pattern with no distinct band on the size of *Dicer*.

Expression of *Lamin A/C* (87 bp), which serves as reference, was detectable in sample of both control and knockout mice. In the negative controls, either no or unspecific products were detected for *Lamin A/C*.

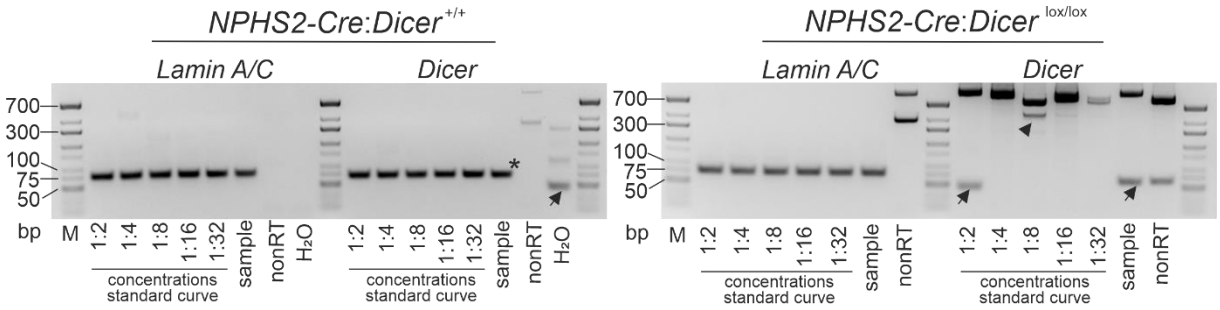

Figure 4.39 ***Dicer expression in control and knockout mice after three days of induction.*** *One Dicer control and one Dicer knockout animal was used. As reference gene murine Lamin A/C (size 87 bp) was used. cDNA was pre-diluted 1:2 and used for standard curve dilutions (1:2; 1:4, 1:8; 1:16, 1:32) and sample (1:8 diluted); nonRT was treated like sample; negative control: H_2O. * indicates Dicer band, arrows and arrowhead indicates unspecific products.*

Taken together, after an induction time of three days, *Dicer* mRNA expression is not detectable in knockout mice compared to control mice.

Target mRNA levels in murine podocytes of Dicer knockout and control mice

mRNA expression levels of *Dicer* knockout mice compared to control mice were analyzed by qPCR analysis at three, seven and 24 days postinduction. Analyzed target mRNAs were chosen due to identified miRNA interaction within this, and in a previous study (Baumgarten et al., unpublished).

After three days, almost all target mRNA levels were increased compared to control mice (Fig. 4.40 A). For three of the shown targets significant upregulation was observed in the knockout mice compared to the control mice: *VegfA* level was increased about 24 %, *Npnt* level about 12 % and *Dusp1* level

about 22 %. *Sparc* levels were increased about 30 % and *Cd2ap* levels were nearly doubled (98 %). Only *Fyn* kinase showed a reduction of mRNA level to 71 % compared to the control mice.

After seven days of induction all analyzed targets showed a varyingly strong decrease in the knockout mice compared to the control mice (Fig. 4.40 B). While expression of *Sparc*, *Npnt*, *VegfA* and *Cd2ap* showed no significant difference compared to control expression, *Dusp1* and *Fyn* levels were markedly decreased to 25 % and 46 %.

With further progressing time of *Dicer* absence, mRNA expression level of targets was also decreased except for *Cd2ap*, which was increased (Fig. 4.40 C). It is very likely that secondary effects cannot be excluded due to long induction time.

Taken together, a trend is visible that after three days mRNA levels are upregulated in knockout mice compared to control mice. After seven and 24 days mRNA levels were decreased for almost all targets.

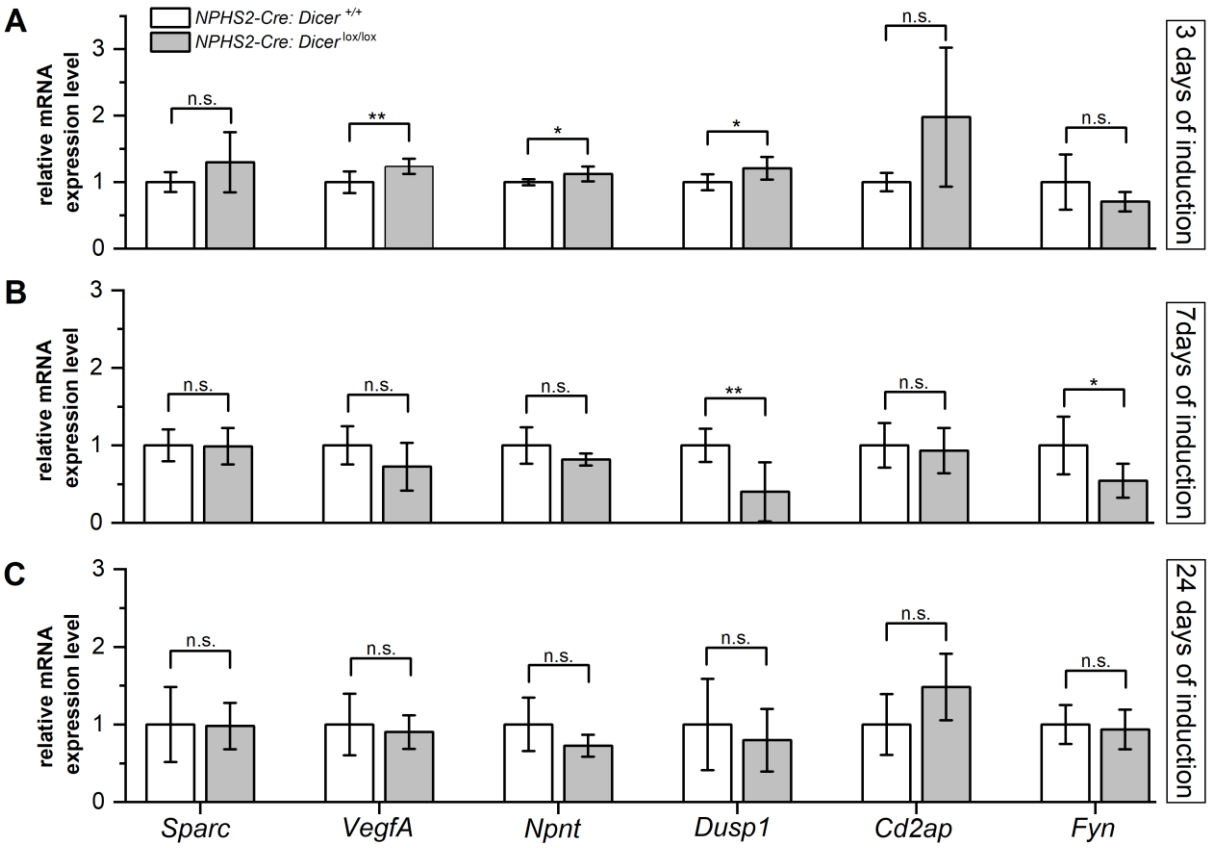

Figure 4.40 ***qPCR quantification of mRNA targets in control and knockout mice****.(A) mRNA expressions after three days of induction (control n=5-7, knockout n=5-7); (B) mRNA expression after seven days of induction (control n=6-8, knockout n=4-7); (C) mRNA expressions after 24 days (control n=5-6, knockout n=5-6); Expression of control =1; reference: Lamin A/C, S9; Quantitative analysis of data are presented as mean ± SEM; p-value: n.s. not significant, * p<0.05, ** p<0.01.*

5. Discussion

miRNAs are short, non-coding RNAs which post-transcriptionally regulate the intracellular levels of specific mRNAs. They are known to play crucial roles in various biological processes such as proliferation, differentiation or apoptosis. In 2008, it was shown that miRNAs are important for the development and also maintenance of podocyte structure and renal filtration function (Harvey et al., 2008; Ho et al., 2008; Shi et al., 2008; Zhdanova et al., 2011). Moreover, miRNAs contribute to the development and the progression of various diseases, showing the great impact of miRNA-mediated regulation. In the present study, analyses to identify specific miRNA targets were performed in order to further unravel the miRNA-mediated regulatory network that is involved in the maintenance of functional podocyte structure.

5.1. Podocyte-specific miRNA-mRNA interactions

Over the last decades, a variety of mature miRNAs were identified in glomerular cell types, however their potential target mRNAs are still not fully established. For a better understanding of the role of miRNAs for kidney structure and filtration function, it is necessary to identify specific target genes. In order to change this bias, specific miRNA-mRNA interactions in podocyte and analysis of their physiological and structural functions were performed.

Over the last years, the role of miRNAs particularly in the development and progression of kidney diseases was analyzed. For example, overexpression of miR-27b lead to enhanced PAN-induced cell death and cytoskeleton destruction by targeting Adora2b, while its inhibition showed a protective effect (Zheng et al., 2018). miR-193a was shown to induce FSGS by inhibiting the expression of WT1, a regulator of podocyte differentiation (Gebeshuber et al., 2013). Reduced levels of WT1 lead to downregulation of its target genes podocalyxin (PODXL) and nephrin, which are essential for podocyte architecture (Gebeshuber et al., 2013).

Identification of miRNA targets will not only further contribute to the revelation of miRNA-mediated regulation in kidney structure and function, but also allow for novel therapeutical treatments.

5.1.1. Predictions of miRNA-mRNA interactions based on specific data set

The great number of miRNAs (mirbase: 38.589) and mRNAs (podocyte transcriptome database: 8.922) makes it challenging to identify a single miRNA-mRNA interaction. To predict possible miRNA binding

site interactions many programs were published over the last years, which are based on different algorithms (e.g. miRWALK2, miRanda, PicTar or TargetScan). Besides base pairing (e.g. Watson-Crick complementarity) as prediction criteria, thermodynamics of mRNA-miRNA duplexes, evolutionary conservation and multiplicity of miRNA binding sites are used for prediction of putative miRNA-mRNA interactions (Dweep et al., 2013). Especially miRWALK2 uses comparison of binding sites resulting from 12 existing miRNA-target prediction programs (Dweep and Gretz, 2015). These programs result in an overwhelming output of possible miRNA-mRNA pairs, because miRNAs can potentially regulate a variety of mRNAs and additionally one mRNA can be regulated by a variety of miRNAs. Compared to published studies, which used mainly whole transcriptome information, a data set of combined podocyte expressed miRNA and AGO2-bound mRNA were used for running target prediction analysis, which was performed in previous studies (Baumgarten et al., unpublished). Using these data a more focused data set of miRNA-mRNA predictions was generated. Moreover, the output of possible interactions is manageable due to lower number of predictions and allows a systematic investigation. Since more than twofold enriched and abundantly expressed (>1‰ of total reads) miRNAs in podocytes were used for *in silico* prediction, putative binding sites for miRNAs with a lower expression level might be missing.

In the present work, predicted miRNA-mRNA interactions of podocytes under physiological conditions have been examined for the maintenance of podocyte structure and function. However, under pathophysiological conditions additional interactions might play an important role (e.g. miR-193a expression in FSGS). Additionally, specific miRNAs and thus interaction with target mRNAs might be important especially at a specific developmental stage. Quantitative analyses of miRNA expression in fetal and adult organs showed that several miRNA species have a higher expression in fetal kidney (e.g. let-7a, mir-26a, miR-199b, miR-17) compared to adult human kidney, indicating a specific role of these miRNA for the development (Aguilar et al., 2010; Tang et al., 2011).

5.1.2. Specific miRNA-mRNA interaction in podocytes

In silico prediction generated putative miRNA-mRNA interactions based on identified podocyte expressed miRNAs and mRNAs (Baumgarten et al., unpublished). To verify the focused predictions, luciferase assays were performed.

To investigate miRNA regulation, reporter constructs of mRNA targets were used to transfect HEK293T cells together with pSuper constructs overexpressing respective miRNA. For a total of nine candidate target transcripts, murine and human 3'UTR were cloned into the pMIR-Report plasmid: *Arrdc3, Fosb, Npnt, Serinc3, Sparc, VegfA, Per1, Zfp36, Stt3a*.

For *Npnt/NPNT*, specific regulation by mmu-miR-101b-3p/has-miR-101-3p could be detected within the present work for human and murine transcript. Regulation of *Sparc/SPARC* by miR-29a-3p and *VegfA/VEGFA* by miR-503-5p was also observed by luciferase reporter assay. Destroying the respective miRNA binding sites lead to a derepression of luciferase activity in all three constructs harboring the mutated binding sites, verifying the specific miRNA-mRNA interaction. In an initial screening experiment, only one species of *Arrdc3/ARRDC3* and *Serinc3/SERINC3*, respectively was regulated by the respective miRNA: murine *Arrdc3* 3'UTR was regulated by miR-19b-3p and human *SERINC3* 3'UTR was regulated by miR-340-5p. Due to non-conserved regulation between murine and human transcript, no further experiments to verify the miRNA binding site were performed. For *Fosb/FOSB*, the initial screening experiment revealed no regulation by the predicted miR-19b-5p and miR-374-5p. In 2017, Müller-Deile et al. demonstrated a specific interaction between the miR-378a-3p and the human *NPNT*, which was also analyzed within this study. No regulation could be observed for either the murine or human transcript at least under the chosen conditions. No regulation was overserved for murine *Per1, Zfp36* and human *STT3A* transcript. Despite modifications in PCR amplification, use of different polymerases and various primer designs, the homologous sequences of these three candidates could not be generated. Due to the fact that not much is known about the role of these candidates in kidney function and no regulation could be detected in the cloned constructs, further attempts of cloning the homologues sequences were not performed.

Luciferase reporter assays were performed using constructs overexpressing the respective miRNA to guarantee sufficient miRNA levels for luciferase transcripts. Since several predicted binding pairs did not show regulation despite miRNA overexpression, demonstrating that overexpression of a putative miRNA is not sufficient to artificially enforce unspecific binding.

5.1.3. Effect of miRNA knockout for human podocyte integrity

The hPCL is an immortalized cell line derived from isolated human podocytes, which were transfected with a retroviral construct coding for the SV40 large T antigen. This cell line proliferates at 33°C and differentiates if cultured at 37°C. During differentiation the cells increase size, form short and long processes and express specific podocyte proteins, e.g. synaptopodin or nephrin (Saleem et al., 2002; Baumgarten, 2017).

In order to further analyze the effect of dysregulated miRNA levels on podocyte structure, specific miRNA knockout cells were used. Since specific interaction between miR-30a-5p and *CD2AP* as well as miR-146b-5p and *FYN* were demonstrated in a previous study (Baumgarten, 2017), the two miRNAs were chosen for miRNA knockout models. hPCL-mir-30a-5p knockout and hPCL-mir-146b-5p knockout

were generated using TALENs (Baumgarten, 2017). TALEN pairs, each composed of a sequence specific TALE array and a part of an unspecific nuclease, binds to the DNA and generates double-strand breaks in the genome. For the TALEN system, a perfect match of two times around 9 to 18 nt is needed, minimizing the risk of off-target effects and thus, making it the favorable method for generating miRNA knockout. Meanwhile, as alternative genome editing method also CRISPR/Cas9 can been used.

Within this study, the knockout cells were unable to differentiate properly in contrast to the control cells. The knockout cells stayed significantly smaller and showed less typical arborization (Saleem et al., 2002), which could be confirmed by cell area measurement. To minimize the possibility of clonal variation, for each control and miRNA knockout of mir-30a-5p and mir-146b-5p two different clones were used for quantitative analysis. For complementation of the observed phenotype, exogenous miR-30a-5p and miR-146b-5p constructs, so-called miRNA-mimics, were used to transfect the control and knockout cells. Two weeks after differentiation, cell area should be measured after control or miRNA-mimic transfection to see if proper differentiation could be obtained. Mimics were gained from Exqion and concentration was used according to manufacturer's recommendation (0.005-50 nM). Cell transfection with control or respective miRNA-mimic with a concentration of 10 nM lead to no GFP signal, indicating too low concentration of miRNA-mimic. Peng et al. (2015) could demonstrate successful transfection of miR-30a mimic using a concentration of 50 nM in MPC5 cells. Therefore, the same concentration was applied for the experiment using the hPCL knockout cell lines, resulting in positive transfection. However, GFP signal was low and not detectable in all cells. Moreover, a strong background noise was obtained in the GFP chancel, unfortunately making the analysis of cell area challenging. Staining of α-actinin-4 was observed as distinct pattern in both transfection conditions. Mimic concentration of 100 nM lead to cell death, suggesting a toxic effect of the high concentration. Thus, further test of different concentration between 50 and 100 nM might be needed to analyze a positive effect of mimic on cell size, arborization and expression of podocyte specific markers, e.g. synaptopodin. Due to strong background noise, a different evaluation method is needed. One possibility could be the evaluation of cell area only in the red channel (α-actinin-4 staining), where no background noise is observed and distinct cell areas could be measured. However, not all cells were transfected and therefore possible cell area changes cannot be attributed only to mimic effect.

In the future, these cells could be used for proteome analysis. The effect of miRNA-knockout on specific podocyte proteins using this comprehensive approach would further contribute to enlighten the regulatory network of miRNA regulation.

5.1.4. Regulation of target genes by miRNAs

The identified interactions between miRNA and mRNAs within the present work contributes to the complexity of the regulatory miRNA-network and fine tuning of diverse cellular functions.

Luciferase reporter assay revealed for *Npnt*, *Sparc* and *VegfA* conserved regulation in murine and human transcript by the respective miRNA. Moreover, regulation in only one specie (either human or mouse) for *Arrdc3* and *SERINC3* were observed. The repression levels observed in all experiments vary between about 10 % up to 44 % of luciferase activity compared to the control. Within the 3'UTR of transcripts, often binding sites of different miRNAs exists, which often show a cooperative effect. Therefore, it is likely that one target is regulated by various miRNAs and additionally one miRNA regulates various mRNAs (Fig. 5.1). Within this study, it could be shown that miR-101-3p regulates the podocyte targets mRNA encoding *Npnt/NPNT*. In a previous study, it was shown that miR-101-3p also regulates *Dusp1/DUSP1,* another podocyte target mRNA (Baumgarten et al., unpublished). There are miRNA-mRNA interactions described where one miRNA is responsible for the complete knockdown of specific mRNA. An example in podocytes is the transcription factor WT1, which is almost completely downregulated by the upregulation of miR-193a leading to FSGS (Gebeshuber et al., 2013). Within this study, the transfection of cells using one miRNA construct lead to slight to moderate changes of the luciferase activity, e.g. 15 % and 19 % repression of luciferase activity of murine and human *VegfA/VEGFA* constructs.

Also, multiple binding sites of the same miRNA can be present in the 3'UTR, which might have an accumulating effect leading to a strong repression. For example, in the 3'UTR of FYN, two binding sites for the miR-146b-5p exist, however only one binding site was functional as shown by loss-of-function luciferase assay (Bachelor thesis Heizler, 2015). Within the 3'UTR of *Sparc/SPARC*, also two binding sites of miR-29a-3p exist. Initial screening of wildtype pMIR_3'UTR construct, miR-29a-3p expression lead to a strong repression of luciferase activity (44 %, 34 %) in the present work. Constructs with both seed regions inactivated demonstrated a stronger depression of firefly/renilla intensity (79 %, 73 %) compared to the construct with one destroyed seed region (28-29 %, 41-48 %), reinforcing the accumulative effect of both miR-29a-3p binding sites. If multiple binding sites are present in the 3'untranslated region of target mRNA, it could be assumed that miRNA binding would lead to a strong reduction of mRNA expression at least if all binding sites are functional under the same condition. In the present work, multiple binding sites of miR-340-5p exist in the 3'UTR of *SERINC3*. Luciferase assay demonstrated a slight effect on luciferase activity (10 % repression), suggesting that either not all binding sites are functional or that even small changes might already have effects. Another possibility would be that a cooperative work with other miRNAs is needed to lead to stronger repression. In cases of miRNA clusters like miR-17~92 or miR-106b~25, studies demonstrated such a cooperative effect.

Mice lacking both miR-17~92 and miR-106b~25 displayed severe cardiac defects and additional defects, which were not observed in miR-17~92 single knockout. Single knockout of miR-106b~25 whereas showed no obvious abnormalities, suggesting interactions among the miRNA clusters (Ventura et al., 2008). miR-17~92 cluster is known to be important for kidney development (Marrone et al., 2014) and overexpression lead to various cancer types by targeting tumor-suppressive proteins and pathways such as PTEN and TGFβ signaling (Fuziwara and Kimura, 2015). The cluster contains six miRNAs (miR-17, miR-18a, miR-19a, miR-19b, miR-20a, miR-92a), however, not all miRNA regulate the same target gene, e.g. tumor suppressor PTEN is regulated among others by miR-17 and miR-92a while SMAD is regulated by miR-18a and miR-19a and miR-19b (Fuziwara and Kimura, 2015).

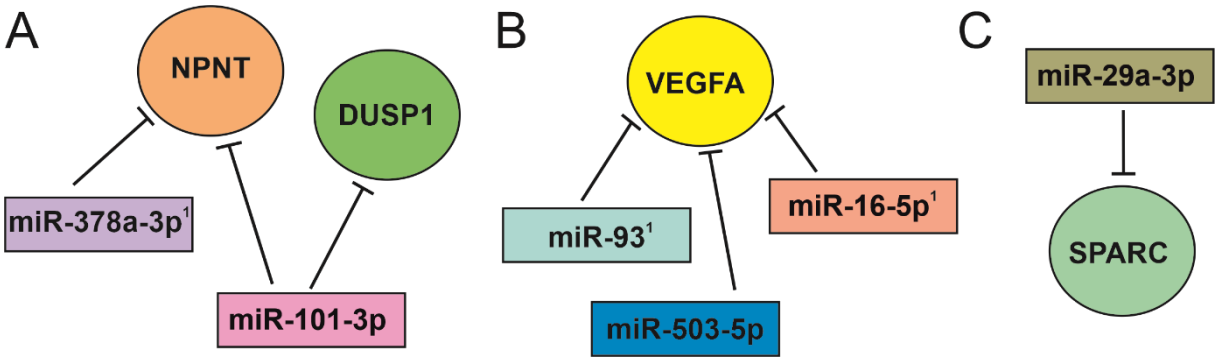

Figure 5.1 ***Regulation of target genes by miRNAs in the kidney****.(A) The targets Npnt/NPNT and Dusp1/DUSP1 (Baumgarten et al., unpublished) are both regulated by the miR-101-3p. Additionally, NPNT is regulated by the miR-378a-3p (Müller-Deile et al., 2017) (B) VEGFA is shown to be regulated by miR-503-5p within this study and also regulated by miRNAs miR-93,, miR-16-5p under pathophysiological conditions (Long et al., 2010; Duan et al., 2019), (C) Sparc/SPARC is regulated by miR-29a-3p as shown within this study in podocytes.* [1] *reported interactions.*

Additionally, interactions are reported for the analyzed candidate VEGFA. For example, miR-16-5p overexpression alleviated the damage of diabetic nephropathy by downregulation of *VEGFA* in HG-stimulated human podocytes (Duan et al., 2019). Also it was shown that miR-93 has a modulatory effect on *VEGFA* expression in diabetic environment (Long et al., 2010). miR-16-5p as well as miR-93 are not enriched in murine podocytes under physiological conditions and thus, were not included in the *in silico* study that revealed the data basis of this work. Within the present work, *NPNT* is regulated by miR-101-3p but it is also regulated by the miR-378a-5p as shown by Müller-Deile et al. (2017). However, this interaction could not be confirmed unambiguously within the work at least under the chosen conditions. Beside the identified interaction between *Sparc/SPARC* and the miR-29a-3p within this study, not much is known about other miRNA interaction in the podocytes or the kidney.

5.1.5. Consequences of miRNA dysregulation in podocytes

Dysregulation of miRNAs is often correlated with different renal diseases, e.g. FSGS, diabetic nephropathy or lupus nephritis (Trionfini and Benigni, 2017). Over the last years, multiple injurious stimuli have been found to contribute to podocyte dedifferentiation leading to loss of podocyte-specific proteins, gain of mesenchymal features and thus to podocyte dysfunction. Therefore, miRNAs are suggested as markers and novel targets for therapeutic methods.

Since miR-29 family targets genes like *Sparc*, identified within this study, or *Spry1* (Long et al., 2011) which are known to be involved in the development of renal diseases, it is crucial to maintain physiological miR-29 family levels for normal kidney function. Loss of podocyte-specific makers like synaptopodin or nephrin are a characteristic of diabetic nephropathy. In streptozotocin induced hyperglycemia, miR-29a-3p levels were decreased in glomeruli of affected mice (Lin et al., 2014). Reduced levels of nephrin were observed in hyperglycemia, which accelerates podocyte injury. Overexpression of miR-29a improved nephrin levels, podocyte viability and renal function with less glomerular fibrosis and inflammation reaction in diabetic transgenic mice compared to diabetic wild-type mice by suppressing histone deacetylase 4 (HDAC4) (Lin et al., 2014).

In the present work, miR-503-5p was identified to be a regulator of *VegfA/VEGFA*, which is also a target of miR-16-5p and miR-93 (Long et al., 2010; Duan et al., 2019) and known to be involved in DN. It was shown that VEGFA was mainly enriched in the PI3K/AKT pathway, which promotes renal fibrosis. Thereby VEGFA was also identified as a target of miR-200 (Park et al., 2013). Since high glucose induces increased AKT expression leading to renal fibrosis, inducing of DN by miR-200 via targeting VEGFA through PI3K/AKT signaling pathway was suggested (Yang et al., 2019). Moreover, miR-503 was identified as a regulator of E2F transcription factor 3 (E2F3). Overexpression of miR-503 promotes podocyte injury by targeting E2F2 in diabetic nephropathy (Zha et al., 2019), suggesting miR-503 as a key player in the development of diabetic nephropathy. Since both VEGFA and miR-503-5p are involved in DN, regulation of VEGFA by miR-503-5p might contribute to its development.

Another miRNA involved with the PI3K/AKT signaling pathway is the miR-340-5p, which was identified as highly expressed miRNA in podocytes (Baumgarten et al., unpublished) and identified as a regulator of *SERINC3* within this study. In oxygen-glucose deprivation/reoxygenation (OGDR) induced neuronal injury, low expression of miR-340-5p was observed (Zheng et al., 2020). miR-340-5p directly regulated PDCD4 and its inhibition leads to protection of hippocampus neurons against OGDR injury. Moreover, by targeting PDCD4, miR-340-5p influences PI3K/AKT signaling. In the kidney, the signaling pathway is involved in the promotion of renal fibrosis, making it reasonable to assume that also in the kidney miR-340-5p might effect PI3K/AKT signaling maybe via targeting SERINC3.

Table 5.1 ***miRNAs in podocyte and their role for kidney health and disease***

miRNA / miRNA family	Described function in podocytes / glomerular function	Source
miR-17~92 cluster	deletion lead to defective proliferation of progenitor cells and reduces number of nephrons during kidney development	Marrone et al., 2014
miR-16-5p	protective effect against podocyte injury by targeting VEGFA	Duan et al., 2019
miR-21-5p	important role in the progression of kidney fibrosis	reviewed in Patel and Noureddine, 2012
	miR-21-5p promotes kidney fibrosis by silencing of metabolic pathways	Chau et al., 2012
	in Alport nephropathy model, silencing resulted in milder disease	Gomez et al., 2015
	can ameliorate glomerular injury caused by TGF-b1	Lai et al., 2015
miR-26a-5p	decreased levels in post-stenotic kidneys	Zhu et al., 2015
	decreased levels in patients with nephritis or IgA nephropathy	Ichii et al., 2014
	inhibits TGF-β-induced extracellular matrix protein expression by targeting CTGF, downregulated in diabetic nephropathy	Koga et al., 2015
	Regulator of *Tob1/TOB1* level	Baumgarten et al., unpublished
miR-27a	promotes podocyte injury via PPARγ-mediated β-catenin activation in diabetic nephropathy	Zhou et al., 2017
miR-27b	overexpression of miR-27b enhanced PAN-induced apoptosis and cytoskeleton destruction in podocytes through targeting adenosine receptor 2B	Zheng et al., 2018
miR-29 family	regulates several collagenes in kidney cortex and medulla	Liu et al., 2010
	targets Sprouty homolog 1 and activates Rho kinase activity, thus favoring fibronectin assembly and apoptosis	Long et al., 2011
	decreased levels in mice with hyperglycemia, overexpression improve nephrin levels and renal function	Lin et al., 2014
	Regulator of *Sparc/SPARC* level	Meisinger, 2021
miR-30a-5p/ miR-30 family	putative targets are upregulated in podocyte specific knockout mice	Shi et al., 2008
	miR-30a-5p targets Xlim1/Lhx1, a transcriptional factor for kidney development in *Xenopous*	Agrawal et al., 2009
	protection against podocyte apoptosis by targeting Notch1 and p53	Wu et al., 2014
	upregulated in injured podocytes, its inhibition prevents PAN induced apoptosis	Xie et al., 2015
	mir-30 family regulates calcium signaling in podocytes	Wu et al., 2015
	inhibits the epithelial-mesenchymal transition through downregulation of NFATc3	Peng et al., 2015
	overexpression of miR-30 family prevents HG-induced podocyte injury by modulating Cx43 expression	Li et al., 2020
	Regulator of CD2AP level	Baumgarten et al., unpublished
miR-93	regulates VEGFA under high glucose conditions	Long et al., 2010
miR-101-3p	Regulator of *Npnt*/*NPNT* level, regulator of *Dusp1/DUSP1* level	Meisinger, 2021; Baumgarten et al., unpublished
miR-124-3p	regulates Itga3 under mechanical or diabetic stress	Li et al., 2013
miR-134/miR-132	BDNF upregulates Limk1 translation and phosphorylation by affecting miR-134 and miR-132 signaling; increases cofilin phosphorylation resulting in actin polymerization	Li et al., 2015
miR-135a-5p	regulates TRPC1 during renal injury, promoting renal fibrosis	He et al., 2014; Yang et al., 2017
miR-146a-5p	absence increases risk of diabetic nephropathy via upregulation of ErbB4 and Notch1	Lee et al., 2017
miR-146b-5p	Regulator of *FYN* level	Baumgarten et al., unpublished
miR-150-5p	promotes renal fibrosis by downregulation of SOCS1	Zhou et al., 2013
miR-193a-5p	upregulation induces FSGS by targeting WT1	Gebeshuber et al., 2013
	loss of miR-193-5p expression induces switch from PECs to podocytes	Kietzmann et al., 2015
miR-200	induces DN by targeting VEGFA through the PI3K/AKT signaling pathway	Yang et al., 2019
miR-206	overexpression promotes podocyte injury via downregulation of WT1	Guo et al., 2016
miR-340-5p	Regulator of *SERINC3* level	Meisinger, 2021

miR-503	contributes to podocyte injury via targeting E2F3 in diabetic nephropathy	Zha et al., 2019
	Regulator of *VegfA/VEGFA* level	Meisinger, 2021

5.2. The transcription factor LMX1B is regulated by miRNAs

The transcription factor LMX1B is an important regulator of the development of podocyte foot processes and slit diaphragms as well as for the maintenance of podocyte structures. Mutations of LMX1B causes the Nail-patella syndrome, which lead in 40 % to nephropathy (Witzgall, 2017). LMX1B regulates important proteins of the filtration barrier and the actin cytoskeleton. In 2013, a regulatory negative feedback loop between *Lmx1b* and the miR-135a-2 was described in the midbrain determining the size of the dopaminergic progenitor pool through the *Wnt1*/Wnt signaling pathway (Anderegg et al., 2013). On the one hand, *Lmx1b* drives the expression of miR-135a-2, while on the other hand the miRNA negatively regulates *Lmx1b* levels.

Since in the midbrain *Lmx1b* not only acts as a regulator of miRNA expression but is also negatively regulated by the miR-135a-2, the addressed question within the present work was if *Lmx1b* is regulated by miRNAs in the podocytes. To answer this question, the 3'UTR of murine and human *Lmx1b/LMX1B* were used for *in silico* prediction of putative miRNA binding sites using mirWALK2. *In silico* analysis predicted miRNA binding sites for miR-210-3p, miR-101a-5p, miR-149-5p, miR-615-3p and miR-615-5p for the 3'UTR of *Lmx1b*, which were also conserved in the human homologue. miR-210-3p, miR-149-5p as well as miR-615-3p were shown to be enriched in murine podocytes (Baumgarten et al., unpublished). The described interaction of miR-135a-5p and *Lmx1b* was also analyzed within this study. For the pMIR_3'UTR-*Lmx1b*-2, the overexpression of miR-210-3p lead to a significant repression of luciferase activity in a screening experiment. For *LMX1B 3'UTR*, specific interaction with the miR-135a-5p, miR-101a-5p and miR-615-3p was observed. The described interaction between the miR-135a-5p and the murine transcript by Anderegg et al. could not be demonstrated under the chosen conditions. Expression of one specific miRNA lead to slight to moderate changes in the luciferase activity (6-17 % repression), however it is most likely that also the regulation of *Lmx1b/LMX1B* is performed by several miRNAs leading to a cooperative effect. Especially for the human transcript, a transfection experiment with a combination of all three miRNAs (miR-135-5p, miR-101a-5p and miR-615-3p) might lead to even stronger repression compared to transfection with a single miRNA. For the verification of miRNA binding sites, further experiments with mutated seed regions are needed. Since no interaction was conserved between murine and human transcript, loss-of function luciferase reporter assays were not performed.

It is known that miR-135a-5p regulates *Lmx1b* in midbrain and within this study, it could be shown that pMIR_3'UTR-*LMX1B*-1 construct had a reduced luminescence by the overexpression of miR-135-5p. Under physiological conditions miR-135a-5p is not enriched in the murine podocytes, however it was described to be involved in diabetic nephropathy (He et al., 2014). In the kidney, overexpression of miR-135a is associated with the development of microalbuminuria and renal fibrosis in patients with diabetic nephropathy by suppressing TRPC1 (transient receptor potential cation channel) (He et al., 2014). TRPC1 activates Ca^{2+} entry into cells and its preventing might be the mechanism to promote renal fibrosis. It was demonstrated that upregulated miR-135a-5p lead to mesangial cell proliferation and increased synthesis of extracellular matrix proteins (He et al., 2014). Therefore, regulation of Lmx1b through miR-135a-5p might also contribute to the development of kidney disease.

In the present work, specific interaction between miR-101a-5p and the constructs pMIR_3'UTR-*LMX1B*-3/4 as well as miR-210-3p and pMIR_3'UTR-*Lmx1b*-2was shown. The expression of miR-101a is poor in chronic renal fibrosis tissues while its target KDM3A is upregulated. KDM3A plays a role in the YAP-TGF-ß Smad signaling pathway and overexpression of miR-101a could attenuate renal fibrosis through its inactivation (Ding et al., 2020). In clear cell renal cell carcinoma (ccRCC), miR-210-3p was found to be increased in FFPE-tissue and urine samples of ccRCC patient (Petrozza et al., 2017; Yoshino et al., 2017). Depletion of miR-210-3p in RCC cell lines lead to increased tumorigenesis and characteristic of epithelial-mesenchymal transition (EMT). TWIST1 was identified as direct target of miR-210-3p that is a regulator of epithelial-mesenchymal transition. High levels of TWIST1 are associated with poor prognosis and short disease-free survival rate, indicating that progression of RCC is promoted by TWIST1 suppression mediated by miR-210-3p (Yoshino et al., 2017). In case of the miR-615-3p which was identified as putative regulator of *LMX1B* within this study not much is known about its target genes or role in kidney function. In metastatic kidney, overexpression of miR-615-3p lead to poor prognosis and overall survival, but the underlying mechanism was not described (Du et al., 2017).

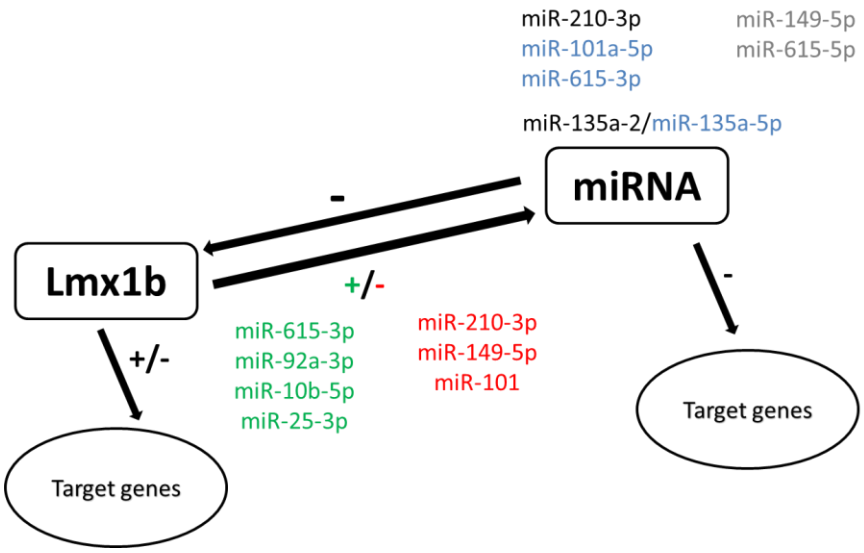

Figure 5.2 ***Putative regulatory pathways of the transcription factor Lmx1b.*** *Lmx1b acting as suppressor (red) or activator of specific miRNAs (green) and identified miRNAs regulating Lmx1b 3'UTR of murine (black) or human transcript (blue). miR-135a-2 interaction with Lmx1b was shown by Anderegg et al. Gray marked miRNAs revealed no regulation.*

Since miRNAs are generated by RNA polymerase II or III from primary transcripts, their expression can also be regulated by transcription factors. In a previous study, the effects of *Lmx1b* knockout on miRNA levels were investigated by *deep sequencing* analysis using freshly isolated podocytes (Baumgarten, 2017), showing that 54 miRNA were upregulated and 38 were downregulated more than two fold in knockout podocytes compared to control podocytes. This indicates that Lmx1b is not only regulated by miRNAs but might also act as either a suppressor or activator of miRNA expression (Fig. 5.2). Interestingly, both miR-101 and miR-210-3p were upregulated in Lmx1b knockout mice, suggesting an enhancing function of Lmx1b in the miRNA expressions. miR-615-3p was downregulated in the knockout podocytes and therefore indicating a suppressing function of Lmx1b (Baumgarten, 2017).

Since the miRNAs miR-210-3p, miR-101a-5p and miR-615-3p seems to be putative regulator of *Lmx1b/LMX1B* and were also suggested as potential Lmx1b targets, it might be possible that also in the podocytes a regulatory feedback loop exists as described for *Lmx1b* in the midbrain. Such regulatory circuits might modulate various pathways and other target genes, which are essential for kidney function.

5.3. Podocyte-specific inducible *Dicer* knockout in mice leading to glomerular injury

It has been shown previously that a constitutive deletion of *Dicer* as well as inducible podocyte-specific deletion of *Drosha* results in severe proteinuria and glomerular injury (Harvey et al., 2008; Ho et al., 2008; Shi et al., 2008; Zhdanova et al., 2011). To prove the consequences of *Dicer* loss in fully developed kidneys, inducible podocyte-specific *Dicer* knockout in adult mice was analyzed.

It could be shown that inducible *Dicer* deletion in adult mice lead to a comparable phenotypes as in the constitutive *Dicer* and inducible *Drosha* knockout mice (Harvey et al., 2008; Ho et al., 2008; Shi et al., 2008; Zhdanova et al., 2011). Mice development proteinuria after three weeks of induction with further progression. EM analysis of the ultrastructure of filtration barrier revealed that with the onset of proteinuria first abnormalities were observed in the knockout mice (e.g. mild foot process effacement). After six weeks of *Dicer* knockout induction, severe foot process effacement was detected in the knockout mice, showing the importance of miRNAs alone for not only the development, but also, for the maintenance of normal podocyte structure and kidney function. To maintain kidney function especially the structural proteins of the filtration barrier and their signaling processes are particularly essential and are suspected to be targets of miRNA regulation.

Interestingly, phenotypes occur at about the same time points after induction or birth respectively, suggesting that the disturbance of podocyte structure and function occurs quite fast in the inducible system. After already three days postinduction, no *Dicer* mRNA was detectable in the knockout mice compared to the control mice (Fig. 4.39). So, to analyze possible differences in target mRNA expression between *Dicer* knockout mice and control mice, freshly isolated podocytes were used for qPCR analysis.

5.3.1. Effect of *Dicer* absence on target mRNAs

In the present work, podocyte-specific miRNA-mRNA interactions were identified *in vitro* using luciferase assays. To further investigate the effect of *Dicer* loss on murine podocytes, the mRNA expression levels of the identified miRNA-regulated mRNAs were analyzed by qPCR: *Sparc, Vegfa, Npnt, Dusp1, Cd2ap and Fyn*. These proteins are important components of the filtration barrier and dysregulation contributes to the development of podocyte injury and kidney diseases.

To observe putative changes in expression, mRNA levels were analyzed at three different time points: three, seven and 24 days. After 24 days of induction, knockout mice showed beginning proteinuria and

first abnormalities in ultrastructure compared to control mice (see 4.4). After three and seven days of induction, no proteinuria is observed and therefore also no ultrastructural changes are expected. However, there might be changes on the molecular level and therefore also in mRNA expression.

Within the study, the trend was observed that after three days postinduction mRNA expression of identified miRNA targets in podocytes are upregulated in the knockout mice compared to the control mice. Expression levels of *VegfA, Npnt* and *Dusp1* were significantly increased in the knockout mice compared to the control mice (Fig. 4.40). Since miRNA binding to target mRNA leads to its inhibition and degradation, mRNA expression levels would be unaltered in normal podocytes. With altered miRNA-mediated regulation, the expression levels of target mRNAs are suspected to be increased, which could be observed in the mice lacking *Dicer*.

After seven days, mRNA expression levels in knockout mice were downregulated compared to the control mice as well as after 24 day postinduction. This can most likely be explained by secondary effects due to perturbation. In the pilot experiment, knockout mice showed first signs of proteinuria and ultrastructural abnormalities after 24 days (see 4.4). Incongruently, within the experiment, for five mice no proteinuria was detectable at days 24 that was set as perfusion time point. However, since molecular changes obviously already take place, animals were used for mRNA expression analysis. Since podocytes of all animals showed a green fluorescence (*Dicer*$^{+/+}$ and *Dicer*$^{lox/lox}$ animals), it can be assumed that knockout of *mT/mG* and thus, also of *Dicer* in one cell was successful. Moreover, after three days *Dicer* expression was not detectable in knockout mice any more, reinforcing the successful knockout and perturbation of miRNA biogenesis. Therefore, with the onset of visible ultrastructural defects, which were observed in the pilot knockout mice experiment, downregulation of the target mRNA expression at day 24 and maybe also already on day seven might be due to secondary effects.

5.3.2. miRNA levels in DICER deletion models

Constitutive deletion of *Dicer* and *Drosha* in mice lead to glomerular injury (Harvey et al., 2008; Ho et al., 2008; Shi et al., 2008; Zhdanova et al., 2011) resulting from altered miRNA biogenesis. After three weeks and with onset of proteinuria, miR-30a could not be detected in knockout mice compared to control mice by *in situ* hybridization (Harvey et al., 2008), revealing the incapability of affected podocytes to synthesize mature miRNAs.

Within the present work about 1/3 reduced levels of miR-30a/d/e-5p could still be detected in three of six knockout mice after seven days of induction by qPCR (data not shown). Detection of other miRNAs could not be verified since the primers also amplified a similar product in the negative control.

One explanation can be technical reasons. qPCR analysis is not the favorable method for miRNA detection since it reveals disadvantages as discussed later on in more detail (see 5.3.2). Another explanation can be that a basic level of mature miRNAs might be present in the knockout cells. For example, in human colorectal cancer cell line (HCT116) some canonical miRNAs were still detectable, albeit at markedly reduced levels after DICER ablation, e.g. miR-16-5p (Kim et al., 2016). To investigate half-lives of mature miRNAs in murine podocytes *in vivo* other RNA detection techniques would be necessary, such as additional Northern blotting, d*eep sequencing* or ISH/RNA scope.

Nevertheless, mice develop proteinuria and ultrastructural changes of the filtration barrier. The amount of residual miRNAs has no essential functional role at least for ultrastructural maintenance in adult podocytes. Moreover, it indicates that even small changes in miRNA levels can have severe effects on podocyte structure and function.

So far, only miR-451 was identified to be produced independently from DICER activity. Due to its short length, the miRNA is not recognizes by DICER and cleaved by AGO2 instead (Cheloufi et al., 2010). In *DICER*-deficient cells it was observed that most of the detected miRNA belonged to the 5p miRNA species (Kim et al., 2016). It was demonstrated that with *DICER* absence, some pre-miRNA can be loaded directly onto AGO, as shown by IP and Northern blotting of pre-miR-16 and AGO. Therefore, it might be possible that beside miR-451 some other pre-miRNA can be loaded onto AGO, enabling maturation of the 5p miRNAs based on 3'-5' trimming (Kim et al., 2016).

Also, the recruitment of miRNAs from other components of the filtration barrier, e.g. the mesangial cells or even other tissues could be a possible explanation for residual miRNA levels. Over the last years, circulating miRNAs became a target of the miRNA research field. Circulating miRNA were detected in various body fluids, e.g. urine or serum and their resistance to high endogenous RNase activity makes them good clinical biomarkers. *In vitro*, it was already demonstrated that the extracellular miRNAs were transferred from one cell to another through exosomes (Kogure et al., 2011; Montecalvo et al., 2012; Sohel et al., 2013). Moreover, it was shown that the miRNAs could regulate their target genes in the recipient cells, indicating circulating miRNA-mediated intercellular communication and a potential role in target gene regulation.

Not much is known about miRNA degradation and turnover rate in podocytes. Several *in vitro* studies demonstrated that the half-live of miRNA are basically stable (Bail et al., 2010; Gantier et al., 2011; Zhang et al., 2011). Moreover, the stability of miRNA depend on specific environment (e.g. cell cycle, growth factors) and therefore can varies from a few hours to days or even weeks (Rüegger and Großhans, 2012; Zhang et al., 2012). In HEK293 cells, the treatment with an transcription inhibitor showed no decay of miRNAs after 8 h (Bail et al., 2010) while certain miRNAs survived for over 12 h

after transfection of HeLa cells with miRNA mimickers (Zhang et al., 2011). Compared to miR-29a (>12h), the miR-29b was rapidly decayed due to uracil at positions 9-11 (7h) (Zhang et al., 2011). Conditionally ablation of *Dicer* in mouse embryonic fibroblasts (Gantier et al., 2011) demonstrated that the majority of tested miRNAs were even more stable than mRNAs (miRNAs: 28-220 h, mRNA: ~10h), showing the variability of turnover for specific miRNAs. Konopka et al. observed that *in vivo* at least in mature neurons, the turnover rate of miRNA was very slow and that they were detectable for several weeks (Konopka et al., 2010). These results indicate that miRNA seems to, in general, have a long life span. Therefore, it might be possible that also in podocytes, the miRNAs have a slow decay rate and might be detectable for a specific time period. Since not much is known about turnover of podocyte miRNAs, especially *in vivo*, the inducible *Dicer* knockout mouse could be used as model for the investigation of miRNA half-lives.

5.3.3. Limitations of qPCR analysis and alternative methods for miRNA detection

Several methods have been developed for the identification and quantitation of mRNA and miRNA expression, which offer advantages and disadvantages.

qPCR analysis is a sensitive method of mRNA detection allowing analysis of RNA with small abundance. This makes it a very suitable method if the sample amount is limited like form laboratory animals. With less material and depending on their expression levels, many mRNAs can be detected using one RNA sample. Thus, saving of material is a big advantage of the qPCR method compared to other techniques.

However, for miRNA detection it can be technically challenging. Their short length offers a great disadvantage. For hybridization with their target sequence, PCR primers need a minimum length of 18-20 nt, which is the length of mature miRNAs. Therefore, miRNA detection is based on a miRNA-specific forward primer and a universal reverse primer as described in Hurteau et al. (2006). Due to the limitation of primer design, amplification of unspecific products or genomic DNA might be performed. Moreover, there is no possibility to control products by sequencing. Since an internal control is used to normalize the samples, it is also crucial to choose an internal control with a constant level of expression. Concerning miRNAs, another drawback of qPCR method is overserved. Single mismatches between miRNAs of the same family cannot be detected. In case of the miR-30 family, qPCR Primers against the miR-30a-5p also detects the expression level of miR-30d-5p and miR-30e-5p. However, mismatches of 5 and 7 nucleotides can be distinguished (e.g. miR-30b-5p and miR-30c-5p) (Baumgarten, 2017).

Another RNA quantification method is Northern blotting. It allows the determination of transcript size and the identification of alternatively spliced variants, family members, as well as mutations (Reue, 1998) and concerning miRNAs also single mismatches between family members. The most limitation associated with Northern analysis, is the need of huge high quality RNA. Even slightly degraded RNA can comprise the quality of RNA abundance measurement and at least 10 µg of total RNA is used for Northern blotting, which would translate to 1.5 million cells in cell culture and up to six mice needed for one validated miRNA. Although Northern blotting analysis would be the most specific method, limited RNA output of animals did not allow the detection of miRNA by this method within the present work.

RNA detection techniques using cells or tissue samples are also often used for the quantification of RNAs. *In situ* hybridization can be used especially for the localization of specific miRNAs in cells or tissues. Therefore, no isolation or electrophoretic separation of RNA is needed as with Northern blotting and qPCR analysis. Analysis of tissue samples enables maximum use, allowing the performance of hundreds of different hybridizations on the same tissue. However, the identification of targets with low DNA or RNA copies is difficult. A novel RNA ISH-technologies was described in 2012 (Wang et al.). *RNAScope* steps are similar to ISH and uses cells or tissue sample for RNA detection. Single-molecule visualization in individual cells or tissue samples is achieved through the use of specific designed probes and a hybridization-based signal amplification system. Therewith multiplex detection of up to four targets and background suppression is possible (Wang et al., 2012), making it a favorable method for stimulations amplification and detection of miRNA and its mRNA target. Moreover, it should display a higher sensitivity compared to standard ISH, also allowing also detection of low levels. However, no probes for mature miRNAs were available at the time of the experiments.

5.3.4. miRNA-mediated regulation and its consequence for the filtration barrier

The filtration barrier is composed of the fenestrated endothelium, the glomerular basement membrane and the podocytes with the slit diaphragm in-between neighboring foot processes. Since all components are crucial, tight regulation and even cross talk between the glomerular cells is necessary for functional filtration barrier (Lennon and Hosawi, 2016). Three of the identified miRNA-regulated targets display podocyte-derived proteins with main function in neighboring glomerular cells and the GBM. Therefore, it might be possible that the integrity of the renal filtration is substantially regulated through podocyte miRNA-regulatory processes.

Nephronectin is a podocyte-derived extracellular matrix protein, which localizes to the GBM. Its interaction with α8β1-integrin, which is produced in mesangial cells, connects the GBM to the

mesangium through specialized adhesion structures (Fig. 5.3) (Zimmerman et al., 2018). Within the present work, *Npnt/NPNT* was identified to interact with the miR-101-3p and was significantly increased after three days of DICER absence. Dysregulation of NPNT is known to play a role in kidney dysfunction, which might be miRNA-mediated. Podocyte-specific deletion of NPNT lead to mesangial expansion and sclerosis as well as to loss of mesangial cell adhesion, decreasing the stability of capillary loops (Zimmerman et al., 2018). In diabetic nephropathy, NPNT was increased in mesangial matrix expansion (Nakatani et al., 2012), indicating that NPNT expression level is crucial for kidney function. In zebrafish and mice suppression of *Npnt* by the miR-378a-3p resulted in proteinuria (Müller-Deile et al., 2017), reporting a miRNA- mediated regulation of the renal function. Together with the identified interaction within this study, a relevance of a miRNA-mediated nephronectin pathway in the regulation of podocyte-GBM interaction might be essential for the integrity of filtration barrier.

The other extracellular matrix protein SPARC contains antiproliferative and counter-adhesive properties. It is known to be a regulator of the composition of ECM proteins in mesangial cells and to be a mediator of podocyte detachment (Sussman et al., 2009). *Sparc/SPARC* is regulated by the miR-29a-3p, as shown in this study. In *Dicer* knockout mice, *Sparc* mRNA levels were increased after three days of doxycycline administration, indicating a functional role of SPARC for podocyte structure and function. Under non-pathological conditions, SPARC is only expressed by podocytes however under pathological conditions it is expressed in all glomerular cell types (Francki and Sage, 2001). SPARC binds to several collagens (e.g. collagen type I or IV) and regulates the expression of several secreted proteins as well as matrix metalloproteinases to mediate extracellular matrix deposition (Francki and Sage, 2001). Through its modulation of cell shape and ECM composition, it might control glomerular permeability by influencing interactions between cells and the surrounding ECM. In case of podocyte diseases, increased SPARC levels resulted in likely maladaptive and worsen renal disease. Alteration of miRNA-mediated regulation of SPARC level might therefore be involved in the progression of various kidney diseases. In a passive nephrotoxic nephritis model using SPARC $^{+/+}$ and SPARC $^{-/-}$ mice (Sussman et al., 2009), increased SPARC levels lead to accelerating glomerulosclerosis in the SPARC $^{+/+}$ mice compared to the null-mutant mice. Moreover, matrix accumulation and foot process effacement were observed in the affected mice. It was further shown that SPARC also disrupt focal adhesion. In SPARC $^{+/+}$ mice, podocyte number was decreased indicating primary podocyte detachment (Sussman et al., 2009). Cell attachment is based on cell transition from an adhesive state to de-adhesive state. Cells in an adhesive state are characterized by focal adhesions and stress fibers, while cell in de-adhesive state lacks stress fiber and are marked by cell shape changes from a spread to round morphology (Greenwood and Murphy-Ullrich, 1998). As an anti-adhesive protein, SPARC was shown that it signals de-adhesion by downregulation of focal adhesions, integrin heterodimer formation and reduction of paxillin phosphorylation in lens epithelial cells (Weaver et al., 2006). Disruption of matrix

–integrin interaction lead to detachment of rounded cells from underlying matrix. Moreover, it was described that SPARC also regulates the activity of certain growth factors like VEGF, which is responsible for the fenestration of glomerular endothelium. Binding of SPARC to VEGF prevents the binding of VEGF to its receptors in endothelial cells, which might function as a counterbalance for potential effects of VEGF in the glomerulus (Francki and Sage, 2001). Thus, the interaction between SPARC and VEGF, which both are under miRNA-mediated regulation, might influence the integrity of the filtration barrier.

Especially, the tight regulation of VEGFA dose is important for development and maintenance of the glomerular filtration barrier (Eremina et al., 2007). Within this study, *VegfA*/*VEGFA* was identified as target of miR-503-5p and significantly increased in *Dicer* knockout podocytes after three days postinduction. VEGFA is expressed by podocytes in high amounts during fetal development but in lower doses in the fully differentiated podocytes. In studies analyzing the effect of dose sensitivity of VEGFA (Eremina et al., 2003; Eremina et al., 2007; Satchell and Braet, 2009) showed that dysregulation of VEGFA expression level lead to different phenotypes. Downregulation of VEGFA lead to missing fenestration, GBM thickening and proliferation of mesangial cells (Eremina et al., 2003; Zhang et al., 2010). Changes of the GBM might affect the function of GBM as the signal cross-talk platform between the podocytes and glomerular endothelial cells (Wang et al., 2015). Overexpression of VEGFA resulted in collapsing glomerulopathy, reduced number of endothelial cells as well as the lack of well- formed slit diaphragms in the glomeruli (Eremina et al., 2003; Satchell and Braet, 2009). Since *VegfA/VEGFA* is miRNA- regulated, dysregulation of miRNA expression might contribute to the observed abnormalities causes by altered VEGFA expression.

The architecture of podocytes foot processes is regulated by several proteins that build up the slit diaphragm. CD2AP is an essential component for the slit diaphragm and mutations in CD2AP lead to renal diseases (Takano et al., 2019). In *Dicer* knockout mice, *Cd2ap* mRNA level was increased compared to control mice within the present work and a specific interaction between *CD2AP* and the miR-30a-5p was demonstrated previously (Baumgarten et al., unpublished). CD2AP directly interacts with actin cytoskeleton by connecting it to the plasma membrane proteins (Lehtonen et al., 2002). Together with nephrin, CD2AP interacts with the p85 regulatory subunit of PI3K and lead to its recruitment to the plasma membrane. PI3K recruitment stimulates the AKT signaling, which controls many cellular processes like cell proliferation, survival and metabolism (Hers et al., 2011). If expression level of CD2AP is essential for the initial signaling step, upregulation of CD2AP would enhance AKT signaling. Induced AKT activation by nephrin, podocin and CD2AP was shown to lead to inhibition of detachment-induced apoptosis (anoikis) in podocytes. Lack of CD2AP lead to apoptotic cell death of podocytes, which is one characterization of glomerulosclerosis (Huber et al., 2003). AKT influence

pathways involved in tumorgenesis, thus upregulation might be responsible among that factors to changes in podocytes after miRNA-knockout. Moreover, CD2AP interacts with podocin, which organizes a complex containing the ion channel TRPC6. Since TRPC6 acts a sensor of mechanically and osmotically induced membrane stretch (Huber et al., 2007), dysregulation of CD2AP levels might reduce podocytes ability to adapt to changing pressure and thus easing podocyte injury. In *Cd2ap* deficient mice, defects in podocyte foot processes and extra cellular matrix deposition was observed (Shih et al., 1999). miRNA-mediated regulation of *CD2AP* was demonstrated in a previous study (Baumgarten, 2017) and might contribute to the development of kidney diseases. Tossidou et al. (2019) could demonstrate that VEGFA stimulation induces tyrosine kinases phosphorylation of CD2AP, which lead to changes in affinity of CD2AP to nephrin, and therefore display another crosstalk between the filtration barrier components.

Specific interaction between miR-146b-5p and *FYN* was demonstrated in a previous study (Baumgarten et al., unpublished) and therefore *Fyn* was analyzed in podocytes of Dicer knockout and control mice within this study. mRNA level of *Fyn* was significantly decreased in knockout mice compared to control mice after seven days postinduction. Dysregulation of FYN expression, either overexpression or downregulation, might be due to lacking miRNA regulation. In several studies, altered FYN expression was observed in different kidney diseases. The two slit diaphragm components Neph1 and Nephrin are phosphorylated by FYN tyrosine, which is necessary for the recruitment of NCK adapter protein or Grb2. Both interactions induce actin polymerization (Verma et al., 2006; Garg et al., 2007) and upregulation of FYN by miRNA knockout might lead to its increment. Non-physiological levels of actin polymerization disturb the maintenance of podocyte structure and function. In familial FSGS, mutations of ACTN4 gene lead to higher binding activity of mutant α-actinin-4 to actin fibers and thus leading to stiffening of the actin network. Therefore, altered actin cytoskeleton might be a possible mechanism in the development of the disease (Kaplan et al., 2000; Weins et al., 2005). Also, in the Nail-Patella Syndrome a stiffer actin cytoskeleton was proposed to be a reason for podocyte injury (Burghardt et al., 2013). So dysregulation of FYN activity and hence resulting stiffer actin cytoskeleton might be one mechanism leading to podocyte injury. Downregulation of FYN was also reported to lead to podocyte damage. In $Fyn^{-/-}$ mice the majority of foot processes were effaced and mesangial matrix increased (Verma et al., 2003), indicating the sensitive mechanism and the need of tight regulation.

The podocyte-derived protein DUSP1 (Dual-specificity protein phosphatase-1) was identified as a target of miR-101-3p (Baumgarten et al., unpublished), however not much is known about its final localization or its role for kidney function. DUSP1 is a threonine-tyrosine dual-specificity phosphatase, which is known to play a role in various biological processes. It is a negative regulator of MAPKs activity by dephosphorylating and inactivating extracellular signal-regulated kinases (ERKs), p38 or JNKs (Sheng et al., 2019). Cell proliferation, differentiation and transformation as well as inflammation and

apoptosis are regulated by MAPK signaling. Sheng et al. (2019) demonstrated that downregulation of DUSP1 promotes mitochondrial fission factor (Mff) phosphorylation by amplifying JNK pathway and therefore enhances fatal mitochondrial fission leading to glomerular apoptosis, renal hypertrophy and fibrosis in diabetic nephropathy (Sheng et al., 2019). Overexpression of DUSP1 in contrast attenuated the renal injury. However, in different epithelial tumors like breast, prostate or bladder cancer higher levels of DUSP1 were found showing an important role in tumor carcinogenesis progression (Shen et al., 2016). Thus, regulation of DUSP1 by miRNA might be an important mechanism to balance DUSP1-JNK-Mff pathway and the development of diabetic nephropathy.

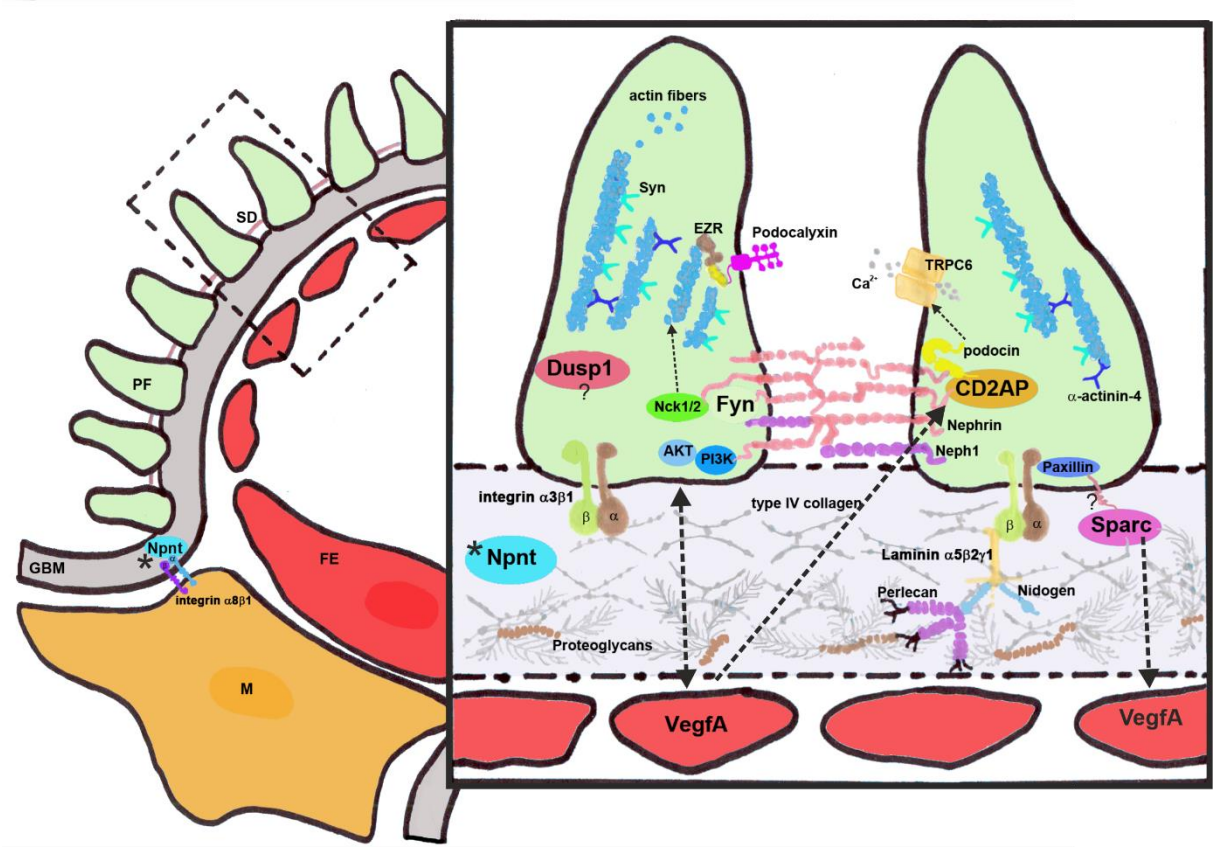

Figure 5.3 ***Crosstalk between components of the filtration barrier.*** *Arrows show reported interaction. Abbreviations: AKT: Protein kinase B, Ca^{2+}: calcium, CD2AP: CD2 associated protein, Dusp1: Dual-specificity protein phosphatase-1, ERZ: Ezrin, FE: Fenestrated endothelium, Fyn: Proto-oncogene tyrosine kinase Fyn, GBM: Glomerular basement membrane, M: Mesangium, Nck1/2:Non-catalytic region of tyrosine kinase adaptor protein 1/2, Npnt: Nephronectin, PF: podocyte foot process, PI3K: Phosphatidylinositol-4,5-bisphosphate 3-kinase, SD: slit diaphragm, Sparc: Secreted acidic cysteine rich glycoprotein, Syn: Synaptopodin, TRPC6: Transient receptor potential cation channel, subfamily C, member 6, VegfA: Vascular endothelial growth factor A.*

6. Summary

Improvement of sequencing techniques lead to identification of more than 38.500 miRNAs in the last decades. In 2019 the human genome contained 2654 mature miRNAs while the murine genome encodes 2013 mature miRNAs (Kozomara et al., 2019). Constitutive deletion of the two miRNA processing enzymes in mice (Drosha and Dicer) revealed the importance of miRNA not only for development, but also for maintenance of normal podocyte structure and function (Harvey et al., 2008; Ho et al., 2008; Shi et al., 2008; Zhdanova et al., 2011). miRNAs post-transcriptionally regulate specific target mRNAs and are involved in various cellular processes. Podocytes are specialized cells which cover the glomerular tuft and show a complex cytoarchitecture. In-between their foot processes, a delicate membrane called slit diaphragm (SD) is build up by specific proteins. Together with the GBM and the fenestrated endothelium, the podocytes (including the SD) form the renal filtration barrier, where the blood filtration takes place. Loss of Dicer or Drosha and thus disturbed canonical miRNA biogenesis leads to podocyte foot processes effacement and following proteinuria, indicating that proteins of the filtration barrier might be targets of miRNA-mediated regulation. For a better understanding of the role of miRNAs for podocyte structure and filtration function, it is necessary to identify target genes of specific miRNAs.

In the present work, the main focus lied on the identification of podocyte-specific miRNA-mRNA interactions that play an important role for podocyte structure and function. In previous studies potential miRNA regulated target genes were identified by using *in silico* predictions (Baumgarten et al., unpublished). These putative interactions between miRNAs and their target mRNAs were analyzed using luciferase assay. An interaction between miR-29a-3p and murine and human *Sparc* was identified. Mutations of the miRNA binding site within the 3'UTR of the target mRNA lead to a derepression of luciferase activity, thus, the observed interaction was verified to be specific. Also an interaction between miR-101-3p and *Npnt/NPNT* as well as miR-503-5p and *VegfA/VEGFA* could be confirmed. For the two target mRNAs *Arrdc3* and *SERINC3*, an interaction was observed in only one specie. However, due to non-conserved interaction between murine and human transcript, loss-of-function luciferase assay was not performed for further verification. For *Per1*, *Zfp36* and *STT3A* no interaction could be identified.

In addition, generated mir-30a-5p and mir-146b-5p knockout cell lines (Baumgarten et al., unpublished) were used to analyze the effect of miRNA loss in podocytes for differentiation. Knockout cells showed differentiation difficulties and stayed smaller than the control cells. Measurement of cell area was used to reinforce the observation. Cells were differentiated for two weeks and staining with HSC Cell Mask Red stain. Using ImageJ analysis cell area was measured showing significant smaller cells in miRNA knockout cells compared to the control cells. Rescue experiment using specific miRNA mimics

was performed, however, a possible positive effect of miRNA mimics on cell area, arborization or specific podocyte markers could not be evaluated due to technical problems. To further investigate the effect of miRNAs on podocyte integrity, optimization of the evaluation method must be carried out.

The transcription factor LMX1B plays an important role for the maintenance of podocyte structure and function and is known to regulate miRNA expression. However, *Lmx1b* is also a potential target of miRNA regulation. To identify the interactions between *Lmx1b/LMX1B* and the predicted miRNAs, luciferase assays were used. For the murine transcript, a positive interaction with the miR-210-3p could be demonstrated at position 1665-1670 in the 3'UTR sequence. The second binding site at position 3236-3274 seems to be not active. For the human transcript, interactions with miR-135a-5p, miR-615-3p and miR-101a-5p were identified. Verification of miRNA binding sites by loss-of function luciferase assay were not performed due to non-conserved interactions between murine and human transcript however might be performed in the future.

Constitutive deletion of *Dicer* and *Drosha* as well as inducible podocyte-specific deletion of *Drosha* demonstrated the importance of miRNAs for the kidney function (Harvey et al., 2008; Ho et al., 2008; Shi et al., 2008; Zhdanova et al., 2011). However, a knockout of *Dicer* in fully developed adult kidneys has not been characterized so far. Therefore, a mouse line with inducible deletion of Dicer in podocytes were generated and used to investigate the effect of miRNA loss in adult kidneys. Knockout mice developed proteinuria after three weeks of induction with further progression. Glomeruli of knockout mice displayed matrix proliferation and glomerular tuft collapse as well as vacuolization of epithelial cells after six weeks of induction. Moreover, proteinaceous casts were observed in the mildly diluted renal tubules. Ultrastructural visualization showed beginning abnormalities after three weeks with further progression after six weeks. With beginning onset of proteinuria, some podocyte foot processes were effaced with still normal formed foot processes. After six weeks, all podocyte foot processes showed an effacement. The observed phenotype is comparable to the constitutive *Dicer* and *Drosha* mice, reinforcing the importance of miRNA for the maintenance of podocyte structure and kidney function.

To investigate the effect of miRNA on target mRNAs *in vivo*, freshly isolated podocyte from *Dicer* knockout and control mice were analyzed using qPCR analysis. The six examined target mRNAs *Sparc*, *Npnt*, *VegfA*, *Dusp*1, *Cd2ap* and *Fyn* were chosen due to identified specific miRNA-mRNA interaction by luciferase assay within this study and in previous studies (Baumgarten et al., unpublished). *Dicer* knockout was induced for three, seven and 24 days by administration of doxycycline. After FACS analysis, RNA was isolated from podocyte cells and transcribed to cDNA. After three days, no more *Dicer* expression could be observed in the knockout mice. Five out of the six examined mRNAs,

expression levels were increased in knockout mice compared to control mice. For *VegfA*, *Npnt* and *Dusp1* significant increment was observed. For *Sparc* and *Cd2ap* no marked difference could be measured. After seven days, all mRNAs displayed decreased levels in the knockout-mice as well as after 24 days. Since *Dicer* expression was not detectable after three days postinduction, decreased levels of mRNAs after seven and 24 days might already be due to secondary effect.

Altogether, the present work further contributes to enlighten the miRNA-mediated regulatory network in podocytes, which is crucial for the maintenance of podocyte structure and function in renal filtration.

7. List of abbreviations

In general, abbreviations of human and murine proteins are written in capital letters. Human genes are written in capital letters and in italics, while murine genes only start with capital letter and are written in italics.

27G	Needle size; outer diameter: 0.4128 mm; inner diameter: 0.210 mm
3'-end	Strand terminating at the hydroxyl group of the third carbon in the sugar-ring
5'-end	Strand terminating at the phosphate of the fifth carbon in the sugar-ring
3p	Mature miRNA derived from the 3'-end of the precursor
5p	Mature miRNA derived from the 5'-end of the precursor
β	Mass concentration
µg	Microgram(s)
µl	Microliter(s)
µm	Micrometer(s)
-/-	Null-mutant
+/+	Wildtype
+/-	Heterozygous
A	
A	Adenine
Abra	Actin-Binding Rho Activating Protein
ABCC1	ATP Binding Cassette Subfamily C Member 1
ACTN4	α-Actinin-4 gene
Adora2b	Adenosine A2b Receptor
AGO 1-4	Argonaute protein 1-4
AKT	Protein kinase B
Anoikis	detachment-induced apoptosis
APS	Ammoniumpersulfate
Arl4c	ADP-Ribosylation Factor-Like 4C
Arrdc3	Arrestin domain containing 3
ATP	Adenosine triphosphate
B	
BDNF	Brain-derived neurotrophic factor
Bgl	*Bacillus globigii*
BLAST	Basic Local Alignment Search Tool
bp	Base pairs
BSA	Bovine serum albumin
C	
c	Molar concentration
C	Cytosine
Ca^{2+}	Bivalent calcium ion
$CaCl_2$	Calcium chloride
Caco buffer	Sodium cacodylate trihydrate buffer
Cas9	CRISPR associated protein 9
ccRCC	clear cell renal cell carcinoma
CCR4	carbon catabolite repressor 4
CD2AP	CD2 associated protein
cDNA	complementary DNA
cm^2	square centimeter(s)
CMV	Cytomegalovirus
CO_2	Carbon dioxide
Cp	Crossing point
Cre	Cre Recombinase
CRISPR	Clustered regularly interspaced short palindromic repeats
CTGF	Connective tissues growth factor
Cx43	Connexin 43
CXCR4	C-X-C chemokine receptor type 4
D	
d	day(s)
d2eGFP	destabilized GFP
DABCO	1, 4-Diazabicyclo[2.2.2]octane
db/db mice	Mice with deficient leptin receptor activity
DCP1-2	decapping protein 1-2
DEPC	Diethylpyrocarbonate
DePex	mounting medium for histology
DGCR8	DiGeorge syndrome critical region gene 8
ddH_2O	double-distillated water
DMEM	Dulbecco's modified Eagle's Medium
DMP30	2,4,6-Tris(dimethylaminomethyl) phenol
DMSO	Dimethyl sulfoxide
DN	Diabetic nephropathy
DNA	Deoxyribonucleic acid
DNase	Deoxyribonuclease
dNTPs	Deoxynucleotide triphosphates
dsRBP	double-stranded RNA-binding protein

Dox	Doxycycline
DTT	1, 4-Dithio-DL-threitol
Dusp1	Dual-specificity protein phosphatase-1

E

e.g.	exempli gratia
E3	ubiquitin-protein ligase
E2F3	Transcription factor E2F3
ECM	Extracellular Matrix
EDTA	Ethylenediaminetetraacetic acid
eGFP	Enhanced green fluorescent protein
EM	Electron microscopy
EMT	Epithelial mesenchymal transition
ENCODE	Encyclopedia of DNA Elements
EPAP	*E.coli* poly-A polymerase
ERK	Extracellular-signal-regulated Kinase
Exp1	cap-binding complex-exportin 1
Exp5	Exportin 5

F

FE	Fenestrated endothelium
FACS	Fluorescent activated cell sorting
FCS	Fetal calf serum
FFPE	Formalin-Fixed Paraffin-Embedded
FGR	Tyrosine kinase family member
Fig	Figure
FLAT	Far linked AT rich elements
FLuc	Firefly luciferase activity
FOSB	FBJ osteosarcoma oncogene B
FSGS	Focal segmental glomerulosclerosis
FYN	Proto-oncogene tyrosine kinase Fyn

G

G	Guanine
g	Gram(s)
g	Multiple of acceleration of gravity
GA	Glutaraldehyde
GBM	Glomerular basement membrane
GFB	Glomerular filtration barrier
GFP	Green fluorescent protein
GRB2	Growth factor receptor-bound protein 2
GW	Glycin-tryptophan repeat Containing

H

h	Hour(s)
H_2O	Water
HBSS	Hank's buffered saline solution
HCC	Hepatocellular carcinoma
HCL	Hydrochloric acid
HDAC4	Histone deacetylase 4
HEK293T	Human Embryonic Kidney 293 cells containing SV40 Large T-antigen
HeLa	HeLa cell line, human cervical cancer cell line
HEPES	4-(2-Hydroxyethyl)-1-piperazineethanesulfonic acid
HF	High Fidelity
Hind	*Haemophilus influenzae*
hnRNP D0	AU-rich element RNA-binding protein 1
hPCL	Human podocyte cell line
hsa	*Homo sapiens*
HSP90	Heat shock protein 90

I

i.e.	id est
IFN	interferon
IgA	Immunoglobulin A
IRF-1	interferon regulatory factor 1
Itga3	Integrin alpha 3
ISH	*In situ* hybridization
ITS-G	Insulin-Transferrin-Selenium

J

JNK	c-Jun N-terminal kinase

K

kb	Kilobase(s)
KCL	Potassium chloride
kDa	Kilodalton
KDM3A	Lysine Demethylase 3A
KH_2PO_4	Potassiumdihydrogen phosphate

L

L	Liter(s)
LB	Lysogeny broth
LC1	Tet-On inducible Cre recombinase
Lim domain	Domain discovered in Lin11, Isl-1, Mec-3
Limk1	LIM domain kinase 1
Lmx1b	LIM Homeobox Transcription Factor 1, Beta
LN	Lupus nephritis
LNA	Locked nucleic acid
loxP sites	Locus of X-over P1, Cre recombinase recognition site

M

M	Molar
MAPK	mitogen-activated protein kinase

MDR1	Multi-Drug-Resistance-Genes 1
MDM2	mouse double minute 2 homologue
Mff	mitochondrial fission factor
m^7G	7-methylguanylate
mG	Monomeric green fluorescent protein
$MgSO_4$	Magnesiumsulfate
min	Minute(s)
miR	Mature miRNA
miRNA	microRNA
mir	Precursor miRNA
mL	Milliliter(s)
mm	Millimeter(s)
mM	Millimolar
mmu	Mus musculus
MPC5	Mouse Podocyte Clone-5
mRNA	Messenger RNA
mT	Targeted tandem dimer Tomato
mT/mG	Tomato mouse reporter cassette
mTor	Mammalian target of rapamycin
mut	Mutant

N

ncRNA	non-coding RNA
n.s.	Not significant
NaCl	Sodiumchloride
Na_2HPO_4	Sodiumhydrogenphosphate
NaN_3	Sodiumazide
NaOH	Sodium hydroxide
Nck1/2	Non-catalytic region of tyrosine kinase adaptor protein 1/2
Neph1	Kin of IRRE-like protein 1
NFATc3	Nuclear factor of activated T-cells, cytoplasmic 3
NIH 3T3	Murine fibroblast cell line
ng	Nanogram(s)
NHP	non-human primates
nm	Nanometer(s)
nM	Nanomolar
NPNT	Nephronectin
non-RT	Not reversely transcribed sample
NOT	Negative regulator of transcription
Notch1	Notch homolog 1, translocationassociated
NPHS1	Nephrin
NPHS2	Podocin
NPS	Nail patella syndrome
nt	Nucleotide

O

OH	Hydroxyl group
OGDR	Oxygen-glucose deprivation/reoxygenation

P

P	Phosphate
PF	Podocyte foot process
p53	Tumor protein P53
p63	Tumor protein p63
p73	Tumor protein p73
p85	regulatory subunit of PI3K
PAGE	Polyacrylamide gel electrophoresis
PAN	Puromycin amino-glycoside
PAN2	Poly(A) Specific Ribonuclease Subunit 2
PAN3	Poly(A) Specific Ribonuclease Subunit 3
PARN	Poly(A) specific ribonuclease
PAS	periodic acid–Schiff
PBS	Phosphate buffered saline
PCR	*Polymerase chain reaction*
PDCD4	Programmed cell death protein 4
PECs	Pariethal endothelial cells
Per1	Period circadian protein homolog 1
PFA	Paraformaldehyde
Pfu	*Pyrococcus furiosus*
PI3K	Phosphatidylinositol-4,5-bisphosphate 3-kinase
piRNAs	piwi-interacting RNA
Pol II/III	RNA polymerase II /III
PODXL	Podocalyxin
PPARγ	Peroxisome proliferator-activated receptor γ
pre-miRNA	miRNA precursor
pri-miRNA	Primary transcript of a miRNA
PTEN	Phosphatase and tensin homolog
PV-1	plasmalemmal vesicle-associated protein 1

Q

qPCR	Quantitative polymerase chain reaction

R

R	Ribosome
RHO	Ras homolog gene family
RISC	RNA induced silencing complex
RLuc	Renilla Luciferase activity
RNA	Ribonucleic acic
RNAse	Ribonuclease, RNA degrading enzyme

Rpm	revolutions per minute
RPMI	Roswell Park Memorial Institute
RT	Room temperature
RT-PCR	Reverse transcription polymerase chain reaction
rtTA	Reverse tetracyclin transactivator
S	
s	Second(s)
S9	RPS9 ribosomal protein
Sac	*Streptomyces achromogenes*
SDS	Sodium dodecylsulfate
shRNA	short hairpin RNA
siRNAs	small interference RNA
SMAD	small mothers against decapentaplegic
snRNA	small nuclear RNA
SOCS1	Suppressor of cytokine signaling 1
SPARC	Secreted protein acidic and rich in cysteine
Spe	*Sphaerotilus natans*
Spry1	Sprouty homolog 1
Src	SRC proto-oncogene, non-receptor tyrosine kinase
Stt3A	subunit of the oligosaccharyl-transferase complex, homolog A
SV40	Simian vacuolating virus 40
T	
T	Thymine
T4 PNK	T4 Polynucleotide Kinase
Tab	Table
TAE buffer	Tris-acetate-EDTA buffer
TALE	Transcription activator-like effector
TALEN	Transcription activator-like effector nuclease
Taq	*Thermus aquaticus*
TEM	Transmission electron microscopy
TEMED	Tetramethylethylenediamine
Tet-On	Tetracycline-Controlled Transcriptional Activation
TDP43	Transactive response DNA binding protein 43 kDa
TGFß	Transforming growth factor-β
TK	Thymidin kinase promoter
TRBP	*trans*-activation-responsive RNA-binding protein
TRIS	Tris(hydroxymethyl)-aminomethan
TRPC1	Transient receptor potential cation channel, subfamily C, member 1
TRPC6	Transient receptor potential cation channel, subfamily C, member 6
Tub	Tubules
TWIST1	Twist-related protein 1
U	
U	Enzyme unit (1 µm/min)
U6	U6 snRNA, spliceosomal RNA
UTR	untranslated region
UV	Ultraviolet
V	
V	Volt(s)
VEGF(A)	Vascular endothelial growth factor(A)
VIS	visible
W	
Wnt1	Proto-oncogene protein Wnt-1/Wnt
wt	Wildtype
WT1	Wilms Tumor protein 1
X	
Xlim1/Lhx1	Lim homeobox 1
XRN1	exoribonuclease 1
Y	
YAP	Yes-associated protein
Z	
Zfp36	Zinc finger protein 36

8. Reference list

Agrawal, R., Tran, U. & Wessely, O. (2009). The miR-30 miRNA family regulates Xenopus pronephros development and targets the transcription factor Xlim1/Lhx1. *Development,* 136: 3927-3936.

Aguilar, A.L.G., Piskol, R., Beitzinger, M., Zhu, J.Y., Kruspe, D. & Aszodi, A. *et al. (*2010). The small RNA expression profile of the developing murine urinary and reproductive systems. *FEBS Letters,* 584: 4426-4434.

Anderegg, A., Lin, H.-P., Chen, J.-A., Caronia-Brown, G., Cherepanova, N. & Yun, B. *et al. (*2013). An Lmx1b-miR135a2 regulatory circuit modulates Wnt1/Wnt signaling and determines the size of the midbrain dopaminergic progenitor pool. *PLoS Genetics,* 9: e1003973.

Appel, D., Kershaw, D.B., Smeets, B., Yuan, G., Fuss, A. & Frye, B. *et al. (*2009). Recruitment of podocytes from glomerular parietal epithelial cells. *Journal of the American Society of Nephrology : JASN,* 20: 333-343.

Atambayeva, S., Niyazova, R., Ivashchenko, A., Pyrkova, A., Pinsky, I. & Akimniyazova, A. *et al. (*2017). The Binding Sites of miR-619-5p in the mRNAs of Human and Orthologous Genes. *BMC Genomics,* 18: 428.

Bail, S., Swerdel, M., Liu, H., Jiao, X., Goff, L.A. & Hart, R.P. *et al. (*2010). Differential regulation of microRNA stability. *RNA (New York, N.Y.),* 16: 1032-1039.

Baumgarten, S. (2017). miRNAs in the kidney and their role in podocyte (dys)function (Regensburg).

Baumgarten, S., Meisinger, S., Dueck, A., Maier, O., Eichner, N. & Fahrenberg, M. *et al. (*unpublished). Role of microRNAs in podocyte (dys)function: Comprehensive search for mRNA targets in podocytes.

Boerries, M., Grahammer, F., Eiselein, S., Buck, M., Meyer, C. & Goedel, M. *et al. (*2013). Molecular fingerprinting of the podocyte reveals novel gene and protein regulatory networks. *Kidney International,* 83: 1052-1064.

Burghardt, T., Kastner, J., Suleiman, H., Rivera-Milla, E., Stepanova, N. & Lottaz, C. *et al. (*2013). LMX1B is essential for the maintenance of differentiated podocytes in adult kidneys. *Journal of the American Society of Nephrology : JASN,* 24: 1830-1848.

Chau, B.N., Xin, C., Hartner, J., Ren, S., Castano, A.P. & Linn, G. *et al. (*2012). MicroRNA-21 promotes fibrosis of the kidney by silencing metabolic pathways. *Science Translational Medicine,* 4: 121ra18.

Cheloufi, S., Dos Santos, C.O., Chong, M.M.W. & Hannon, G.J. (2010). A dicer-independent miRNA biogenesis pathway that requires Ago catalysis. *Nature,* 465: 584-589.

Chong, M.M.W., Rasmussen, J.P., Rudensky, A.Y., Rundensky, A.Y. & Littman, D.R. (2008). The RNAseIII enzyme Drosha is critical in T cells for preventing lethal inflammatory disease. *The Journal of Experimental Medicine,* 205: 2005-2017.

Ding, H., Xu, Y. & Jiang, N. (2020). Upregulation of miR-101a Suppresses Chronic Renal Fibrosis by Regulating KDM3A via Blockade of the YAP-TGF-β-Smad Signaling Pathway. *Molecular Therapy. Nucleic Acids,* 19: 1276-1289.

Donoviel, D.B., Freed, D.D., Vogel, H., Potter, D.G., Hawkins, E. & Barrish, J.P. *et al. (*2001). Proteinuria and perinatal lethality in mice lacking NEPH1, a novel protein with homology to NEPHRIN. *Molecular and Cellular Biology,* 21: 4829-4836.

Du, M., Giridhar, K.V., Tian, Y., Tschannen, M.R., Zhu, J. & Huang, C.-C. *et al. (*2017). Plasma exosomal miRNAs-based prognosis in metastatic kidney cancer. *Oncotarget,* 8: 63703-63714.

Duan, Y.-R., Chen, B.-P., Chen, F., Yang, S.-X., Zhu, C.-Y. & Ma, Y.-L. *et al. (*2019). Exosomal microRNA-16-5p from human urine-derived stem cells ameliorates diabetic nephropathy through protection of podocyte*. Journal of Cellular and Molecular Medicine*.

Dustin, M.L., Olszowy, M.W., Holdorf, A.D., Li, J., Bromley, S. & Desai, N. *et al. (*1998). A Novel Adaptor Protein Orchestrates Receptor Patterning and Cytoskeletal Polarity in T-Cell Contacts*. Cell,* 94: 667-677.

Dweep, H. & Gretz, N. (2015). miRWalk2.0: a comprehensive atlas of microRNA-target interactions*. Nature Methods,* 12: 697.

Dweep, H., Sticht, C. & Gretz, N. (2013). In-Silico Algorithms for the Screening of Possible microRNA Binding Sites and Their Interactions*. Current Genomics,* 14: 127-136.

Ebert, M.S., Neilson, J.R. & Sharp, P.A. (2007). MicroRNA sponges: competitive inhibitors of small RNAs in mammalian cells*. Nature Methods,* 4: 721-726.

Eremina, V., Baelde, H.J. & Quaggin, S.E. (2007). Role of the VEGF--a signaling pathway in the glomerulus: evidence for crosstalk between components of the glomerular filtration barrier*. Nephron Physiology,* 106: p32-7.

Eremina, V., Sood, M., Haigh, J., Nagy, A., Lajoie, G. & Ferrara, N. *et al. (*2003). Glomerular-specific alterations of VEGF-A expression lead to distinct congenital and acquired renal diseases*. The Journal of Clinical Investigation,* 111: 707-716.

Francki, A. & Sage, E.H. (2001). SPARC and the Kidney Glomerulus Matricellular Proteins Exhibit Diverse Functions under Normal and Pathological Conditions*. Trends in Cardiovascular Medicine,* 11: 32-37.

Fuziwara, C.S. & Kimura, E.T. (2015). Insights into Regulation of the miR-17-92 Cluster of miRNAs in Cancer*. Frontiers in Medicine,* 2: 64.

Gantier, M.P., McCoy, C.E., Rusinova, I., Saulep, D., Wang, D. & Xu, D. *et al. (*2011). Analysis of microRNA turnover in mammalian cells following Dicer1 ablation*. Nucleic Acids Research,* 39: 5692-5703.

Garg, P., Verma, R., Nihalani, D., Johnstone, D.B. & Holzman, L.B. (2007). Neph1 cooperates with nephrin to transduce a signal that induces actin polymerization*. Molecular and Cellular Biology,* 27: 8698-8712.

Gebeshuber, C.A., Kornauth, C., Dong, L., Sierig, R., Seibler, J. & Reiss, M. *et al. (*2013). Focal segmental glomerulosclerosis is induced by microRNA-193a and its downregulation of WT1*. Nature Medicine,* 19: 481-487.

Gomez, I.G., MacKenna, D.A., Johnson, B.G., Kaimal, V., Roach, A.M. & Ren, S. *et al. (*2015). Anti-microRNA-21 oligonucleotides prevent Alport nephropathy progression by stimulating metabolic pathways*. The Journal of Clinical Investigation,* 125: 141-156.

Greenwood, J.A. & Murphy-Ullrich, J.E. (1998). Signaling of de-adhesion in cellular regulation and motility*. Microscopy Research and Technique,* 43: 420-432.

Griffiths-Jones, S. (2004). The microRNA Registry*. Nucleic Acids Research,* 32: D109-11.

Griffiths-Jones, S., Grocock, R.J., van Dongen, S., Bateman, A. & Enright, A.J. (2006). miRBase: microRNA sequences, targets and gene nomenclature*. Nucleic Acids Research,* 34: D140-4.

Griffiths-Jones, S., Saini, H.K., van Dongen, S. & Enright, A.J. (2008). miRBase: tools for microRNA genomics*. Nucleic Acids Research,* 36: D154-8.

Gulyaeva, L.F. & Kushlinskiy, N.E. (2016). Regulatory mechanisms of microRNA expression*. Journal of Translational Medicine,* 14: 143.

Guo, N., Guo, J. & Su, D. (2016). MicroRNA-206 and its down-regulation of Wilms'Tumor-1 dictate podocyte health in adriamycin-induced nephropathy. *Renal Failure,* 38: 989-995.

Han, X., Wang, Y., Zhang, X., Qin, Y., Qu, B. & Wu, L. *et al. (*2016). MicroRNA-130b Ameliorates Murine Lupus Nephritis Through Targeting the Type I Interferon Pathway on Renal Mesangial Cells. *Arthritis and Rheumatology (Hoboken, N.J.),* 68: 2232-2243.

Haraldsson, B., Nyström, J. & Deen, W.M. (2008). Properties of the glomerular barrier and mechanisms of proteinuria. *Physiological Reviews,* 88: 451-487.

Harfe, B.D., McManus, M.T., Mansfield, J.H., Hornstein, E. & Tabin, C.J. (2005). The RNaseIII enzyme Dicer is required for morphogenesis but not patterning of the vertebrate limb. *Proceedings of the National Academy of Sciences of the United States of America,* 102: 10898-10903.

Harita, Y., Kitanaka, S., Isojima, T., Ashida, A. & Hattori, M. (2017). Spectrum of LMX1B mutations: from nail-patella syndrome to isolated nephropathy. *Pediatric Nephrology (Berlin, Germany),* 32: 1845-1850.

Harvey, S.J., Jarad, G., Cunningham, J., Goldberg, S., Schermer, B. & Harfe, B.D. *et al. (*2008). Podocyte-specific deletion of dicer alters cytoskeletal dynamics and causes glomerular disease. *Journal of the American Society of Nephrology : JASN,* 19: 2150-2158.

Hausmann, R., Kuppe, C., Egger, H., Schweda, F., Knecht, V. & Elger, M. *et al. (*2010). Electrical forces determine glomerular permeability. *Journal of the American Society of Nephrology : JASN,* 21: 2053-2058.

He, F., Peng, F., Xia, X., Zhao, C., Luo, Q. & Guan, W. *et al. (*2014). MiR-135a promotes renal fibrosis in diabetic nephropathy by regulating TRPC1. *Diabetologia,* 57: 1726-1736.

He, L., Thomson, J.M., Hemann, M.T., Hernando-Monge, E., Mu, D. & Goodson, S. *et al. (*2005). A microRNA polycistron as a potential human oncogene. *Nature,* 435: 828-833.

Heidet, L., Bongers, E.M.H.F., Sich, M., Zhang, S.-Y., Loirat, C. & Meyrier, A. *et al. (*2003). In Vivo Expression of Putative LMX1B Targets in Nail-Patella Syndrome Kidneys. *The American Journal of Pathology,* 163: 145-155.

Herrera-Carrillo, E. & Berkhout, B. (2017). Dicer-independent processing of small RNA duplexes: mechanistic insights and applications. *Nucleic Acids Research,* 45: 10369-10379.

Hers, I., Vincent, E.E. & Tavaré, J.M. (2011). Akt signalling in health and disease. *Cellular Signalling,* 23: 1515-1527.

Ho, J., Ng, K.H., Rosen, S., Dostal, A., Gregory, R.I. & Kreidberg, J.A. (2008). Podocyte-specific loss of functional microRNAs leads to rapid glomerular and tubular injury. *Journal of the American Society of Nephrology : JASN,* 19: 2069-2075.

Huber, T.B. & Benzing, T. (2005). The slit diaphragm: a signaling platform to regulate podocyte function. *Current Opinion in Nephrology and Hypertension,* 14: 211-216.

Huber, T.B., Hartleben, B., Kim, J., Schmidts, M., Schermer, B. & Keil, A. *et al. (*2003). Nephrin and CD2AP associate with phosphoinositide 3-OH kinase and stimulate AKT-dependent signaling. *Molecular and Cellular Biology,* 23: 4917-4928.

Huber, T.B., Kottgen, M., Schilling, B., Walz, G. & Benzing, T. (2001). Interaction with podocin facilitates nephrin signaling. *The Journal of Biological Chemistry,* 276: 41543-41546.

Huber, T.B., Schermer, B. & Benzing, T. (2007). Podocin organizes ion channel-lipid supercomplexes: implications for mechanosensation at the slit diaphragm. *Nephron. Experimental Nephrology,* 106: e27-31.

Hurteau, G.J., Spivack, S.D. & Brock, G.J. (2006). Potential mRNA degradation targets of hsa-miR-200c, identified using informatics and qRT-PCR. *Cell Cycle,* 5: 1951-1956.

Ichii, O., Otsuka-Kanazawa, S., Horino, T., Kimura, J., Nakamura, T. & Matsumoto, M. *et al. (*2014). Decreased miR-26a expression correlates with the progression of podocyte injury in autoimmune glomerulonephritis*. PloS One,* 9: e110383.

Ichimura, K., Kurihara, H. & Sakai, T. (2003). Actin filament organization of foot processes in rat podocytes*. The Journal of Histochemistry and Cytochemistry : Official Journal of the Histochemistry Society,* 51: 1589-1600.

Jonas, S. & Izaurralde, E. (2015). Towards a molecular understanding of microRNA-mediated gene silencing*. Nature Reviews Genetics,* 16: 421-433.

Joung, J.K. & Sander, J.D. (2013). TALENs: a widely applicable technology for targeted genome editing*. Nature Reviews Molecular Cell Biology,* 14: 49-55.

Kang, Y.S., Li, Y., Dai, C., Kiss, L.P., Wu, C. & Liu, Y. (2010). Inhibition of integrin-linked kinase blocks podocyte epithelial-mesenchymal transition and ameliorates proteinuria*. Kidney International,* 78: 363-373.

Kaplan, J.M., Kim, S.H., North, K.N., Rennke, H., Correia, L.A. & Tong, H.Q. *et al. (*2000). Mutations in ACTN4, encoding alpha-actinin-4, cause familial focal segmental glomerulosclerosis*. Nature Genetics,* 24: 251-256.

Kietzmann, L., Guhr, S.S.O., Meyer, T.N., Ni, L., Sachs, M. & Panzer, U. *et al. (*2015). MicroRNA-193a Regulates the Transdifferentiation of Human Parietal Epithelial Cells toward a Podocyte Phenotype*. Journal of the American Society of Nephrology : JASN,* 26: 1389-1401.

Kim, V.N. (2005). MicroRNA biogenesis: coordinated cropping and dicing*. Nature Reviews Molecular Cell Biology,* 6: 376-385.

Kim, Y.-K., Kim, B. & Kim, V.N. (2016). Re-evaluation of the roles of DROSHA, Export in 5, and DICER in microRNA biogenesis*. Proceedings of the National Academy of Sciences of the United States of America,* 113: E1881-9.

King, I.N., Yartseva, V., Salas, D., Kumar, A., Heidersbach, A. & Ando, D.M. *et al. (*2014). The RNA-binding protein TDP-43 selectively disrupts microRNA-1/206 incorporation into the RNA-induced silencing complex*. Journal of Biological Chemistry,* 289: 14263-14271.

Knouf, E.C., Garg, K., Arroyo, J.D., Correa, Y., Sarkar, D. & Parkin, R.K. *et al. (*2012). An integrative genomic approach identifies p73 and p63 as activators of miR-200 microRNA family transcription*. Nucleic Acids Research,* 40: 499-510.

Koga, K., Yokoi, H., Mori, K., Kasahara, M., Kuwabara, T. & Imamaki, H. *et al. (*2015). MicroRNA-26a inhibits TGF-β-induced extracellular matrix protein expression in podocytes by targeting CTGF and is downregulated in diabetic nephropathy*. Diabetologia,* 58: 2169-2180.

Kogure, T., Lin, W.-L., Yan, I.K., Braconi, C. & Patel, T. (2011). Intercellular nanovesicle-mediated microRNA transfer: a mechanism of environmental modulation of hepatocellular cancer cell growth*. Hepatology (Baltimore, Md.),* 54: 1237-1248.

Konopka, W., Kiryk, A., Novak, M., Herwerth, M., Parkitna, J.R. & Wawrzyniak, M. *et al. (*2010). MicroRNA loss enhances learning and memory in mice*. The Journal of Neuroscience : the Official Journal of the Society for Neuroscience,* 30: 14835-14842.

Kozomara, A., Birgaoanu, M. & Griffiths-Jones, S. (2019). miRBase: from microRNA sequences to function*. Nucleic Acids Research,* 47: D155-D162.

Kozomara, A. & Griffiths-Jones, S. (2011). miRBase: integrating microRNA annotation and deep-sequencing data*. Nucleic Acids Research,* 39: D152-7.

Kozomara, A. & Griffiths-Jones, S. (2014). miRBase: annotating high confidence microRNAs using deep sequencing data*. Nucleic Acids Research,* 42: D68-73.

Kriz, W. & Lemley, K.V. (2015). A potential role for mechanical forces in the detachment of podocytes and the progression of CKD. *Journal of the American Society of Nephrology : JASN,* 26: 258-269.

Lai, J.Y., Luo, J., O'Connor, C., Jing, X., Nair, V. & Ju, W. *et al. (*2015). MicroRNA-21 in glomerular injury. *Journal of the American Society of Nephrology : JASN,* 26: 805-816.

Lee, H.W., Khan, S.Q., Khaliqdina, S., Altintas, M.M., Grahammer, F. & Zhao, J.L. *et al. (*2017). Absence of miR-146a in Podocytes Increases Risk of Diabetic Glomerulopathy via Up-regulation of ErbB4 and Notch-1. *Journal of Biological Chemistry,* 292: 732-747.

Lee, R.C., Feinbaum, R.L. & Ambros, V. (1993). The C. elegans heterochronic gene lin-4 encodes small RNAs with antisense complementarity to lin-14. *Cell,* 75: 843-854.

Lehtonen, S., Zhao, F. & Lehtonen, E. (2002). CD2-associated protein directly interacts with the actin cytoskeleton. *American Journal of Physiology-Renal Physiology,* 283: F734-43.

Lennon, R. & Hosawi, S. (2016). Glomerular cell crosstalk. *Current Opinion in Nephrology and Hypertension,* 25: 187-193.

Li, D., Lu, Z., Jia, J., Zheng, Z. & Lin, S. (2013). MiR-124 is related to podocytic adhesive capacity damage in STZ-induced uninephrectomized diabetic rats. *Kidney and Blood Pressure Research,* 37: 422-431.

Li, M., Armelloni, S., Zennaro, C., Wei, C., Corbelli, A. & Ikehata, M. *et al. (*2015). BDNF repairs podocyte damage by microRNA-mediated increase of actin polymerization. *The Journal of Pathology,* 235: 731-744.

Li, M., Ni, W., Zhang, M., Liu, S., Chen, M. & Hong, X. *et al. (*2020). MicroRNA-30/Cx43 axis contributes to podocyte injury by regulating ER stress in diabetic nephropathy. *Annals of Translational Medicine,* 8: 1674.

Li, X. & He, J.C. (2015). An update: the role of Nephrin inside and outside the kidney. *Science China. Life Sciences,* 58: 649-657.

Lin, C.-L., Lee, P.-H., Hsu, Y.-C., Lei, C.-C., Ko, J.-Y. & Chuang, P.-C. *et al. (*2014). MicroRNA-29a promotion of nephrin acetylation ameliorates hyperglycemia-induced podocyte dysfunction. *Journal of the American Society of Nephrology : JASN,* 25: 1698-1709.

Liu, X., Fan, Q., Yang, G., Liu, N., Chen, D. & Jiang, Y. *et al. (*2013). Isolating glomeruli from mice: A practical approach for beginners. *Experimental and Therapeutic Medicine,* 5: 1322-1326.

Liu, Y., Taylor, N.E., Lu, L., Usa, K., Cowley, A.W. & Ferreri, N.R. *et al. (*2010). Renal medullary microRNAs in Dahl salt-sensitive rats: miR-29b regulates several collagens and related genes. *Hypertension (Dallas, Tex. : 1979),* 55: 974-982.

Long, J., Wang, Y., Wang, W., Chang, B.H.J. & Danesh, F.R. (2010). Identification of microRNA-93 as a novel regulator of vascular endothelial growth factor in hyperglycemic conditions. *Journal of Biological Chemistry,* 285: 23457-23465.

Long, J., Wang, Y., Wang, W., Chang, B.H.J. & Danesh, F.R. (2011). MicroRNA-29c is a signature microRNA under high glucose conditions that targets Sprouty homolog 1, and its in vivo knockdown prevents progression of diabetic nephropathy. *Journal of Biological Chemistry,* 286: 11837-11848.

Lüllmann-Rauch, R. & Asan, E. (2019). Harnorgane. In: *Taschenlehrbuch Histologie.* E.A. Renate Lüllmann-Rauch, ed. (Stuttgart: Thieme), pp. 539–566.

Maezawa, Y., Cina, D. & Quaggin, S.E. (2013). Glomerular Cell Biology. In: *Seldin and Giebisch's the kidney. Physiology and pathophysiology.* D.W. Seldin, G.H. Giebisch, M. Caplan, O.W. Moe & R.J. Alpern, eds. (London: Academic Press), pp. 721–755.

Marrone, A.K., Stolz, D.B., Bastacky, S.I., Kostka, D., Bodnar, A.J. & Ho, J. (2014). MicroRNA-17~92 is required for nephrogenesis and renal function. *Journal of the American Society of Nephrology : JASN,* 25: 1440-1452.

Meister, G. (2013). Argonaute proteins: functional insights and emerging roles. *Nature Reviews Genetics,* 14: 447-459.

Miner, J.H. (2012). The glomerular basement membrane. *Experimental Cell Research,* 318: 973-978.

Miosge, N., Sasaki, T. & Timpl, R. (2002). Evidence of nidogen-2 compensation for nidogen-1 deficiency in transgenic mice. *Matrix Biology,* 21: 611-621.

Moeller, M.J., Sanden, S.K., Soofi, A., Wiggins, R.C. & Holzman, L.B. (2003). Podocyte-specific expression of cre recombinase in transgenic mice. *Genesis (New York, N.Y. : 2000),* 35: 39-42.

Montecalvo, A., Larregina, A.T., Shufesky, W.J., Stolz, D.B., Sullivan, M.L.G. & Karlsson, J.M. *et al. (*2012). Mechanism of transfer of functional microRNAs between mouse dendritic cells via exosomes. *Blood,* 119: 756-766.

Moorthy, A.V. & Blichfeldt, T.C. (2009). Anatomy and Physiology of the Kidney. In: *Pathophysiology of kidney disease and hypertension.* A.V. Moorthy, ed. (Philadelphia, Pa: Saunders/Elsevier), pp. 1–15.

Mount, D.B. (2014). Thick ascending limb of the loop of Henle. *Clinical Journal of the American Society of Nephrology : CJASN,* 9: 1974-1986.

Moyano, M. & Stefani, G. (2015). piRNA involvement in genome stability and human cancer. *Journal of Hematology & Oncology,* 8: 38.

Müller-Deile, J., Dannenberg, J., Schroder, P., Lin, M.-H., Miner, J.H. & Chen, R. *et al. (*2017). Podocytes regulate the glomerular basement membrane protein nephronectin by means of miR-378a-3p in glomerular diseases. *Kidney International,* 92: 836-849.

Muzumdar, M.D., Tasic, B., Miyamichi, K., Li, L. & Luo, L. (2007). A global double-fluorescent Cre reporter mouse. *Genesis (New York, N.Y. : 2000),* 45: 593-605.

Nakatani, S., Wei, M., Ishimura, E., Kakehashi, A., Mori, K. & Nishizawa, Y. *et al. (*2012). Proteome analysis of laser microdissected glomeruli from formalin-fixed paraffin-embedded kidneys of autopsies of diabetic patients: nephronectin is associated with the development of diabetic glomerulosclerosis. *Nephrology, Dialysis, Transplantation,* 27: 1889-1897.

Park, J.T., Kato, M., Yuan, H., Castro, N., Lanting, L. & Wang, M. *et al. (*2013). FOG2 protein down-regulation by transforming growth factor-β1-induced microRNA-200b/c leads to Akt kinase activation and glomerular mesangial hypertrophy related to diabetic nephropathy. *Journal of Biological Chemistry,* 288: 22469-22480.

Paroo, Z., Ye, X., Chen, S. & Liu, Q. (2009). Phosphorylation of the human microRNA-generating complex mediates MAPK/Erk signaling. *Cell,* 139: 112-122.

Patel, V. & Noureddine, L. (2012). MicroRNAs and fibrosis. *Current Opinion in Nephrology and Hypertension,* 21: 410-416.

Peng, R., Zhou, L., Zhou, Y., Zhao, Y., Li, Q. & Ni, D. *et al. (*2015). MiR-30a Inhibits the Epithelial--Mesenchymal Transition of Podocytes through Downregulation of NFATc3. *International Journal of Molecular Sciences,* 16: 24032-24047.

Pennisi, E. (2012). Genomics. ENCODE project writes eulogy for junk DNA. *Science,* 337: 1159, 1161.

Petrozza, V., Pastore, A.L., Palleschi, G., Tito, C., Porta, N. & Ricci, S. *et al. (*2017). Secreted miR-210-3p as non-invasive biomarker in clear cell renal cell carcinoma. *Oncotarget,* 8: 69551-69558.

Pollak, M.R., Quaggin, S.E., Hoenig, M.P. & Dworkin, L.D. (2014). The glomerulus: the sphere of influence. *Clinical Journal of the American Society of Nephrology : CJASN,* 9: 1461-1469.

Pöschl, E., Schlötzer-Schrehardt, U., Brachvogel, B., Saito, K., Ninomiya, Y. & Mayer, U. (2004). Collagen IV is essential for basement membrane stability but dispensable for initiation of its assembly during early development. *Development (Cambridge, England),* 131: 1619-1628.

Pozzi, A., Jarad, G., Moeckel, G.W., Coffa, S., Zhang, X. & Gewin, L. *et al. (*2008). Beta1 integrin expression by podocytes is required to maintain glomerular structural integrity. *Developmental Biology,* 316: 288-301.

Qin, J., Ke, J., Xu, J., Wang, F., Zhou, Y. & Jiang, Y. *et al. (*2015). Downregulation of microRNA-132 by DNA hypermethylation is associated with cell invasion in colorectal cancer. *OncoTargets and Therapy,* 8: 3639-3648.

Rabelink, T.J., Heerspink, H.J.L. & Zeeuw, D. de (2015). The Pathophysiology of Proteinuria. In: *Chronic Renal Disease.* P.L. Kimmel & M.E. Rosenberg, eds. (Burlington: Elsevier Science), pp. 92–105.

Reitsma, S., Slaaf, D.W., Vink, H., van Zandvoort, M.A.M.J. & oude Egbrink, Mirjam G. A. (2007). The endothelial glycocalyx: composition, functions, and visualization. *Pflugers Archiv : European Journal of Physiology,* 454: 345-359.

Reue, K. (1998). mRNA quantitation techniques: considerations for experimental design and application. *The Journal of Nutrition,* 128: 2038-2044.

Rüegger, S. & Großhans, H. (2012). MicroRNA turnover: when, how, and why. *Trends in Biochemical Sciences,* 37: 436-446.

Saleem, M.A., O'Hare, M.J., Reiser, J., Coward, R.J., Inward, C.D. & Farren, T. *et al. (*2002). A conditionally immortalized human podocyte cell line demonstrating nephrin and podocin expression. *Journal of the American Society of Nephrology : JASN,* 13: 630-638.

Satchell, S.C. & Braet, F. (2009). Glomerular endothelial cell fenestrations: an integral component of the glomerular filtration barrier. *American Journal of Physiology-Renal Physiology,* 296: F947-56.

Shen, J., Xia, W., Khotskaya, Y.B., Huo, L., Nakanishi, K. & Lim, S.-O. *et al. (*2013). EGFR modulates microRNA maturation in response to hypoxia through phosphorylation of AGO2. *Nature,* 497: 383-387.

Shen, J., Zhang, Y., Yu, H., Shen, B., Liang, Y. & Jin, R. *et al. (*2016). Role of DUSP1/MKP1 in tumorigenesis, tumor progression and therapy. *Cancer Medicine,* 5: 2061-2068.

Sheng, J., Li, H., Dai, Q., Lu, C., Xu, M. & Zhang, J. *et al. (*2019). DUSP1 recuses diabetic nephropathy via repressing JNK-Mff-mitochondrial fission pathways. *Journal of Cellular Physiology,* 234: 3043-3057.

Shi, S., Yu, L., Chiu, C., Sun, Y., Chen, J. & Khitrov, G. *et al. (*2008). Podocyte-selective deletion of dicer induces proteinuria and glomerulosclerosis. *Journal of the American Society of Nephrology : JASN,* 19: 2159-2169.

Shih, N.Y., Li, J., Karpitskii, V., Nguyen, A., Dustin, M.L. & Kanagawa, O. *et al. (*1999). Congenital nephrotic syndrome in mice lacking CD2-associated protein. *Science (New York, N.Y.),* 286: 312-315.

Sohel, M.M.H., Hoelker, M., Noferesti, S.S., Salilew-Wondim, D., Tholen, E. & Looft, C. *et al. (*2013). Exosomal and Non-Exosomal Transport of Extra-Cellular microRNAs in Follicular Fluid: Implications for Bovine Oocyte Developmental Competence. *PloS One,* 8: e78505.

Sussman, A.N., Sun, T., Krofft, R.M. & Durvasula, R.V. (2009). SPARC accelerates disease progression in experimental crescentic glomerulonephritis. *The American Journal of Pathology,* 174: 1827-1836.

Takano, T., Bareke, E., Takeda, N., Aoudjit, L., Baldwin, C. & Pisano, P. *et al. (*2019). Recessive mutation in CD2AP causes focal segmental glomerulosclerosis in humans and mice. *Kidney International,* 95: 57-61.

Tang, Y., Liu, D., Zhang, L., Ingvarsson, S. & Chen, H. (2011). Quantitative analysis of miRNA expression in seven human foetal and adult organs. *PloS One,* 6: e28730.

The ENCODE Project Consortium (2004). The ENCODE (ENCyclopedia Of DNA Elements) Project. *Science,* 306: 636-640.

Tossidou, I., Teng, B., Worthmann, K., Müller-Deile, J., Jobst-Schwan, T. & Kardinal, C. *et al. (*2019). Tyrosine Phosphorylation of CD2AP Affects Stability of the Slit Diaphragm Complex. *Journal of the American Society of Nephrology : JASN,* 30: 1220-1237.

Treiber, T., Treiber, N. & Meister, G. (2019). Regulation of microRNA biogenesis and its crosstalk with other cellular pathways. *Nature Reviews Molecular Cell Biology,* 20: 5-20.

Trionfini, P. & Benigni, A. (2017). MicroRNAs as Master Regulators of Glomerular Function in Health and Disease. *Journal of the American Society of Nephrology : JASN,* 28: 1686-1696.

Tryggvason, K. & Wartiovaara, J. (2005). How does the kidney filter plasma? *Physiology (Bethesda, Md.),* 20: 96-101.

Uddin, M.J., Dorotea, D., Pak, E.S. & Ha, H. (2020). Fyn Kinase: A Potential Therapeutic Target in Acute Kidney Injury. *Biomolecules and Therapeutics,* 28: 213-221.

Vasmant, D., Maurice, M. & Feldmann, G. (1984). Cytoskeleton ultrastructure of podocytes and glomerular endothelial cells in man and in the rat. *The Anatomical Record,* 210: 17-24.

Ventura, A., Young, A.G., Winslow, M.M., Lintault, L., Meissner, A. & Erkeland, S.J. *et al. (*2008). Targeted deletion reveals essential and overlapping functions of the miR-17 through 92 family of miRNA clusters. *Cell,* 132: 875-886.

Verma, R., Kovari, I., Soofi, A., Nihalani, D., Patrie, K. & Holzman, L.B. (2006). Nephrin ectodomain engagement results in Src kinase activation, nephrin phosphorylation, Nck recruitment, and actin polymerization. *The Journal of Clinical Investigation,* 116: 1346-1359.

Verma, R., Wharram, B., Kovari, I., Kunkel, R., Nihalani, D. & Wary, K.K. *et al. (*2003). Fyn binds to and phosphorylates the kidney slit diaphragm component Nephrin. *The Journal of Biological Chemistry,* 278: 20716-20723.

Wang, F., Flanagan, J., Su, N., Wang, L.-C., Bui, S. & Nielson, A. *et al. (*2012). RNAscope: a novel in situ RNA analysis platform for formalin-fixed, paraffin-embedded tissues. *The Journal of Molecular Diagnostics : JMD,* 14: 22-29.

Wang, H., Yue, Z., Wu, J., Liu, T., Mo, Y. & Jiang, X. *et al. (*2015). The Accumulation of VEGFA in the Glomerular Basement Membrane and Its Relationship with Podocyte Injury and Proteinuria in Alport Syndrome. *PloS One,* 10: e0135648.

Wang, Z. (2011). The guideline of the design and validation of MiRNA mimics. *Methods in Molecular Biology (Clifton, N.J.),* 676: 211-223.

Weaver, M.S., Sage, E.H. & Yan, Q. (2006). Absence of SPARC in lens epithelial cells results in altered adhesion and extracellular matrix production in vitro. *Journal of Cellular Biochemistry,* 97: 423-432.

Weinbaum, S., Tarbell, J.M. & Damiano, E.R. (2007). The structure and function of the endothelial glycocalyx layer. *Annual Review of Biomedical Engineering,* 9: 121-167.

Weins, A., Kenlan, P., Herbert, S., Le, T.C., Villegas, I. & Kaplan, B.S. *et al. (*2005). Mutational and Biological Analysis of alpha-actinin-4 in focal segmental glomerulosclerosis. *Journal of the American Society of Nephrology : JASN,* 16: 3694-3701.

Welsh, G.I. & Saleem, M.A. (2011). The podocyte cytoskeleton--key to a functioning glomerulus in health and disease. *Nature reviews. Nephrology,* 8: 14-21.

Wennemuth, G. (2017). Niere und Urogenitalsystem. In: *Taschenbuch Histologie.* G. Wennemuth, M. Albrecht, G. Aumüller, R. Bock, E. Eppler & A. Hofmann *et al.*, eds. (München: Elsevier), pp. 218–235.

Wiggins, R.C. (2007). The spectrum of podocytopathies: a unifying view of glomerular diseases. *Kidney International,* 71: 1205-1214.

Wightman, B., Ha, I. & Ruvkun, G. (1993). Posttranscriptional regulation of the heterochronic gene lin-14 by lin-4 mediates temporal pattern formation in C. elegans. *Cell,* 75: 855-862.

Witzgall, R. (2017). Nail-patella syndrome. *Pflugers Archiv : European Journal of Physiology,* 469: 927-936.

Wu, J., Zheng, C., Fan, Y., Zeng, C., Chen, Z. & Qin, W. *et al. (*2014). Downregulation of microRNA-30 facilitates podocyte injury and is prevented by glucocorticoids. *Journal of the American Society of Nephrology : JASN,* 25: 92-104.

Wu, J., Zheng, C., Wang, X., Yun, S., Zhao, Y. & Liu, L. *et al. (*2015). MicroRNA-30 family members regulate calcium/calcineurin signaling in podocytes. *The Journal of Clinical Investigation,* 125: 4091-4106.

Xie, H., Lin, H.-L., Wang, N., Sun, Y.-L., Kan, Y. & Guo, H. *et al. (*2015). Inhibition of microRNA-30a prevents puromycin aminonucleoside-induced podocytic apoptosis by upregulating the glucocorticoid receptor α. *Molecular medicine reports,* 12: 6043-6052.

Yang, F., Cui, Z., Deng, H., Wang, Y., Chen, Y. & Li, H. *et al. (*2019). Identification of miRNAs-genes regulatory network in diabetic nephropathy based on bioinformatics analysis. *Medicine,* 98: e16225.

Yang, X., Wu, D., Du, H., Nie, F., Pang, X. & Xu, Y. (2017). MicroRNA-135a is involved in podocyte injury in a transient receptor potential channel 1-dependent manner. *International Journal of Molecular Medicine,* 40: 1511-1519.

Ye, P., Liu, Y., Chen, C., Tang, F., Wu, Q. & Wang, X. *et al. (*2015). An mTORC1-Mdm2-Drosha axis for miRNA biogenesis in response to glucose- and amino acid-deprivation. *Molecular cell,* 57: 708-720.

Yoon, J.-H., Jo, M.H., White, E.J.F., De, S., Hafner, M. & Zucconi, B.E. *et al. (*2015). AUF1 promotes let-7b loading on Argonaute 2. *Genes and Development,* 29: 1599-1604.

Yoshino, H., Yonemori, M., Miyamoto, K., Tatarano, S., Kofuji, S. & Nohata, N. *et al. (*2017). microRNA-210-3p depletion by CRISPR/Cas9 promoted tumorigenesis through revival of TWIST1 in renal cell carcinoma. *Oncotarget,* 8: 20881-20894.

Zha, F., Bai, L., Tang, B., Li, J., Wang, Y. & Zheng, P. *et al. (*2019). MicroRNA-503 contributes to podocyte injury via targeting E2F3 in diabetic nephropathy. *Journal of Cellular Biochemistry,* 120: 12574-12581.

Zhang, S., Ji, Y., Liu, X., Lu, X., Su, W. & Di Zhang *et al. (*2010). Podocyte-specific VEGF down-regulation and pathophysiological development. *IUBMB life,* 62: 677-683.

Zhang, Z., Qin, Y.-W., Brewer, G. & Jing, Q. (2012). MicroRNA degradation and turnover: regulating the regulators. *Wiley Interdisciplinary Reviews. RNA,* 3: 593-600.

Zhang, Z., Zou, J., Wang, G.-K., Zhang, J.-T., Huang, S. & Qin, Y.-W. *et al. (*2011). Uracils at nucleotide position 9-11 are required for the rapid turnover of miR-29 family. *Nucleic Acids Research,* 39: 4387-4395.

Zhdanova, O., Srivastava, S., Di, L., Li, Z., Tchelebi, L. & Dworkin, S. *et al. (*2011). The inducible deletion of Drosha and microRNAs in mature podocytes results in a collapsing glomerulopathy. *Kidney International,* 80: 719-730.

Zheng, Y., Zhao, P., Lian, Y., Li, S., Chen, Y. & Li, L. (2020). MiR-340-5p alleviates oxygen-glucose deprivation/reoxygenation-induced neuronal injury via PI3K/Akt activation by targeting PDCD4. *Neurochemistry International,* 134: 104650.

Zheng, Z., Hu, H., Tong, Y., Hu, Z., Cao, S. & Shan, C. *et al. (*2018). MiR-27b regulates podocyte survival through targeting adenosine receptor 2B in podocytes from non-human primate. *Cell Death and Disease,* 9: 1133.

Zhou, H., Hasni, S.A., Perez, P., Tandon, M., Jang, S.-I. & Zheng, C. *et al. (*2013). miR-150 promotes renal fibrosis in lupus nephritis by downregulating SOCS1. *Journal of the American Society of Nephrology : JASN,* 24: 1073-1087.

Zhou, Z., Wan, J., Hou, X., Geng, J., Li, X. & Bai, X. (2017). MicroRNA-27a promotes podocyte injury via PPARγ-mediated β-catenin activation in diabetic nephropathy. *Cell Death and Disease,* 8: e2658.

Zhu, X.-Y., Ebrahimi, B., Eirin, A., Woollard, J.R., Tang, H. & Jordan, K.L. *et al. (*2015). Renal Vein Levels of MicroRNA-26a Are Lower in the Poststenotic Kidney. *Journal of the American Society of Nephrology : JASN,* 26: 1378-1388.

Zimmerman, S.E., Hiremath, C., Tsunezumi, J., Yang, Z., Finney, B. & Marciano, D.K. (2018). Nephronectin Regulates Mesangial Cell Adhesion and Behavior in Glomeruli. *Journal of the American Society of Nephrology : JASN,* 29: 1128-1140.

9. Supplement

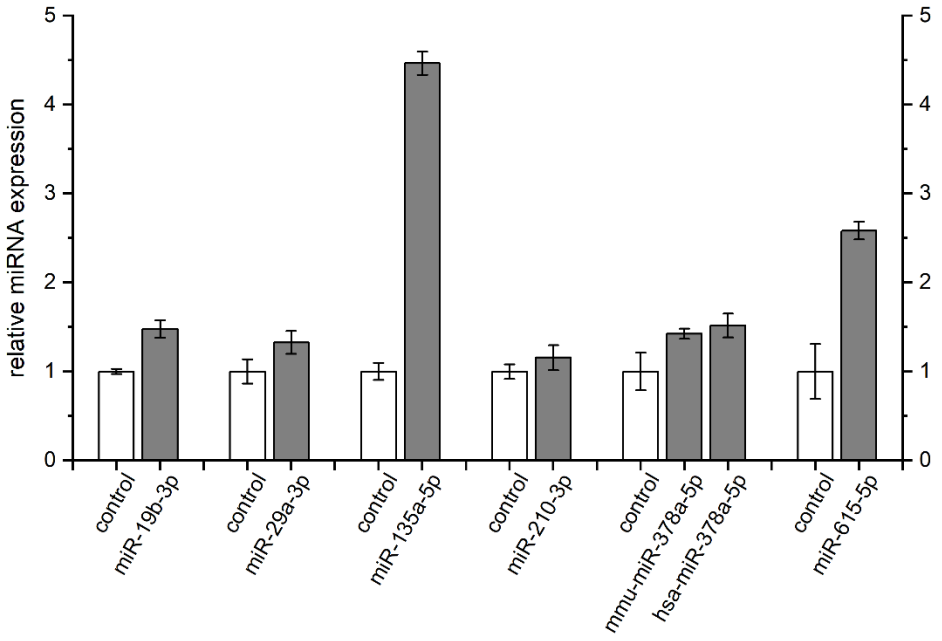

Figure 9.1 ***Overexpression of generic miRNAs****. Either control or respective miRNA pSuper plasmid were used for transfection of HEK293T cells. After 24h small RNA was isolated and used for qPCR analysis.*

```
Query  721   GGCAGGGGACCCCCCAGTTCTTAAGAGCGATTGGAAAGGGAGGAAGGGGAGAGGAAGAGG  780
              ||||||||||||||||||||||||||||||||||||||||||||||||||||||||||||
Sbjct  2452  GGCAGGGGACCCCCCAGTTCTTAAGAGCGATTGGAAAGGGAGGAAGGGGAGAGGAAGAGG  2511

Query  781   CGAACTTGAAGCATCGGACCCAGTTGTATCCCAGCCTGGGCCCAAATGGGGGCAGCCTGG  840
              ||||||||||||||||||||||||||||||||||||||||||||||||||||||||||||
Sbjct  2512  CGAACTTGAAGCATCGGACCCAGTTGTATCCCAGCCTGGGCCCAAATGGGGGCAGCCTGG  2571

Query  841   GCAGGGAGGGCAGCCCCAGGCCCCACCAACTCTAGAGGCAGATGGAGCCCCCAGAACCAG  900
              ||||||||||||||||||||||||||||||||||||||||||||||||||||||||||||
Sbjct  2572  GCAGGGAGGGCAGCCCCAGGCCCCACCAACTCTAGAGGCAGATGGAGCCCCCAGAACCAG  2631

Query  901   GTAGCATCAGACCAGACAACAGAGCCTCCAGTGGTCAGGGACTTCAGAAGCACCTGCTGG  960
              |||||||||||||||||||||||||||||| ||||||||||||||||||||||||||||
Sbjct  2632  GTAGCATCAGACCAGACAACAGAGCCTCCAGGGGTCAGGGACTTCAGAAGCACCTGCTGG  2691
```

Figure 9.2 ***Alignment of fragment 2 of LMX1B 3'UTR with point-mutation at position 2.663 in transcript sequence*** *(marked in bold and red). 198 bp downstream of miR-615-5p binding site (bold brown, 2.459-2.464); Query = cloned sequence of fragment, Sbjct= transcript sequence of LMX1B*

```
Query  836   AGAGCAAAAGAGAATGAGAGGTGGGCAGGGGGAGTCTTGGCAAAAGACCAAGTTCCACTT  895
              ||||||||||||||||||||||||||||||||||||||||||||||||||||||||||||
Sbjct  5233  AGAGCAAAAGAGAATGAGAGGTGGGCAGGGGGAGTCTTGGCAAAAGACCAAGTTCCACTT  5292

Query  896   CCCTGCTGGGGAAGTCGAGGCTCAGAAAGAGGAAATAATTGCCCCAGGTAACACAGGGCA  955
              ||||||||||||||| ||||||||||||||||||||||||||||||||||||||||||||
Sbjct  5293  CCCTGCTGGGGAAGTCAAGGCTCAGAAAGAGGAAATAATTGCCCCAGGTAACACAGGGCA  5352

Query  956   GAGGAGGGACAAAAAGCTGGGCATGGCCCCAGCCAGAGCCCCATCTGCCTACTCCGTGAA  1015
              |||||||||||||||||||||||||||||||||||| ||||||||||||||||||||
Sbjct  5353  GAGGAGGGACAAAAAGCTGGGCATGGCCCCAGCCAGAGCCTCATCTGCCTACTCCGTGAA  5412

Query  1016  GCCTCCCAGGTACTCTGCTATCCTGGGAAACGCACAGGGAGGCCACACAGAGACACTGCT  1075
              ||||||||||||||||||||||||||||||||||||||||||||||||||||||||||||
Sbjct  5413  GCCTCCCAGGTACTCTGCTATCCTGGGAAACGCACAGGGAGGCCACACAGAGACACTGCT  5472

Query  1076  CACAAGAGTCAGACCAAGGTGCCAGCACAGCCTGGAAAGAGCTC  1119
              |||||||||||||||||||||||||||||||||||||||||||
Sbjct  5473  CACAAGAGTCAGACCAAGGTGCCAGCACAGCCTGGAAAGAGCTC  5516
```

Figure 9.3 ***Alignment of fragment 3 of LMX1B 3'UTR with point-mutations at position 5.310 and 5.393 in transcript sequence*** *(marked in bold and red). 74 bp upstream and 5 bp downstream of miR-149-5p binding site (bold cyan, 5.383-5.388), 144 bp and 60 bp upstream of miR-210-3p binding site (bold red, 5.443-5.448); Query = cloned sequence of fragment, Sbjct= transcript sequence of LMX1B; Box indicates SacI- restriction site.*

Numbering of 3'UTR sequence is based on transcript sequence. Blue letters indicate flanking exon while green letters indicate 3'downstream sequence. Restriction sites of *Spe*I (ACTAGT) and *Sac*I (GAGCTC), which are inserted in the primer sequence (box), are indicated as dark yellow.

Arrdc3/ARRDC3

```
1417  ATTGATCCAAATCCTGATCAGTCATCCGAGGACAGACCATCATGCCCCTCTCGCTGAAGC  1476
1477  AACACTTGACTGAGTCAAGTTGACATGGGTTCTGAACTGTATCTCTTCCAGCTGAGGACA  1536
1537  GAGAAGTATCTTGGAGACACGTTTGCAGAGGAAGTGGAATTGCCTTTGCCCAGACAGATG  1596
1597  GCAAACACATGAAACAACCAGTGATCATGCTTTAGAATCCTACAGCATCATTTGGGGCTG  1656
1657  TTCCAACATGCTTGAAGATCTGAGCTTTCCTTCTTTAAAACTGGCACATGTTAAGGGCAG  1716
1717  TCTTCTTAGCCTGTGGTCATCCGTGTCAAGACACCATTGCAAAGAAGGATGTTGTCCTTC  1776
1777  CTATTTGAAAATTTGCACATGCTCAATGCTTACATTGTGCAGTTCAGTGTCACTACAGCA  1836
1837  TTTTTTTTCCATTTATGCCAGACTCTTGATACTCTTACAACTTGTTTATGGTCAGCACAA  1896
1897  CATGGAACAAAAGAAAGCTTTGAAAAACTTTGACATTAAAAAAACAAAACAAAATGCACT  1956
1957  GACAGGTTTTTTTTCTTAGTTTTTTGTTTTGTTTTGTTTTTTGGGTTTTTTGTTTGTTTG  2016
2017  TTAAGTTAATGTAGCCTGGACTCTACCTGCATATGCACATGCTCAGAATTGTCCTACTAG  2076
```

2077 GCTGACCATGTATCACCTCTTCAGCTTGGATCCTACTGTGGATTTATTTACAAACATCAA 2136
2137 ATGCCTTCAAGCCAATCCTTTTGCTGTATGTTTTGCAGCCTACTGTAGTAGATAAGCAAC 2196
2197 AGATACAAGGAGAAAAGAGACAAGAGGAGGAGGCTGACAAGAGACTTTGTATGGCTGTTG 2256
2257 TTTGGTTTTCTGTGAGAGTGTTGCCTTTCTACTATTGATAGCAGAGCAGCCTTGTGTTAC 2316
2317 TGACTGCCTAACATCACTCAATCTCAGGTGAATGCATCACTTGCCAAACTGTTGGAATGC 2376
2377 CGTCTATGTTTGTTGCACTGTTATGTTGTTGTTGTTGTTAATTGTTGTTATTTGGTT 2436
2437 GGATTTTTTGGAGAGGGATATTCGGAAATGGGACATACACAAAACTGATAACCCACCCAC 2496
2497 ATTCCCCTTTTTATCATTACATATAAGAAGAAACAAAGCTCAGAGTGGAGAAAGACAGTA 2556
2557 GGGCGGGCACCAGCAGAGGCAAGGGCTGTTGCTCTGGAAAAATATTTTTATTATTTTAAA 2616
2617 AACGAGTGGAAGCTGCCCGGTCACTAGGGAAGGGAGGGAAAAGTGCATTTATTTTTATAC 2676
2677 AGAGTTACTTAATTACCTCCAAAACACATATGTTGGAAATCAGTTTTGCTGATGCAAGGT 2736
2737 ACTTCAATAAGCCAGAATATATCAAGGTCATGATGGGGGAAGCTTCATTTATACATTTGC 2796
2797 TCAAGTTTGAGAGAATAAAATCCCAAATTTGTTTCCAAAGTGTGTAACTTTATAAGTAGA 2856
2857 AAAACTAGAATGTTTGCTGGGATAAGTAGCTTTAGTTTGTACACGTGTATAATATTGTTT 2916
2917 TTCAACAATTTTTCCTGTCATCTAAGAAACATTGATAGGTCTCTAGCTTTGAGTATATAT 2976
2977 AGGTAGAGCAACACATGAGTAAATTATTTTTAAAGATAATTTATGGTTGGATTGTAACCA 3036
3037 TATACTAACATTCATGAAACAACTAAAACCCCCACCTTCTCAAAGTACAAAATAGAGTGA 3096
3097 TTTTGTAAGAGTTGGCTTGTGTTCTTAGTGACACCAGCATCTCTGATGTTACAACATCAT 3156
3157 GTGTGAGATGGAGCTTGTCATCTGCCCACCTTGCCCTCTGCCCCACAGTTACAGTGCCTG 3216
3217 AGAAGACTCGGAACGCTGGCCTGGTGCTTGACCTGGTTAAATACTGTCTTAAAGCTTCAT 3276
3277 ACAAAATAGGCTTTTCCATAAGTGGCCTTTAAGAAAACATGGAAGATAATTCATGTTTGA 3336
3337 AATAATGCTGACAGGGTGAAGAAAGCCCGTTGTAAAAATGAATCGCGTTTTAAGTGATTC 3396
3397 AGTTAAAGGGTTTGTGCTCCCATAGCAAACTAATACTAGATAATAAGGAAATGGGGTGAA 3456
3457 TTATTTTTTTAATTGTTAAATCATTTTGTGAATGTCCCCCACCCCCAGAAGAAGCTGATG 3516
3517 GGATATTTGGCATAAAGGGCATTTGGTGGTTTTGTTTTCGTTGGTAGGGATTGTCTGAAA 3576
3577 ACACCTGACTCTGTGTTATGTCTAACTAGGGAACAATTGTTGGTGTGCATGGCCTTGGGC 3636
3637 ACTCACTACCATGTTCGACAAAGTACTCTATTAGCAAGAATGACCAATATTCTGATTAAT 3696
3697 TGGCACTGGTGACAAAATTCTTTTACGATTTGGCAAAATAAGGTTTTACTTTTCCCATTA 3756
3757 ATTATTTCTTTACTCTTTAGAGGCATTATACTTCTAAATATTGGTCAATTCTTGACATAA 3816
3817 CACCTGAGGGCCACAGTCATGCTCTAGTATTCAAGATAGCTTCCTAATTTTTCATTTAGG 3876
3877 AAAAGTCAAATCCAAAATGTTTGAGAAACAAAGTGCAATATTAAATGTTTGCTTTATAGA 3936
3937 TTATATTCTATGGCTGTTGTAATCTTTTATTTGGTGCTGAATATGTCCTTGTAGGCTCTG 3996
3997 TTTTAAGAAAACCATGTGGGAAATGATTTAACTTTTCCTATTGCTCTTCCTTGTGGAAAA 4056
4057 TAAAAGTGTTTTTTTTTTTCTGTTTTTGTATAA 4089

Figure 9.4 ***Complete 3'UTR of Arrdc3.*** *Primer positions (box) in transcript sequence and miRNA binding site of miR-19b-3p (bold green).*

1414 ATTGATCCAAATCCTGATCAGTCAGCAGATGATAGACCATCCTGCCCCTCTCGTTGAAGG 1473
1474 AACACTTGGTTGAATCAAGTTGATGTGGGTTCCGAACTGTATCTCTTCCGGCTGAGGACA 1533
1534 GAGAAGTATCTTGGAGACACGTTTCAGAGGAAGTGGAATTACTTTTGCCCAGAAAAATGG 1593

```
1594  CGAATACATGAAACAACCAGTGATCATGCTTTAGAAGCCTACAGCAACATTCTGAGACTG  1653
1654  CTCCAACATGCTTGAAGATCTAAGCTTTTCTCTTTTAAAACTGGCACATACTCAGAGCAG  1713
1714  TCTTCTTAGCCTATGGTCGTACGTGTCAAGACATCACGTTGTAAAGAGGGATGATTTCCT  1773
1774  TCTTTTGATTTGAAAATTTGCACATGCTCAATGCTTACATTGTGCGGTTCGACGTCACTA  1833
1834  CAGCTTCTTTTTTTTTTTTTTTTTTTTCTATTTTTGCCAGACTCTTGATACTCTTAAAA  1893
1894  CTTGTTTGTGGTCAGCACAACAAGGAACAAAACAAAGCTTTGAAAAAACTTTAACATGAA  1953
1954  AAAACGCACTGACATTTTTTTTTATTTAATATAGCCTGGACTTTACCTGCGTATGCACAT  2013
2014  GCTCAGAATTGTCTACTAGGCTGACTATGTATCACCTCTTCAGCTTGGATCCAATTGTGG  2073
2074  ATTTATTTACAAACATCAAATGCCTTCAAGCCAATCCTTTTTGCTGTATGTTTTGCAGCC  2133
2134  TACTGTAGTAGATACGCAACAGATAATGTGGGAAAAAAAGAGATAAGAGGAGGAAGCTAA  2193
2194  TAAGAGACTGTCAAGATTGTATACCTTCTTGGTTTCTTTTAAGAATTTGTTGCCTTTCTA  2253
2254  CTATTACAGCAAAGCAGCATTTTGTTACTGACTGCCTAAAATCACTTAATCTCAGGTGAA  2313
2314  CGCATCACTTGCCAAACTGTTGGAATGCTATTTGTGTTTTGTTGCACTGTTTTTTTCGTT  2373
2374  TGTTTGTTTGTTTATTTGGTTGGCTTTTTGGAGAGGGAAATTTGGAAACGGGACATACAC  2433
2434  AAAAGTTACACACCCACATTCCCTTTTTATCATGACATACAAGAAGAAACTAGCAGAGCT  2493
2494  AAGAATGGAGTGAAGAAAGGCAGTATGGCAGGCACCAGCAAAGAGTTGAGGGCTGTTGCT  2553
2554  CTTAAAAATTATTTTTTTTATTATTATTTTGAAAGTATGGAAGTTTTCCATTCACTGGGG  2613
2614  AAAGGAGGGAAAAGTGCATTTATTTTTATACAGAGTTACTTAATTACCTCCAAAACACAT  2673
2674  ATGTTGGAAATCGCTTTTGCTGGTGCAAAGTATATTAATGAGCAGGAATACATACATTGA  2733
2734  GGTTATGAATAGAGAGCTCAATTTGTACCTTTGCTGTCTTGCTCAAGCTTGGTATGGCAT  2793
2794  GAAAACTCGACTTTATTCCAAAAGTAACTTCAAAATTTAAAATACTAGAACGTTTGCTGC  2853
2854  GATAAATCTTTTGGATTTTTGTGTTTTTCTAATGAGAATACTGTTTTTCATTACCTAAAG  2913
2914  AACAATTTGCTAAACATGAGAAATCACTCACTTTGATTATGTATAGATTACATAGGAAGA  2973
2974  ACAATCACATCAGTAAGTTATAGTTTATATTAAAGGTAATTTTCTGTTGGCTCATAACAA  3033
3034  ATATACCAGCATTCATGATAGCATTTCAGCATTTTCCAAGGTACCAAGTGTACTTATTTT  3093
3094  GTTGTTGTTGTTGTTGTATTTTAGAAGGAATTCAGCTCTGATGTTTTTAAAGAAAAC  3153
3154  CAGCATCTCTGATGTTGCAACATACGTGTAAAATGGGTGTTACATCTATCCTGCCATTTA  3213
3214  ACCCCACAGTTAATAAAGTGGCTGAAAATAATAGTAGCTCTGGCTTGGTGCTTGACCTGG  3273
3274  TTAAATACTGTCTTAAAGCTCATACAAAACAAATAGGCTTTTCCATAAGTGGCCTTTAAG  3333
3334  AAAACATGGAAGACAATTCATGTTTGACAAATGCTGACAGGGTGAAGAAAGCCCAGTGTA  3393
3394  AAAATGAATCGCGTTTTAAGTGATTCGGTTAAAGAGTTTGGGCTCCCGTAGCAAACTAAT  3453
3454  ACTAGATAATAAGGAAATGGGGGTGAAATATTTTTTTATTGTTGAATCATTTTGTGAATG  3513
3514  TCCCCCTCAAAAAAAGCTAATGGAATATTTGGCATAAAGGGCATTTGGTGGTTTTATTTT  3573
3574  TGTTTGAGGGGGATTGTCAGAAAATCCCTTTTCTCTCTTACGTCTAACTGACTAGGGAAC  3633
3634  AATTGTTGATATGCATAGCATTGGAATACTTGTCATTATATACTCTTACAAATAACACAT  3693
3694  GAAGCAAGAATGACCAATATTCTGATAATTGGCACTGGATCACAAAATGTGATAAAACTT  3753
3754  TAAATGTATAAAACTTTATCAAATAAAGTTTTATTTTCCCCTTTAAAATGTATTTCTTTA  3813
3814  GAGGCATTACTTTTTTAAAAATATTGGTCAATTCCTGACATAAGATGTGAGGTTCACAGT  3873
3874  TGTATTCCAGTATTCAAGATAGATTCCTGATTTTTCAATTAGGAAAAGTAAAATCCAAAA  3933
3934  TGTTAGCAAAACAAAGTGCAATATTAAATGTTTGCTTTATAGATTATATTCTATGGCTGT  3993
3994  TTGTAATTTCTCTTTTTTTCCTTTTTTATTTGGTGCTGAATATGTCCTTGTAGGCTCTGT  4053
4054  TTTAAGAAAACAATATGTGGGAAATGATTTAATTTTTCCTATTGCTCTTCCTTGTGGAAA  4113
4114  ATAAAGTGTTTTGTTTTTTTCTGTTTTGTATAATTGTTTGGAGATTTATTTGAATCTTGA  4173
```

4174 TCATATTAGTAACTCACCATACATGCAAACACATTAAATTAAACTATTAAACTCTATTTT 4233

4234 AAGCCA 4239

Figure 9.5 ***Complete 3'UTR of ARRDC3.*** *Primer positios (box) in transcript sequence and miRNA binding site of miR-19b-3p (bold green). Internal SacI-restriction site marked in yellow.*

Fosb/FOSB

1444 GAGCAGCCGTCCGACCCGCTGAACTCGCCCTCCCTTCTTGCTCTGTAAACTCTTTAGACA 1503

1504 AACAAAACAAACAAACCCGCAAGGAACAAGGAGGAGGAAGATGAGGAGGAGAGGGGAGGA 1563

1564 AGCAGTCCGGGGGGTGTGTGTGTGGACCCTTTGACTCTTCTGTCTGACCACCTGCCGCCTC 1623

1624 TGCCATCGGACATGACGGAAGGACCTCCTTTGTGTTTTGTGCTCCGTCTCTGGTTTTCTG 1683

1684 TGCCCCGGCGAGACCGGAGAGCTGGTGACTTTGGGGACAGGGGGTGGGGCGGGGATGGAC 1743

1744 ACCCCTCCTGCATATCTTTGTCCTGTTACTTCAACCCAACTTCTGGGGATAGATGGCTGG 1803

1804 CTGGGTGGGTAGGGTGGGGTGCAACGCCCACCTTTGGCGTCTTGCGTGAGGCTGGAGGGG 1863

1864 AAAGGGTGCTGAGTGTGGGGTGCAGGGTGGGTTGAGGTCGAGCTGGCATGCACCTCCAGA 1923

1924 GAGACCCAACGAGGAAATGACAGCACCGTCCTGTCCTTCTTTTCCCCCACCCACCCATCC 1983

1984 ACCCTCAAGGGTGCAGGGTGACCAAGATAGCTCTGTTTTGCTCCCTCGGGCCTTAGCTGA 2043

2044 TTAACTTAACATTTCCAAGAGGTTACAACCTCCTCCTGGACGAATTGAGCCCCCGACTGA 2103

2104 GGGAAGTCGATGCCCCCTTTGGGAGTCTGCTAACCCCACTTCCCGCTGATTCCAAAATGT 2163

2164 GAACCCCTATCTGACTGCTCAGTCTTTCCCTCCTGGGAAAACTGGCTCAGGTTGGATTTT 2223

2224 TTTCCTCGTCTGCTACAGAGCCCCCTCCCAACTCAGGCCCGCTCCCACCCCTGTGCAGTA 2283

2284 TTATGCTATGTCCCTCTCACCCTCACCCCCACCCCAGGCGCCCTTGGCCGTCCTCGTTGG 2343

2344 GCCTTACTGGTTTTGGGCAGCAGGGGGCGCTGCGACGCCCATCTTGCTGGAGCGCTTTAT 2403

2404 ACTGTGAATGAGTGGTCGGATTGCTGGGTGCGCCGGATGGGATTGACCCCCAGCCCTCCA 2463

2464 AAACTTTCCCTGGGCCTCCCCTTCTTCCACTTGCTTCCTCCCTCCCCTTGACAGGGAGTT 2523

2524 AGACTCGAAAGGATGACCACGACGCATCCCGGTGGCCTTCTTGCTCAGGCCCCAGACTTT 2583

2584 TTCTCTTTAAGTCCTTCGCCTTCCCCAGCCTAGGACGCCAACTTCTCCCCACCCTGGGAG 2643

2644 CCCCGCATCCTCTCACAGAGGTCGAGGCAATTTTCAGAGAAGTTTTCAGGGCTGAGGCTT 2703

2704 TGGCTCCCCTATCCTCGATATTTGAATCCCCAAATATTTTTGGACTAGCATACTTAAGAG 2763

2764 GGGGCTGAGTTCCCACTATCCCACTCCATCCAATTCCTTCAGTCCCAAAGACGAGTTCTG 2823

2824 TCCCTTCCCTCCAGCTTTCACCTCGTGAGAATCCCACGAGTCAGATTTCTATTTTTTAAT 2883

2884 ATTGGGGAGATGGGCCCTACCGCCCGTCCCCCGTGCTGCATGGAACATTCCATACCCTGT 2943

2944 CCTGGGCCCTAGGTTCCAAACCTAATCCCAAACCCCACCCCCAGCTATTTATCCCTTTCC 3003

3004 TGGTTCCCAAAAAGCACTTATATCTATTATGTATAAATAAATATATTATATATGAGTGTG 3063

3064 CGTGTGTGTGCGTGTGCGTGCGTGCGTGCGTGCGTGCGAGCTTCCTTGTTTTCAAGTGTG 3123

3124 CTGTGGAGTTCAAAATCGCTTCTGGGGATTTGAGTCAGACTTTCTGGCTGTCCCTTTTTG 3183

3184 TCACTTTTTTGTTGTTGTCTCGGCTCCTCTGGCTGTTGGAGACAGTCCCGGCCTCTCCCT 3243

3244 TTATCCTTTCTCAAGTCTGTCTCGCTCAGACCACTTCCAACATGTCTCCACTCTCAATGA 3303

3304 CTCTGATCTCCGGTCTGTCTGTTAATTCTGGATTTGTCGGGGACATGCAATTTTACTTCT 3363

3364 GTAAGTAAGTGTGACTGGGTGGTAGATTTTTTACAATCTATATCGTTGAGAATTCTGGGT 3423

3424 GGAAATGTCTGATCAGGAGAAGGGCCTGCCACTGCCGACCACAATTCATTGACTCCATAG 3483

3484 CCCTCACCCAGGCTGTATTTGTGATTTTTTTCATTTTGTTTTTTTGTATTTTGCACCTGA 3543

3544 CCCCGGGGGTGCTGGGGCAGTCTAGCACTGGGCAGCTCCCCTCCCCCCCTTGGTTCTGCA 3603

3604 CTGTCGCCAATAAAAAGCTTTTAAAAAACTGTA 3636

Figure 9.6 ***Complete 3'UTR of Fosb.*** *Primer positions (box) in transcript sequence and miRNA binding site of miR-374a-5p (bold dark green) and miR-19b-3p (bold green).*

1567 CCTTCCGATCCCCTGAACTCGCCCTCCCTCCTCGCTCTGTGAACTCTTTAGACACACAAA 1626

1627 ACAAACAAACACATGGGGGAGAGAGACTTGGAAGAGGAGGAGGAGGAGGAGAAGGAGGAG 1686

1687 AGAGAGGGGAAGAGACAAAGTGGGTGTGTGGCCTCCCTGGCTCCTCCGTCTGACCCTCTG 1746

1747 CGGCCACTGCGCCACTGCCATCGGACAGGAGGATTCCTTGTGTTTTGTCCTGCCTCTTGT 1806

1807 TTCTGTGCCCCGGCGAGGCCGGAGAGCTGGTGACTTTGGGGACAGGGGGTGGGAAGGGGA 1866

1867 TGGACACCCCCAGCTGACTGTTGGCTCTCTGACGTCAACCCAAGCTCTGGGGATGGGTGG 1926

1927 GGAGGGGGGCGGGTGACGCCCACCTTCGGGCAGTCCTGTGTGAGGATTAAGGGACGGGGG 1986

1987 TGGGAGGTAGGCTGTGGGGTGGGCTGGAGTCCTCTCCAGAGAGGCTCAACAAGGAAAAAT 2046

2047 GCCACTCCCTACCCAATGTCTCCCACACCCACCCTTTTTTTGGGGTGCCTAGGTTGGTTT 2106

2107 CCCCTGCACTCCCGACCTTAGCTTATTGATCCCACATTTCCATGGTGTGAGATCCTCTTT 2166

2167 ACTCTGGGCAGAAGTGAGCCCCCCCCTTAAAGGGAATTCGATGCCCCCCTAGAATAATCT 2226

2227 CATCCCCCCACCCGACTTCTTTTGAAATGTGAACGTCCTTCCTTGACTGTCTAGCCACTC 2286

2287 CCTCCCAGAAAAACTGGCTCTGATTGGAATTTCTGGCCTCCTAAGGCTCCCCACCCCGAA 2346

2347 ATCAGCCCCCAGCCTTGTTTCTGATGACAGTGTTATCCCAAGACCCTGCCCCCTGCCAGC 2406

2407 CGACCCTCCTGGCCTTCCTCGTTGGGCCGCTCTGATTTCAGGCAGCAGGGGCTGCTGTGA 2466

2467 TGCCGTCCTGCTGGAGTGATTTATACTGTGAAATGAGTTGGCCAGATTGTGGGGTGCAGC 2526

2527 TGGGTGGGGCAGCACACCTCTGGGGGGATAATGTCCCCACTCCCGAAAGCCTTTCCTCGG 2586

2587 TCTCCCTTCCGTCCATCCCCCTTCTTCCTCCCCTCAACAGTGAGTTAGACTCAAGGGGGT 2646

2647 GACAGAACCGAGAAGGGGGTGACAGTCCTCCATCCACGTGGCCTCTCTCTCTCCTCAG 2706

2707 GACCCTCAGCCCTGGCCTTTTTCTTTAAGGTCCCCCGACCAATCCCCAGCCTAGGACGCC 2766

2767 AACTTCTCCCACCCCTTGGCCCCTCACATCCTCTCCAGGAAGGGAGTGAGGGGCTGTGAC 2826

2827 ATTTTTCCGGAGAAGATTTCAGAGCTGAGGCTTTGGTACCCCCAAACCCCCAATATTTTT 2886

2887 GGACTGGCAGACTCAAGGGGCTGGAATCTCATGATTCCATGCCCGAGTCCGCCCATCCCT 2946

2947 GACCATGGTTTTGGCTCTCCCACCCCGCCGTTCCCTGCGCTTCATCTCATGAGGATTTCT 3006

3007 TTATGAGGCAAATTTATATTTTTTAATATCGGGGGGTGGACCACGCCGCCCTCCATCCGT 3066

3067 GCTGCATGAAAAACATTCCACGTGCCCCTTGTCGCGCGTCTCCCATCCTGATCCCAGACC 3126

3127 CATTCCTTAGCTATTTATCCCTTTCCTGGTTTCCGAAAGGCA**ATTATA**TCTATTATGTAT 3186

3187 AAGTAAATAT**ATTATA**TATGGATGTGTGTGTGTGCGTGCGCGTGAGTGTGTGAGCGCTTC 3246

3247 TGCAGCCTCGGCCTAGGTCACGTTGGCCCTCAAAGCGAGCCGTTGAATTGGAAACTGCTT 3306

3307 CTAGAAACTCTGGCTCAGCCTGTCTCGGGCTGACCCTTTTCTGATCGTCTCGGCCCCTCT 3366

3367 GATTGTTCCCGATGGTCTCTCTCCCTCTGTCTTTTCTCCTCCGCCTGTGTCCATCTGACC 3426

3427 GTTTTCACTTGTCTCCTTTCTGACTGTCCCTGCCAATGCTCCAGCTGTCGTCTGACTCTG 3486

3487 GGTTCGTTGGGGACATGAGATTTTATTTTTTGTGAGTGAGACTGAGGGATCGTAGATTTT 3546

3547 TACAATCTGTATCTTTGACAATTCTGGGTGCGAGTGTGAGAGTGTGAGCAGGGCTTGCTC 3606

3607 CTGCCAACCACAATTCAATGAATCCCCGACCCCCCTACCCCATGCTGTACTTGTGGTTCT 3666

```
3667  CTTTTTGTATTTTGCATCTGACCCCGGGGGGCTGGGACAGATTGGCAATGGGCCGTCCCC  3726
3727  TCTCCCCTTGGTTCTGCACTGTTGCCAATAAAAAGCTCTTAAAAACGCA  3775
```

Figure 9.7 ***Complete 3'UTR of FOSB.*** *Primer positions (box) in transcript sequence and miRNA binding site of miR-374a-5p (bold dark green).*

Npnt/NPNT

```
1851  GTCATCTTCAAAGGTGAAAAAAGGCGTGGTCACACGGGGGAGATTGGATTGGATGATGTG  1910
1911  AGCTTGAAAAGAGGTCGCTGCTGAGAAGACCCCTGGCAGCTCCCGAGCTAGCAGTGAATT  1970
1971  TGTCGCTCTCCCTCATTTCCCAATGCTTGCCCTCTTGTCTCCCTCTTATCAGGCCTAGGG  2030
2031  CAGGAGTGGGTCAGGAGGAAGGTTGCTTGGTGACTCGGGTCTCGGTGGCCTGTTTTGGTG  2090
2091  CAATCCCAGTGAACAGTGACACTCTCGAAGTACAGGAGCATCTGGAGACACCTCCGGGCC  2150
2151  CTTCTGGGGTGTTACCTTATATGGTGTCTTCTTTAGGAAGGCCTTTTGGCATGTGTGACCG  2210
2211  GGACCATCCTTCATCCTGGTTATAGAGTGGGCCTGCTAGCCAACTACGGGAGACGTTTTC  2270
2271  ATTCTGTGCAAATGGTATTCTGTGATCTGTCCAGTGTTGTACCATGAGTAGTACTGACTT  2330
2331  TGCTTACAGTATGACAGTATGATGTACAGCGTGCTTGTGAAACTAGTGTATCTTTTTTCAC  2390
2391  TTCAGTTACTTCTGGCCTGACCTCAATCCATATTCTTTATAACGGAGGGGTGTGCAACAT  2450
2451  ATTAAGATGCATTTATTCTTGTAAACTGTGTCTTTCTGTTAAAGACAGTTATATAGGGTG  2510
2511  GGCATGGAATTTCCTGGTTAGCAGTACTGTGTTTGTGTAAATGTGCTATTACTATAAGTA  2570
2571  TTTACATGTTCCGAATATCCACAGACTCTAGTTGCAAGGTCAAAGGCAGCTTATGATCCC  2630
2631  CTGAGTTAAAAAAAAAATACATGGTGACCTGTCATCTATGCTATGACTTAAACCAGCAGC  2690
2691  AAGAAAACTGGCAAAGGTGTGCGGCTTGGGGTAGTGTCATGATGGCTTTGTTTCTGTGTC  2750
2751  CTTGAGTTTGACCTATTCAGAAAACCATTCAAGGGAAGCAAGGACCTGCAGTTAATATAT  2810
2811  AAAACCCCTATGCTTCCGGTTATACTTTAAACTGACAGCCTTCACCACTGTTACATGCCT  2870
2871  CCACCAGTAAGAAGCTTTGTAAAGATTCTGGGGGGGGGAGCGGAGGACCAGAGGACAGCC  2930
2931  CATAAGACAGGTGCTTTAAATCAGCAAGGTTTCCACGAGTGCAGCTAATGTGTTACCTGA  2990
2991  GGCTGGGCTAGGAAGCAGGCCTGTGCACAGAGGTGACGCTGCCGATGATGGAGCAACACT  3050
3051  AGCACTGTCGAGGAGGACAAGATTGGAATTTTAATATCGACAGAGCCCCAACTTCGTCTC  3110
3111  CTCCCTGTCAGACCGCTGTTTTAAAAAAACACATAGCTTTAGAGAGTCAACTTTTCTCCT  3170
3171  TAGCATTTCTCACCCTTCTGATTAAGTAATCAAAATATTTTCTGCTGTTTTTGCCAGGAG  3230
3231  ACACAAAGATGATTAAAGGGTTGGAAAAAAAGATCTATGGTGACAAACTAAAGGAACTGG  3290
3291  GAGTGTTCTGCCTGGAGAAGAGAAGACTGAGGGGCAGGCCGTGGGGGCTCCTCCAGGCTG  3350
3351  CGAAGGGTTGGCACCAAGAGCTTGGGGAGCGGCTGTTCTCCATGTGTCCTGAGAATAGGA  3410
3411  CCAGAGGGAACAGGCTTAGGCTAGAGTGTGAGGGGGACTTTCCTGGCAGGGACAGTTGCT  3470
3471  AAGCCCAATCCTTTACAAAAAAGAAGTGTGATCATATTCATTCTCCTCCTACTCCCTCCT  3530
3531  TCCCTCCCTCCCTTCCTTCCTTCTTTCCTCCCTCCCTTCCTTCTTTCCTCCCCCCCTTAC  3590
3591  TTCTACCTTCATCTCTCTCTCTCCCTTTCTGTTCTCTTCTCTTCCTCTCTATCTTCTTTG  3650
3651  TCCCTTCCCTCCATTAAAAAAAAAAAAAAAAACTACATAAAATGTTAGGTATTTAAGGTGT  3710
3711  ACGTACTTCAAGGTAAAGTCCCTGATCATGGACACTAGAAGACACTTTGGTCTCCAAAGT  3770
3771  AGTCCATGATAATGACCATCTTCAGAACTGAGCAGTTTGGACTGAGCTCCAAGGTAGACT  3830
3831  TTCTGCTCTTGGCCTCCTCCTGTAAAGGGCACAAAAGGAAATGTCAAGCTCACTGAAAGG  3890
3891  GTCTTCACTCAACAGCCAACCCAGCAGTATTAACAGAACAAATCCCCAAATTCTTTATTC  3950
```

3951 CTGGAGAGGGTGTGTCACACAGGTGCTATCGAATCTTAATAATGTCCTAATATGGTGGTG 4010

4011 TTAATGTTTGATTCCTGGGTAAGGGTGCGACCCCCCACGGTTTGTTCAGTCGATGCTTAG 4070

4071 ACTTGTTTTTCAAAGAGACCCCCAAGAAACATGAGGCAGAGAGAGCCTGTCTGGTGCATT 4130

4131 GCCTGGCTTGCATTGACAAGTTAACATGGCTACTGAAGGTGTGTCAACCACAGCACCGTT 4190

4191 AGCCCTCGTCCTTGCCTCCTTCCATGACTCACTTTCTCACCAGGAGCCTTCCAAGTTCCA 4250

4251 CGAGCTGGTAATGCTTTTTGAACAGCTCCAAGTGACTTTGCCATTTAGCTCAACAGACAC 4310

4311 AGATTTGGGGCTTCTGAAGTAGAAGTAAAGAGCACCTAAGATGTCCTTAGGTCCATTTTT 4370

4371 TTTAATGATTCATTTCCTTCTTGGTCATGTAACTGCACAGCTGATTCAGAAGAAAGGGGA 4430

4431 ACGTAATCGAGAATTTCACTCCCAGGTGCCAATAAGACATTGCACTACACTGATGGAGGA 4490

4491 AGTTATCCAAAGTACTGTATAACATCTTGTTTATTATTTAATGTTCTCTCAAGTGAGAAT 4550

4551 TGTTTGTGGTTTTCAAAATGAACAAATAAAAGCAATCTTTGTAAATAAAAATCACTGTTC 4610

4611 CTACTGCCACctgcctcttcctggttttttttgacttctgatttttgggactgggctc 4669

Figure 9.8 ***Complete 3'UTR of Npnt.*** *Primer positions (box) in transcript sequence: NPNT-2 (----) and NPNT-1 (——), miRNAs binding site of miR-378a-3p (bold black) and miR-101-3p (bold orange).*

1785 GTCGTCTTCAAAGGTGAAAAAAGGCGTGGTCACACTGGGGAGATTGGATTAGATGATGTG 1844

1845 AGCTTGAAAAAAGGCCACTGCTCTGAAGAACGCTAACAACTCCAGAACTAACAATGAACT 1904

1905 CCTATGTTGCTCTATCCTCTTTTTCCAATTCTCATCTTCTCTCCTCTTCTCCCTTTTATC 1964

1965 AGGCCTAGGAGAAGAGTGGGTCAGTGGGTCAGAAGGAAGTCTATTTGGTGACCCAGGTTT 2024

2025 TTCTGGCCTGCTTTTGTGCAATCCCAATGAACAGTGATACCCTCCTTGAAATACAGGGGC 2084

2085 ATCGCAGACACATCAAAGCCATCTGTGGGTGTTGCCTTCCATCCTGTGTCTCTTTCAGGA 2144

2145 AGGCATTCAGCATGCGTGAGCCATACCATCCTCCATCCTGATTACAAGGTGCTCCTTGTA 2204

2205 GCAAATTATGAGAGTGAGTTACGGGAGCAGTTTTTAAAAGAAATCTTTGCAGATGGCTAT 2264

2265 GATGTTATGTGTTCGGTGTTGTACCATGAGTAGTATTGACTTCCCTTGAGATATGATGTA 2324

2325 CAATGTGCTTGTGAAATTGACTTACCCTCTTCACTTAAGTTAGTTCTGGCCTGACCTGAA 2384

2385 CTCTGACTTTTACTGCCATTCACTTTATAAAATAAGGGTGTGTAACATATCAAGATACAT 2444

2445 TTATTTTTATCTGTTTTTTTTTTCCTGTTAAAGACAATTATGTAGAGTGGGCACGTAATC 2504

2505 CCTCCTTAGTAGTATTGTGTTTTGTGTAAATGTGCTATTGATATTAAGTATTTACATGTT 2564

2565 CCAAATATTTACAGACTCTAGTTGCAAGGTAAAGGGCAGCTTGTGATCTCAAAAAAATAC 2624

2625 ATGGTGAAATGTCATCCAGTTCCATGACCTTATATTGGCAGCAGTAGGAAATTGGCAGAA 2684

2685 GTGTTGGGTTGTGGTAACGGAGTGATGAATTTTTTTTTAATGGCCTTGAGTTTGATCTCT 2744

2745 GCAAAGGATAGGAAACCTTTAGGAAGACAAGAAACTGCAGTTAATTTAGAACTGTCACTG 2804

2805 TTTCAAGTTACACTTTAAAACCACAGCTTTTACCATCATAACATGGCTCTGGTAATATGT 2864

2865 AGGAAGCTTTATAAAAGTTTTGGTTGATTCAGAAAAAGGATCCTGTTGCAGAGTGAGAGG 2924

2925 AAGCATAGGGGGAAACTCCATTGGAACAGATTTTCACACAACGTTTTAAATTGATATAAG 2984

2985 TTTAGGCAGTTGTAGTTCATAACTTATGTTGCTCATGTTGTGCTGTGTCAGGATGGGATA 3044

3045 GGAAGCAAGTCCCATGCTTAGAGGCATGGGATGTGTTGGAACGGGATTTACACACACTGG 3104

3105 AGGAGCAGGGCAAGTTGGAATTCTAAGATCCATGAACCCCCAACTGTATTTCCTCCCTGC 3164

3165 ATATTTTACCAATATATTAAAAAACAATGTAACTTTTAAAAGGCATCATTCCTGAGGTTT 3224

3225 GTCTTAATTTCTGATTAAGTAATCAGAATATTTTCTGCTATTTTTGCCAGGAATCACAAA 3284

3285 GATGATTAAAGGGTTGGAAAAAAAGATCTATGATGGAAAATTAAAGGAACTGGGATTATT 3344

3345 GAGCCTGGAGAAGAGAAGACTGAGGGGCAAACCATTGATGGTTTTCAAGTATATGAAGGG 3404

3405 TTGGCACAGAGAGGGTGGCGACCAGCTGTTCTCCATATGCACTAAGAATAGAACAAGAGG 3464

3465 AAACTGGCTTAGACTAGAGTATAAGGGAGCATTTCTTGGCAGGGGCCATTGTTAGAATAC 3524

3525 TTCATAAAAAAAGAAGTGTGAAAATCTCAGTATCTCTCTCTCTTTCTAAAAAATTAGATA 3584

3585 AAAATTTGTCTATTTAAGATGGTTAAAGATGTTCTTACCCAAGGAAAAGTAACAAATTAT 3644

3645 AGAATTTCCCAAAAGATGTTTTGATCCTACTAGTAGTATGCAGTGAAAATCTTTAGAACT 3704

3705 AAATAATTTGGACAAGGCTTAATTTAGGCATTTCCCTCTTGACCTCCTAATGGAGAGGGA 3764

3765 TTGAAAGGGGAAGAGCCCACCAAATGCTGAGCTCACTGAAATATCTCTCCCTTATGGCAA 3824

3825 TCCTAGCAGTATTAAAGAAAAAAGGAAACTATTTATTCCAAATGAGAGTATGATGGACAG 3884

3885 ATATTTTAGTATCTCAGTAATGTCCTAGTGTGGCGGTGGTTTTCAATGTTTCTTCATGTT 3944

3945 AAAGGTATAAGCCTTTCATTTGTTCAATGGATGATGTTTCAGATTTTTTTTTTTTAAGA 4004

4005 GATCCTTCAAGGAACACA**GTTCAG**AGAGATTTTCATCGGGTGCATTCTCTCTGCTTCGTG 4064

4065 TGTGACAAGTTATCTTGGCTGCTGAGAAAGAGTGCCCTGCCCCACACCGGCAGACCTTTC 4124

4125 CTTCACCTCATCAGTATGATTCAGTTTCTCTTATTCAATTGGACTCTCCCAGGTTCCACAG 4184

4185 AACAGTAATATTTTTTGAACAATAGGTACAATAGAAGGTCTTCTGTCATTTAACCTGGTA 4244

4245 AAGGCAGGGCTGGAGGGGGAAAATAAATCATTAAGCCTTTGAGTAACGGCAGAATATATG 4304

4305 GCTGTAGATCCATTTTTAATGGTTCATTTCCTTTATGGTCATATAACTGCACAGCTGAAG 4364

4365 ATGAAAGGGGAAAATAAATGAAAATTTTACTTTTCGATGCCAATGATACATTGCACTAAA 4424

4425 CTGATGGAAGAAGTTATCCAAAGT**ACTGTA**TAACATCTTGTTTATTATTTAATGTTTTCT 4484

4485 AAAATAAAAAATGTTAGTGGTTTTCCAAATGGCCTAATAAAAACAATTATTTGTAAATAA 4544

4545 AAACACTGTTAGTAATACcagttgtctattcttgttttttgagttttgttttttttgac 4604

4605 ttggaaa 4611

Figure 9.9 ***Complete 3'UTR of NPNT.*** *Primer positions (box) in transcript sequence: NPNT-2 (----) and NPNT-1 (——), miRNAs binding site of miR-378a-3p (bold black) and miR-101-3p (bold orange).*

Serinc3/SERINC3

1448 CTCCAGCTGGTTGTGCCTCCTCCTTTACCTCTGGACTCTTGTGGCTCCCCTGGTCCTCAC 1507

1508 AGGTCGGGACTTCAGCTGAGCTCAGTGTGTCAAGGACACTGATAAAGCTGACCAGAGTCT 1567

1568 CCTTTTCTGAAAATGCATATCCATTTTGCGTTTCATCAACGAGACTATTAAGTGAACGCT 1627

1628 TTGCAGATTTGGCTGTATTCAGG**TTTATA**TCAAAAGGCAAGATTGAGTAATGCTTGATGC 1687

1688 AGAATCTGAGCTTTCATATATATATATATATATATATATATACACACACACACACACA 1747

1748 CATATATATGTTTATTTGTAAGGCTATAGCACAAAGGGAACATTTTTGTGTTTTAACATG 1807

1808 AACTACAGCTGTGCTGTGAAGAGAATTC**TTTATA**AAGACCTGTAGATTCCTACAACTTTG 1867

1868 GTTTAAGTTTTAAGTTAGAAGATTGTTGGATATTTAAGGCTATTTTTAATTTCTATTACA 1927

1928 GTCTCCTTAAAAACCAAAAAGGAATGCATTAATCCACATTTCCCTTCTTCAGAGGTGTAG 1987

1988 TGTCCTGGCTCTTGGCAAGGAATTATGTATTTAGGTCAGTCCCCAGAAATGCAGCTGCTC 2047

2048 ATACAGCTGAGAGAAGGCTATTATTGAGTTCCTTTACTTACTT**TTTATA**CTACACTGATG 2107

2108 CTGCTTGATAGAAGTCTGTGGCTTTGTCAGATATGTCACCCAAGTAAATGCTTTGTAGAT 2167

2168 CTGATTAAAATGAAAAGCTCACTTGAGAAACACTGCAGAGTTATGTAATGATCTTGTTGT 2227

2228 GAGTGTGTGAAAGTCAAAGGCATGTCAGTTTATTACATTTGCAACATAAAAGTACTTAAT 2287

2288 TAAAATAGATATTTAGTTTCTTGTTTGTTTGTGTATTTGTTTAGAAAGGGTCTTTTCCAC 2347

```
2348  ATAACCCAGACTTGCTTGGAATGCAGATCATCCTATCTCCACTTCCAAGTACTGAGGAGG  2407
2408  AGGTTTCTATCACCATAGCTAGTCTTTTCTTAAAGATCCTTCTGCAGTGGGGTTGATAGG  2467
2468  TTTTCTTTTATTGTTGTTTTCTTGTTTAGAGAGTCCCAAATCAATCTGACATTTCAGGCA  2527
2528  AAATGCTCCTCTTCTAACACTTAAGATTTGACTAGTCAAGTTTTTAAGTTCATTTAGAAA  2587
2588  CTACCCTAAATATTTTCTCTGGGGAAGATCAAAGTAGGTAAGAAACAGTTTAGGCACTGT  2647
2648  CAAAAAAGATATTCCTGAAAAGCAGTGTGCAAAGGAGGTATGATAAAACAGGCTTTTCAA  2707
2708  GAGAAACTAGTATCGGTTCTGCACTAGGCCCTGTTGGGGTGAAGACAAGACAGACATTCT  2767
2768  TCCATCTAAGGAAAATGAGCGGACCAGCCTGGTAAATTAGTGCTGAAAACTCATAAACAG  2827
2828  AAATCAGTGGATAGAGGCTAGCACAGTGACTTCCTCGAGAGAGTGCTGTTAGGATTTGTA  2887
2888  ACGTAGGTTCACACCAGGTATCAGGGCAGTTCATCTGAGATTTGAACTAAAGATGTAAGG  2947
2948  GGGTTTGGGGAAAAATTGACAGCTTAGAGAATTTCCACATTGGTGTTTAAGGGGATAGGA  3007
3008  AAAACTTATTTCCAGTTTAATCTGTGTACATAGGTTCTGCTTGGGATCCTGGTTGGGATG  3067
3068  GAGGTGGTCCCTTCATATGATGAATAGGTTTGGGAGTCAGACCTCTGGGGTCTGCCTGAC  3127
3128  CTCTGCTATTTTCTAGGTTGAGTGGCTGTCTAATGCTCACTGAGTACATGCTGTGCTTGT  3187
3188  GACCTTGAGCACTCTGCCTGGGCCTCATGCAGAACTTAGTACCAGAGATTATTTGAAGAT  3247
3248  AAAGTTGTCTCAGAATGGATATGTTGTAAGGATGTTTGACAGTAAGTGCCAATGTCACTA  3307
3308  TGGATTAAAGCAAGACTAAATGTACTTAAAAGGTCAGAAGTGTTCAGAATCTGATAGAGG  3367
3368  CTGGGTTGAATGTAGTTTTAGAGAATTAAACATAGTTGTAATATAGACAGCTAGGTAGAG  3427
3428  CTGGAGGCTAGGGAAGCTGGGTTTGATGGGTTGTTGGAACTACTGTCCTTTAGGATCATG  3487
3488  TGTCAAAGCAAACTACAAAGGATTTGTGAAGCAGATAATTGTGGCCCTTAAGCTTAACTG  3547
3548  TGTGAGACAAATACCTGTTTTTAACAGTAGGGGAACCATAAATTTCAAAGCGGATCCTAT  3607
3608  TCTTTGTCTTATATGATTAAAAATAAATGGAGTTCTAAACTACCAAATAATGTAATAGAG  3667
3668  TTCAATAAAGGGTTTTTTTTTTTTTC  3694
```

Figure 9.10 ***Complete 3'UTR of Serinc3.*** *Primer positions (box) in transcript sequence and miRNA binding site of miR-340-5p (bold pink).*

```
1463  CTCCAGCTGGGTCTGCCTCCTGCTTTACGTCTGGACCCTTGTGGCTCCACTTGTCCTCAC  1522
1523  CAGTCGGGACTTCAGCTGAACCTCTGAGTGCCAAGGACACCACTGGAACTCACAAAGGTC  1582
1583  TCCTTCACCGAAAACCCATATACCTTTTAAGTTTGTTTCAACTAAAATATTAAGTGAATG  1642
1643  CTTTGCAAGTTTGACTGTATGCAGGTTTATATCAGAAGGTGAGATTGAATAATGCTTGAT  1702
1703  GCAGAATCGAAACTTCTCATTTATCTGTATATTATGTTTACTTCTAAGGATATAGCACAA  1762
1763  AGGGAACATTTTTTGTTTAAAGTGAACTACAGCTGTGCTGTGAAGAGAGTTCTTTATAAA  1822
1823  GCCTGTAGGTTCTTTTAACTTTGGTTTAAAATGTAAGATAGGAAAATGTTGGATATTTGA  1882
1883  GGCCATGCTTAATATATTTTATATTGCAGTATCCTTTAAAAGCAAAAAAAAAAAAAATGCAT  1942
1943  TTATATTACAGTTTTCCTCTATGAAAGTCCTTACTTATATGATACAAGCACTGTGTTTTG  2002
2003  TGCTTAAACTCTTCAGCGGGGTAGCATCAAAGTTCTTGGGGAAGGATCGTATATGTGGGT  2062
2063  CCCTTCCCTAGAAGAATGGTTGCTGATATGGCTACTGCTTCTACATCTTGAGTTTTTTAA  2122
2123  TTTACTTTTTTTACACTGTAGCATTGAGACTGCTTGATTCAAGTCTGGTGCTTTGCCAGA  2182
2183  TGTATTAATTTCCATAAATGCTTTGTGAGTTTGGTTAAAATGAAGATTCACTTGGGAAAA  2242
2243  CACTGCAGCTTTAGTCTGTGTTACTATCTTGTTATGAGTATGTAAAAGTAAAATGCATGT  2302
2303  GAATTTATCATATTTGCACTATGAAGGTATTTGGTTAAAATACAAAGACTTTTAAGATTT  2362
2363  TAAGGCCCTTTCTTCCAACAGCTTTTATAGTTAGCAGCCATTCTTTATTTTCTGGATAGC  2422
```

```
2423  CAGGTTTTATCACGCTTCTAGTCAGGATGCTCCTATTCCTTCTAAAAATTACGGTCTGAC  2482
2483  TAGTGAGCAAAGTCTTGAATTTATTCAAAAGTCCTAAATACCTTCTCTAGGTAAGACACT  2542
2543  TGGTAGATGAGAGACGGAAGGCATTGTCAAGAACCATTTTCATGAGAGGTGGTGTGCAAA  2602
2603  AAGGTAGAATAAAAGAGTTCTTTCAACAAAGATTTACTGTCTATTCTGTACTAGACCCTG  2662
2663  TAGGTTTTGGGGTACAGTGTTAAACATGATAGAGGCTCTGCCGTCTTGGACTTTAATAGC  2722
2723  TTAGAGAAGAGAGCAAATGAGCTGACAGGTGGTTATAATGTGAATTAGTGCTGTGGTTTA  2782
2783  GGAATTGGAGAGAACTCAAAGGAGAGGTATTTGGTGTAATGGTAGGCTTTCTGGAGAAAA  2842
2843  TGATATTTAAGCCAAGAACTCTTAGAAGTTAGCTAAGAGAGAGATGGGAAAATGAGACGA  2902
2903  CATTGCTGGAGTAGATAAAACTGCATGTTAAAGGCAGGAAGATGGGGAAAAAAAGTTCAG  2962
2963  TAAAGCTGGAATGGGGAAATGTAGTCAGGGACTGAATTTTAAAGGGCTTTATCAACCTCA  3022
3023  GTAAAGAGTTTGGACCTTATGTTGAGGGTGGCTGAAAACATATTCATAGTGTCATGAACA  3082
3083  AATTTTATCTTCAGTCACTTGGGCTGATATATAGAGAATGGATTTAGAGAGATGAGACCA  3142
3143  GGTGCAGTCCATATGAGATGTGAAATAGAGAAGTGGAATCGTAGGGACGGGGAGAAATTG  3202
3203  ACAGGTGAGGGCTACTTAGCAATTAGAATTTTTTTTTTTCAATTTTAATTTTTTTTTTTG  3262
3263  AGACGGAGTCTTGCTCTGTCGCCCAGGCTGGAGTGCAATGGTGCGATCTCCGCTCACTGC  3322
3323  AGGCTCCGCCTCCCGGGTTCACGCCATTCTCCCGCCTCAGCCTCCCTAGTAGCTGGGACT  3382
3383  ACAGGCACCCACCACCACGCCTGGCTAATTTTTTTTGTATTTTTAGTAGAGACAGGGTTT  3442
3443  CACCATGTTAGCCAGGATGGTCTCGATCTCCTGACCTCGTGATCCACCTGCCGCGGCCTC  3502
3503  CCAAAGTTCTAGGATTACTGGCATGAGCCACCGTGCCTGGCCAGCAATTAGAATTTTAAC  3562
3563  ACTGGCAGTTATGAATAATATGAAGGAGAGGTAGATTTCTGAGTGATTCTGGTTTAACCA  3622
3623  GCTGGGTGGATGGTGGTTCCACGTATTCAGGTGGCAAACAGGAAAAACATGTGTTCGAAG  3682
3683  AAGAATGGAGGTAGGTGGTCTCTTAAGAATGGTTAAGAGGCTTGGGAGTCAGACTGCTTG  3742
3743  GGTTTGCATCCCAGCTTTGCCGTTTTCTGGCTATCAAACTTGTCAGCTATTATTTGTTGA  3802
3803  GTACGTACTATTTGATTTATGACCACAGGCAGCTGAGCCTCAGTGTTGGTGCCTAGTGTA  3862
3863  CAAGATTGTTAAAGAATAAAGTTATTTTGCAAAGTGTAACCCATTTTTAGCACTGACATA  3922
3923  GCACTGACAGTAGCTGCTGATCTCATTATGGGCTAAAATAAGACAATATTCAAAGGTCAG  3982
3983  AGATATCTAGCCAGAATCTGATGGAGGCTGGATTTCAGATTTTGTTACAGAATTAGACAG  4042
4043  AGGAACACAGAGGGGACAGGCTCAGTTAGGGTGGAGGTGTGGGGTAGGGAAGCAGGACTT  4102
4103  GATATAAATTATTGGAATCATTGTCTTTTAAACCAGTGGTTTATGTCAGGGTATAGCGTT  4162
4163  TCAAGGGATTTGAGGGTCAGATGGGGAAATGTAGCCCCTTATTTTGCCAGTGTGAAGCAG  4222
4223  ATACCCTGCTTTTCTTTACAGTAGCGGAGTCAGCTTAAGAGCTTTAAAGGTCCTAAACTT  4282
4283  CAAAAACATTACAGTGCCCCATCCTCCGCCTTAATGTAATTCAAAATACAAACAATACTA  4342
4343  AACTGTAAAATAAATGTAACAAAGTCCAATAAAGTTTTTATTTTTTTCTCATGA  4396
```

Figure 9.11 ***Complete 3'UTR of SERINC3.*** *Primer positions (box) in transcript sequence and miRNA binding site of miR-340-5p (bold pink).*

Sparc/SPARC

```
1187  AGGACATCAACAAGGATCTGGTGATCTAAGTTCACGCCTCCTGCTGCAGTCCTGAACTCT  1246
1247  CTCCCTCTGATGTGTCCCCCCTCCCATTACCCCCTTGTTTAAAATGTTTGGATGGTTGGC  1306
1307  TGTTCCGCCTGGGGATAAGGTGCTAACATAGATTTAACTGAATACATTAACGGTGCTAAA  1366
1367  AAAAAAAAAAAAACAAAGTAAGAAAGAAACTAGAACCCAAGTCACAGCATTTTCCCACAT  1426
```

1427 AACTCTGAGGCCATGGCCCATCCACAGCCTCCTGGTCCCCTGCACTACCCAGTGTCTCAC 1486

1487 TGGCTGTGTTGGAAACGGAGTTGCATAAGCTCACCGTCCACAAGCACGAGGAGATATCTC 1546

1547 TAGCTTTCATTTCTGTTTTGCATTTGACTCTTAACACTCACCCAGACTCTGTGCTTATTT 1606

1607 CATTTTGGGGGATGTGGGCTTTTTCCCCTGGTGGTTTGGAGTTAGGCAGAGGGAAGTTAC 1666

1667 AGACACAGGTACAAAATTTGGGTAAAGATGCTGTGAGACCTGAGGACCCACCAGTCAGAA 1726

1727 CCCACATGGCAAGTCTTAGTAGCCTAGGTCAAGGAAAGACAGAATAATCCAGAGCTGTGG 1786

1787 CACACATGACAGACTCCCAGCAGCCCGGGACCTTGCTGTCTTCTCGACTCTTAGGGCGTT 1846

1847 TCTTTCCATGTTTGGCTGTTGGTTTTAGTTTTGGTGAGCCATGGGTGGGCCAGAACATCA 1906

1907 CTCAACTGCAATTGGGCTTTCAGGTTCTTGCCGGGAGCTCTAGGCACTGGGAGGCTGTTT 1966

1967 CAGGAAAGTGAGACTCAAGAGGAAGACAGAAAAGGTTGTAACGTAGAGGAAGTGAGACTG 2026

2027 GTGAATTGGTTTGATTTTTTTCACATCTAGATGGCTGTCATAAAGTTTCTAGCATGTTCC 2086

2087 CCCTCACCTCTCCCCACCCCCTGCCACTTGAAACCTTCTACTAATCAAGAGAAACTTCCA 2146

2147 AGCCAACGGAATGGTCAGATCTCACAGGCTGAGAAATTGTTCCCCTCCAAGCATTTCATG 2206

2207 AAAAAGCTGCTTCTCATTAACCATGCAAACTCTCACAGCAATGTGAAGAGCTTGACAAGT 2266

2267 CTTTCAAAATAAAAAGTAACAACTTAGAAACGGC 2300

Figure 9.12 ***Complete 3'UTR of Sparc.*** *Primer positions (box) in transcript sequence and miRNA binding site of miR-29a-3p (bold cyan). Internal SacI-restriction site marked in yellow.*

948 AGGATATCGACAAGGATCTTGTGATCTAAATCCACTCCTTCCACAGTACCGGATTCTCTC 1007

1008 TTTAACCCTCCCCTTCGTGTTTCCCCCAATGTTTAAAATGTTTGGATGGTTTGTTGTTCT 1067

1068 GCCTGGAGACAA**GGTGCT**AACATAGATTTAAGTGAATACATTAAC**GGTGCT**AAAAATGAA 1127

1128 AATTCTAACCCAAGACATGACATTCTTAGCTGTAACTTAACTATTAAGGCCTTTTCCACA 1187

1188 CGCATTAATAGTCCCATTTTTCTCTTGCCATTTGTAGCTTTGCCCATTGTCTTATTGGCA 1247

1248 CATGGGTGGACACGGATCTGCTGGGCTCTGCCTTAAACACACATTGCAGCTTCAACTTTT 1307

1308 CTCTTTAGTGTTCTGTTTGAAACTAATACTTACCGAGTCAGACTTTGTGTTCATTTCATT 1367

1368 TCAGGGTCTTGGCTGCCTGTGGGCTTCCCCAGGTGGCCTGGAGGTGGGCAAAGGGAAGTA 1427

1428 ACAGACACACGATGTTGTCAAGGATGGTTTTGGGACTAGAGGCTCAGTGGTGGGAGAGAT 1487

1488 CCCTGCAGAACCCACCAACCAGAACGTGGTTTGCCTGAGGCTGTAACTGAGAGAAAGATT 1547

1548 CTGGGGCTGTGTTATGAAAATATAGACATTCTCACATAAGCCCAGTTCATCACCATTTCC 1607

1608 TCCTTTACCTTTCAGTGCAGTTTCTTTTCACATTAGGCTGTTGGTTCAAACTTTTGGGAG 1667

1668 CACGGACTGTCAGTTCTCTGGGAAGTGGTCAGCGCATCCTGCAGGGCTTCTCCTCCTCTG 1727

1728 TCTTTTGGAGAACCAGGGCTCTTCTCAGGGGCTCTAGGGACTGCCAGGCTGTTTCAGCCA 1787

1788 GGAAGGCCAAAATCAAGAGTGAGATGTAGAAAGTTGTAAAATAGAAAAAGTGGAGTTGGT 1847

1848 GAATCGGTTGTTCTTTCCTCACATTTGGATGATTGTCATAAGGTTTTTAGCATGTTCCTC 1907

1908 CTTTTCTTCACCCTCCCCTTTTTTCTTCTATTAATCAAGAGAAACTTCAAAGTTAATGGG 1967

1968 ATGGTCGGATCTCACAGGCTGAGAACTCGTTCACCTCCAAGCATTTCATGAAAAAGCTGC 2027

2028 TTCTTATTAATCATACAAACTCTCACCATGATGTGAAGAGTTTCACAAATCCTTCAAAAT 2087

2088 AAAAAGTAATGACTTAGAAACTGCCTTCCTGGGTGATTTGCATGTGTCTTAGTCTTAGTC 2147

2148 ACCTTATTATCCTGACACAAAAACACATGAGCATACATGTCTACACATGACTACACAAAT 2207

2208 GCAAACCTTTGCAAACACATTATGCTTTTGCACACACACACCTGTACACACACACCGGCA 2267

2268 TGTTTATACACAGGGAGTGTATGGTTCCTGTAAGCACTAAGTTAGCTGTTTTCATTTAAT 2327

2328 GACCTGTGGTTTAACCCTTTTGATCACTACCACCATTATCAGCACCAGACTGAGCAGCTA 2387

2388 TATCCTTTTATTAATCATGGTCATTCATTCATTCATTCATTCACAAAATATTTATGATGT 2447

2448 ATTTACTCTGCACCAGGTCCCATGCCAAGCACTGGGGACACAGTTATGGCAAAGTAGACA 2507

2508 AAGCATTTGTTCATTTGGAGCTTAGAGTCCAGGAGGAATACATTAGATAATGACACAATC 2567

2568 AAATATAAATTGCAAGATGTCACAGGTGTGATGAAGGGAGAGTAGGAGAGACCATGAGTA 2627

2628 TGTGTAACAGGAGGACACAGCATTATTCTAGTGCTGTACTGTTCCGTACGGCAGCCACTA 2687

2688 CCCACATGTAACTTTTTAAGATTTAAATTTAAATTAGTTAACATTCAAAACGCAGCTCCC 2747

2748 CAATCACACTAGCAACATTTCAAGTGCTTGAGAGCCATGCATGATTAGTGGTTACCCTAT 2807

2808 TGAATAGGTCAGAAGTAGAATCTTTTCATCATCACAGAAAGTTCTATTGGACAGTGCTCT 2867

2868 TCTAGATCATCATAAGACTACAGAGCACTTTTCAAAGCTCATGCATGTTCATCATGTTAG 2927

2928 TGTCGTATTTTGAGCTGGGGTTTTGAGACTCCCCTTAGAGATAGAGAAACAGACCCAAGA 2987

2988 AATGTGCTCAATTGCAATGGGCCACATACCTAGATCTCCAGATGTCATTTCCCCTCTCTT 3047

3048 ATTTTAAGTTATGTTAAGATTACTAAAACAATAAAAGCTCCTAAAAAATCAAACTGTATT 3107

3108 CTGGTGTTCTCTTCTACACAGTGGGAGGGCGAGCAGTAGGAGAGATTGGCCCATTTGGTG 3167

3168 CTGGCCATTTGAGGAATGCAAGCCCAGCACTAGTCTCATAATCTCTAGGAATCTGTAGAG 3227

3228 AGAGGAATTGAAGTAAATTTCAGCATTGGCTCATTCAGTCATTCGGCGACATTCATCAGG 3287

3288 TACCTGCAATGTGTTAGGGGATCTTATGAGTAGGCAGCGTGCGTGATCCTTGCTCCCCTG 3347

3348 GAGCTTTCTAACATTCTAGCAGGCAGACCACACATAAATTTGCAATACTGTTTCTGATAA 3407

3408 AAACGTGCTGTAAAGGAAATAAAGCAGAGAACTATCATGGAAAA 3451

Figure 9.13 ***Complete 3'UTR of SPARC.*** *Primer positions (box) in transcript sequence and miRNA binding site of miR-29a-3p (bold cyan).*

VegfA/VEGFA

1573 ATGTGACAAGCCAAGGCGGTGAGCCAGGCTGCAGGAAGGAGCCTCCCTCAGGGTTTCGGG 1632

1633 AACCAGACCTCTCACCGGAAAGACCGATTAACCATGTCACCACCACGCCATCATCGTCAC 1692

1693 CGTTGACAGAACAGTCCTTAATCCAGAAAGCCTGACATGAAGGAAGAGGAGACTCTTCGA 1752

1753 GGAGCACTTTGGGTCCGGAGGGCGAGACTCCGGCAGACGCATTCCCGGGCAGGTGACCAA 1812

1813 GCACGGTCCCTCGTGGGACTGGATTCGCCATTTTCTTATATCT**GCTGCT**AAATCGCCAAG 1872

1873 CCCGGAAGATTAGGGTTGTTTCTGGGATTCCTGTAGACACACCCACCCACATACACACAT 1932

1933 ATATATATATTATATATATAAATAAAT 1959

Figure 9.14 ***Complete 3'UTR of VegfA.*** *Primer positions (box) in transcript sequence and miRNA binding site of miR-503-5p (bold dark blue).*

1591 ATGTGACAAGCCGAGGCGGTGAGCCGGGCAGGAGGAAGGAGCCTCCCTCAGGGTTTCGGG 1650

1651 AACCAGATCTCTCACCAGGAAAGACTGATACAGAACGATCGATACAGAAACCACGCTGCC 1710

1711 GCCACCACACCATCACCATCGACAGAACAGTCCTTAATCCAGAAACCTGAAATGAAGGAA 1770

1771 GAGGAGACTCTGCGCAGAGCACTTTGGGTCCGGAGGGCGAGACTCCGGCGGAAGCATTCC 1830

1831 CGGGCGGGTGACCCAGCACGGTCCCTCTTGGAATTGGATTCGCCATTTTATTTTCTT**GC** 1890

1891 **TGCT**AAATCACCGAGCCCGGAAGATTAGAGAGTTTTATTTCTGGGATTCCTGTAGACACA 1950

```
1951  CCCACCCACATACATACATTTATATATATATATATTATATATATATAAAAATAAATATCT  2010
2011  CTATTTTATATATATAAAATATATATATTCTTTTTTTAAATTAACAGTGCTAATGTTATT  2070
2071  GGTGTCTTCACTGGATGTATTTGACTGCTGTGGACTTGAGTTGGGAGGGGAATGTTCCCA  2130
2131  CTCAGATCCTGACAGGGAAGAGGAGGAGATGAGAGACTCTGGCATGATCTTTTTTTTGTC  2190
2191  CCACTTGGTGGGGCCAGGGTCCTCTCCCCTGCCCAGGAATGTGCAAGGCCAGGGCATGGG  2250
2251  GGCAAATATGACCCAGTTTTGGGAACACCGACAAACCCAGCCCTGGCGCTGAGCCTCTCT  2310
2311  ACCCCAGGTCAGACGGACAGAAAGACAGATCACAGGTACAGGGATGAGGACACCGGCTCT  2370
2371  GACCAGGAGTTTGGGGAGCTTCAGGACATTGCTGTGCTTTGGGGATTCCCTCCACATGCT  2430
2431  GCACGCGCATCTCGCCCCCAGGGGCACTGCCTGGAAGATTCAGGAGCCTGGGCGGCCTTC  2490
2491  GCTTACTCTCACCTGCTTCTGAGTTGCCCAGGAGACCACTGGCAGATGTCCCGGCGAAGA  2550
2551  GAAGAGACACATTGTTGGAAGAAGCAGCCCATGACAGCTCCCCTTCCTGGGACTCGCCCT  2610
2611  CATCCTCTTCCTGCTCCCCTTCCTGGGGTGCAGCCTAAAAGGACCTATGTCCTCACACCA  2670
2671  TTGAAACCACTAGTTCTGTCCCCCCAGGAGACCTGGTTGTGTGTGTGTGAGTGGTTGACC  2730
2731  TTCCTCCATCCCCTGGTCCTTCCCTTCCCTTCCCGAGGCACAGAGAGACAGGGCAGGATC  2790
2791  CACGTGCCCATTGTGGAGGCAGAGAAAAGAGAAAGTGTTTTATATACGGTACTTATTTAA  2850
2851  TATCCCTTTTTAATTAGAAATTAAAACAGTTAATTTAATTAAAGAGTAGGGTTTTTTTTC  2910
2911  AGTATTCTTGGTTAATATTTAATTTCAACTATTTATGAGATGTATCTTTTGCTCTCTCTT  2970
2971  GCTCTCTTATTTGTACCGGTTTTTGTATATAAAATTCATGTTTCCAATCTCTCTCTCCCT  3030
3031  GATCGGTGACAGTCACTAGCTTATCTTGAACAGATATTTAATTTTGCTAACACTCAGCTC  3090
3091  TGCCCTCCCCGATCCCCTGGCTCCCCAGCACACATTCCTTTGAAATAAGGTTTCAATATA  3150
3151  CATCTACATACTATATATATATTTGGCAACTTGTATTTGTGTGTATATATATATATATAT  3210
3211  GTTTATGTATATATGTGATTCTGATAAAATAGACATTGCTATTCTGTTTTTTATATGTAA  3270
3271  AAACAAAACAAGAAAAAATAGAGAATTCTACATACTAAATCTCTCTCCTTTTTTAATTTT  3330
3331  AATATTTGTTATCATTTATTTATTGGTGCTACTGTTTATCCGTAATAATTGTGGGGAAAA  3390
3391  GATATTAACATCACGTCTTTGTCTCTAGTGCAGTTTTTCGAGATATTCCGTAGTACATAT  3450
3451  TTATTTTTAAACAACGACAAAGAAATACAGATATATCTTAAAAAAAAAAAAGCATTTTGT  3510
3511  ATTAAAGAATTTAATTCTGATCTCAAA  3537
```

Figure 9.15 ***Complete 3'UTR of VEGFA.*** *Primer positions (box) in transcript sequence and miRNA binding site of miR-503-5p (bold dark blue).*

Per1, Zfp36 and STT3A

```
3971  AAGGGTTCAAGCTCTCAGGACTCTGCCATGGAGGAAGAAGAGCAAGGTGGGGGCTCATCC  4030
4031  AGCCCAGCTTTACCTGCAGAAGAAAACAGCACCAGCTAGACTCCATTTTGGGGCCGCTTA  4090
4091  CAGCAGTCTAATGAGAGGCTTCCTTTCGACCATGTTGGGGTTCTTATAACTCAAGATACA  4150
4151  GCTGGACCAACCAATAGGAAACTGCCCCAGCTTCTCCCAACATAGGGGGCTGGACCCCCA  4210
4211  TTACCAGCCCAGGCACAGGAGCTGCCTCTAGCTTCTTAGCAGAGTGGAAGTTCTCAGCCC  4270
4271  CATTTGGAGGATTGTCCACGCCCGTCCCACTGAGGAGACGGGCGGGTCTTCGGTTAAGGT  4330
4331  TGCTGACAAGCTGCTGAAGTGGTCTGTCCAAATCCCAGCTGAGCCTGAGTCCCAGTCGCA  4390
4391  GGGTTGGGGCTGCACTTATTTATTTGGGAGAGACAGCTCACTCTCCCACCTCACCCCAAG  4450
4451  ATGGGAGGAGGGGAACCTGGGATCTGTGTAGGATCCAGGTCCGTGAACCCCTAGCTGCTC  4510
4511  CAGGGTGGGGGAGGTTGGTGGACCATGGAGTCCCTGGTGCTGCCCCTCAGGTGGGACCCA  4570
```

```
4571  GGTGTTCTCAGCTCTACCCTCTACCAATGACATTTGTGTTTTTGATATTGTGTCTGTTAT  4630
4631  TTTTTTTTTAATACAAAATGACAAAATGAAAAACCAAAAACccaagactttgtgaaatga  4690
4691  agttgggagtttgggtgaggggaggggtgg  4720
```

Figure 9.16 ***Complete 3'UTR of Per1.*** *Primer positions (box) in transcript sequence and miRNA binding site of miR-29a-3p (bold cyan).*

```
896   TCACCTGTCTTTGAGGCAGGGGTGTTTGGGCCTCCCCAGACCCCTGCACCCCCAAGGCGT  955
956   CTCCCCATCTTCAATCGTATCTCTGTCTCTGAGTGACAAGTGCCTACCTACCCAGTATGG  1015
1016  ATCAGCTAGATCTCAAAGAGAGGGCAGGGACTGCTCATTGCTGTGGGGACCTGGGGCACT  1075
1076  CCTCTAAGTTAATAAGTCCCATCTTCTGGACATTCCAAGATGCAATAACCCATTTCCCTG  1135
1136  GTGCTGGGCTGGGGCAGGTCCCTAGTTTGCAAATTCAGTGTTTGGGTGGATCCGTTCCTA  1195
1196  GGGTACCTAAGATGTTTGAGGGAGACAGTTGACAGTTGGTCTTCCAGGCCCCAAGTCTTC  1255
1256  TGTTGTTTTTGAGATAGGAGCTTATTATGGTACCCCAGGCTGGCTTTGAACTCAATATAA  1315
1316  TCCTGCCTTAGCCTTTTCCAAGTTCTGGGGTTACAGGTATGCACCAGCCCCTCTGCAACT  1375
1376  CTGGTCTCCTGGAATCTTAAGTGCTGTGAAGAGCCGGCTCCCACAATACTATCCTAATTT  1435
1436  TTACTAGACCCTGAAGTTCAGTGTCCGGTGGTCGAAGCCTCTCCTGAGAATCCTGGTGCT  1495
1496  CAAATTTCCCTCCTAAAGCAAATAGCCAAAGCCATTGCCAAATCCCTTCTCCCCCAACCA  1555
1556  GTGGGCCCTTTATTTATGACGACTTTATTTATTGTATTAAGATTTTATAGTATTTATATA  1615
1616  TATTGGGTCGTCTACTCCGTTTTTCTTTTTGTAATGTTAAAACTGATACTGTATTAAGTA  1675
1676  TATGCTATAATATATTAATATATTGCTACCGTACAAGTCTATTTTTTGGGGGGGGTTGGA  1735
1736  ATTTTTAAATAAAATCTTGAGTGTGAACTGagatgaaatttgtctttttcgcggctcaca  1795
1796  gccttgtgatggtgggtaaa  1815
```

Figure 9.17 ***Complete 3'UTR of Zfp36.*** *Primer positions (box) in transcript sequence and miRNA binding site of miR-29a-3p (bold cyan).*

```
2182  GTAAAGGACCTGGATAATCGAGGCTTGTCAAGGACATAAATGTCACGTCCAGCTCTGATA  2241
2242  TGCTTCGCACTGAGCACATCACATTTAGGACGTTGAAGATTTTTTTTTTTTTTTTTTTTT  2301
2302  AATATGCAGTTTGTAAGAACAAAACTGGATGGCATCAGAATTGTCTGGAAGTTTTGTCTT  2361
2362  GGGCAGTATGGGCTGGGCCAAATGAAATGATTTTTATAATTCTAAACAGGTTACCAAATG  2421
2422  AAATGTCATGGCTTTACTTTGGTCAATTAAAGGGGGGAATTTTTTTAAAAAATGTGCCTT  2481
2482  ATTTGTTTTGACTTATAACTGATTTGAGGGAGGCAAAAGCTATGCTAGGCTGCCAGAAGG  2541
2542  ACATAAGCAGACCTTGTCCATTCTCTTAGCTCCCTAAATTAGCCAAATAGAGACTTCTTT  2601
2602  CTCAAATCAGGAAAACTATCAAAGACCAATTCAGATCCTACATTTACAGACAGTTTTGTC  2661
2662  ATAACCCTTTGCATTGCAGCACCTAGTACAATTCCTTGGAAACAGCGTGGCTCAATAAAT  2721
2722  TTTTATTGAATGAATAAATGTGGGACCAGAAGAGTGCTAGAAGAGTGCCTTTCTGGGCTA  2781
2782  CTATGTCTCTGTTCTCAATGTCTTTTATCCTTAGACGCTCTTTGACTTTATAAATCAGCA  2841
2842  GTTTTGAAGACTCAAGACAAACAGTGAAATTATTGGTTTATCAATGGAGAGGAAGAAACT  2901
2902  CTTCCAGCATTACATATAGAGCTTGATGGTCAGTAGGTGTTTTTGAATCAGCTTAAATAT  2961
2962  AATCATACATATCAATTTGAAATGGAGCTTTTCAGTACTCTCACTTATTCATGACACAGG  3021
```

3022 AATGACCCTTTACTCAAAACTCTTGTGGTTGTTCAAAGGTGAGCTTCTTTTTCCCTTAGT 3081
3082 CTTAGCCTATGTGTTGCTGTTGTATATTGTTACCAAGTTCAACTACCTAATTTTGAAGCT 3141
3142 CTTTCCAAATAAGATACAAATTAAAAGGGGAAGCATTGCCAGTAACAGGTCCCTAGAGAG 3201
3202 CAGTGCCAGCCTGCCTGCAAGAAAAGAGGAGAAACTTCTTAAAAAGTTTTAAGCCTGGGC 3261
3262 AACATAAGGAGATTGTTTCTATGAAAAATAAAAATTAGCCAGGTATGGTGGTGTACACCT 3321
3322 GTAGTCCCAGCTACTCGGGAAGATGAGATTGGAGGATCACTTGGGCCTGGGAGGTTGAGG 3381
3382 CTACAGTGAACTGTGATTGTGCCACTGTACTCCAGTCTGGGCGACAGTGAAATCTTGTCT 3441
3442 AAACAAAAACAATTTAACTGGGAAGCACAGTGGTCCTTGAGGACATTTAATATCAGGACA 3501
3502 AAGAGCCTATGAATATATCACTGATGTATATAAACCCTAAGGCGTTAATAAAAGCTAACT 3561
3562 GTTTAGTGTTATCCATTTAAGGGAACAGGAGGAATTGCATAACTTTTAGATTAGTCATAG 3621
3622 TGGTGCTCCTAAGGGATATGCTGTTGTATATTTGTATAGCCAGGGCACTTAGCCTTCCAA 3681
3682 ACCAA**TTTATA**TACCATGTTCTTCAACTGTGGGTGAGATTTAGCCTCAAGATTTGATTTA 3741
3742 CTATATGTAAGTACATTACTTGATTTCTATAAAGAATCTTTAGTGGAAGAGGTTATTCTG 3801
3802 AATTATTTATCAATATGATTAATACCAGTTAGAAATTATTAATGATCTTCC**TTTATA**CTA 3861
3862 TACATAGGATAACTTTTAACTTGTCGCTACAGTTGTTGCTCTGAGGATCTTAATTTTGTT 3921
3922 ACTTTCTAGGCTACATGAAGCTATCTTTTTAAAAAGTGTACTCTTCATTTTCACTGTTAT 3981
3982 TGTGTACTTAGCATAAAAAACTCAAATCTAGGCCAGGTGCAGTGGCTCATGCCTGTAATC 4041
4042 CCAGCACTTTGGGAGGCTGAAGCATGCGGATCACTTGAGCCCAGGAGTTCAAGACCAGCC 4101
4102 TGGGCAACATGGCTAATGAACACTAAGCATAGTTTTGATGTCTTTCATATTAAAGACTTT 4161
4162 CTCAAATTCTTGCTAGTCTGCTCCTCTTTAAGAGTGGGACCCTAGGCAGGGCGCAGTGGA 4221
4222 TCATGCCTGTAATCCCAGCACTTTGGGAGGCCGAGGCAGGCAGATCACTTGAGGCCAGGA 4281
4282 GTTTGAGACCGGCCTGGCAACGTGGGAAAACTCTGTCTCTACTAAAAATACAAAAATTAG 4341
4342 CTGGGTGTGGGGTACACACCCTGTAATCTCAGCTACTGGGGAGGCTGAGGCATGAGAATT 4401
4402 GCCCAGGAGGTGGAGGTTGCAGTGAGCAGACATCATGCCACTGCACTCCAACCTGGGAGA 4461
4462 CAGAGCAAGACTGTCTCAAAAAAAAAAAAAAAAAAAAAAAAgagtgggacccaaaaaagc 4521
4522 tgattgaaaggtctgtttgtaggggggtgta 4551

Figure 9.18 ***Complete 3'UTR of STT3A.*** *Primer positions (box) in transcript sequence and miRNA binding site of miR-340-5p (bold pink).*

Lmx1b/LMX1B

1609 GCTTCCTCGGCTCTTCCGACGTGGGCTCCCTGCAGGCCCGCGTGGGGAACCCCATTGACC 1668
1669 GGCTCTACTCCATGCAGAGCTCCTACTTTGCCTCCTGAG**AGCCAG**CCGGGCCGCATGGAC 1728
1729 GCTTGGGCCTGGGCCTAGGGTGGAGCCACAGGCCTCTGC**AGCCAG**CCGGCCCCCCAGCCC 1788
1789 ACCACCCGCTCAGACTCTTCAGAC**AGCCAT**ACGGTGCCCTCCCCTCGGCC**AGCCAG**ACCT 1848
1849 GGCTCAAGTGCCCACCGGGCAC**AGCCAG**GCAAGGCAGATGGGTGCAGCCTGGGCAGGGAC 1908
1909 TGTGTCCTGCCCACAGAGACCTTGT**GACCCC**TGGGGACCCAGAGCTCTTGGACAGTCACT 1968
1969 TGCCTCCCAGTCCTTTGACTTCATCACTACCTTCCCCGTCCCCGCCTCTTTTTGGGGGAA 2028
2029 GCTTAAATTTGTTCGTTCTTTCTTTTCTTTCTTTCTTTCTTTCTTTCTTTCTTTCT 2088
2089 TTCTTTCTTTCTTTCTTTTTTTTTATAAACATTCTGTTTCCAGCCAACCTCCATTGTCCC 2148
2149 TGCAAGGCCAGCCCTGGGACAGTGCCTGGTACCCGAGAAACAGTTATACGGGTGTCCTGC 2208

```
2209  GCTGGAGACCACTTCCCCTTCTGGTTAGCTCGGGGGATGGTTTCTGGGTCCTGGGAGGCC  2268
2269  CAGGGTCACTGTTCCCAGCCCTAGGCTGGAGCACAGGAGAGGAGGGCCCATGCAGGTGTG  2328
2329  ACAGGCTCTTTGGCCCTGCCTGAACTGGGAGTCTCAGCAAGAGGAGGGATGTGGACAAAG  2388
2389  CCCAGAGAGACCCAAAGGGACAGAGATGCGCGCACGTAAAGCCACTCACATCTGTAGGCA  2448
2449  CACCTGTGCAAGCATGCATATATACACCTGGTGCACACGCACACAAAGATGGAAGAGCTG  2508
2509  CCTTTCCTTTCCAGAAGCAGCGGTGAGGTCAGCGAGCAGGGCCTACCTCTAAGAGCAATT  2568
2569  GGAGAGGGAGGAAGGACGTAGGCCTGAGGTGTGAGCAGACAGACCTGGGTGGACCCCAGG  2628
2629  CTCTGTACAGGTCATGACTGCCAGGGCAGGAGGGTAGTCACAAACCTACAGGTCCCAGGG  2688
2689  CAAAGCTGGAGTCCAGAGAACCCAGTATACACAGACCTCAGCAGACACTCCAGATGGAGA  2748
2749  GGACCTCAAGAGTCTGACCCTTGGTACCATCCGATACTTAACTCCCTCGGTCCTTCTTCT  2808
2809  TACCCAGGGCCAGCGATGGCCAGCTGCCCTCCTTGTGGGCTCCCCTGACCCTCAATCTCC  2868
2869  TCTTGCCTGTCAGCTGAGGCTGTCCGCTGGCAGGGCTCCTGACCTTAGCCAGCTCGCACT  2928
2929  CAACAAGGCCAGCACCTTCTCTGCTCTTGGCACCTTAGCTCTGCTGATGCGGCTTAGGTC  2988
2989  TCATGACTTTGGAGCCCCATCCTTGTTCCATAATGACCCCCCTCCCCGGGGCCTCACACA  3048
3049  GGCACAGTGACAAGCTACAAACTCCTTCAATATGTGTGGATGGGATGTTGATTGCTTAGA  3108
3109  GCCCATGGAAGACCACCGCTTGTACCTGGTTGCCTTTCCTTTTGTTGGCTCAGTCAGCTT  3168
3169  GGGGCGTTACTCTGAAGCCACTGTATCTGTTCCCTCTGTCTCAGCTGCATCAGGTCAGCC  3228
3229  CTGTGGGGCGCCCCACAGAATCCTTGCACAGTTATAGGCCACCAGCATTTCAGCCTCCTG  3288
3289  AGTCACCCCCAGCCCCCAGTCTCCTGGACTCTTCCTGCCTGAAGCTGAAGCAGCCGTGGT  3348
3349  TCTTTCCTTGTCACCCCCCCCCCGCACACCACCCCCCAACCTCTGGCAAGCACTGTGTTC  3408
3409  CAGGCCAGAAGCCCAGGAGAAGGCTGCCATTCATTTAACGCAGACTCCTAGCCACCCCTC  3468
3469  ACCCACCAACCCACCCGTCCTGATGTCTGCCGAGCTCTAGCTGTGAGCACGGCAGGATGA  3528
3529  GTATCTCTCTGTCGCCCGCCATTTTGGGCTCCTGTGCCTGGTTAGTTAAGCTGCGTGGGT  3588
3589  TAATTTCCTGTCTCTGGGGAGACCTCAGACCCCCTTAGCCCCACCCAGATGTCACAATAT  3648
3649  GGAGTCAGCAGGGAAGAGCAGCTAGCACAGCCCTCCCGTGTCCCCCATTCTATCACTATC  3708
3709  CTCCATGCTGAAGGTGTGGTCCTGAGCTAGCTGCTTGTGTGGCTCGCCCTTGCCTCCTCT  3768
3769  GGCACAGGCCCCTGGCTGAATGGTACAGTGCATACTCCGGGCAGACCCAGGGTAAATAGG  3828
3829  AGCTCCAGGAACCCGGGCCTACTCTCATCCACTTTTTAAGTTGGGAGATGCAATCCAGTA  3888
3889  GACTGTGTCGCTGCTGAGAAACCTGAGACAGGAGAAGAGCTGGGATGTGCTCAAGGCTTC  3948
3949  ACAGCAACGTAGTGACAGAGCCACAGATGAGGAGAGGACATTAGGTCTGTCCCCATCTCT  4008
4009  GTCTCACATATGCACCCCACCACCACCACCAGGGACCAATGCGTTCTCACCACACCTGCT  4068
4069  GACCCCAAGGGTCCTCCAAACCGAGTCCAGCCCTGGCCTCTGCTGTTGCCATGCTGGTGT  4128
4129  CCCCAAGCCAGAAGATGTTATCACTTCTAAGTTGCCAGAGGAGGGTCCCCCCAGCCACCA  4188
4189  CACCAGAGATGCCCTGGCAGCCACTCTCAGCATTCTTTCACCACGGCTGTGGCCTGCTGC  4248
4249  CCTGCTGAGACAACATGGCTGCTGCAGGGACAAGGGCTTCTGTCCCGTGGGAAGAGACAG  4308
4309  CCTTTGATCTTGCCCAGACCTTGTTAGATAGCACACTCAGGCTTCTGGAACTGAGGCTGG  4368
4369  AAGGAGGCAGTGGTGGAGGGTTGAAGGTGGGGGGTGGGGCTAGCCTGCAGCCTGAAAGGG  4428
4429  CAGAGGGATATGGGAGAATGAGGTAGAAATTGAGAGAGAAAATCCAAGTTCCACCTCCTG  4488
4489  GCTGGGGGTGTGGCATGTTGAGGCTCAGGCAGAGAGGAAGGAGCCTGTCCAGGTGTCACA  4548
4549  CAGGAGTGACAAGAACCTGAGCTTTGTCCCAGCCAGGGCCCTATCTGTAGATTCATTCCA  4608
4609  TGAGGCTTCCCTTCTCTCTGCTGTCCTCAGAGACTCAGAAGAGGCCCCACACACAGACAC  4668
4669  CACACCAGGGGTGAGAGTCAGACCAAGGGGTGGCACAGACAGCCTGCTGTTATGGAGGCT  4728
```

4729 TCCTTAGTGGCAGGTGGGCATTGAGAAACTGCCCTTACATAAGAGATCCAGCTCAAGGGC 4788

4789 AGCCTCTCCTCCTTTAGGGACATCCCTTTGAAGTGAGACCACCTCCCTGTCTGTCTGATT 4848

4849 GTACCCCCCCCCCCCCCGCTCAGCAGGGGAAGATGGACTCAGAGCTCTGGGCACCCCTAG 4908

4909 GACCAGGGGGACGCTGCAGCCCAGGGCTGACCGATGCGTGGAAGGGGCAGCACACTCACA 4968

4969 CACGTG**CGCACA**CACTCACACCCGAAACAAGGAGGCTCACACATGGCCTGGGAGCAGGGA 5028

5029 GACAGGAAGGACCCTTCAACATGTGGCCCTTGACAGGGGCAATTGCCAATGGTCTCTGGG 5088

5089 CTGCTGCCCTGCCCTGGGGTCCCGCTTGGAGGGCGTTTGTTGCAGCTGGACTGGGGCCAG 5148

5149 GCCACCCATCGTATTCTTTCCGTTTACCTTGTACAGACTGCCCGCCTGCCATCCCCACAC 5208

5209 ACATTTTATTTA**ATAACT**TGTCATTGTTAAATTATTTATTAGCGTTTCCACATCACCACC 5268

5269 CCCGCCTTCCACTCACCTTCTGCCTCTTCCCACAAAAGCAGAAAATGGAAACAGCAAGAA 5328

5329 AAAAAGACAAGATGTTGGTATATTTGTAAATAAACAACCTGTACACTCC 5377

Figure 9.19 ***Complete 3'UTR of Lmx1b.*** *Primer positions (box) in transcript sequence: fragment 1 (—), fragment 2(---), fragment 3 (- – -) and fragment 4 (·····), miRNA binding site are indicated as followed: miR-149-5p (bold cyan), miR-135a-5p (bold pink), miR-210-3p (bold red), miR-615-3p (bold blue), miR-615-5p (bold brown) and miR-101a-5p (bold black). Internal SacI-restriction sites marked in yellow.*

1574 GGAACGACTCCATCTTCCATGACATCGACAGCGATACCTCCTTAACCAGCCTCAGCGACCT 1633

1634 GCTTCCTCGGCTCCTCAGACGTGGGCTCCCTGCAGGCCCGCGTGGGGAACCCCATCGACC 1693

1694 GGCTCTACTCCATGCAGAGTTCCTACTTCGCCTCCTGAG**AGCCAG**CCAGGCGCACGGACG 1753

1754 CTTGGGCAGGGGCCTGGGGGGGACTGCCAGCCTCTGCGGCCAGCCTGGCCACCCCCGCCC 1813

1814 TGCTCTC**CGCACA**GACTACAGAC**AGCCAT**ACGGTGCCCTCCCCTCGGCCAGCTGGGCCTG 1873

1874 ACCACTGTGCCCGTTGGGTAC**AGCCAG**ACCGGTAGATGGGCACAGCCTGGGCAGGGGCTG 1933

1934 TGTCCTGCCCACAGAGACCTTGTCATCCCCAGGGACCCAGAGCTCTCGGACGGCCACTCG 1993

1934 TGTCCTGCCCACAGAGACCTTGTCATCCCCAGGGACCCAGAGCTCTCGGACGGCCACTCG 1993

1994 CCTCCCAGCCCCACCTCGGCCTCCATCGCCTCCTCCCCATCTCTTTTTTGGGAAGCTTAA 2053

2054 ATTCTCTCTATTTTTTTAAATGTCCTCTCTGTGTCCATGGCCCTCCATGCAAGCCCCAGG 2113

2114 ACAATGGTGTCATGAGGCGGTGACCTGAGAAGCGTGTGTACCTGTGCCCCAGCAAGGGCA 2173

2174 GGGGTGGCCTCTGGGGGCAGGCCCACTGCCTGGAACCGCACACCCCTCAGCCTGAGTCTG 2233

2234 GAGCAGCAGTGGAGAGGGGCCTGAGGGGAGGCACTGTCAGGAGGCGG**GCTCGG**AGCCTGA 2293

2294 GCCTGGGCAGGCGCAAAGGGACAGAGAGGCACGTGCAGACACATGCACACTTGCAGACAA 2353

2354 ACCCACGCAAACACACACACAGCTGTATGGGGACACCAGAAGGGACAGGGATGCTCAGCG 2413

2414 GGTCTGTCCTGCCTTGTCAGAAAGAGAAAAGGAGGCCAGGCAGGG**GACCCC**CCAGTTCTT 2473

2474 AAGAGCGATTGGAAAGGGAGGAAGGGGAGAGGAAGAGGCGAACTTGAAGCATCGGACCCA 2533

2534 GTTGTATCCCAGCCTGGGCCCAAATGGGGGCAGCCTGGGCAGGGAGGGCAGCCCCAGGCC 2593

2594 CCACCAACTCTAGAGGCAGATGGAGCCCCCAGAACCAGGTAGCATCAGACCAGACAACAG 2653

2654 AGCCTCCAGGGGTCAGGGACTTCAGAAGCACCTGCTGGGCACCCCATCTGCAATGTGGTC 2713

2714 CTCTCCCCAGCCACCTCTGCCTCCCCTCACATACCTCCAGTGACAAGGAGCTCACTAGGT 2773

2774 CAGCGAGCCCACAGCAGCTGTGCTGTCCTGCATCCCAGAGCCAGGCTTCCCCAGCTCTCC 2833

2834 CTCTTAACACTGTCCCCCAGCAGGCCTCCGGCTGTCCCTCTAAAGGTGTGGGGCAGGTAT 2893

2894 CACTTCACCTTCCCACTGATGTCAGCCGGCCAGAAGTGAGCAGGCACATCACCTCTCCTG 2953

2954 CTGTGGCACCCTTCCTCTGTTAATTTGGCCCAAAAGACAATGATTTGGCCACATGACCTT 3013

3014 AGAGATTCACCCTGCCCTGCTGTAGCTAAATCCCTGGGCCCCACACGCAAGTGACAGCTA 3073

3074 AGCCACATCTGTTTTCTGTGTATATGCAGGATGGGGGCACCTACTGTTTTGTTTTGTTTT 3133

3134 GTTTTGTTTTGTTTTGTTTTGTTTTGTTTTGTTTTGTTTGAGACGGAGTTTCGCTCTTGT 3193

3194 TGCCCAGGCTGGAGTGCAATGGCGCGATCTCGGCTCACCACAACCTCCGCCTCCCAGGTT 3253

3254 CAAGTGATTCTGATGCCTCAGCCTCCCTAGTAGCTGAGATTACAGGCATGCGCCACCACA 3313

3314 CCCAGCTAATTTTGTATTTTTAGTAGCAACGGGGTTTCTCCATGTTGGTCAGGCTGGTCT 3373

3374 CCAACCCCCGACCTCAGGTGATCCGCCTGCCTCGGCCTCCCAAAGTGCTGGGATTACAGG 3433

3434 CGTGAGCCACCGCACCCAGTCTGCACTTACTGTTTAGACTGAATGAGGGACCGTGACCTC 3493

3494 TTTCCTTTTCCATTCCTTCTTACTCGATTCATTCCAGCCTGTGGAATTTCTCTGCACCCT 3553

3554 GATTCAGTGACCACTGCTCTCCTCTCTCCCAGCACATCTGCCCAGTGAGGAGTTGGCCCT 3613

3614 GGGTCTCACCTGAGGTGTGTGGACCGGGCTGGCCTCTCCCTGTTTGACATTGGCCCATTA 3673

3674 ATGCATCCTCTTTGGGGGACACATTCCAATTGCATTTCCTGCCCCCTTCTCCCAGGGCAA 3733

3734 TTGCAGAAGATTGTGTCAGGCGCCCTGCTGGAAGTCAGGTGCACTAGATCCATCCCCAGC 3793

3794 CCCAGTCTGCTCAACTCTATCCCTGTCAGAGCAAGGAGGCTGGGCTGCTGGGGCCTGACT 3853

3854 GGTGAGCCCACCCTGTCCCCTGGTGATCACTGTGTCCCCTTGTTCAGGTGCTCACAACCC 3913

3914 TACCTTTAACTCTGAGGTCAAGCCCTAGGCCACCACCCTAAAGTCTGCCTGGTCCAACCT 3973

3974 TTGAGCAAGTAAGGATAATGAATGTCCCTTTTCCACCTTTGGGGCCCTCTGCCTGGATCT 4033

4034 CTGGAATCCTCTAAGTTCAACCTGTTCTGTGGTTTTGCTCCCGTTTGCTGGGAAATTCAG 4093

4094 TCCCCCCAGAATGTCCTGGGCCAACCTCCTTGCCTGACATGTGGCCTCGTGTCACCCATT 4153

4154 GGGCCCCAGCAGCCAGCTAGCCCTTCTGCAGCTCTTCTTACAAACAGAGCCTCTCCAAGG 4213

4214 ACCTCAGTTGATGTTCTGGTCCTTCTGCCGCCTCAGCCCACCAGGGTCCGTGCCACCATG 4273

4274 GGTCTCTTGAGCAGCAGCTGCACTGGCTTCTGGAGAGACACCCCTCTTTCTCCTTTTGCA 4333

4334 CATGCACCATCTGAATCGTGCCAGGGACATCCTGGGCAGATTCAGGGGCAGATGCCCTAT 4393

4394 CCCCCAGGAGACCTGGCCCTTCTCTCTCAGACCCAATAAGTTGGAAGGGACGTCAGAAGC 4453

4454 GGTCATCTCATCTGCCCCTTATTTTATAGTTGGAAACCCTGAGGCAAGAGAGGGAAAGAG 4513

4514 GCCTGTCCAAGGTCCGGGTTAGTGACAGAGCTGAGCTGAGAACAGGGACGTTGTGCCCCA 4573

4574 CTGTCCCCTGTGGTTTGTGAATGACCTCCAGGTCAGGGGGTCACAACTTGTTCTTAGTAA 4633

4634 ACTTGCCAGCTGTTGGGGTCACATATTCCCATTCTGGGGCCTCACAAACCCCCGAATCCA 4693

4694 GCCGGGACCCCATGCCAGGAGCTGGTCTAGGGACAGCATGCTTGTGACCCACAGACTGTT 4753

4754 AAAGCCAGAAGGGACCTCAGAGAGTCCCTTATGCTGGAGGCGCCCTGTCAGCCGTGGCTA 4813

4814 GGGGCCCCTTGCTCTATGCTGTGCCTTGCTGCCCACAGGCTCCCAGACACCAGTGCCCAC 4873

4874 TCTGCCCAGCCCCGGACTGGGTGTGGCTCGCAGATGAACAAGATGCAGGGCCTGCCTTGA 4933

4934 GGGGTGTCTCCTAGAAGGAAAGCCAGACTCTCCGGCCCAGCCAGAGAGTCCAGACATGGC 4993

4994 AGGGACCCGTTTCTCAGATGAGGAGCCTGAGGCTCAGAGAAGGGAGGCGATGTGTTCAGG 5053

5054 GCCACCCAGCAGAAGCCTGTGGGGCTGGGCAACCTTCTCCCACTTTATGGGAGGAGCTGC 5113

5114 AGCCTTGGCTGGGAGCTGGGCGGGGAGTAGCCAGGACCACCCCTTGCCCGTGCCGTGACA 5173

5174 TGGAACCTTCATCACTAAGGGGGCTGGAGTGGGAAGAGGGAGATAACTGTGTGGTCTCCA 5233

5234 GAGCAAAAGAGAATGAGAGGTGGGCAGGGGGAGTCTTGGCAAAAGACCAAGTTCCACTTC 5293

5294 CCTGCTGGGGAAGTCAAGGCTCAGAAAGAGGAAATAATTGCCCCAGGTAACACAGGGCAG 5353

5354 AGGAGGGACAAAAAGCTGGGCATGGCCCCAGCCAGAGCCTCATCTGCCTACTCCGTGAAG 5413

5414 CCTCCCAGGTACTCTGCTATCCTGGGAAACGCACAGGGAGGCCACACAGAGACACTGCTC 5473

```
5474  ACAAGAGTCAGACCAAGGTGCCAGCACAGCCTGGAAAGAGCTCAGAAAGGGGGTTGGTGC  5533
5534  ACGTGGCTGGGCATCTTAGGAGGCTTCCTGAGGGTGGGTAAAGGTGGGAAGGCCCTGGCG  5593
5594  CTGCATCAGATGAGCAGGGCCTGGCAGGGACAAGCCTCTTCTCCTTTGGGAAGCCCTGCA  5653
5654  GCCTCCTAGCAAGAGGCTGATTCCCCACTCTGCCCCCATCTGAATGTCCTTTTCATGTTG  5713
5714  CACGCAGGGAACCTCAGGAAGGAGGATTGCCTGATGCCTGCCTGGCTCCATCCTTGAGCT  5773
5774  CTGGCGCACCACCTAGGGTGAGGGAGAGCCTGCAGCTCTGGGGCTAAGTCTGCCCTGGGGG 5833
5834  GAAAGGGCTCCACGCTCACACGCACGCGCTCGCACACACACTCACACCTGGACGCACA  5893
5894  CGGAGGCTTGCGGACCCATACTCACAGGCACATGTGGCCTGGGGACTGGGGGAGCAGGAA  5953
5954  AGACCCCTCCAACATTTGGCCCTTGGAAGGCACCATTGCCAATGAGCCTCTTTGCTGGTT  6013
6014  CCCCCGACCCCACCTGGGGGTCCCATGGGAGCCCAGCCCAGCCAGGTGTGGGGATGGGCC  6073
6074  ACCGGCCATTCCTGTTTTCCTTGTACAGACAGATTCTCACTACCCACCCGCCATCCCCAG  6133
6134  ACACATTTTATTTAATAACTTGTCATTGTTAAATTATTTATTAGCGTTTACCACACCACC  6193
6194  ACCCCCACCCTGCCCTCCACTCTCACCTTCCACCTCTTCCCACAACAGCAGAAAATGGAA  6253
6254  ACAACAACAAAAAAAGATGAGACATCAGTATATTTGTAAATAAACCGACCTGTACACTC   6312
```

Figure 9.20 ***Complete 3'UTR of LMX1B.*** *Primer positions (box) in transcript sequence: fragment 1 (—), fragment 2(---), fragment 3 (- – -) and fragment 4 (⋯⋯), miRNA binding site are indicated as followed: miR-149-5p (bold cyan), miR-135a-5p (bold pink), miR-210-3p (bold red), miR-615-3p (bold blue), miR-615-5p (bold brown) and miR-101a-5p(bold black). Internal SacI-restriction sites marked in yellow.*

Table 9.1 ***Body weight of Dicer mice on day 31 and on day 41.*** *Differences are written in g and corresponding %. – indicating loss of weight.*

		body weigth [g]			
Genotype	Animals	31 d	41 d	Δ differences [g]	
NPHS2-Cre: Dicer $^{lox/lox}$	mouse 1	26.07	21.90	- Δ 4.17	16 %
	mouse 2	20.05	14.90	- Δ 5.15	26 %
	mouse 3	22.84	15.00	- Δ 7.84	34 %
	mouse 4	22.92	18.00	- Δ 4.92	21 %
	mouse 5	19.80	20.70	Δ 0.9	5 %
NPHS2-Cre: Dicer $^{+/+}$	mouse 1	23.15	22.90	- Δ 0.25	1 %
	mouse 2	22.66	22.83	Δ 0.17	1 %
	mouse 3	26.19	26.30	Δ 0.11	0.1 %
	mouse 4	22.86	23.12	Δ 0.26	1 %
	mouse 5	25.32	26.35	Δ 1.03	4 %
	mouse 6	22.30	22.61	Δ 0.31	1 %
NPHS2-Cre: Dicer $^{lox/+}$	mouse 1	27.57	27.80	Δ 0.23	1 %
	mouse 2	22.85	24.24	Δ 1.39	6 %
	mouse 3	20.63	22.14	Δ 1.51	7 %

Table 9.2 ***Body weigth of Dicer mice for podocyte isolation on induction day and on the respective perfusion day.*** *Mice used for podocyte isolation after three days, seven days and 24 days of induction. Differences are written in g and corresponding %. – indicating loss of weight.*

		body weigth [g]						body weigth [g]			
Genotype	Animals	0 d	3 d	Δ differences [g]		Genotype	Animals	0 d	3 d	Δ differences [g]	
NPHS2-Cre: Dicer $^{+/+}$	mouse 1	23.04	22.69	- Δ 0.35	2 %	*NPHS2-Cre: Dicer* $^{lox/lox}$	mouse 1	26.68	26.10	- Δ 0.58	2 %
	mouse 2	23.67	23.49	- Δ 0.18	1 %		mouse 2	27.57	27.79	Δ 0.22	1 %
	mouse 3	29.44	29.48	Δ 0.04	0.1 %		mouse 3	17.50	18.52	Δ 1.02	6 %
	mouse 4	22.82	23.70	Δ 0.88	4 %		mouse 4	15.50	17.03	Δ 1.53	10 %
	mouse 5	29.82	31.10	Δ 1.28	4 %		mouse 5	30.70	30.30	- Δ 0.4	1 %
	mouse 6	23.46	23.99	Δ 0.53	2 %		mouse 6	12.63	15.43	Δ 2.8	22 %
	mouse 7	23.15	24.23	Δ 1.08	5 %		mouse 7	19.25	20.30	Δ 1.05	5 %
	mouse 8	22.00	23.61	Δ 1.61	7 %						
	mouse 9	18.01	20.23	Δ 2.22	12 %						
	mouse 10	27.52	28.18	Δ 0.66	2 %						
	mouse 11	15.72	18.00	Δ 2.28	15 %						
		body weigth [g]						body weigth [g]			
Genotype	Animals	0 d	7 d	Δ differences [g]		Genotype	Animals	0 d	7 d	Δ differences [g]	
NPHS2-Cre: Dicer $^{+/+}$	mouse 1	24.38	23.76	- Δ 0.62	3 %	*NPHS2-Cre: Dicer* $^{lox/lox}$	mouse 1	21.54	21.98	Δ 0.44	2 %
	mouse 2	31.00	31.09	Δ 0.09	0.3 %		mouse 2	32.01	32.10	Δ 0.09	0.3 %
	mouse 3	24.70	24.64	- Δ 0.06	0.2%		mouse 3	26.85	27.88	Δ 1.03	4 %
	mouse 4	30.57	31.11	Δ 0.54	2 %		mouse 4	22.07	23.23	Δ 1.16	5 %
	mouse 5	14.25	15.24	Δ 0.99	7 %		mouse 5	23.50	24.13	Δ 0.63	3 %
	mouse 6	29.62	29.33	- Δ 0.29	1 %		mouse 6	23.27	24.12	Δ 0.85	4 %
	mouse 7	23.61	24.41	Δ 0.8	3 %		mouse 7	24.54	25.70	Δ 1.16	5 %
	mouse 8	30.70	30.98	Δ 0.28	1 %		mouse 8	26.15	26.40	Δ 0.25	1 %
	mouse 9	35.45	34.27	- Δ 1.18	3 %						
	mouse 10	25.30	25.90	Δ 0.6	2 %						
	mouse 11	25.65	26.00	Δ 0.35	1 %						
		body weigth [g]						body weigth [g]			
Genotype	Animals	0 d	24 d	Δ differences [g]		Genotype	Animals	0 d	24 d	Δ differences [g]	
NPHS2-Cre: Dicer $^{+/+}$	mouse 1	22.54	23.60	Δ 1.06	5 %	*NPHS2-Cre: Dicer* $^{lox/lox}$	mouse 1	29,84	30,61	Δ 0.77	3 %
	mouse 2	21.85	22.66	Δ 0.81	4 %		mouse 2	22,89	23,9	Δ 1.01	4 %
	mouse 3	26.28	28.59	Δ 2.31	9 %		mouse 3	30,59	31,4	Δ 0.81	3 %
	mouse 4	22.65	23.13	Δ 0.48	2 %		mouse 4	22,54	23,64	Δ 1.1	5 %
	mouse 5	21.06	21.87	Δ 0.81	4 %		mouse 5	26,79	27,65	Δ 0.86	3 %
	mouse 6	22.95	23.80	Δ 0.85	4 %		mouse 6	20,01	21,84	Δ 1.83	9 %
	mouse 7	25.66	27.46	Δ 1.8	7 %		mouse 7	21,91	23,63	Δ 1.72	8 %

10. Acknowledgement

At the end of my thesis, I want to thank all the people who helped and encouraged me during all the time from the beginning to the end of this thesis.

Foremost, I want to thank Prof. Dr. Ralph Witzgall for giving me the opportunity to work on the very interesting miRNA project, for his patience, support and advice throughout the thesis.

I am thankful to my mentors, Prof. Dr. Gunter Meister and Prof. Dr. Frank Schweda for their valuable advice and suggestions.

Special thanks to Dr. Melanie Zaparty, who took care of the miRNA project. Without your support and help, your ideas and suggestions over the last four years, none of this would have been possible.

I want to thank Marion Kubitza and Olga Maier for their help and support in technical questions and laboratory work. Thanks to Marion, for her help in the podocyte isolation and the guidance she gave me through the lab and to Olga for her support in the miRNA project.

Also I would to like to thank Kerstin Herrmann and Helga Othmen for performing EM analysis and Jaqueline Dirmeier, Rüdiger Eder and Irina Fink for performing the FACS analysis. I would also like to thank Carmen Zetzschke for her support with the genotyping.

I want to thank my current and former fellow PhD students Dr. Susanne Baumgarten, Tim Braun, Katrin Brunner, Dr. Korbinian Bürger, Julia Dörr, Jasmin Karreis, Dr. Lisa Lucke and Dr. Markus Setzer for creating a great atmosphere and moral support.

I want to thank all students that helped to further the miRNA project through their energetic work: Caroline Gabriel, Tabea Gross, Bianca Lehner and Neha Malagimani.

My gratitude is also extended to all current and former members of Professor Witzgall's group for the pleasant atmosphere at work: Eva Chira, Dr. Melanie Grosch, Anita Hecht, Michal Jirák, Edeltraud Lautenschlager, Ton Maurer, Christine Meese, Larissa Osten, Prof. Dr. Reinhard Rachel, Karin Schadendorf, Dr. Kerstin Schmidt, Lena Seitz, Justin Skotnitzki, Petra Utz, Ludwig Utz, Uwe de Vries, Marina Wuttke, Yulia Zaytseva and Anita Zügner.

Last but not least, I want to thank my parents, Lieselotte and Erich Meisinger, my brothers Thomas and Stephan Meisinger and Hanna for all their support and patience throughout the years.

11. Eidesstattliche Erklärung

Ich erkläre hiermit an Eides statt, dass ich die vorliegende Arbeit ohne unzulässige Hilfe Dritter und ohne Benutzung anderer als der angegebenen Hilfsmittel angefertigt habe. Die aus anderen Quellen direkt oder indirekt übernommenen Daten und Konzepte sind unter Angabe des Literaturzitats gekennzeichnet.

Bei der Auswahl und Auswertung folgenden Materials haben mir die in der Arbeit genannten Personen in der jeweils beschriebenen Weise unentgeltlich geholfen. Weitere Personen waren an der inhaltlich-materiellen Herstellung der vorliegenden Arbeit nicht beteiligt. Insbesondere habe ich hierfür nicht die entgeltliche Hilfe eines Promotionsberaters oder anderer Personen in Anspruch genommen. Niemand hat von mir weder unmittelbar noch mittelbar geldwerte Leistungen für Arbeiten erhalten, die im Zusammenhang mit dem Inhalt der vorgelegten Dissertation stehen.

Die Arbeit wurde bisher weder im In- noch im Ausland in gleicher oder ähnlicher Form einer anderen Prüfungsbehörde vorgelegt.

Ich versichere an Eides statt, dass ich nach bestem Wissen die reine Wahrheit gesagt und nichts verschwiegen habe.

……..

Sandra Meisinger